ELECTROCHEMICAL CHARACTERIZATION OF SOME ELECTROACTIVE NUCLEOPHILIC SUBSTITUTION REACTIONS

by

Md. Rabiul Islam

A thesis submitted in partial fulfillment of the requirements for the degree of Master of Philosophy (M.Phil) in Chemistry

Khulna University of Engineering & Technology
Khulna 9203, Bangladesh.

July, 2016

Declaration

This is to certify that the thesis work entitled “Electrochemical Characterization of Some Electroactive Nucleophilic Substitution Reactions” has been carried out by Md. Rabiul Islam in the Department of Chemistry, Khulna University of Engineering & Technology, Khulna, Bangladesh. The above thesis work or any part of this work has not been submitted anywhere for the award of any degree or diploma.

Signature of the Supervisor

Signature of the Candidate

Acknowledgements

First of all I would like to express my grateful thanks to Allah to complete my task.

I would like to express my deepest sense of gratitude and sincere thanks to my respected supervisor **Dr. Md. Abdul Motin**, Professor and Head, Department of Chemistry, Khulna University of Engineering & Technology, Khulna, Bangladesh for providing me the opportunity of working under his kind supervision. For his proper guidance, co-operation, invaluable suggestions and constant encouragement throughout this research work it is easy to find the right way to fulfill the desire research. I will remember his inspiring guidance and cordial behavior forever in my future life.

I am pleased to express my gratitude to **Md. Abdul Hafiz Mia**, Lecturer, Department of Chemistry, Khulna University of Engineering & Technology, Khulna, Bangladesh for helping my research work. I should take this opportunity to express my sincere thanks to **all teachers and stuffs** of this department for their valuable advice and moral support in my research work.

I wish to convey my hearty thanks to all my friends and class fellows specially **Md. Nazim Uddin, Palash Kumar Dhar** and **Md. Alim Uddin** for helped me according to their ability.

I wish to thank my **parents** for their grate understanding and support.

Md. Rabiul Islam

Abstract

The substitution reaction of Catechol in presence of Imidazole, L-Arginine and L-Serine have been studied by cyclic voltammetry, controlled potential coulometry and differential pulse voltammetry techniques using Glassy carbon (GC), Gold (Au) and Platinum (Pt) electrodes. The voltammetric studies have been carried out by varying the composition of Catechol, Imidazole, L-Arginine and L-Serine in the buffer solution of different pH, different electrodes and scan rate.

Pure Imidazole, L-Arginine and L-Serine are electro-inactive whereas pure Catechol is electro-active. In the second scan of potential, a new anodic peak appears at the lower potential and the oxidation and reduction peak shifted with respect of pure catechol after addition of Imidazole, L- Arginine and L-Serine in catechol solution. At the same time the anodic and cathodic peak current decreases significantly compared with the pure catechol that indicates the participation of reaction of o-benzoquinone with Imidazole, L-Arginine and L-Serine. The reaction products generated from the reaction of catechol in presence of Imidazole, L-Arginine and L-Serine are assumed to be 4-(1H-imidazol-1-yl)cyclohexa-3,5-diene-1,2-dione- 2-amino-4-(1-(3,4-dioxocyclo hexa-1,5-dien-1-yl)guanidino)-4-oxobutanoic acid and 3-hydroxy-2-((3-hydroxy-4-oxocyclohexa-2,5-dien-1-ylidene)amine)propanoic acid respectively that undergo electron transfer at more negative potentials than the Catechol. The electro –synthesized products generated from Catechol with Imidazole, L-Arginine and L-Serine were isolated. The formation of Catechol-nucleophile adducts are also confirmed by FTIR spectra.

The pH effect of catechol in presence of Imidazole, L-Arginine and L-Serine has been investigated in different pH from 3 to 11. From the experiment it has been observed that almost no new anodic peak appeared after repetitive cycling at pH 3-5 (acidic media) and pH 9-11 (basic media). At pH 7, the o-benzoquinone undergoes nucleophilic attack by the amines that is reflected from voltammetric new anodic peak, A_0 appeared after repetitive cycling. The slopes of the peak potential, E_p vs pH plot has determined graphically as the anodic peaks of Catechol-Imidazole (60 mV/pH), Catechol-Arginine (56mV/pH) and Catechol-Serine (61.5 mV/pH) at 0.1V/s. This indicates that the oxidation reaction of

catechol-amine adduct proceeded via the $1e^{-}/1H^{+}$ process. This also suggests that during the reaction not only electron but also proton are released from the catechol-amine adduct.

The reaction is strongly influenced by the pH as well as concentration of Imidazole, L-Arginine and L-Serine. These reactions are mostly favorable in 20 mM of Imidazole, 30 mM of L-Arginine and 90 mM of L-Serine with fixed 2mM of Catechol at pH 7. The electro-oxidation of Catechol is found to be facilitated in neutral media.

Electrode effects on CV and DPV of Catechol in presence of Imidazole, L-Arginine and L-Serine have been investigated. The nature of voltammograms, peak position and current intensity for the studied systems are different for different electrodes. The voltammetric response of GC electrode is better than Au and Pt electrodes.

The scan rate effect on cyclic voltammogram of Catechol in presence of Imidazole, L-Arginine and L-Serine has also been studied. The peak current of both the anodic and the corresponding cathodic peaks increases with the increase of square root of scan rate. The nearly proportionality of the anodic and corresponding cathodic peak suggests that the peak current of the reactant at each redox reaction is controlled by diffusion process. The current function, $I_p/v^{1/2}$ of Catechol derivatives are found to be decreased exponentially with increasing scan rate. In all the studies of Catechol-amine derivatives have been found to undergo electrochemical reaction with ECE (electron transfer- chemical reaction-electron transfer) type mechanism.

During the course of coulometry the appeared anodic and cathodic peak height is increased to the advancement of coulometry, parallel to the decrease in height of existing anodic and cathodic peaks which indicates the reaction product has been produced.

Contents

LIST OF TABLES

LIST OF FIGURES

CHAPTER I

Introduction

1.1 General

Electrochemistry is the study of chemical processes that cause electrons to move and studies the relationship between electricity, as a measurable and quantitative phenomenon, and identifiable chemical change, with either electricity considered an outcome of a particular chemical change or vice-versa. It correlates chemical, surface and electrical properties of the systems. It has strong links to many other fields of science. Modern electrochemistry has vast applications. These include exploration of new inorganic and organic compounds, biochemical and biological systems, energy applications involving fuel cells and solar cells, and nano scale investigations. It also finds applications in electro analysis, industrial electrolysis, electroplating, batteries, electrochemical machining, minimization of corrosion, sensor biosensors nanotechnology and bio- electrochemistry [1]. Electrochemical processes form the basis of large-scale chemical and metallurgical production of a number of materials. Modern electrochemical power sources (primary and secondary batteries) are used in many fields of engineering and their production figures are measured in billions of units. Several electrochemical devices, such as pH or oxygen electrodes, have been used regularly for years in environmental analysis. Recent advances in electrochemical sensor technology will certainly enlarge expand the scope of these devices towards a wide range of organic and inorganic contaminants and will speed their role in field analysis. These advances incorporate the introduction of modified or molecular devices or sensor arrays, and developments in the areas of micro fabrication, computerized instrumentation and flow detectors.

Electrochemical vision have been proved particularly fruitful for studying and interpreting a number of very important biological processes such as cellular respiration, photosynthesis, and in maintaining the redox balance of proteins [2]. Moreover, redox signaling involves the control of cellular processes by redox reactions.

The analytical advantages of the various voltammetric techniques include excellent sensitivity with a very large useful linear concentration for both inorganic and organic species. These voltammetric techniques present irreplaceable tools due to their robustness and ability to provide a vast amount of important thermodynamics and kinetics information. Voltammetric techniques used to characterize electrocatalyst surfaces and kinetics of some of the electrocatalytic reactions being most important in ever-growing fields of fuel cells, electrolysis and battery technologies, such as hydrogen oxidation/evolution reaction, oxygen reduction reaction as well as the oxidation of carbon-monoxide and low-molecular weight alcohols.

Voltammetric techniques has encouraged the development of electroanalytical methods for the determination of analytes in a wide range of concentrations (up to traces) in real samples from different areas of great importance for human being and animal‘s health. The common characteristic of all voltammetric techniques is that they involve the application of a potential (E) to an electrode and the monitoring of the resulting current (i) flowing through the electrochemical cell. In many cases the applied potential is varied or the current is monitored over a period of time (t). Thus, all voltammetric techniques can be described as some function of E, i, and t.

Therefore, voltammetric techniques coupled to pre-concentration adsorptive steps have been developed and look very promising for the quantification of these substrates in real samples.

There has been a growing interest in the study of the reactions between quinones produced from the oxidation of 1,2-dihyroxybenzene (catechol), 1,3-dihyroxy benzene (resorcinol), 1,4-dihyroxy benzene (hydroquinone) and nucleophiles for mechanistic [3-7] reasons. Catechol, resorcinol and hydroquinone are the compounds of dihydroxy isomers in which two hydroxyl groups are substituted onto benzene ring. The nucleophilic attacks that lead to the formation of dihydroxybenzene derivatives with more or less positive oxidation potentials are followed by more E (electron transfer) steps and C (chemical reaction) steps depends on the structure of intermediates by EC reaction [8]. The following drug or drug making compounds for example sulfanilic acid, nicotinamide, diethylamine, metronidazole, diisopropylamine, pyridoxine etc. may be used as nucleophiles. Among

them diethylamine are also used as a precursor to two herbicides, dilate and triallate, as well as formation of certain organosulfur drugs [9]. Due to weak alkaline nature it may act a neutral nucleophile and presence of one lone pair electron on nitrogen enables it to take participation in 1,4-Michael addition reaction with o-benzoquinone. Sulfanilic acid and certain related substituted derivatives are of considerable medicinal importance. As the compound readily forms diazo compounds, it is used to make sulfa drugs and dyes [10].

The electrocatalytic effect of catechol in presence of L-Serine, L-Arginine and imidazol for three different electrodes (Au, GC and Pt) and various concentration of L-Serine, L-Arginine and imidazol at different scan rate are studied. However because of the importance of aminoquinones as biologically important compounds [11] in this direction that demands detail electrochemical studies of catechol in the presence of diethylamine and sulfanilic acid as representative of secondary aliphatic and aromatic amines. Although the peoples have used the above compounds enormously but the reaction mechanism of most of the compounds are still unknown.

The objective of the present study is thus a fundamental pursuit to have better insight of the possible redox interactions of catechol with Imidazole, L-Arginine and L-Serine compounds. These compounds undergo oxidation and/or reduction on the electrode surface within a certain potential range. The electroactivity of such compounds depends upon the pH of the medium, nature of the electrode and active moiety (electrophore) present in their structures. Their redox behavior can be influenced by the change in pH, substituents, concentration and scan rate. The variation in redox behavior can be abused for a number of useful purposes like elucidation of electrode reaction mechanism. Cyclic voltammetry (CV), differential pulse voltammetry (DPV), Chronoamperometry (CA) have used in the present work.

1.2.1 Catechol

A biologically important organic phenol, having two hydroxyl groups attached to the benzene ring called Catechol is also known as 1,2-dihydroxybenzene or pyrocatechol shown in Figure 1.1. It is the ortho isomer of the three isomeric benzenediols. This colorless compound occurs naturally in trace amounts. The Catechol skeleton occurs in a

variety of natural products such as urushiols, which are the skin-irritating poisons are found in plants [12]. It occurs as feathery white crystals which are very rapidly soluble in water.

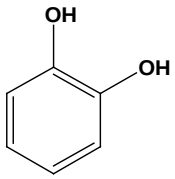

Figure 1.1: Structure of catechol

1.2.2 Natural occurrence of Catechol

Small amounts of catechol occur naturally in fruits and vegetables, tea, tobacco and in crude beet sugar coal and some traditional Chinese medicines. It is also found in the leaves and branches of oak and willow trees. Catechol moieties are also found widely within the natural world.

1.2.3 Use of Catechol

Catechol is used in a variety of applications. Catechol is an organic aromatic compound, appearing under the form of colorless solid flakes which darken upon exposure to air and light. Catechol is mainly used as an intermediate for the synthesis of pharmaceuticals, agrochemicals and in formulation. Catechol is a precursor to various flavorings such as vanillin or eugenol (synthetic “vanilla” aroma and flavor), used in food industry, perfumery, home and personal care products. The Catechol route of vanillin synthesis is far more environmentally friendly than the o-nitrochlorobenzene route. The production is performed using conventional closed vessels.

1.2.4 Imidazole

Imidazole is an organic compound with the formula $(CH)_2N(NH)CH$. It is a white or colourless solid that is soluble in water, producing a mildly alkaline solution. In chemistry, it is an aromatic heterocycle, classified as a diazole, and having non-adjacent nitrogen

atoms. Imidazole is a planar 5-membered ring. It exists in two equivalent tautomeric forms, because the positive charge can be located on either of the two nitrogen atoms. Imidazole is a highly polar compound, as evidenced by its electric dipole moment of 3.67D [13]. It is highly soluble in water. The compound is classified as aromatic due to the presence of a sextet of π-electrons, consisting of a pair of electrons from the protonated nitrogen atom and one from each of the remaining four atoms of the ring.

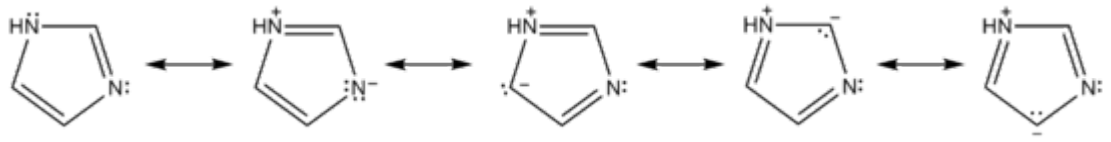

Figure 1.4: Resonance structures of imidazole

Many natural products, especially alkaloids, contain the imidazole ring. This ring system is present in important biological building-blocks, such as histidine and the related hormone histamine. Many drugs contain an imidazole ring, such as certain antifungal drugs, the nitro imidazole series of antibiotics, and the sedative midazolam [14-18].

1.2.5 Functions and uses of Imidazole

Imidazole is incorporated into many important biological molecules. The most pervasive is the amino acid histidine, which has an imidazole side-chain. Histidine is present in many proteins and enzymes and plays a vital part in the structure and binding functions of hemoglobin. Imidazole-based histidine compounds play a very important role in intracellular buffering [19]. Histidine can be decarboxylated to histamine, which is also a common biological compound.

Imidazole has become an important part of many pharmaceuticals. Synthetic imidazoles are present in many fungicides and antifungal, antiprotozoal, and antihypertensive medications. Imidazole is part of the theophylline molecule, found in tea leaves and coffee beans that stimulate the central nervous system. It is present in the anticancer medication mercaptopurine, which combats leukemia by interfering with DNA activities. A number of substituted imidazoles, including clotrimazole, are selective inhibitors of nitric oxide synthase, which makes them interesting drug targets in inflammation, neurodegenerative diseases and tumors of the nervous system [20, 21]. One of the applications of imidazole is

in the purification of His-tagged proteins in immobilised metal affinity chromatography (IMAC). Imidazole is used to elute tagged proteins bound to Ni ions attached to the surface of beads in the chromatography column. An excess of imidazole is passed through the column, which displaces the His-tag from nickel co-ordination, freeing the His-tagged proteins.

1.2.6 L-Arginine

Arginine (abbreviated as Arg or R) is an α-amino acid that is used in the biosynthesis of proteins [6]. It contains an α-amino group (which is in the protonated $-NH_3^+$ form under biological conditions), an α-carboxylic acid group (which is in the deprotonated $-COO^-$ form under biological conditions), and a side chain of a 3-carbon aliphatic straight chain capped by a complex guanidinium, classifying it as a charged (at physiological pH), aliphatic amino acid. Arginine is classified as a semiessential or conditionally essential amino acid, depending on the developmental stage and health status of the individual [22].

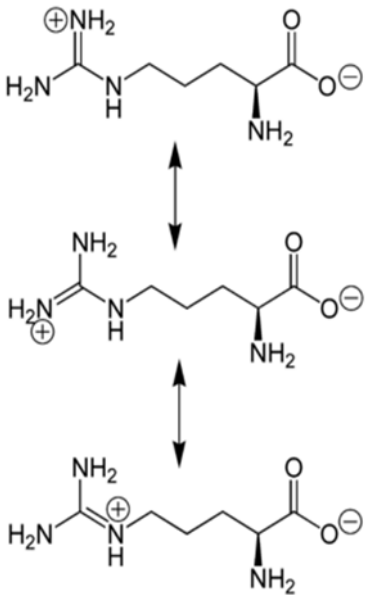

Figure 1.3: Delocalization of charge in guanidinium group of L-Arginine

1.2.7 Occurrence of L-Asparagine

Arginine is one such conditionally essential amino acid. Arginine was first isolated from a lupin seedling extract in 1886 by the German chemist Ernst Schultze [23]. The biosynthetic pathway, however, does not produce sufficient arginine, and some must still

be consumed through diet. Individuals with poor nutrition or certain physical conditions may be advised to increase their intake of foods containing arginine. Arginine is found in a wide variety of foods, including:

- Animal sources:

  dairy products (e.g., cottage cheese, ricotta, milk, yogurt, whey protein drinks), beef, pork (e.g., bacon, ham), gelatin, poultry (e.g. chicken and turkey light meat), wild game (e.g. pheasant, quail), seafood (e.g., halibut, lobster, salmon, shrimp, snails, tuna).

- Plant sources:

  wheat germ and flour, lupins, buckwheat, granola, oatmeal, peanuts, nuts (coconut, pecans, cashews, walnuts, almonds, Brazil nuts, hazelnuts, peanuts), seeds (hemp, pumpkin, sesame, sunflower), chickpeas, cooked soybeans etc.

1.2.8 Functions and uses of L-Arginine

Arginine plays an important role in cell division, the healing of wounds, removing ammonia from the body, immune function, and the release of hormones [24-26]. Other roles of arginine are precursor for the synthesis of nitric oxide (NO). Non-L-arginine derived NO can be generated by the nitrate-nitrite-nitric oxide pathway that is monitored through saliva testing. It reduces healing time of injuries (particularly bone). It also quickens repair time of damaged tissue [27, 28]. It helps to decrease blood pressure in clinical hypertensive subjects [29]. NO-mediated decrease in blood pressure is influenced by both the L-arginine-dependent nitric oxide synthase pathway and non-L-arginine or alternative pathway through nitrate-rich foods such as beets and spinach.

L-arginine is used for heart and blood vessel conditions including congestive heart failure (CHF), chest pain, high blood pressure, and coronary artery disease. L-arginine is also used for recurrent pain in the legs due to blocked arteries (intermittent claudication), decreased mental capacity in the elderly (senile dementia), erectile dysfunction (ED), and male infertility. Some people use L-arginine for preventing the common cold, improving kidney function after a kidney transplant, high blood pressure during pregnancy,

improving athletic performance, boosting the immune system, and preventing inflammation of the digestive tract in premature infants. L-arginine is used in combination with a number of over-the-counter and prescription medications for various conditions. For example, L-arginine is used along with ibuprofen for migraine headaches; with conventional chemotherapy drugs for treating breast cancer; with other amino acids for treating weight loss in people with AIDS; and with fish oil and other supplements for reducing infections, improving wound healing, and shortening recovery time after surgery. Some people apply L-arginine to the skin to speed wound healing and for increasing blood flow to cold hands and feet, especially in people with diabetes [30].

1.2.9 L-Serine

L-Serine (abbreviated as Ser or S) is an α-amino acid that is used in the biosynthesis of proteins. It contains an α-amino group (which is in the protonated $-NH_3^+$ form under biological conditions), a carboxyl group (which is in the deprotonated $–COO^-$ form in physiological conditions), and a side chain consisting of a hydroxymethyl group, classifying it as a polar amino acid [31]. It can be synthesized in the human body under normal physiological circumstances, making it a nonessential amino acid.

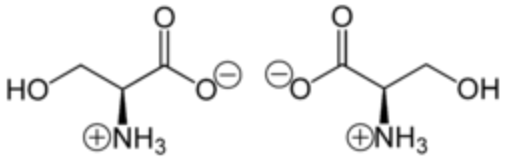

Figure 1.2: (*S*)-Serine (left) and (*R*)-serine (right) in zwitterionic form at neutral pH

1.2.10 Occurrence of L-Serine

This compound is one of the naturally occurring proteinogenic amino acids. Only the L-stereoisomer appears naturally in proteins. It is not essential to the human diet, since it is synthesized in the body from other metabolites, including glycine. Serine was first obtained from silk protein, a particularly rich source, in 1865. Its name is derived from the Latin for silk, *sericum*. Serine's structure was established in 1902 [32].

1.2.11 Uses of L-Serine

L-Serine is an amino acid widely used as nutrition supplements in food production, beverage, pharmaceutical, cosmetics, agriculture/animal feed, and various other industries. Serine is especially important to proper functioning of the brain and central nervous system. It helps form the phospholipids needed to make every cell in animal body. It is also involved in the function of RNA and DNA, fat and fatty acid metabolism, muscle formation, and the maintenance of a healthy immune system. It is needed to produce tryptophan, an amino acid that is used to make serotonin, a mood-determining brain chemical. Serine is important in metabolism in that it participates in the biosynthesis of purines and pyrimidines. It also plays an important role in the catalytic function of many enzymes. It has been shown to occur in the active sites of chymotrypsin, trypsin, and many other enzymes. The so-called nerve gases and many substances used in insecticides have been shown to act by combining with a residue of serine in the active site of acetylcholine esterase, inhibiting the enzyme completely. L-Serine also has the clinical and research for therapeutic uses [32-34].

1.3 Electrochemical properties of Catechol derivatives

The electrochemical study of catechols in the presence of some other nucleophiles such as methanol, 4-hydroxycoumarin, ethanol, 2-thiobarbituric acid, β-diketones, 4-hydroxy-6-methyl-2-pyrone, 2-thiouracil, dimedone, 4,7-dihydroxycoumarin, 4,5,7-trihydroxycoumarin, 4-hydroxy-6-bromocoumarin, 3-hydroxycoumarin, 4-hydroxy-6-methyl-a-pyrone, 4-hydroxy-6-methyl-2-pyridone, 4-hydroxycarbostyrile, sulfonic acid and 4-amino-3-thio-1,2,4-triazole were studied [35-49].

Aminoquinones are biologically important compounds in this direction, therefore, it demands detail electrochemical studies of catechol in the presence of amines. In this research work, we have studied the electrocatalytic effect of catechol in presence of Imidazole, L-Arginine and L-Serine for three different electrodes (Au, GC and Pt) and various concentration Imidazole (2-30 mM), L-Arginine (10-100mM) and L-Serine (10-130 mM)) and different pH (3-11)) at different scan rate. The primary aim of the present study is thus a fundamental realization to have better insight of the possible redox

interactions of 1,2-dihyroxybenzene with Imidazole, L-Arginine and L-Serine compounds. To the best of our knowledge, electrochemical study of catechol with Imidazole, L-Arginine and L-Serine at different conditions has not been reported before this work.

1.4 Objectives of the Thesis

Attempt will be made in the present research work is systematic study of electro-synthesis and mechanism of redox process of biologically important catechol compound and its amine derivatives which may be help to understand the role of the derivatives in the biological processes. Electrochemical study of nucleophilic substitution reactions of catechol in presence of Imidazole, L-Arginine and L-Serine were carried out in different pH media.

The objectives of this study are:

- ❖ to synthesize biologically important Catechol-Imidazole, Catechol-Arginine and Catechol-Arginine derivatives by electrochemically.
- ❖ to diagnose the mechanism of the redox processes of these compounds at different pH and different scan rate.
- ❖ to know the redox interaction of the species by Cyclic voltammetry (CV), Controlled potential coulometry (CPC), Differential pulse voltammetry (DPV) and Chronoamperometry (CA) techniques.
- ❖ to study the effect of pH, scan rate, concentration on the voltammogram.
- ❖ to recognize the most favorable condition (concentration, pH) for the reaction.
- ❖ to characterize the new features of the synthesized species by electrochemical and spectral analysis.

CHAPTER II

Theoretical Background

Electroanalytical chemistry encompasses a group of quantitative analytical methods that are based upon the electrical properties of an analyte solution when it is made part of an electrochemical cell. There are two general types of electrochemical methods. Electroanalytical methods are a class of techniques in analytical chemistry which study an analyte by measuring the potential (volts) and/or current (amperes) in an electrochemical cell containing the analyte. These methods can be broken down into several categories depending on which aspects of the cell are controlled and which are measured. The three main categories are potentiometry (the difference in electrode potentials is measured), coulometry (the cell's current is measured over time), and voltammetry (the cell's current is measured while actively altering the cell's potential). Voltammetry applies a constant and/or varying potential at an electrode's surface and measures the resulting current with a three electrode system. This method can reveal the reduction potential of an analyte and its electrochemical reactivity. This method in practical terms is nondestructive since only a very small amount of the analyte is consumed at the two-dimensional surface of the working and auxiliary electrodes. In practice the analyte solutions is usually disposed of since it is difficult to separate the analyte from the bulk electrolyte and the experiment requires a small amount of analyte. Electrodes are employed for electrochemical determination of organic molecules as well as metal ions. The electrode can act as a source (for reduction) or a sink (for oxidation) of electrons transferred to or from the species in solution:

$$O + ne \rightarrow R$$

Where, O and R are the oxidized and reduced species. In order for the electron transfer to occur, there must be a correspondence between the energies of the electron orbitals where transfer takes place in the donor and acceptor. In the electrode this level is the highest filled orbital, which in a metal is Fermi energy level. In the soluble species it is the orbital of the valence electron to be given or received. For reduction, there is a minimum energy that the transferable electrons from the electrode must have before the transfer can occur,

which corresponds to a sufficiently negative potential. For an oxidation, there is a maximum energy that the lowest unoccupied level in the electrode can have in order to receive electrons from the species in solution, corresponding to a sufficiently positive potential.

In order to study electrode reactions, reproducible experimental conditions must be created which enable minimization of all unwanted factors that can contribute to the measurements and diminish their accuracy. That means to suppress migration effects, confine the interfacial region as close as possible to the electrode, and minimize solution resistance. These objectives are achieved by the addition of large amount (around 1 mol dm^{-3}) of inert electrolyte, the electroactive species being at a concentration of 5 mM or less [28].

Since an electrode predominantly attracts positively and negatively charged species, which may or may not undergo reaction at the surface, it should be remembered that the species may adsorb at the electrode surface. This makes it clear that in the description of any electrode process we have to consider the transport of species to the electrode surface as well as the electrode reaction itself. This transport can occur by diffusion, convection or migration.

2.1 Mass transfer process in voltammetry

Mass transfer is the movement of material from one location to another in solution. In electrochemical systems, three modes of mass transport are generally considered which a substance may be carried to the electrode surface from bulk solution including diffusion, convection and migration. Any of these or more than one might be operating in a given experiment which is depended on the experimental conditions.

In general, there are three types of mass transfer processes:

- Migration
- Diffusion
- Convection

2.1.1 Migration

Migration is the movement of ions through a solution as a result of electrostatic attraction between the ions and the electrodes. It is the primary cause of mass transfer in the bulk of

the solution in a cell. This motion of charged particle through solution, induced by the charges on the electrodes is called migration [29]. This charge movement constitutes a current. This current is called migration current. The larger the number of different kinds of ions in a given solution, the smaller is the fraction of the total charge that is carried by a particular species. Electrolysis is carried out with a large excess of inert electrolyte in the solution so the current of electrons through the external circuit can be balanced by the passage of ions through the solution between the electrodes, and a minimal amount of the electroactive species will be transported by migration. Migration is the movement of charged species due to a potential gradient. In voltammetric experiments, migration is undesirable but can be eliminated by the addition of a large excess of supporting electrolytes in the electrolysis solution. The effect of migration is applied zero by a factor of fifty to hundred ions excess of an inert supporting electrolyte.

2.1.2 Diffusion

Diffusion refers to the process by which molecules intermingle as a result of their kinetic energy of random motion. Whereas a concentration difference between two regions of a solution, ions or molecules move from the more concentrated region to the dilute and leads to a disappearance of the concentration difference. The one kind of mode of mass transfer is diffusion to an electrode surface in an electrochemical cell. The rate of diffusion is directly proportional to the concentration difference. When the potential is applied, the cations are reduced at the electrode surface and the concentration is decreased at the surface film. Hence a concentration gradient is produced. Finally, the result is that the rates of diffusion current become larger.

2.1.3 Convection

By mechanical way reactants can also be transferred to or from an electrode. Thus forced convection is the movement of a substance through solution by stirring or agitation. This will tend to decrease the thickness of the diffuse layer at an electrode surface and thus decrease concentration polarization. Natural convection resulting from temperature or density differences also contributes to the transport of species to and from the electrode [30]. At the same time a type of current is produced. This current is called convection current. Removing the stirring and heating can eliminate this current. Convection is a far more efficient means of mass transport than diffusion.

2.2 Cyclic voltammetry (CV)

Cyclic voltammetry is a very versatile electrochemical technique which allows to probe the mechanics of redox and transport properties of a system in solution. This is accomplished with a three electrode arrangement whereby the potential relative to some reference electrode is scanned at a working electrode while the resulting current flowing through a counter (or auxiliary) electrode is monitored in a quiescent solution. The technique is ideally suited for a quick search of redox couples present in a system; once located, a couple may be characterized by more careful analysis of the cyclic voltammogram. More precisely, the controlling electronic is designed such that the potential between the reference and the working electrodes can be adjusted but the big impedance between these two components effectively forces any resulting current to flow through the auxiliary electrode. Usually the potential is scanned back and forth linearly with time between two extreme values – the switching potentials using triangular potential waveform (see Figure 2.1). When the potential of the working electrode is more positive than that of a redox couple present in the solution, the corresponding species may be oxidized (i.e. electrons going from the solution to the electrode) and produce an anodic current. Similarly, on the return scan, as the working electrode potential becomes more negative than the reduction potential of a redox couple, reduction (i.e. electrons flowing away from the electrode) may occur to cause a cathodic current. By IUPAC convention, anodic currents are positive and cathodic currents negative.

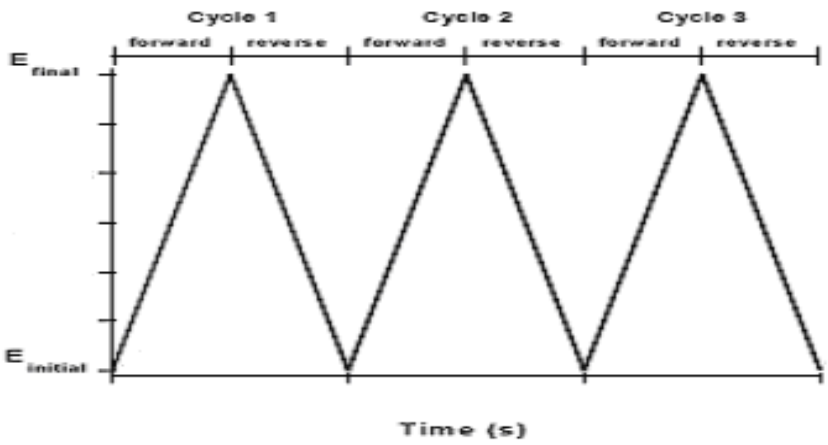

Figure 2.1: A cyclic voltammetry potential waveform with switching potentials

The magnitude of the observed faradaic current can provide information on the overall rate of the many processes occurring at the working electrode surface. As is the case for any

multi–step process, the overall rate is determined by the slowest step. For an redox reaction induced at a working electrode, the rate determining step may be any one of the following individual step depending on the system: rate of mass transport of the electro-active species, rate of adsorption or de-sorption at the electrode surface, rate of the electron transfer between the electro-active species and the electrode, or rates of the individual chemical reactions which are part of the overall reaction scheme.

For the oxidation reaction involving *n* electrons

$$\text{Red} \rightleftarrows \text{Ox} + ne^-$$

the *Nernst Equation* gives the relationship between the potential and the concentrations of the oxidized and reduced form of the redox couple at equilibrium (at 298 K):

$$E = E^{0'} + \frac{0.059}{n}\log_{10}\frac{[\text{Ox}]_s}{[\text{Red}]}$$

where E is the applied potential and $E^{0'}$ the formal potential; [OX] and [Red] represent surface concentrations at the electrode/solution interface, *not* bulk solution concentrations. Note that the Nernst equation may or may not be obeyed depending on the system or on the experimental conditions.

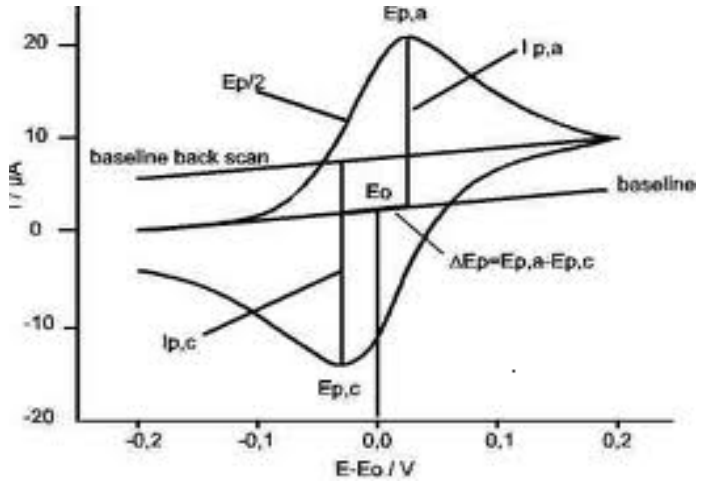

Figure 2.2: The expected response of a reversible redox couple during a single potential cycle

A typical voltammogram is shown in Figure 2.2. The scan shown starts at a slightly negative potential, *(A)* up to some positive switching value, *(D)* at which the scan is reversed back to the starting potential. The current is first observed to peak at E_{pa} (with value i_{pa}) indicating that an oxidation is taking place and then drops due to depletion of the reducing species from the diffusion layer. During the return scan the processes are

reversed (reduction is now occurring) and a peak current is observed at E_{pc} (corresponding value, i_{pc}).

Providing that the charge–transfer reaction is reversible, that there is no surface interaction between the electrode and the reagents, and that the redox products are stable (at least in the time frame of the experiment), the ratio of the reverse and the forward current i_{pr}/i_{pf} = 1.0 (in Figure 2.2 $i_{pa} = i_{pf}$ and $i_{pc} = i_{pr}$). In addition, for such a system it can be shown that:

- the corresponding peak potentials E_{pa} and E_{pc} are independent of scan rate and concentration
- the formal potential for a reversible couple $E^{0'}$ is centered between E_{pa} and E_{pc}: $E^{0'} = (E_{pa} + E_{pc})/2$
- the separation between peaks is given by $\Delta E_p = E_{pa} - E_{pc} = 59/n$ mV (for a n electron transfer reaction) at all scan rates (however, the measured value for a reversible process is generally higher due to uncompensated solution resistance and non-linear diffusion. Larger values of ΔE_p, which increase with increasing scan rate, are characteristic of slow electron transfer kinetics).

It is possible to relate the half-peak potential ($E_{p/2}$, where the current is half of the peak current) to the polarographic half-wave potential, $E_{1/2}$: $E_{p/2} = E_{1/2} \pm 29\text{mV}/n$ (The sign is positive for a reduction process.)

Simply stated, in the forward scan, the reaction is $O + e^- \rightarrow R$, R is electrochemically generated as indicated by the cathodic current. In the reverse scan, $R \rightarrow O + e^-$, R is oxidized back to O as indicated by the anodic current. The CV is capable of rapidly generating a new species during the forward scan and then probing its fate on the reverse scan. This is a very important aspect of the technique [31].

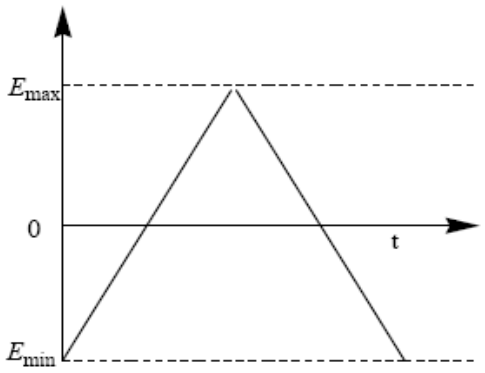

Figure 2.3: Variation of potential with time in cyclic voltammetry

A characteristic feature is the occurrence of peaks, identified by the peak potential $E_{p,}$ which corresponds to electron transfer reactions. The repetitive triangular potential excitation signal for CV causes the potential of the working electrode to sweep backward and forward between two designate values (the switching potentials).

In cyclic voltammetry of reversible system, the product of the initial oxidation or reduction is then reduced or oxidized, respectively, on reversing the scan direction.

Adsorbed species lead to changes in the shape of the cyclic voltammogram, since they do not have to diffuse from the electrode surface. In particular, if only adsorbed species are oxidized or reduced, in the case of fast kinetics the cyclic voltammogram is symmetrical, with coincident oxidation and reduction peak potentials [32].

Cyclic voltammetry is one of the most versatile techniques for the study of electroactive species, as it has a provision for mathematical analysis of an electron transfer process at the electrode [33-36]. It is an electroanalytical tool for monitoring and recognition of many electrochemical processes taking place at the surface of electrode and can be used to study redox processes in biochemistry and macromolecular chemistry [37].

2.2.1 Single electron transfer process

Based upon the values of electrochemical parameters, i.e., peak potential E_p, half peak potential ($E_{p/2}$), half wave potential ($E_{1/2}$), peak current (I_p), anodic peak potential E_{pa}, cathodic peak potential E_{pc} etc, it can be ascertained whether a reaction is reversible, irreversible or quasi-reversible. The electrochemical parameters can be graphically obtained from the voltammogram as shown in the Figure 2.3.
Three types of single electron transfer process can be studied.

a. Reversible process. b. Irreversible process and c. Quasi-reversible.

2.2.1(a) Reversible processes

The peak current for a reversible couple (at 25°C), is given by the Randles-Sevcik equation: $\boldsymbol{i}_p = (2.69 \times 10^5)\, n^{3/2} A C D^{1/2} v^{1/2}$

where n is the number of electrons, A the electrode area (in cm^2), C the concentration (in mol/cm^3), D the diffusion coefficient (in cm^2/s), and v the scan rate (in V/s). Accordingly, the current is directly proportional to concentration and increases with the square root of the scan rate. The ratio of the reverse-to-forward peak currents, $\boldsymbol{i}_{pr}/\boldsymbol{i}_{pf}$, is unity for a simple reversible couple. This peak ratio can be strongly affected by chemical reactions coupled to the redox process. The current peaks are commonly measured by extrapolating the preceding baseline current. The position of the peaks on the potential axis (E_p) is related to the formal potential of the redox process. The formal potential for a reversible couple is centered between E_{pa} and E_{pc}:

$$E° = (E_{pa} + E_{pc})/2$$

The separation between the peak potentials (for a reversible couple) is given by:

$$\Delta E_p = E_{pa} - E_{pc} = 59mV/n$$

Thus, the peak separation can be used to determine the number of electrons transferred, and as a criterion for a Nernstian behavior. Accordingly, a fast one-electron process exhibits a ΔE_p of about 59 mV. Both the cathodic and anodic peak potentials are independent of the scan rate. It is possible to relate the half-peak potential ($E_{p/2}$, where the current is half of the peak current) to the polarographic half-wave potential, $E_{1/2}$

$$E_{p/2} = E_{1/2} \pm 29mV/n$$

(The sign is positive for a reduction process.) For multi electron-transfer (reversible) processes, the cyclic voltammogram consists of several distinct peaks, if the E^o values for the individual steps are successively higher and are well separated. An example of such mechanism is the six-step reduction of the fullerenes C_{60} and C_{70} to yield the hexaanion products C_{60}^{6-} and C_{70}^{6-} where six successive reduction peaks can be observed.

The situation is very different when the redox reaction is slow or coupled with a chemical reaction. Indeed, it is these "nonideal" processes that are usually of greatest chemical interest and for which the diagnostic power of cyclic voltammetry is most useful. Such information is usually obtained by comparing the experimental voltammograms with those derived from theoretical (simulated) ones.

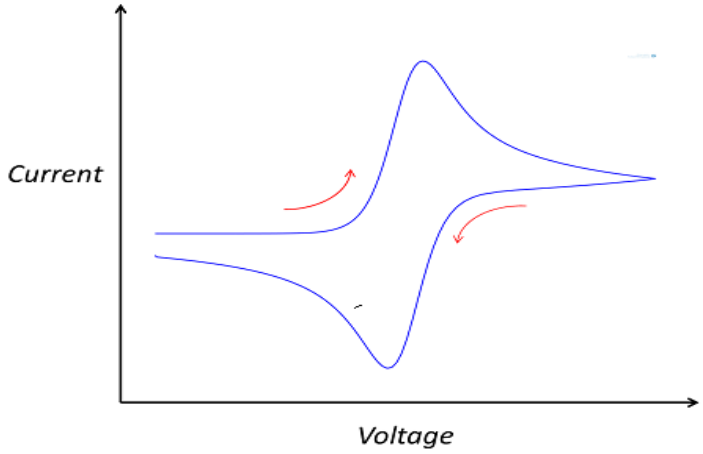

Figure 2.4: Reversible cyclic voltammogram of redox process

2.2.1(b) Irreversible processes

For irreversible processes (those with sluggish electron exchange), the individual peaks are reduced in size and widely separated. Totally irreversible systems are characterized by a shift of the peak potential with the scan rate:

$$E_p = E° - (RT/\alpha n_a F)[0.78 - \ln(k^o/(D)^{1/2}) + \ln (\alpha n_a F\nu/RT)^{1/2}]$$

where α is the transfer coefficient and n_a is the number of electrons involved in the charge-transfer step. Thus, E_p occurs at potentials higher than E°, with the overpotential related to k° and a. Independent of the value k°, such peak displacement can be compensated by an appropriate change of the scan rate. The peak potential and the half-peak potential (at 25°C) will differ by $48/\alpha n$ mV. Hence, the voltammogram becomes more drawn-out as $\alpha\mathbf{n}$ decreases.

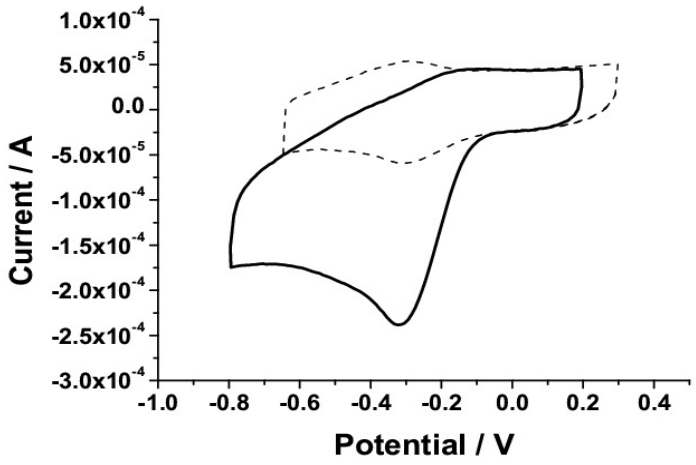

Figure 2.5: Cyclic voltammogram of irreversible redox process

2.2.1(c) Quasi-reversible process

Quasi-reversible process is termed as a process, which shows intermediate behavior between reversible and irreversible processes. In such a process the current is controlled by both the charge transfer and mass transfer.

Cyclic voltammogram for quasi-reversible process is shown in Figure 2.6 [38].

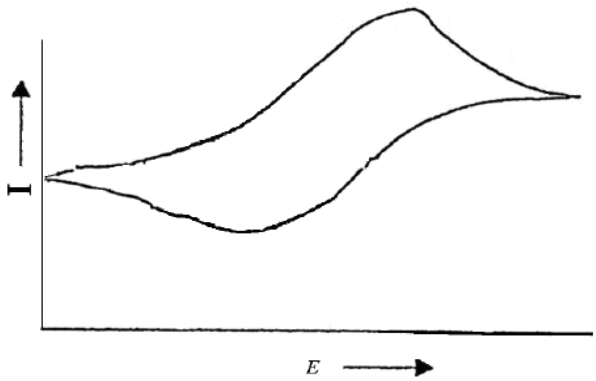

Figure 2.6: Cyclic voltammogram of quasi-reversible redox process

For quasi-reversible process the value of standard heterogeneous electron transfer rate constant, k_{sh}^{o} lies in the range of 10^{-1} to 10^{-5} cm sec^{-1} [39]. An expression relating the current to potential dependent charge transfer rate was first provided by Matsuda and Ayabe [40].

$$I(t) = C_{o(0,t)} k_{sh}^{o} Exp\left[-\frac{\alpha nF}{RT}\left\{E(t) - E^{o}\right\}\right] - C_{R(0,t)} k_{sh}^{o} Exp\left[-\frac{\beta nF}{RT}\left\{E(t) - E^{o}\right\}\right] \ldots.2.1$$

where k_{sh}^{o} is the heterogeneous electron transfer rate constant at standard potential E^{0} of redox system. α is the transfer coefficient and β = 1- α. In this case, the shape of the peak and the various peak parameters are functions of α and the dimensionless parameter, Λ, defined as [41]

$$\Lambda = \frac{k_{s,h}}{D^{1/2}(nF/RT)^{1/2}\upsilon^{1/2}} \quad \text{.....2.2}$$

when $D_o = D_R = D$

D_o and D_R are the diffusion coefficients of oxidized and reduced species respectively.

For quasi-reversible process current value is expressed as a function of ψ(*E)* [41].

$$I = nFAC_o^{*}\frac{k_{sh}^{o}}{\Lambda}\psi(E) \quad \text{.....2.3}$$

where $\psi(E)$ is expressed as

$$\psi(E) = \frac{I}{nFAC_o^{*}D_o^{1/2}(nF/RT)^{1/2}\upsilon^{1/2}} \quad \text{.....2.4}$$

It is observed that when $\Lambda \geq 10$, the behavior approaches that of a reversible system [42].

For three types of electrode processes, Matsuda and Ayabe [40] suggested following zone boundaries.

- Reversible (Nernstian)

  $k_{sh}^{o} \geq 0.3\upsilon^{1/2}$ cm s^{-1}
- Quasi-reversible

  $0.3\upsilon^{1/2} \geq k_{sh}^{o} \geq 2\times10^{-5}\upsilon^{1/2}$ cm s^{-1}
- Totally irreversible

  $k_{sh}^{o} \leq 2\times10^{-5}\upsilon^{1/2}$ cm s^{-1}

2.2.2 Multi electron transfer processes

Multi-electron transfer process usually takes place in different steps. A two-step mechanism each characterized by its own electrochemical parameters is called an "EE mechanism".

A two step reversible "EE mechanism" is represented as;

$$O + n_1 e \leftrightarrow R_1 \qquad (E_1^o) \ldots\ldots\ldots\ldots\ldots\ldots 2.5$$

$$R + n_1 e \leftrightarrow R_2 \qquad (E_2^o) \ldots\ldots\ldots\ldots\ldots\ldots 2.6$$

Each heterogeneous electron transfer step is associated with its own electrochemical parameters i.e., k_{sh}^o and α_i, where i = 1, 2 for the 1st and 2nd electron transfer respectively. The value of k_{sh}^o for first reversible electron transfer limiting case can be calculated as [43]:

$$k_{sh} = k_{sh}^o \exp\left[-\alpha 1 F \Delta E^o / 2RT\right] \ldots\ldots\ldots\ldots\ldots\ldots 2.7$$

where

$$\Delta E^o = E_2^o - E_1^o$$

For ΔE^0 greater than 180 mV, shape of wave does not dependent on the relative values of E^0, otherwise shapes of peak and peak currents depend upon ΔE^0 [44]. Based on the value of ΔE^0, we come across different types of cases as shown in the Figure 2.6.

Types of two electron transfer reactions

***Case 1*:** $\Delta E^0 \geq 150$ mV peaks separation

When $\Delta E^0 \geq 150$ mV the EE mechanism is termed as "disproportionate mechanism [45]. Cyclic voltammogram consists of two typical one-electron reduction waves. The heterogeneous electron transfer reaction may simultaneously be accompanied by homogenous electron transfer reaction, which in multi-electron system leads to disproportionation which can be described as:

$$R_1 \rightarrow O + n_1 e \ldots\ldots\ldots\ldots\ldots\ldots\ldots\ldots\ldots\ldots\ldots\ldots 2.8a$$

$$R_1 + n_2 e \rightarrow R_2 \ldots\ldots\ldots\ldots\ldots\ldots\ldots\ldots\ldots\ldots\ldots\ldots 2.8b$$

$$2R_1 \leftrightarrow O + R_2 \ldots\ldots\ldots\ldots\ldots\ldots\ldots\ldots\ldots\ldots\ldots\ldots 2.8c$$

$$k_{disp} = \frac{[O][R_2]}{[R_1]^2} \ldots\ldots\ldots\ldots\ldots\ldots\ldots\ldots\ldots\ldots\ldots\ldots 2.9$$

$$\ln k_{disp} = \left[\frac{nF}{RT}\right](E_2^o - E_1^o) \ldots\ldots\ldots\ldots\ldots\ldots\ldots\ldots 2.10$$

***Case 2*:** $\Delta E^0 < 100$ mV ----- Peaks overlapped

In this case, the individual waves merge into one broad distorted wave whose peak height and shape are no longer characteristics of a reversible wave. The wave is broadened

similar to an irreversible wave, but can be distinguished from the irreversible voltammogram, in that the distorted wave does not shift on the potential axis as a function of the scan rate.

***Case 3*:** ΔE^0 = 0 mV ----- Single peak

In this case, in cyclic voltammogram, only a single wave would appear with peak current intermediate between those of a single step one electron and two electron transfer reactions and E_p-$E_p/2$ = 56 mV.

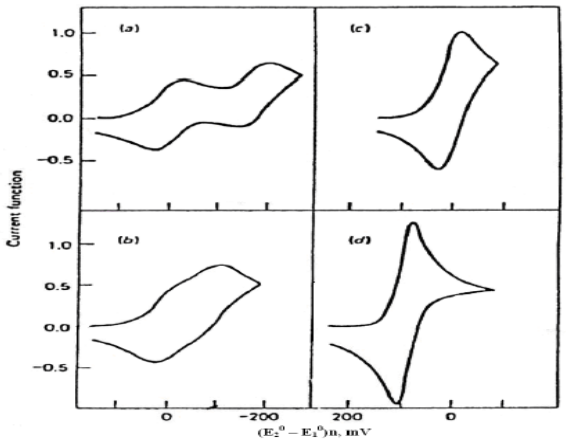

Figure 2.7 Cyclic voltammograms for a reversible two-step system (a) ΔE^0= - 180 mV, (b) ΔE^0 = -90 mV, (c) ΔE^0 = 0 mV, (d) ΔE^0 = 180 mV. (Taken from ref. [46])

Contrary to the convention the direction of the current in these voltammograms has been shown cathodic above the base line and anodic below the base line.

Case 4: $E^0_1 < E^0_2$ ----2nd Reduction is easy than 1st one

If the energy required for the second electron transfer is less than that for the first, one wave is observed, having peak height equal to $2^{3/2}$ times that of a single electron transfer process. In this case, E_p-$E_p/2$ = 29 mV. The effective E^0 for the composite two electron wave is given by $\frac{(E_1^o + E_2^o)}{2}$ as reported in literature [46].

2.3 Pulse techniques

The basis of all pulse techniques is the difference in the rate of decay of the charging and the faradaic currents following a potential step (or pulse). The charging current decays considerably faster than the faradaic current. A step in the applied potential or current

represents an instantaneous alteration of the electrochemical system. Analysis of the evolution of the system after perturbation permits deductions about electrode reactions and their rates to be made. The potential step is the base of pulse voltammetry. After applying a pulse of potential, the capacitive current dies away faster than the faradic one and the current is measured at the end of the pulse. This type of sampling has the advantage of increased sensitivity and better characteristics for analytical applications. At solid electrodes there is an additional advantage of discrimination against blocking of the electrode reaction by adsorption [32].

2.3.1 Differential pulse voltammetry (DPV)

The potential wave form for differential pulse voltammetry (DPV) is shown in Figure 2.8. The potential wave form consists of small pulses (of constant amplitude) superimposed upon a staircase wave form. Unlike Normal pulse voltammetry (NPV**)**, the current is sampled twice in each Pulse Period (once before the pulse, and at the end of the pulse), and the difference between these two current values is recorded and displayed.

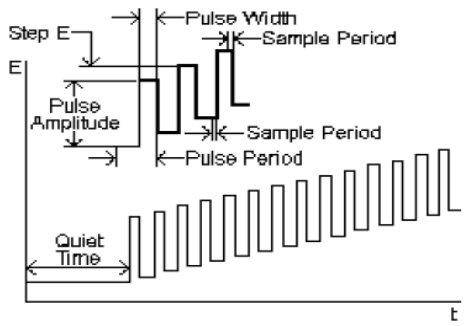

Figure 2.8: Scheme of application of potential

The important parameters for pulse techniques are as follows:

- Pulse amplitude is the height of the potential pulse. This may or may not be constant depending upon the technique.
- Pulse width is the duration of the potential pulse.
- Sample period is the time at the end of the pulse during which the current is measured.

- For some pulse techniques, the pulse period or drop time must also be specified. This parameter defines the time required for one potential cycle, and is particularly significant for polarography (i.e., pulse experiments using a mercury drop electrode), where this time corresponds to the lifetime of each drop (i.e., a new drop is dispensed at the start of the drop time, and is knocked off once the current has been measured at the end of the drop time - note that the end of the drop time coincides with the end of the pulse width).

Quantitative treatments for reversible systems demonstrated that, with only *R* (positive sign) or only *O* (negative sign) initially present, the following equation can be written as

$$E_{max} = E_{1/2} \pm \frac{\Delta E}{2} \quad \text{.....2.11}$$

where ΔE is the pulse amplitude.

2.4 Chronoamperometry (CA)

As with all pulsed techniques, chronoamperometry (**CA**) is one of the simplest potential wave forms. The potential is changed instantaneously from the Initial Potential to the First Step Potential, and it is held at this value for the First Step Time. This is a single potential step experiment. In **CA**, the current is monitored as a function of time. The Faradaic current--which is due to electron transfer events and is most often the current component of interest--decays as described in the Cottrell equation. Since the current is integrated over relatively longer time intervals, CA gives a better signal to noise ratio in comparison to other amperometric technique. A chronoamperometric curve at a disk microelectrode varies from the Cottrell behavior to the steady state current. When potential is stepped to a diffusion-controlled potential domain at the disk electrode with radius, *a*, in the solution including electroactive species with the concentration, c^*, and the diffusion coefficient, *D*, the responding current, *I*, at the electrolysis time, *t*, has been expressed as [47, 48]

$$I = 4nFc^*Da\left(1 + 0.71835\tau^{-1/2} + 0.05626\tau^{-3/2} - 0.00646\tau^{-5/2}\right) \text{..... 2.12}$$

$$I = 4nFc^*Da\left[\left(\pi/4\tau\right)^{1/2} + \pi/4 + 0.094\tau^{1/2}\right] \text{.....2.13}$$

where $\tau = 4Dt/a^2$. Equations 2.12 and 2.13 are valid for $\tau > 1.44$ and $\tau < 0.82$, respectively. Some expressions for the chronoamperometric curves obtained by finite difference or the related methods [49-54] are closed to Equation (2.12) and (2.13). When τ is small enough to neglect the third term in Equation (2.13), the potential-depending current for the reversible case is expressed by

$$I = \left(\pi^{1/2} nFD^{1/2} a^2 t^{-1/2} + \pi nFDa\right) c^* (1 + e^{-\varsigma})^{-1} \text{…….2.14}$$

where $\varsigma = (F/RT)(E - E^{0'})$

The Cottrell plot (I vs. $t^{-1/2}$) gives the slope and the intercept, respectively

$$s = \pi^{1/2} nFD^{1/2} a^2 c^* (1 + e^{-\varsigma})^{-1}$$

$$p = \pi nFDa\, c^* (1 + e^{-\varsigma})^{-1}$$

The ratio of the square of the slope to the intercept is

$$s^2 / p = nFa^3\, c^* (1 + e^{-\varsigma})^{-1} \text{ or } n\left(1 + e^{-\varsigma}\right)^{-1} = s^2 / pFa^3\, c^* \text{ …2.15}$$

This equation does not include D, and hence is the basic equation of evaluating n without knowing D from the chronoamperometric curves.

CHAPTER III

Experimental

The redox behavior of Catechol with Imidazole, L-Arginine and L-Serine in buffer solution at different pH has been measured using Cyclic voltammetry (CV) and Differential pulse voltammetry (DPV) at Glassy carbon (GC), Gold (Au) and Platinum (Pt) electrode. Details of the instrumentation are given in the following sections. The source of different chemicals, the instruments and brief description of the methods are given below.

3.1 Chemicals

All chemicals and solvents used in the electrochemical synthesis and analytical work were of analytical grade. The used chemicals were-

Sl. No.	Chemicals	Molecular formula	Molar mass	Reported purity	Producer
1.	Catechol	$C_6H_4(OH)_2$	110.11	99%	Fisher Scientific UK Ltd.
2.	Imidazole	$C_3H_4N_2$	68.077	99%	E-Merck, Germany
3.	L-Arginine	$C_6H_{14}N_4O_2$	174.20	99%	Merck Specialities Pvt. Ltd., India
4.	L-Serine	$C_3H_7NO_3$	105.09	99%	E-Merck, Germany
5.	Glacial Acetic Acid	CH_3COOH	60.05	99.5%	Loba Chemie Pvt. Ltd., India
6.	Sodium Acetate	$CH_3COONa.3H_2O$	136.08	99%	Merck Specialities Pvt. Ltd., India
7.	Potassium Chloride	KCl	74.6	99.5%	E-Merck, Germany
8.	Sodium Di-hydrogen Orthophosphate	$NaH_2PO_4.2H_2O$	156.01	98-100%	Loba Chemie Pvt. Ltd., India

Sl. No.	Chemicals	Molecular formula	Molar mass	Reported purity	Producer
9.	Di-sodium Hydrogen Orthophosphate	$Na_2HPO_4.2H_2O$	177.99	97-100%	Thermo Fisher Scientific India Pvt. Ltd.
10.	Sodium Hydroxide	NaOH	40.0	97%	E-Merck, Germany
11.	Sodium Bicarbonate	$NaHCO_3$	84.0	99%	E-Merck, Germany

3.2 Equipments

During this research work the following instruments were used-

- The electrochemical studies (CV, DPV) were performed with a computer controlled potentiostats/ galvanostats (μstat 400, Drop Sens, Spain)
- A Pyrex glass micro cell with teflon cap
- Glassy carbon (GC)/ Gold (Au)/ Platinum (Pt)as working electrode (BASi, USA)
- Three carbon rods (Local market Dhaka, Bangladesh)
- Ag/ AgCl as reference electrode (BASi, USA)
- Liquid micro size (0.05um) polishing alumina (BAS Inc. Japan)
- Pt wire as counter electrode (Local market, Dhaka, Bangladesh)
- A HR 200 electronic balance with an accuracy of ± 0.0001g was used for weighting and
- A pH meter (pH Meter, Hanna Instruments, Italy) was employed for maintaining the pH of the solutions.

3.3 Cyclic voltammetry (CV)

In several well established electrochemical techniques for the study of electrochemical reactions, we have chosen the CV technique to study and analyze the redox reactions occurring at the polarizable electrode surface. This technique helps us to understand the mechanism of electron transfer reaction of the compounds as well as the nature of adsorption of reactants or products on the electrode surface. CV is often the first experiment performed in an electrochemical study. CV consists of imposing an excitation potential nature on an electrode immersed in an unstirred solution and measuring the

current and its potential ranges varies from a few millivolts to hundreds of millivolts per second in a cycle. This variation of anodic and cathodic current with imposed potential is termed as voltammogram [30].

The technique involves under the diffusion controlled mass transfer condition at a stationary electrode utilizing symmetrical triangular scan rate ranging from 1 mVs^{-1} to hundreds millivolts per second.

In CV the current function can be measured as a function of scan rate. The potential of the working electrode is controlled vs a reference electrode such as Ag/AgCl electrode. The electrode potential is ramped linearly to a more negative potential and then ramped is reversed back to the starting voltage. The forward scan produces a current peak for any analyte that can be reduced through the range of potential scan. The current will increase as the current reaches to the reduction potential of the analyte [55].

The current at the working electrode is monitored as a triangular excitation potential is applied to the electrode. The resulting voltammogram can be analyzed for fundamental information regarding the redox reaction. The potential at the working electrode is controlled vs a reference electrode, Ag/AgCl(standard NaCl) electrode. The excitation signal varies linearly with time. First scan positively and then the potential is scanned in reverse, causing a negative scan back to the original potential to complete the cycle. Signal on multiple cycles can be used on the scan surface. A cyclic voltammogram is plot of response current at working electrode to the applied excitation potential.

3.4 Important features of CV

An electrochemical system containing species ‘O’ capable of being reversibly reduced to ‘R’ at the electrode is given by,

$$O + ne^- = R \quad \text{……3.1}$$

Nernst equation for the system is

$$E = E^0 + \frac{0.059}{n}\log\frac{C_0^s}{C_R^s} \quad \text{……..3.2}$$

Where,

E = Potential applied to the electrode

E^0 = Standard reduction potential of the couple versus reference electrode

n = Number of electrons in Equation (3.1)

C_0^s = Surface concentration of species 'O'

C_R^s = Surface concentration of species 'R'

A redox couple that changes electrons rapidly with the working electrode is termed as electrochemically reverse couple. The relation gives the peak current i_{pc}

$$i_{pc} = 0.4463\ nFA\ (D\alpha)^{1/2}C \text{.....3.3}$$

$$\alpha = \left(\frac{nFv}{RT}\right) = \left(\frac{nv}{0.026}\right)$$

Where,

i_{pc} = peak current in amperes

F= Faraday`s constant (approximately 96500)

A = Area of the working electrode in cm^2

v= Scan rate in volt/ sec

C= Concentration of the bulk species in mol/L

D= Diffusion coefficient in cm^2 /sec

In terms of adjustable parameters, the peak current is given by the Randless- Sevcik equation,

$$i_{pc}=2.69\times10^5\times n^{3/2}AD^{1/2}Cv^{1/2} \text{ .....3.4}$$

The peak potential E_p for reversible process is related to the half wave potential $E_{1/2}$, by the expression,

$$E_{pc} = E_{1/2} - 1.11\left(\frac{RT}{nF}\right), \quad \text{at } 25^0\text{C .....3.5}$$

$$E_{pc} = E_{1/2} - \left(\frac{0.0285RT}{n}\right) \text{.....} \qquad 3.6$$

The relation relates the half wave potential to the standard electrode potential

$$E_{1/2} = E^0 - \frac{RT}{nF}\ln\frac{f_{red}}{f_{ox}}\left(\frac{D_{ox}}{D_{ox}}\right)^{1/2}$$

$$E_{1/2} = E^0 - \frac{RT}{nF}\ln\left(\frac{D_{ox}}{D_{red}}\right)^{1/2} \text{.....3.7}$$

Assuming that the activity coefficient f_{ox} and f_{red} are equal for the oxidized and reduced species involved in the electrochemical reaction.

From Equation (3.6), we have,

$$E_{pa} - E_{pc} = 2.22\left(\frac{RT}{nF}\right) \quad \text{at } 25^0\text{C}\ldots\ldots\ldots\ldots\ldots\ldots\ 3.8$$

$$\text{or } E_{pa} - E_{pc} = \left(\frac{0.059}{n}\right) \quad \text{at } 25^0\text{C}\ldots\ldots\ldots\ldots\ldots\ldots 3.9$$

This is a good criterion for the reversibility of electrode process. The value of i_{pa} should be close for a simple reversible couple,

$$i_{pa}/i_{pc} = 1\ldots\ldots\ldots\ldots\ldots\ldots\ldots\ldots \quad 3.10$$

And such a system $E_{1/2}$ can be given by,

$$E_{1/2} = \frac{E_{pa} + E_{pc}}{2} \ldots\ldots\ldots\ldots\ldots\ldots 3.11$$

For irreversible processes (those with sluggish electron exchange), the individual peaks are reduced in size and widely separated, Totally irreversible systems are characterized by a shift of the peak potential with the scan rate [56];

$$E_p=E^0-(RT/\alpha n_aF)[0.78-\ln(k^0/(D)^{1/2})+\ln(\alpha n_aF\alpha/RT)^{1/2}]\ldots\ldots..3.12$$

Where α is the transfer coefficient and n_a is the number of electrons involved in the charge transfer step. Thus E_p occurs at potentials higher than E^0, with the over potential related to k^0 (standard rate constant) and α. Independent of the value k^0, such peak displacement can be compensated by an appropriate change of the scan rate. The peak potential and the half-peak potential (at 25^0 C) will differ by 48/ αn mV. Hence, the voltammogram becomes more drawn-out as αn decreases.

The peak current, given by

$$i_p=(2.99\times10^5)n(\alpha n_a)^{1/2}ACD^{1/2}v^{1/2}\ldots\ldots\ldots... \quad 3.13$$

is still proportional to the bulk concentration , but will be lower in height (depending upon the value of α) . Assuming α = 0.5, the ratio of the reversible –to– irreversible current peaks is 1.27 (i.e. the peak current for the irreversible process is about 80% of the peak for a reversible one). For quasi- reversible systems (with $10^{-1}>k^0>10^{-5}$ cm/s) the current is controlled by both the charge transfer and mass transport [57]. The shape of the cyclic voltammogram is a function of the ratio k^0 $(\pi vnFD/RT)^{1/2}$. As the ratio increases, the process approaches the reversible case. For small values of it, the system exhibits an irreversible behavior. Overall, the voltammograms of a quasi-reversible system are more drawn out and exhibit a larger separation in peak potential compared to a reversible system.

Unlike the reversible process in which the current is purely mass transport controlled, currents due to quasi-reversible process are controlled by a mixture of mass transport and charge transfer kinetics [57, 58]. The process occurs when the relative rate of electron transfer with respect to that of mass transport is insufficient to maintain Nernst equilibrium at the electrode surface.

3.5 Differential pulse voltammetry (DPV)

Differential pulse voltammetry (DPV) is a technique that is designed to minimize background charging currents. The waveform in DPV is a sequence of pulses, where a baseline potential is held for a specified period of time prior to the application of a potential pulse. Current is sampled just prior to the application of the potential pulse. The potential is then stepped by a small amount (typically < 100 mV) and current is sampled again at the end of the pulse. The potential of the working electrode is then stepped back by a lesser value than during the forward pulse such that baseline potential of each pulse is incremented throughout the sequence.

By contrast, in normal pulse voltammetry the current resulting from a series of ever larger potential pulse is compared with the current at a constant 'baseline' voltage. Another type of pulse voltammetry is square wave voltammetry, which can be considered a special type of differential pulse voltammetry in which equal time is spent at the potential of the ramped baseline and potential of the superimposed pulse. The potential wave form consists of small pulses (of constant amplitude) superimposed upon a staircase wave form [59]. Unlike NPV, the current is sampled twice in each pulse Period (once before the pulse, and at the end of the pulse), and the difference between these two current values is recorded and displayed.

3.6 Important features of DPV

Differential pulse voltammetry has these prominence:

i) Current is sampled just prior to the application of the potential pulse.

ii) Reversible reactions show symmetrical peaks and irreversible reaction show asymmetrical peaks.

iii) The peak potential is equal to $E_{1/2}^{r}$-ΔE in reversible reactions, and the peak current is proportional to the concentration.

3.7 Chronoamperometry (CA)

Chronoamperometry is an electrochemical technique in which the potential of the working electrode is stepped and the resulting current from faradaic processes occurring at the electrode is monitored as a function of time. This technique has advantage of without knowing a value of a diffusion coefficient [60]. When potential is stepped from a non-reacting domain to *E*, a Cottrell plot (*I* vs. $t^{-1/2}$) shows the slope by the linear diffusion.

$$s = \pi^{1/2} nFD^{1/2} a^2 c^*$$

together with the intercept for the edge effect

$$p = \pi nFDac^*$$

where *a* is the radius of the electrode, *c** is the concentration of the electroactive species, *D* is the diffusion coefficient. The ratio of the square of the slope, *s*, to the intercept, *p*, is

$$n = s^2 / pFa^3 c^* \quad \text{.....3.14}$$

Since this equation does not include *D*, values of *n* can be determined from *s* and *p* without knowing *D* values.

3.8 Computer controlled potentiostats (for CV, DPV and CA experiment)

The main instrument for voltammetry is the Potentiostats/ Galvanostats (µStat 400, DropSens, Spain), which will be applied to the desired potential to the electrochemical cell (i.e. between a working electrode and a reference electrode), and a current-to-voltage converter, which measures the resulting current, and the data acquisition system produces the resulting voltammogram.

3.9 Electrochemical cell

This research work was performed by a three electrode electrochemical cell. The voltammetric cell also contains a Teflon cap. The electrochemical reaction of interest takes place at the working electrode and the electrical current at this electrode due to electron

transfer is termed as faradic current. The counter electrode is driven by the potentiostatic circuit to balance the faradic process at the working electrode with an electron transfer of opposite direction.

3.10 Electrodes

Three types of electrodes are used in this research:

i) Working electrodes are Glassy carbon (GC) electrode with 3.0 mm diameter disc, Gold (Au)&Platinum (Pt) electrode with 1.6 mm diameter disc and three carbon rods (diameter 6.0 mm)

ii) Ag/ AgCl (standard NaCl) electrode used as reference electrode from BASi, USA

iii) Counter electrode is a Pt wire

The working electrode is an electrode on which the reaction of interest is occurring. The reference electrode is a half-cell having a known electrode potential and it keeps the potential between itself and the working electrode. The counter electrode is employed to allow for accurate measurements to be made between the working and reference electrodes.

3.11 Preparation of electrodes

In this study, Glassy carbon (GC), Gold (Au) and Platinum (Pt) electrodes purchase from the BASi, USA are used as working electrode. Electrode preparation includes polishing and conditioning of the electrode. The electrode was polished with 0.05μm alumina powder on a wet polishing cloth. For doing so a part of the cloth was made wet with deionized water and alumina powder was sprinkled over it. Then the electrode was polished by softly pressing the electrode against the polishing surface at least 10 minutes. The electrode surface would look like a shiny mirror after thoroughly washed with deionized water.

3.12 Removing dissolved Oxygen from solution

Dissolved oxygen can interfere with observed current response so it is needed to remove it. Experimental solution was indolented by purging for at least 5-10 minutes with 99.99% pure and dry nitrogen gas (BOC, Bangladesh). By this way, traces of dissolved oxygen were removed from the solution.

3.13 Electrode polishing

Materials may be adsorbed to the surface of a working electrode after each experiment. Then the current response will degrade and the electrode surface needs to clean. In this case, the cleaning required is light polishing with 0.05µm alumina powder. A few drops of polish are placed on a polishing pad and the electrode is held vertically and the polish rubbed on in a figure-eight pattern for a period of 30 seconds to a few minutes depending upon the condition of the electrode surface. After polishing the electrode surface is rinsed thoroughly with deionized water.

3.14 Experimental procedure

The electrochemical cell filled with solution 50mL of the experimental solution and the Teflon cap was placed on the cell. The working electrode together with reference electrode and counter electrode was inserted through the holes. The electrodes were sufficiently immersed. The solution system is deoxygenated by purging the nitrogen gas for about 10 minutes. The solution has been kept quiet for 10 seconds. After determinating the potential window the voltammogram is taken at various scan rates, pH and concentrations from the Drop View Software.

3.15 Preparation of buffer solutions

Acetate Buffer Solution: To prepare acetate buffer (pH 3.0-5.0) solution definite amount of sodium acetate was dissolved in 0.1M acetic acid in a volumetric flask and the pH was measured. The pH of the buffer solution was adjusted by further addition of acetic acid and / or sodium acetate.

Phosphate Buffer Solution: Phosphate buffer solution (pH 6.0-8.0) was prepared by mixing a solution of 0.1M sodium dihydrogen ortho-phosphate ($NaH_2PO_4.2H_2O$) with a solution of 0.1M disodium hydrogen ortho-phosphate ($Na_2HPO_4.2H_2O$). The pH of the prepared solution was measured with pH meter.

Hydroxide Buffer Solution: To prepare hydroxide buffer (pH 9.0-11.0) solution definite amount of sodium hydroxide was dissolved in 0.1M sodium bicarbonate in a volumetric flask. The pH of the prepared solution was measured with pH meter.

Figure 3.1: Experimental setup (Software controlled Potentiostats (μstat 400))

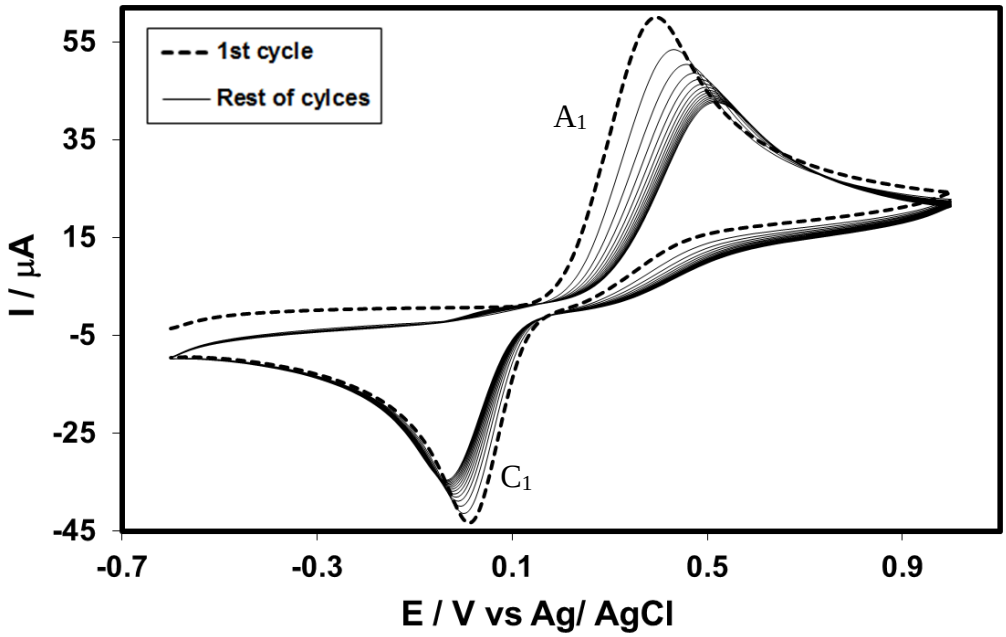

Fig. 4.1: Cyclic voltammogram (CV) of 15 cycles of 2mM catechol of GC electrode in buffer solution (pH 7) at scan rate 0.1V/s.

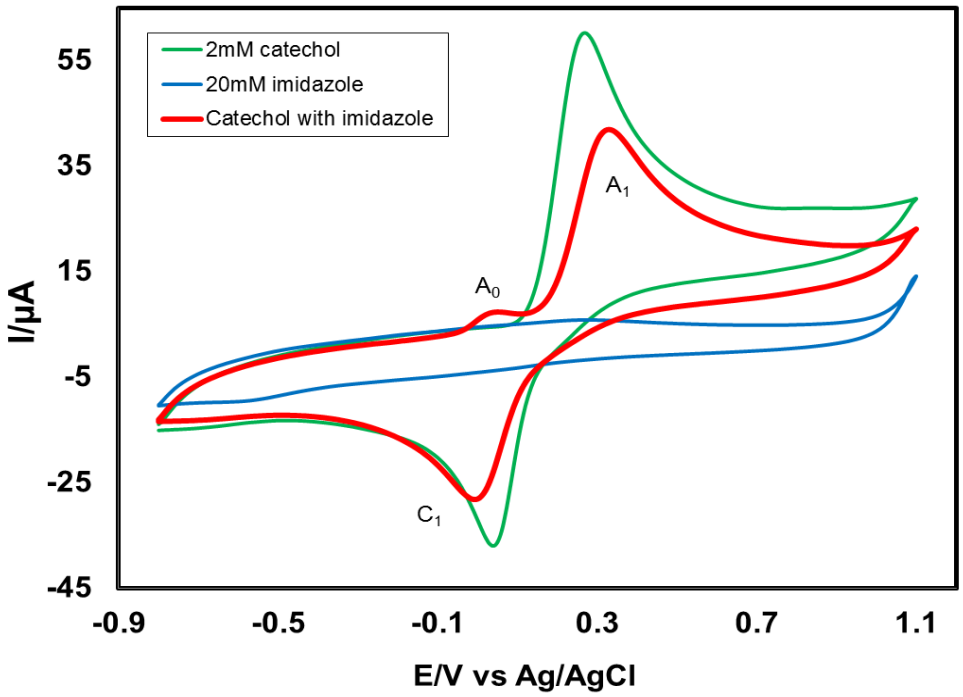

Fig. 4.2: Cyclic voltammogram of 2 mM Catechol, 20mM Imidazole and 2 mM Catechol with 20mM Imidazole of GC electrode in buffer solution (pH 7) at scan rate 0.1 V/s (2nd cycle). A_0 and A_1 is appeared anodic peak and anodic peak, and C_1 is corresponding cathodic peak.

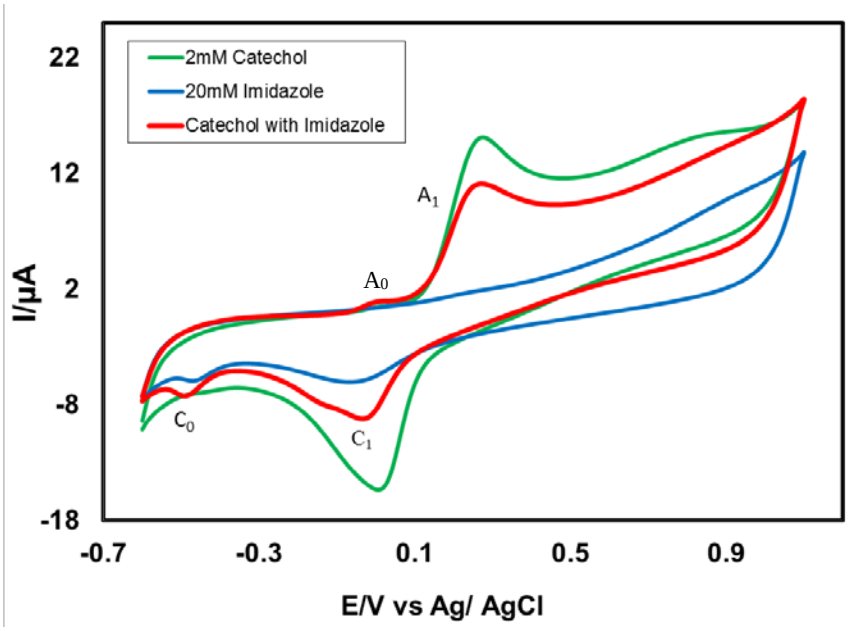

Fig. 4.3: Cyclic voltammogram of 2 mM Catechol, 20mM Imidazole and 2 mM Catechol with 20mM Imidazole of Pt electrode in buffer solution (pH 7) at scan rate 0.1 V/s (2nd cycle). A_0 and A_1 is appeared anodic peak and anodic peak, C_0 and C_1 is corresponding cathodic peak.

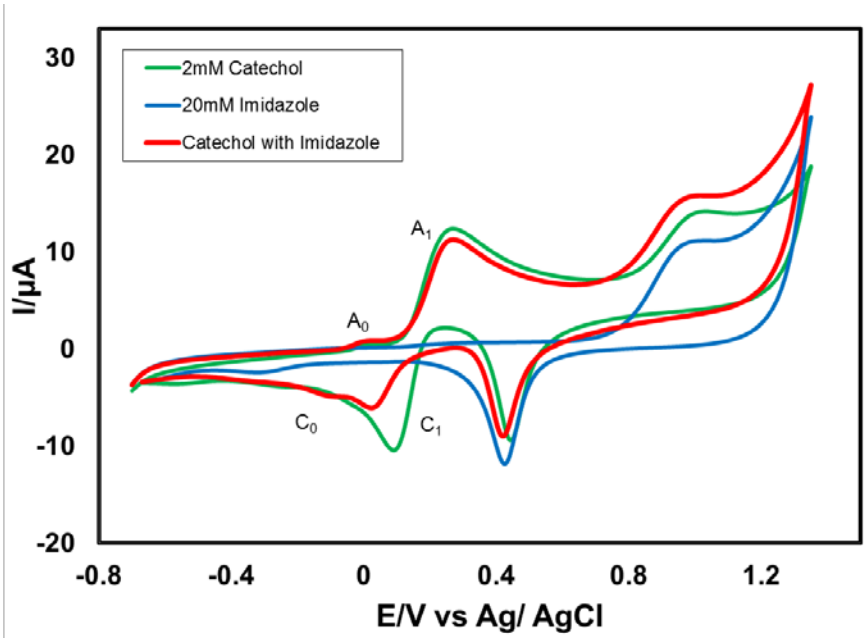

Fig. 4.4: Cyclic voltammogram of 2 mM Catechol, 20mM Imidazole and 2 mM Catechol with 20mM Imidazole of Au electrode in buffer solution (pH 7) at scan rate 0.1 V/s (2nd cycle). A_0 and A_1 is appeared anodic peak and anodic peak, C_0 and C_1 is corresponding cathodic peak.

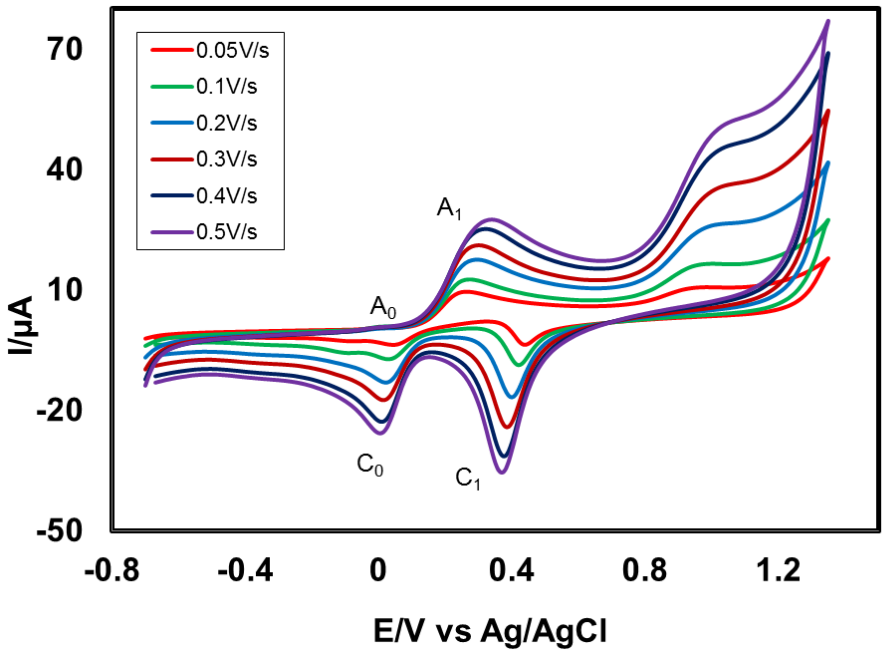

Fig. 4.5: Cyclic voltammogram of 2 mM Catechol with 20mM Imidazole in the second scan of potential at GC electrode in buffer solution (pH 7) at scan rate 0.05 V/s to 0.5 V/s.

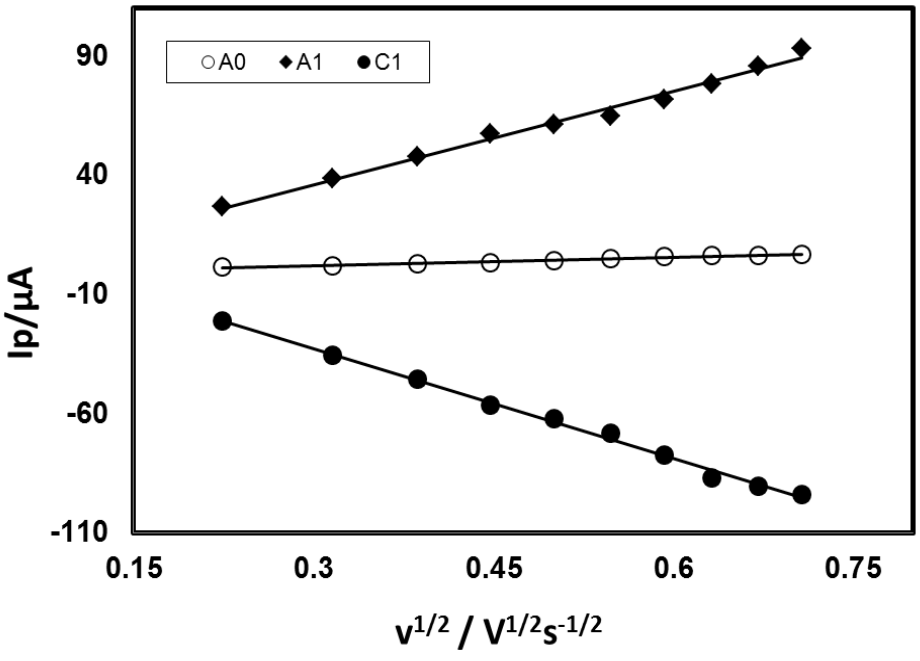

Fig. 4.6: Plots of peak current (I_p) versus square root of scan rate ($v^{1/2}$) of 2 mM Catechol with 20mM Imidazole of GC electrode in buffer solution (pH 7) (2^{nd} cycle).

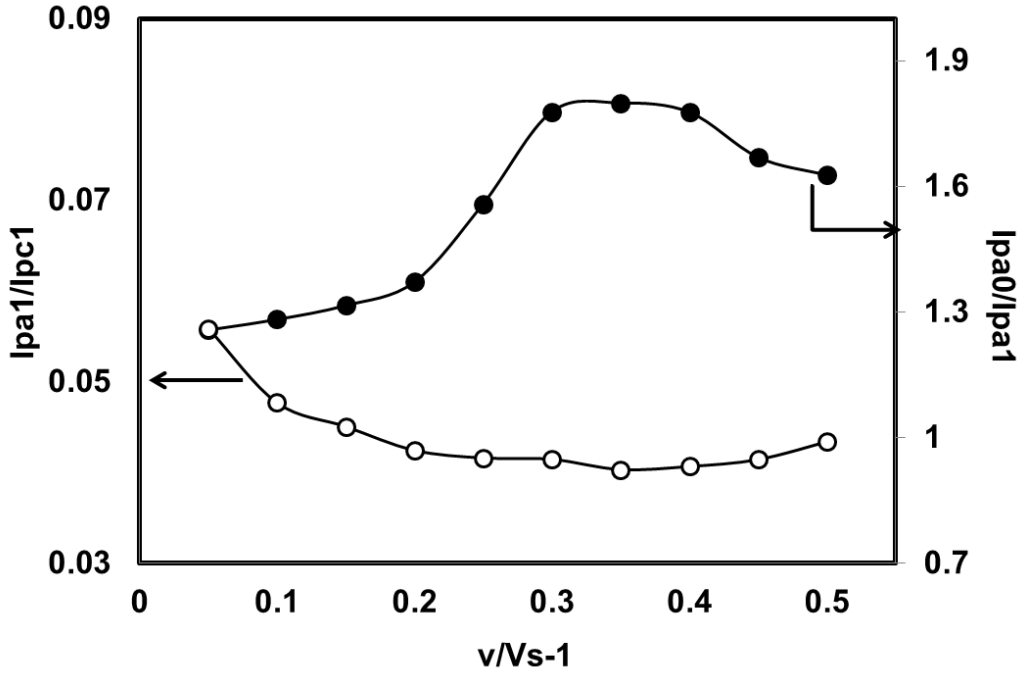

Fig. 4.7: Variation of peak current ratio of corresponding peak (I_{pa1}/I_{pc1}) and anodic peak (I_{pa0}/I_{pa1}) vs scan rate (v) of 2 mM Catechol with 20mM Imidazole of GC electrode in buffer solution (pH 7) at scan rate 0.1 V/s in the second scan of potential.

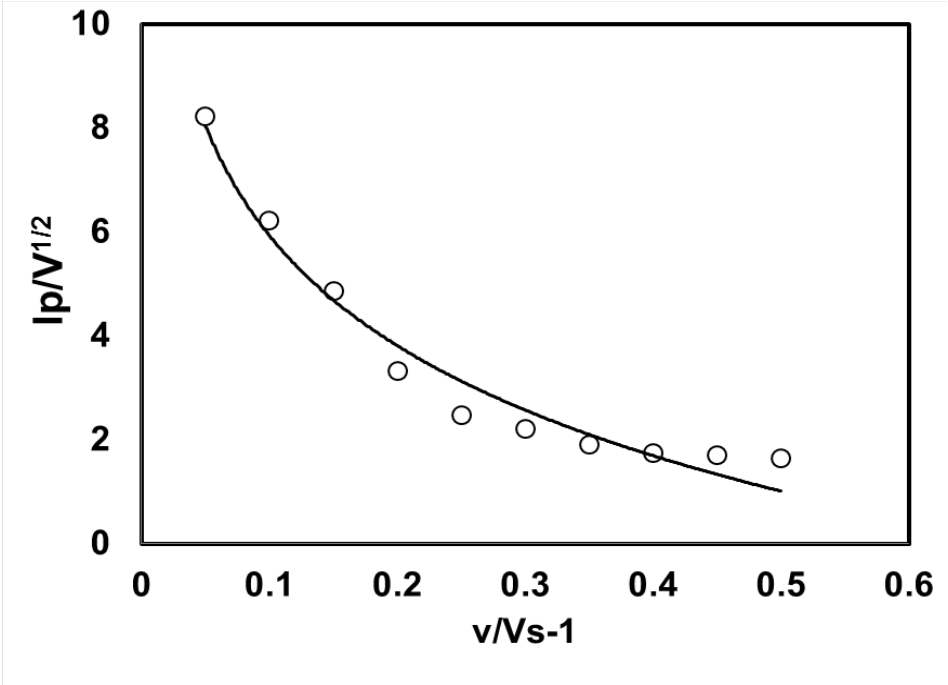

Fig. 4.8: Plot of current function ($I_p/v^{1/2}$) versus scan rate (v) of 2 mM Catechol with 20mM Imidazole of GC electrode in buffer solution (pH 7) of the Appeared anodic peak (A_0).

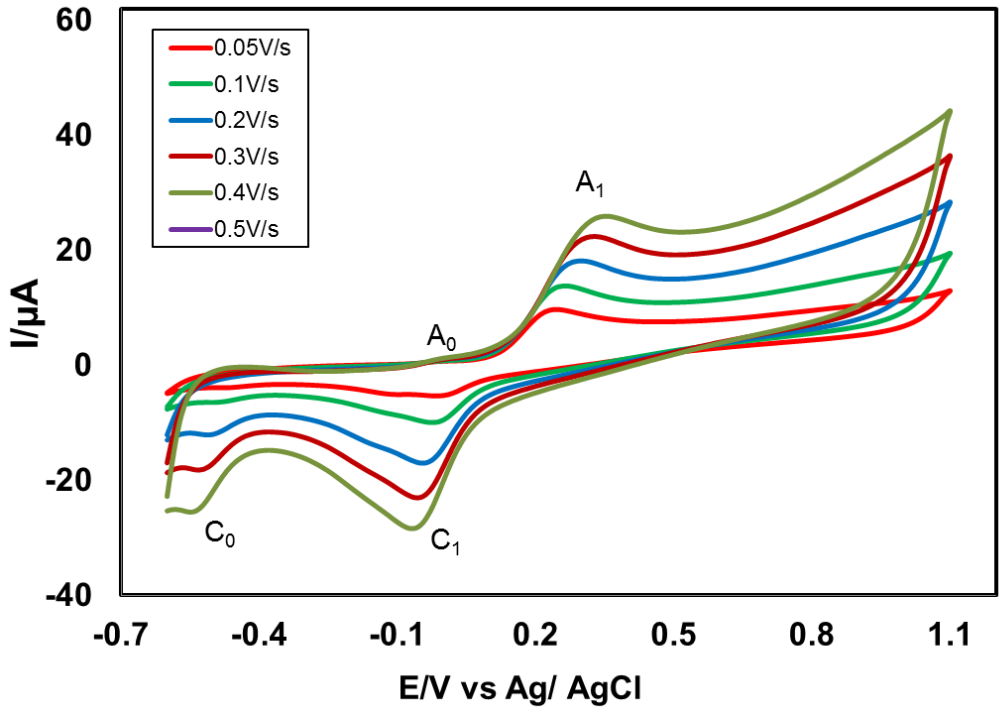

Fig. 4.9: Cyclic voltammogram of 2 mM Catechol with 20mM Imidazole in the second scan of potential at Pt electrode in buffer solution (pH 7) at scan rate 0.05 V/s to 0.5 V/s.

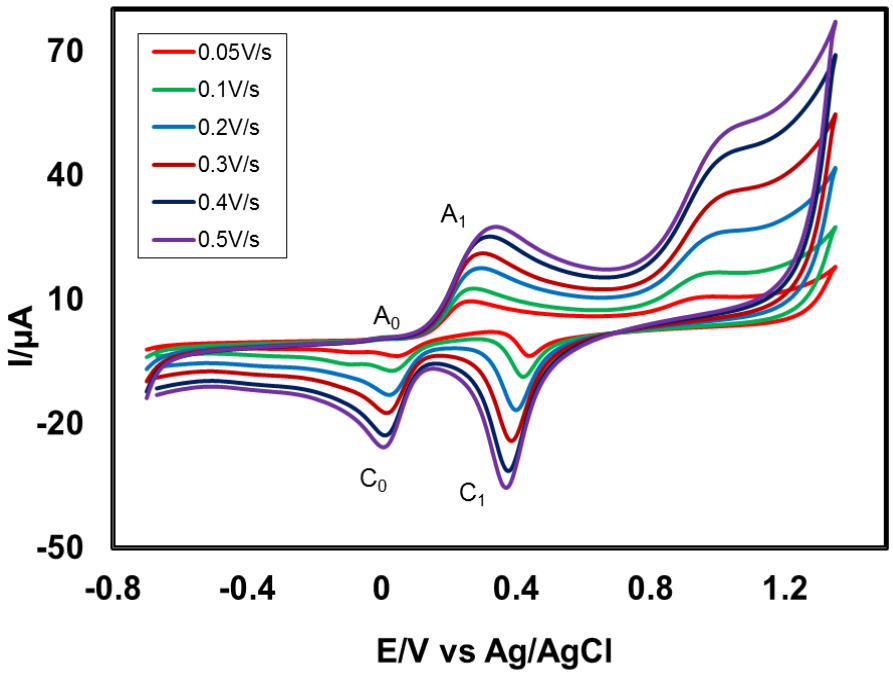

Fig. 4.10: Cyclic voltammogram of 2 mM Catechol with 20mM Imidazole in the second scan of potential at Au electrode in buffer solution (pH 7) at scan rate 0.05 V/s to 0.5 V/s.

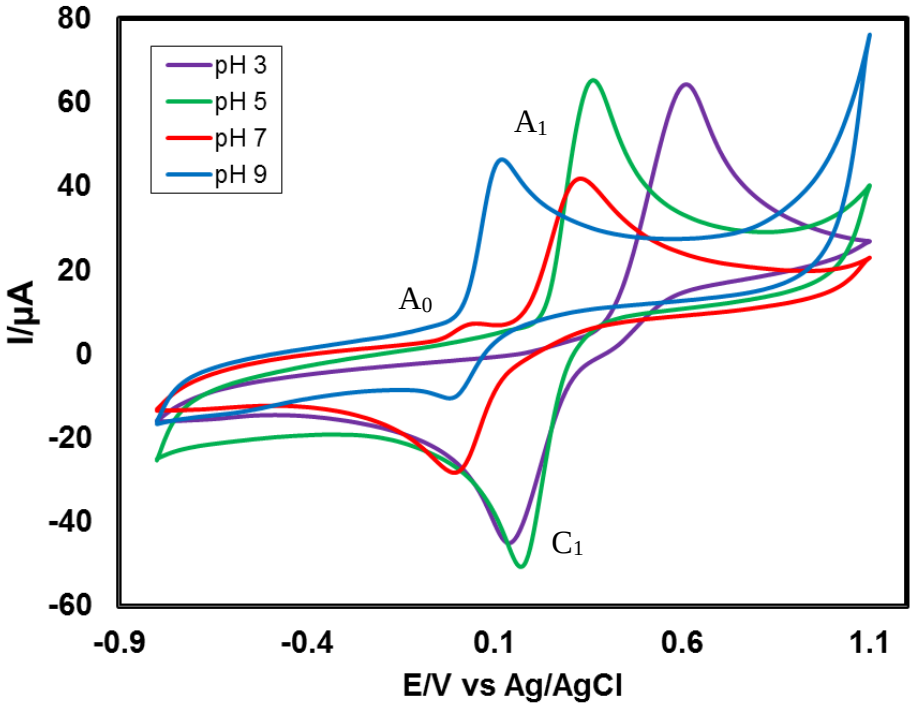

Fig. 4.11: Cyclic voltammogram of 2 mM Catechol with 20mM Imidazole of GC (3 mm) electrode in different pH (3, 5, 7 and 9) at scan rate 0.1 V/s.

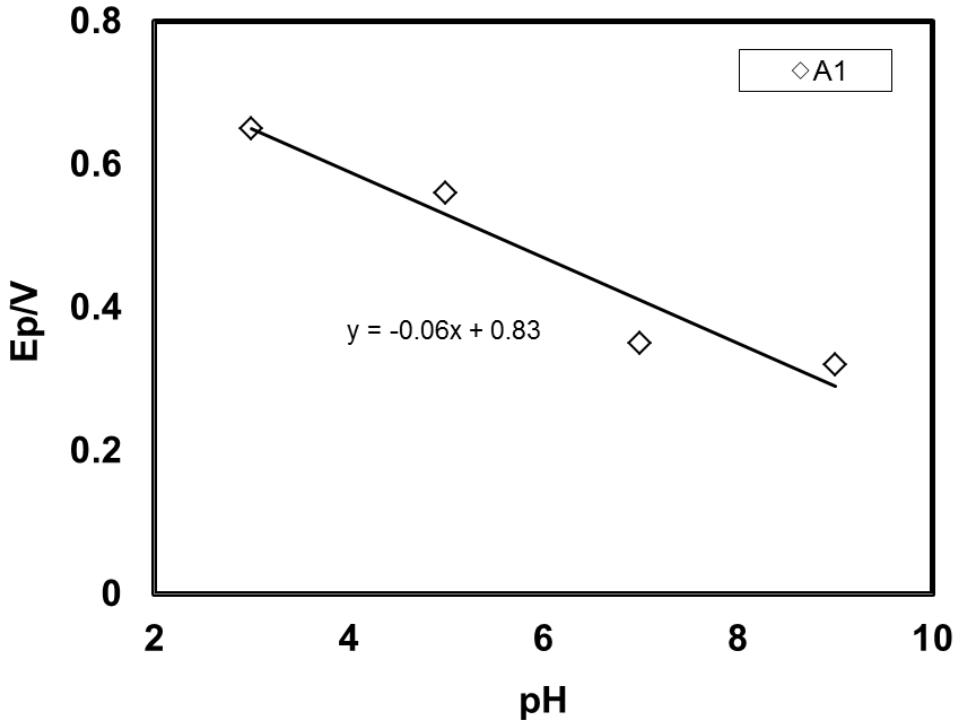

Fig. 4.12: Plots of peak potential (E_p) versus pH (3, 5, 7, 9 and 11) of 2 mM Catechol with 20 mM Imidazole of GC electrode at scan rate 0.1 V/s (2^{nd} cycle).

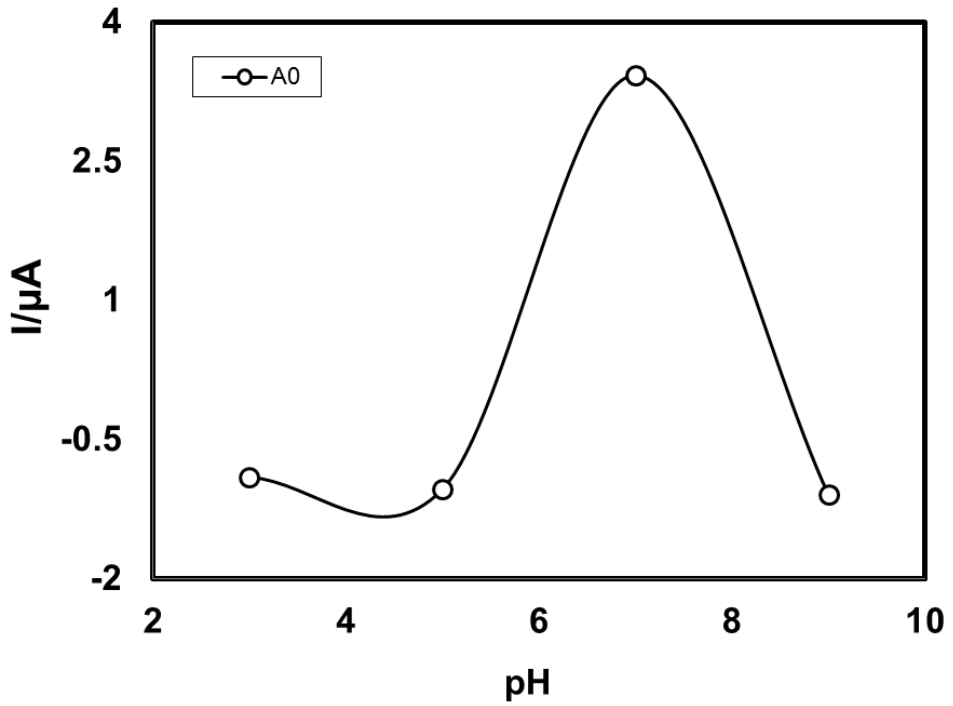

Fig. 4.13: Plot of peak current (I_p) versus pH (3, 5, 7 and 9) of 2 mM Catechol with 20mM Imidazole of GC electrode at scan rate 0.1 V/s (2nd cycle).

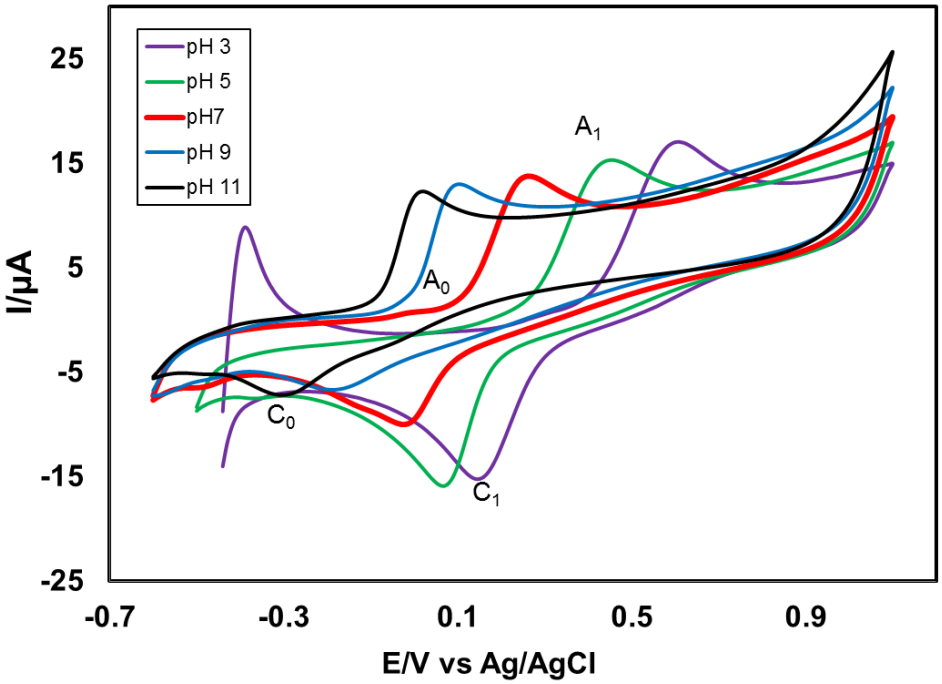

Fig. 4.14: Cyclic voltammogram of 2 mM Catechol with 20mM Imidazole of Pt electrode in different pH (3, 5, 7, 9 and 11) at scan rate 0.1 V/s.

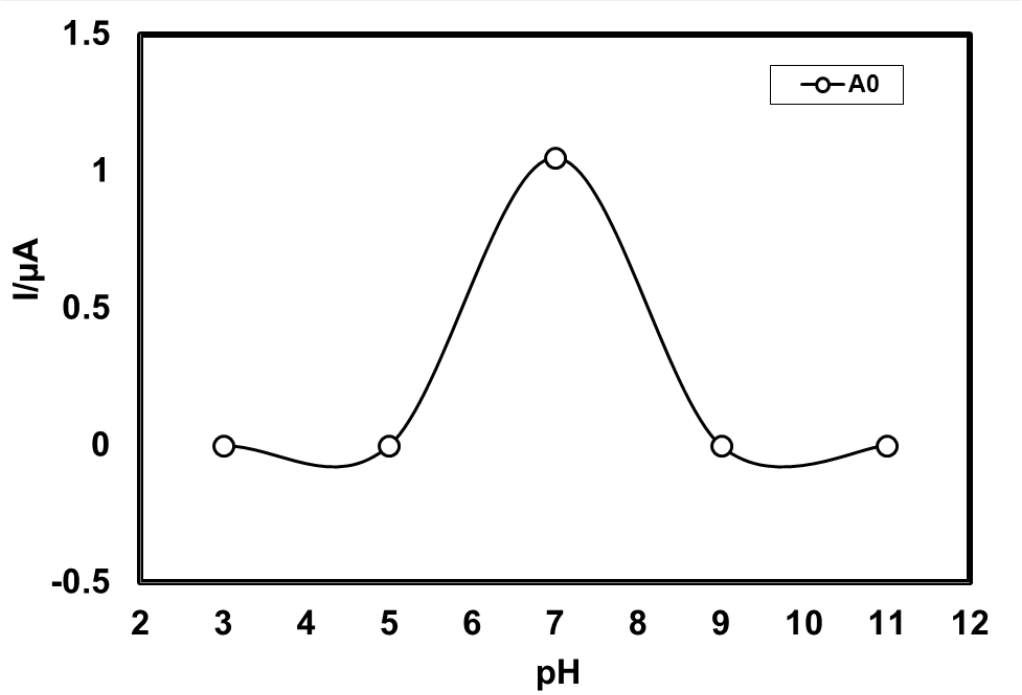

Fig. 4.15: Plots of peak current (I_p) versus pH (3, 5, 7, 9 and 11) of 2 mM Catechol with 20mM Imidazole of Pt electrode at scan rate 0.1 V/s (2nd cycle).

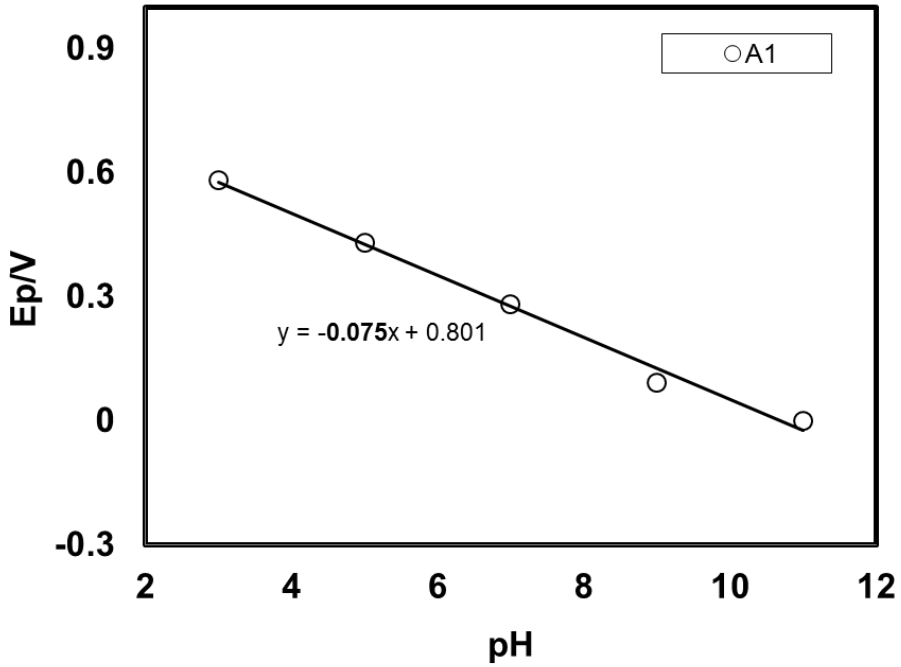

Fig. 4.16: Plot of peak potential (E_p) versus pH (3, 5, 7, 9 and 11) of 2 mM Catechol with 20mM Imidazole of Pt electrode at scan rate 0.1 V/s (2nd cycle).

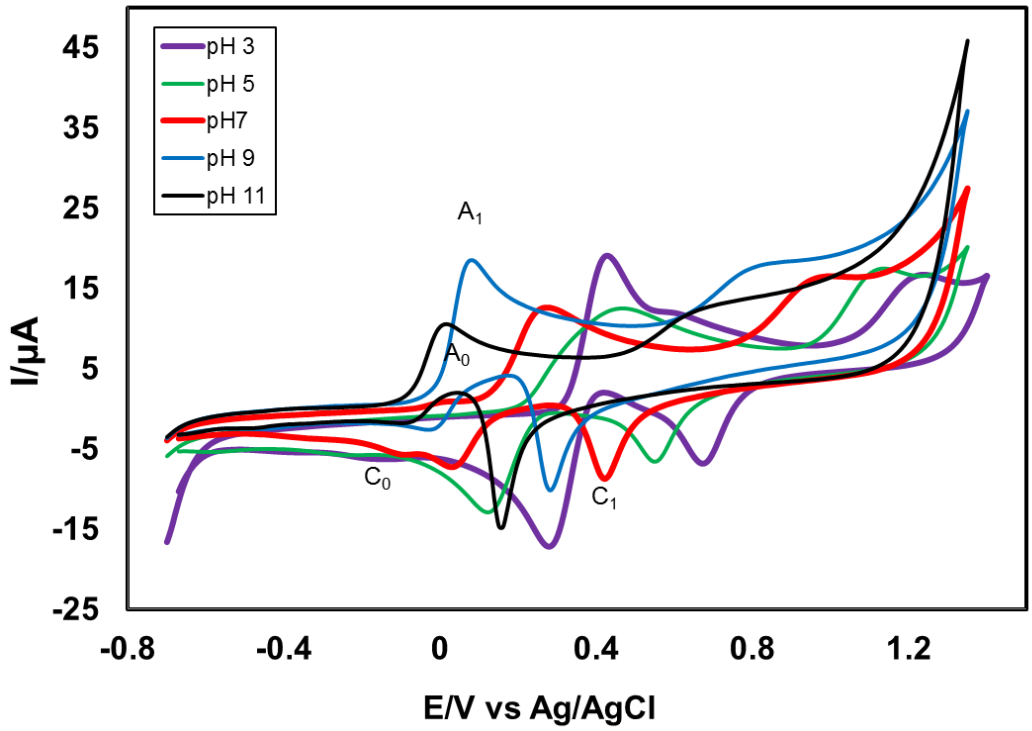

Fig. 4.17: Cyclic voltammogram of 2 mM Catechol with 20mM Imidazole of Au electrode in different pH (3, 5, 7, 9 and 11) at scan rate 0.1 V/s.

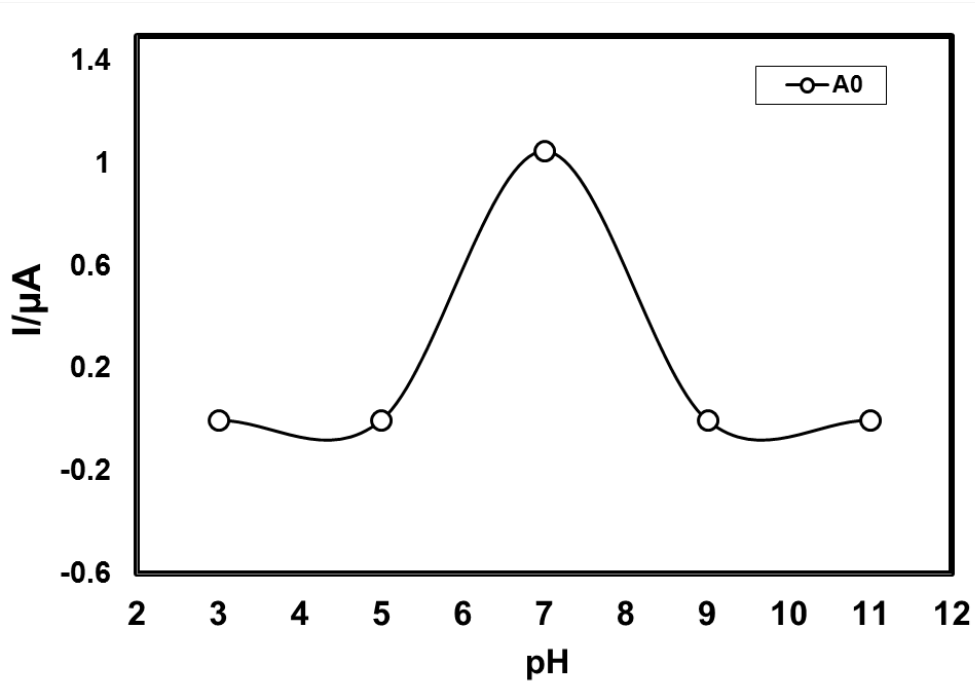

Fig. 4.18: Plots of peak current (I_p) versus pH (3, 5, 7, 9 and 11) of 2 mM Catechol with 20mM Imidazole of Au electrode at scan rate 0.1 V/s (2^{nd} cycle).

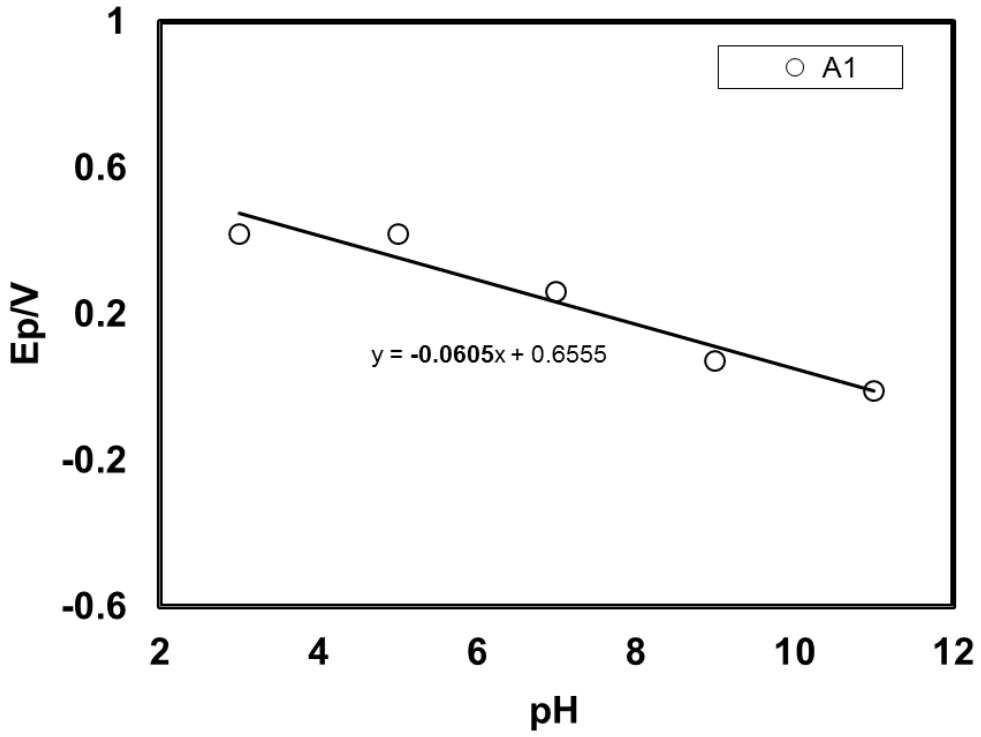

Fig. 4.19: Plot of peak potential (E_p) versus pH (3, 5, 7, 9 and 11) of 2 mM Catechol with 20mM Imidazole of Au electrode at scan rate 0.1 V/s (2nd cycle).

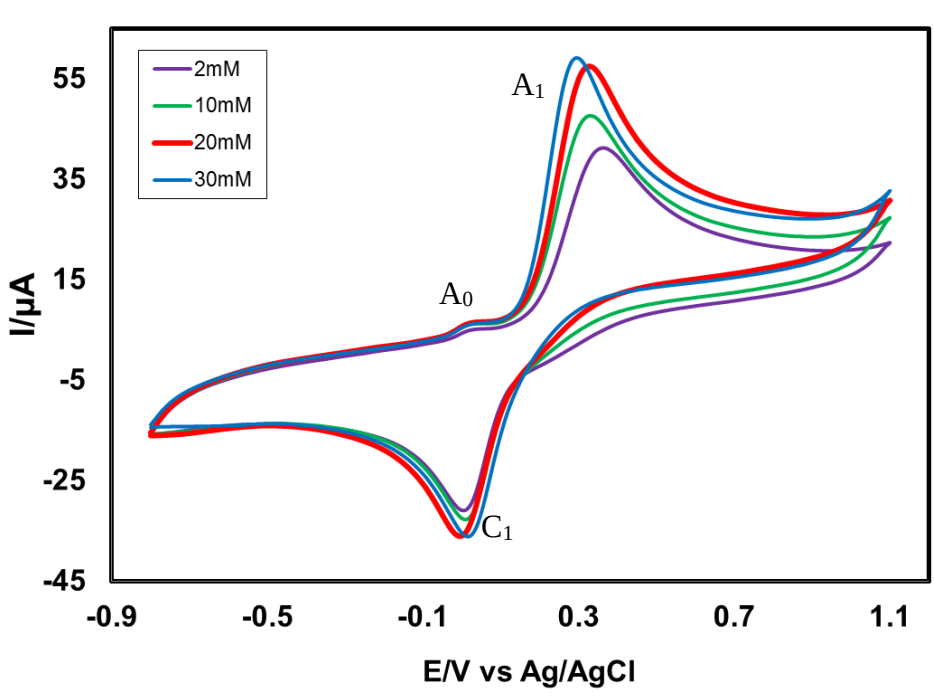

Fig. 4.20: CV of composition changes of Imidazole (2, 10, 20 and 30mM) with fixed 2 mM Catechol of GC electrode at pH 7 and scan rate 0.1 V/s.

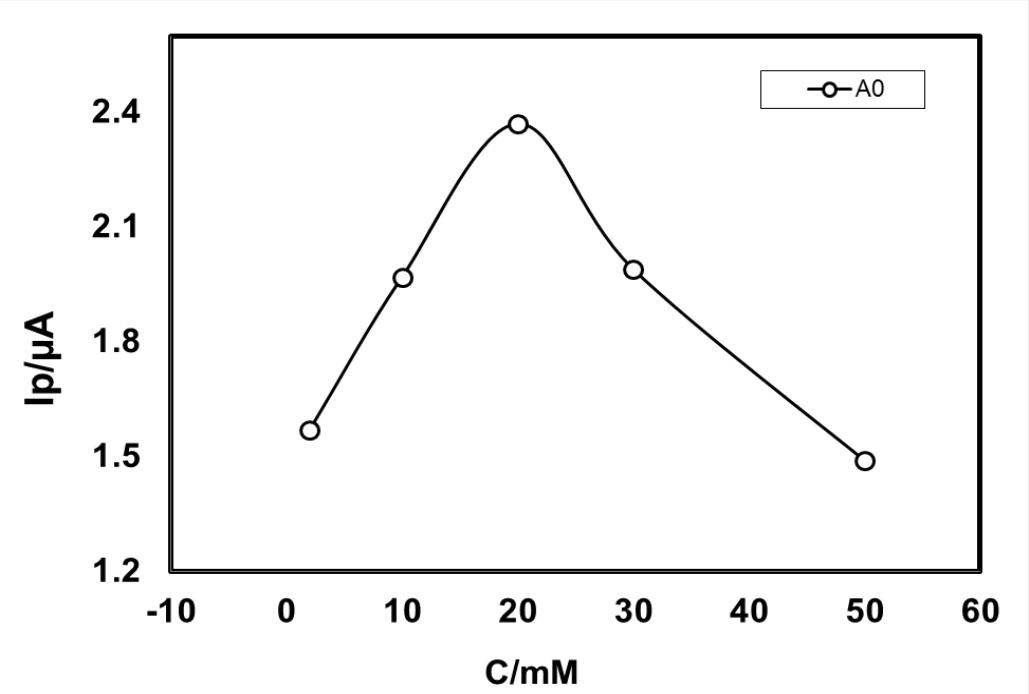

Fig. 4.21: Comparison of cyclic voltammogram of different concentration (2, 10, 20 and 30mM) of 2 mM Catechol with 20mM Imidazole of GC electrode in buffer solution (pH 7) at scan rate 0.1 V/s (2nd cycle).

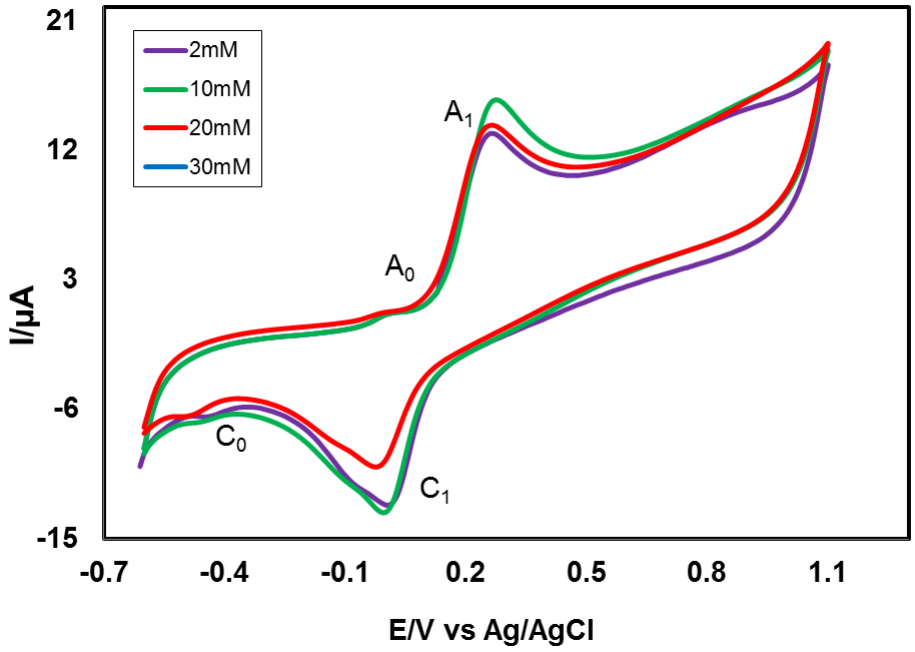

Fig. 4.22: CV of composition changes of Imidazole (2, 10, 20 and 30mM) with fixed 2 mM Catechol of Pt electrode at pH 7 and scan rate 0.1 V/s.

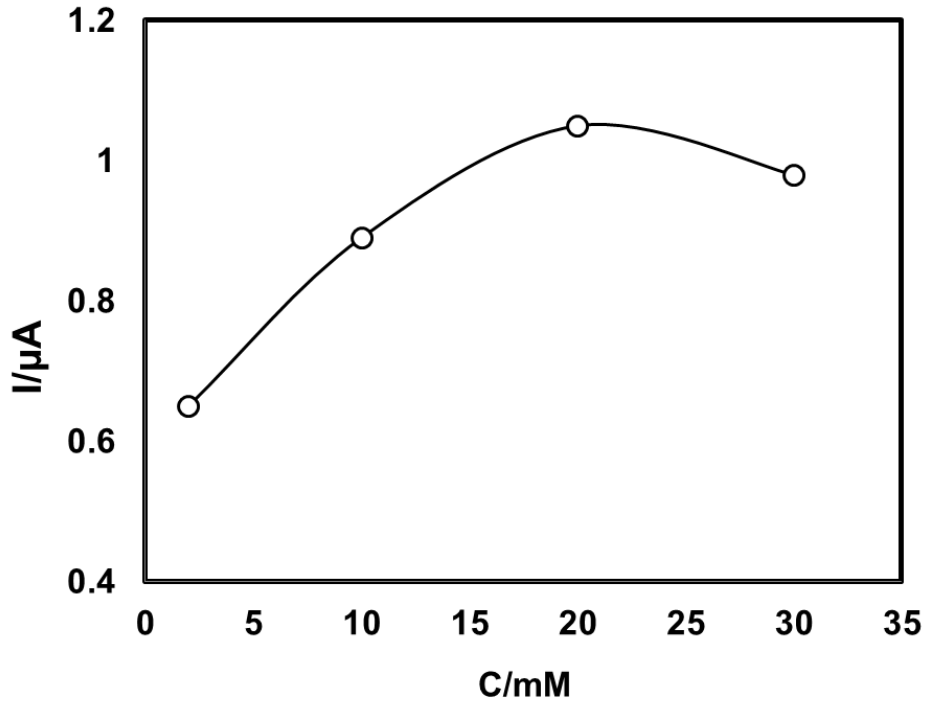

Fig. 4.23: Plots of peak current (I_p) versus concentration (C) of Imidazole (2, 10, 20 and 30mM) with fixed 2 mM Catechol of Pt electrode in buffer solution (pH) at 7 scan rate 0.1 V/s (2^{nd} cycle).

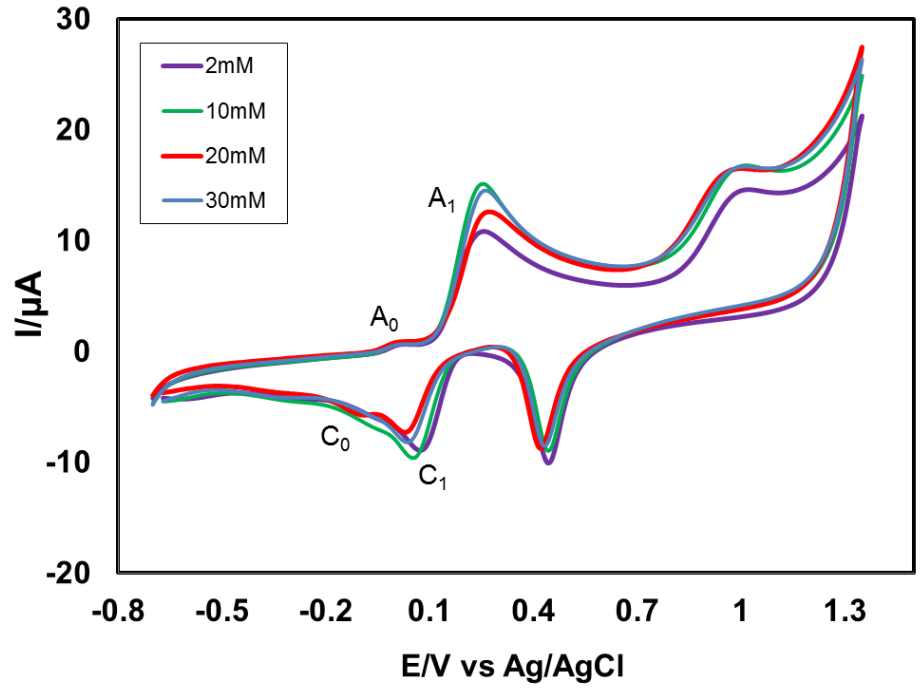

Fig. 4.24: CV of composition changes of Imidazole (2, 10, 20 and 30mM) with fixed 2 mM Catechol of Au electrode at pH 7 and scan rate 0.1 V/s.

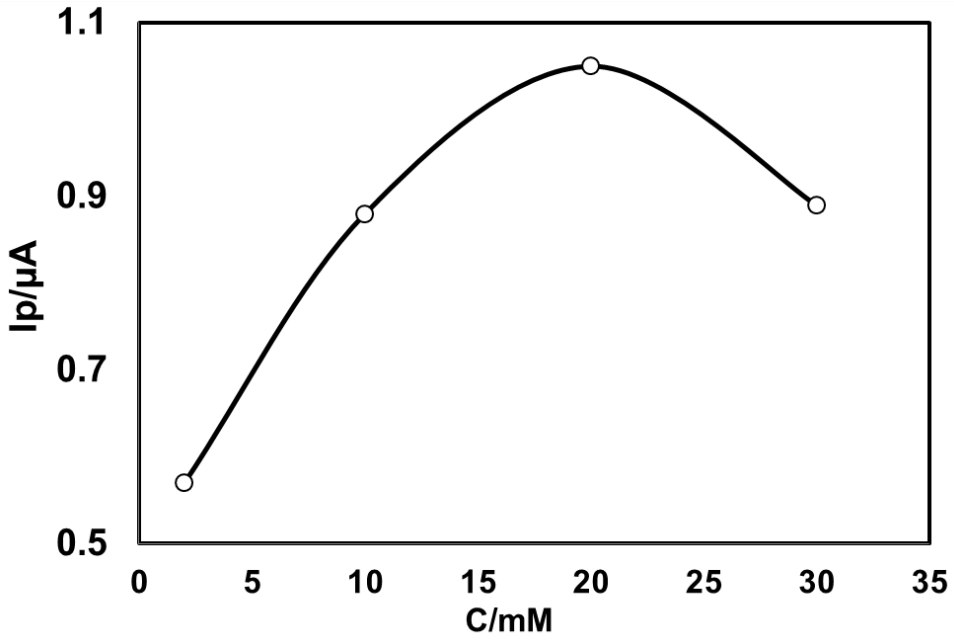

Fig. 4.25: Plots of peak current (I_p) versus concentration (C) of Imidazole (2, 10, 20 and 30mM) with fixed 2 mM Catechol of Au electrode in buffer solution (pH 7) at scan rate 0.1 V/s (2^{nd} cycle).

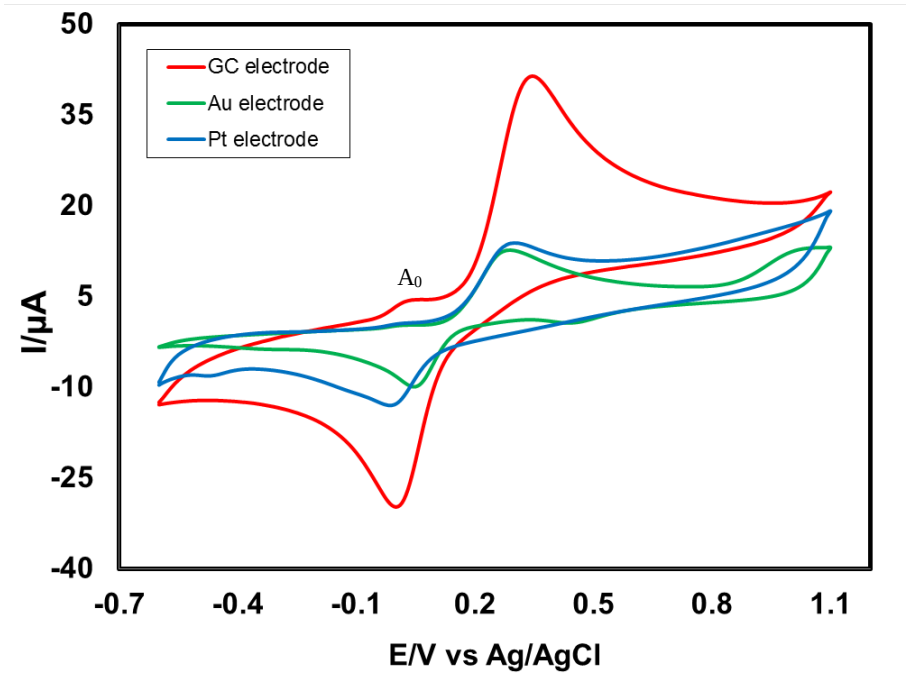

Fig. 4.26: Cyclic voltammogram (CV) of 2 mM catechol with 20mM Imidazole in GC electrode (3.0 mm), Gold electrode (1.6 mm) and Platinum electrode (1.6 mm) at pH 7 and scan rate 0.1 V/s.

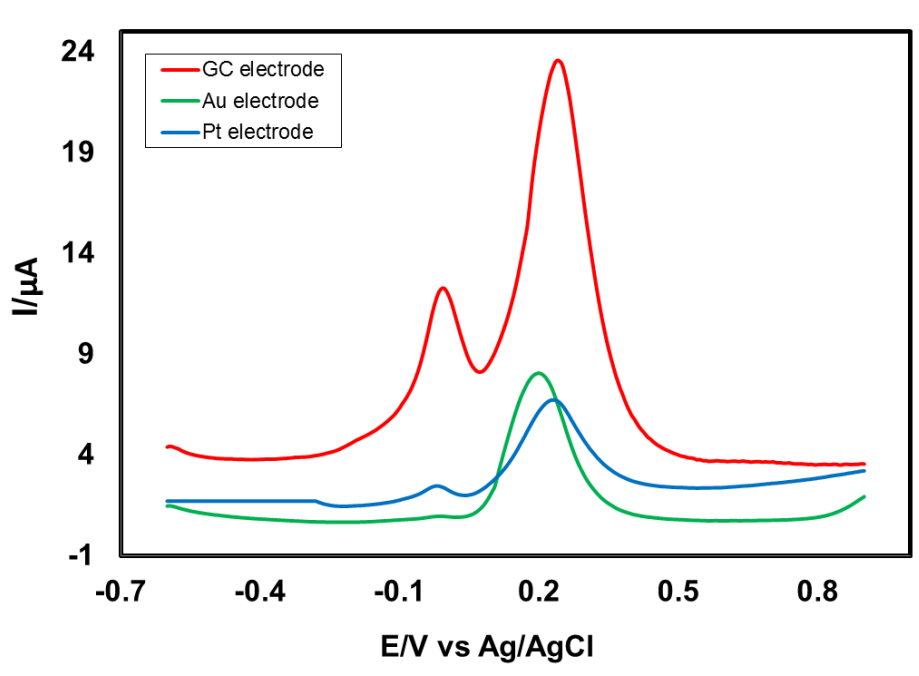

Fig. 4.27: Differential pulse voltammogram (DPV) of 2 mM catechol with 20mM Imidazole in GC electrode (3.0 mm), Gold electrode (1.6 mm) and Platinum electrode (1.6 mm) at pH 7 and scan rate 0.1 V/s.

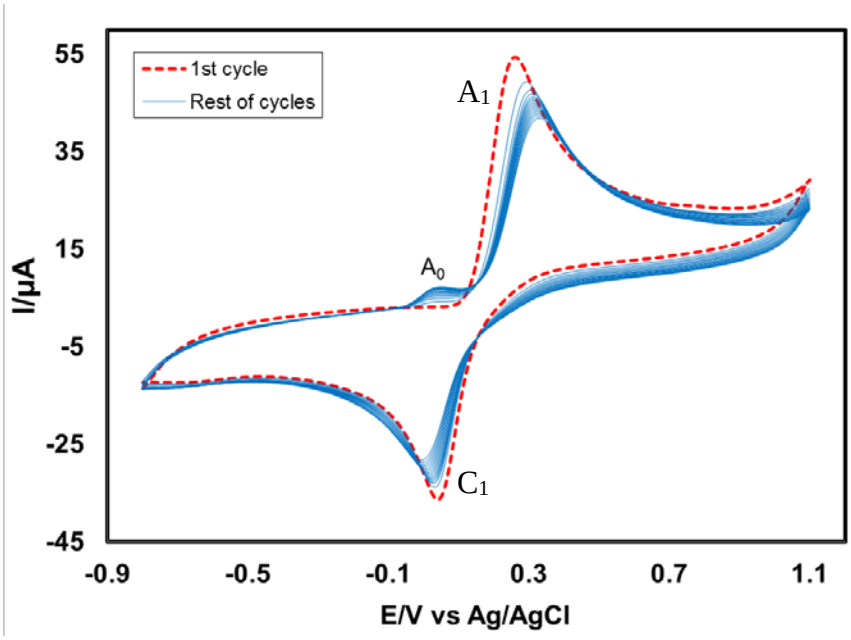

Fig. 4.28: Cyclic voltammogram of 2 mM Catechol with 20mMImidazole of GC (3 mm) electrode in the buffer solution of pH 7 at scan rate 0.1 V/s (15 cycles). The appeared anodic peak current (A_0) increased with the iteration scan from the first cycle.

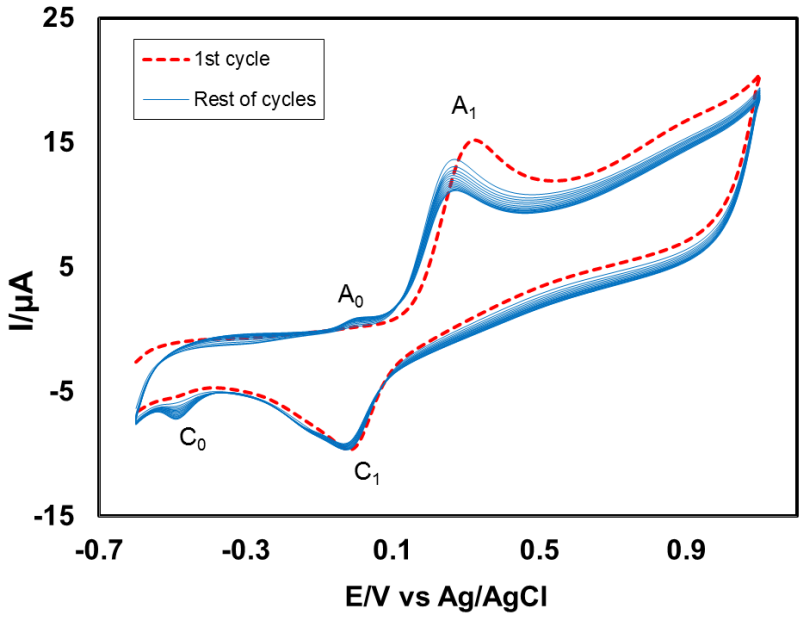

Fig. 4.29: Cyclic voltammogram of 2 mM Catechol with 20mM Imidazole of Pt electrode in the buffer solution of pH 7 at scan rate 0.1 V/s (15 cycles). The appeared anodic peak current (A_0) and cathodic peak current (C_0) increased with the iteration scan from the first cycle.

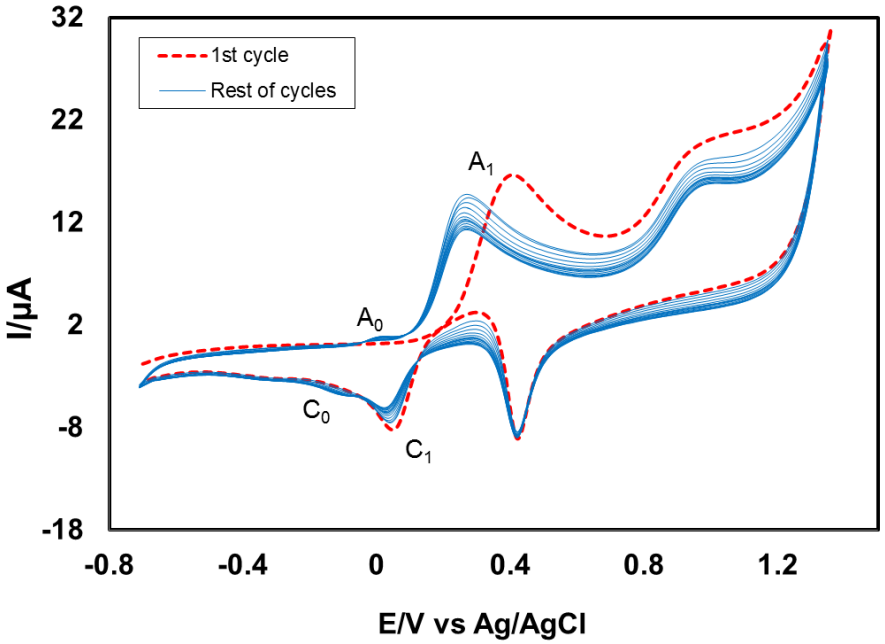

Fig. 4.30: Cyclic voltammogram of 2 mM Catechol with 20mM Imidazole of Au electrode in the buffer solution of pH 7 at scan rate 0.1 V/s (15 cycles). The appeared anodic peak current (A_0) and cathodic peak current (C_0) increased with the iteration scan from the first cycle.

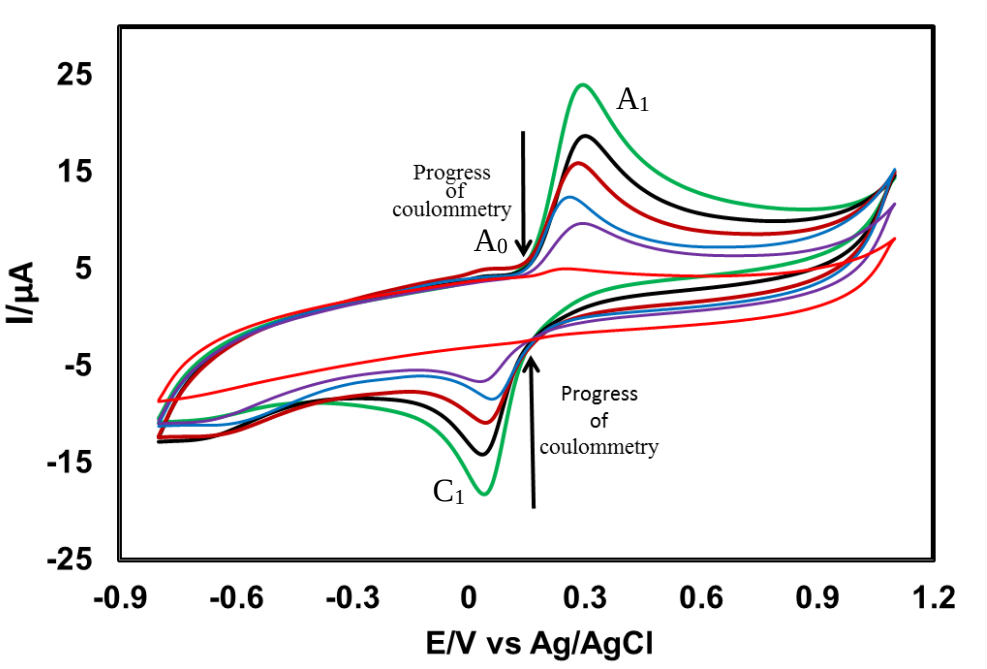

Fig. 4.31: Cyclic voltammogram and (CV) of 1 mM Catechol in presence of 10mM Imidazole of GC electrode during controlled potential coulometry at 0.45 V in pH 7 at scan rate 0.1 V/s after consumption of 0-20C.

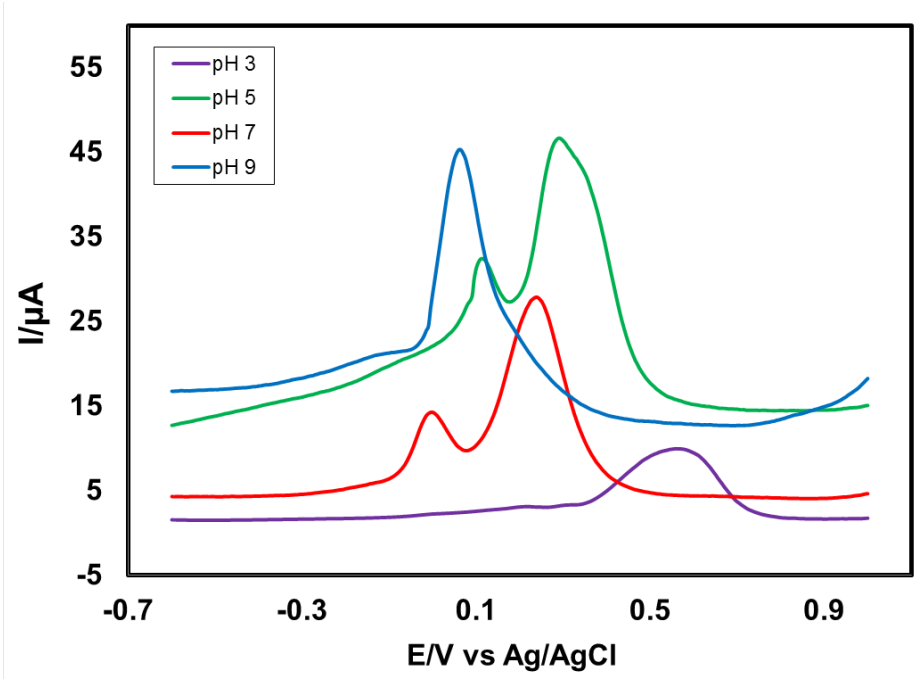

Fig. 4.32: Differential pulse voltammogram (DPV) of 2 mM Catechol with 20mM Imidazole of GC electrode in second scan of different pH (3, 5, 7 and 9) and scan rate 0.1 V/s.

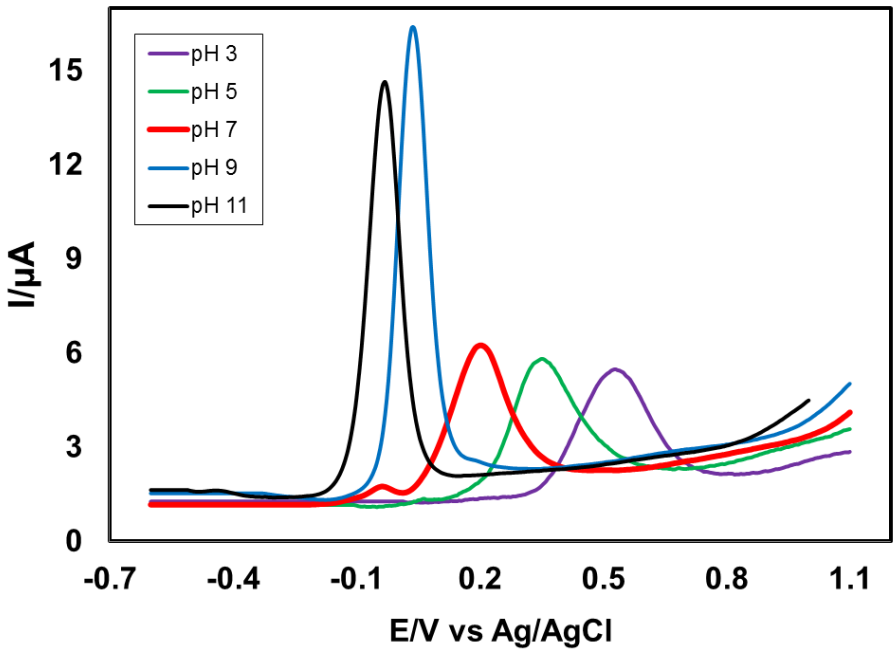

Fig. 4.33: Differential pulse voltammogram (DPV) of 2 mM Catechol with 20mM Imidazole of Pt electrode in second scans of different pH (3, 5, 7 , 9 and 11) and scan rate 0.1 V/s.

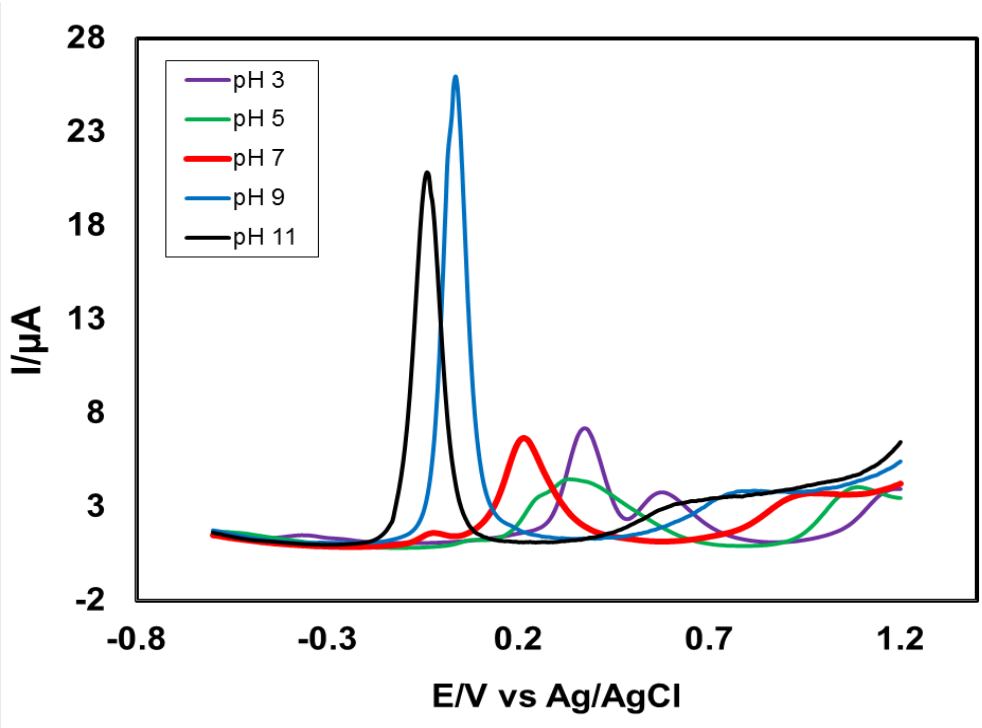

Fig. 4.34: Differential pulse voltammogram (DPV) of 2 mM Catechol with 20mM Imidazole of Au electrode in second scans of different pH (3, 5, 7, 9 and 11) and scan rate 0.1 V/s.

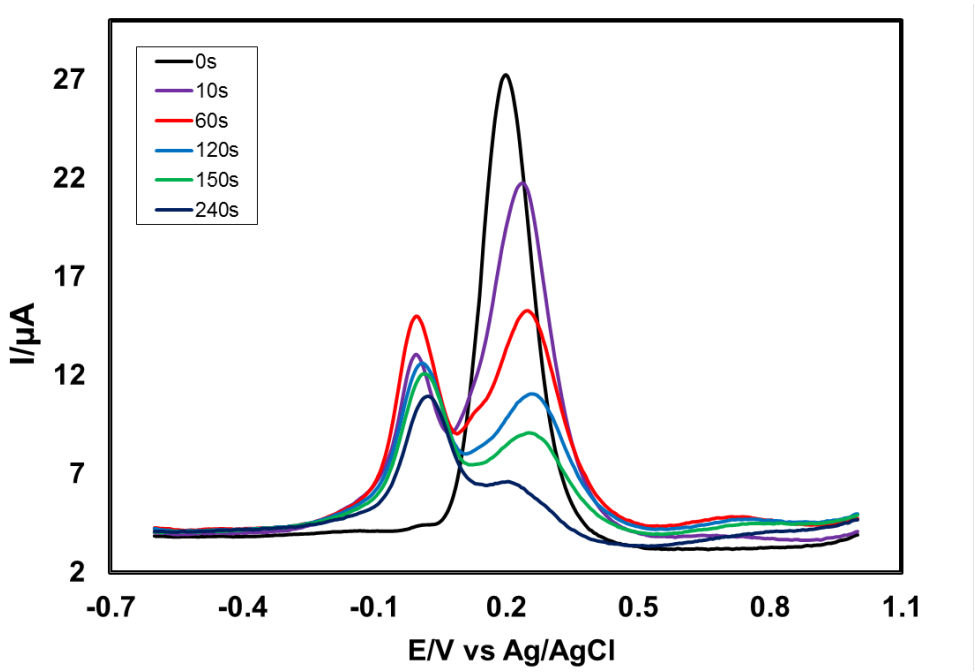

Fig. 4.35: Differential pulse voltammogram (DPV) of deposition time change (0, 10, 60, 120, 150 and 240 s) of 2 mM catechol with 20mM Imidazole of pH 7 at *E*puls 0.02 V, tpuls 20ms and scan rate 0.1 Vs^{-1}.

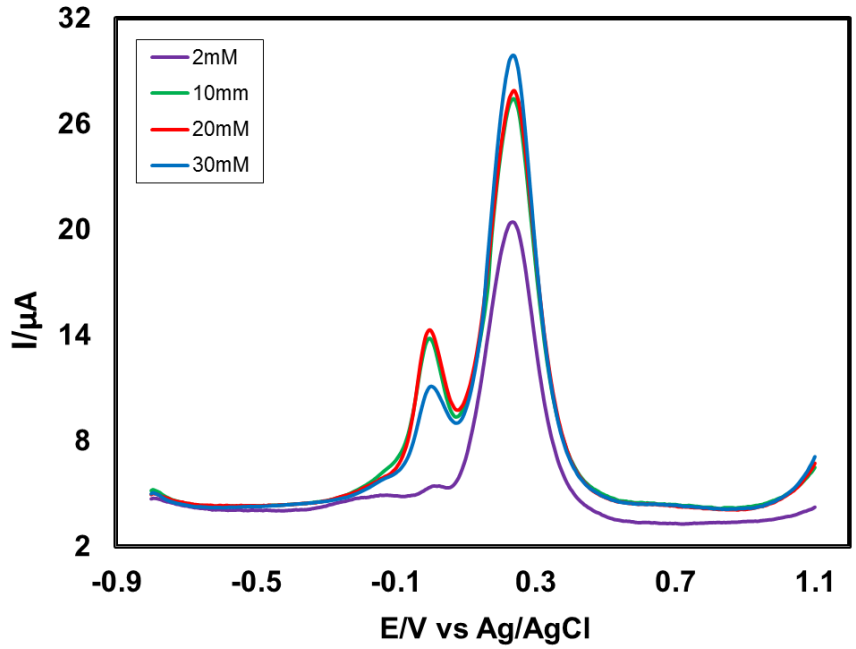

Fig. 4.36: Differential pulse voltammogram (DPV) of composition change of Imidazole (2, 10, 20 and 30mM) with the fixed composition of 2 mM Catechol in second scan of pH7 at *E*puls 0.02 V, tpuls 20ms of GC electrode and scan rate 0.1 Vs^{-1}.

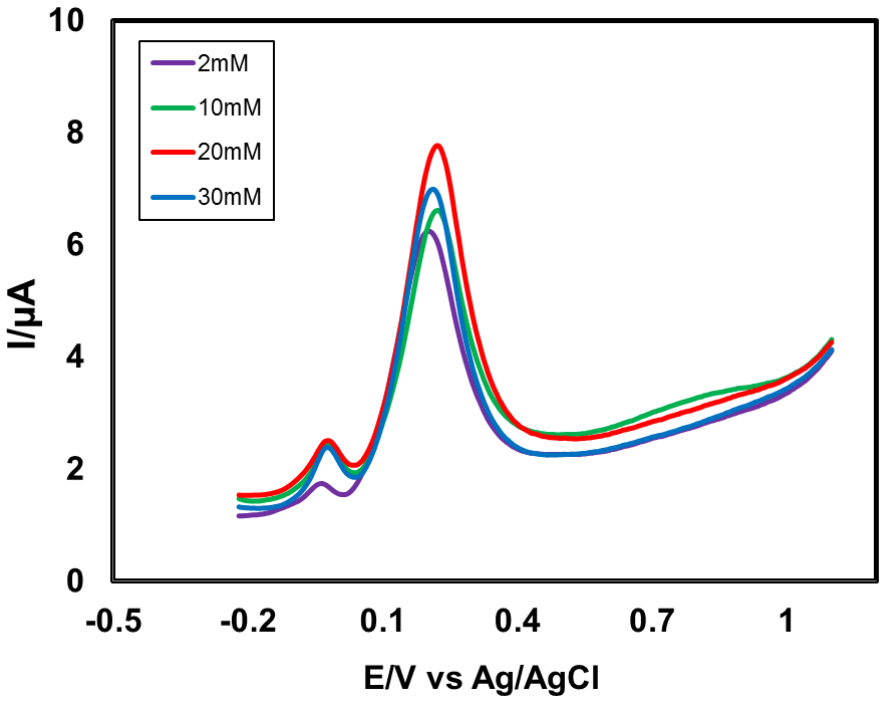

Fig. 4.37: Differential pulse voltammogram (DPV) of composition change of Imidazole (2, 10, 20 and 30mM) with the fixed composition of 2 mM Catechol in second scan of pH 7 at *E*puls 0.02 V, tpuls 20ms of Pt electrode and scan rate 0.1 Vs^{-1}.

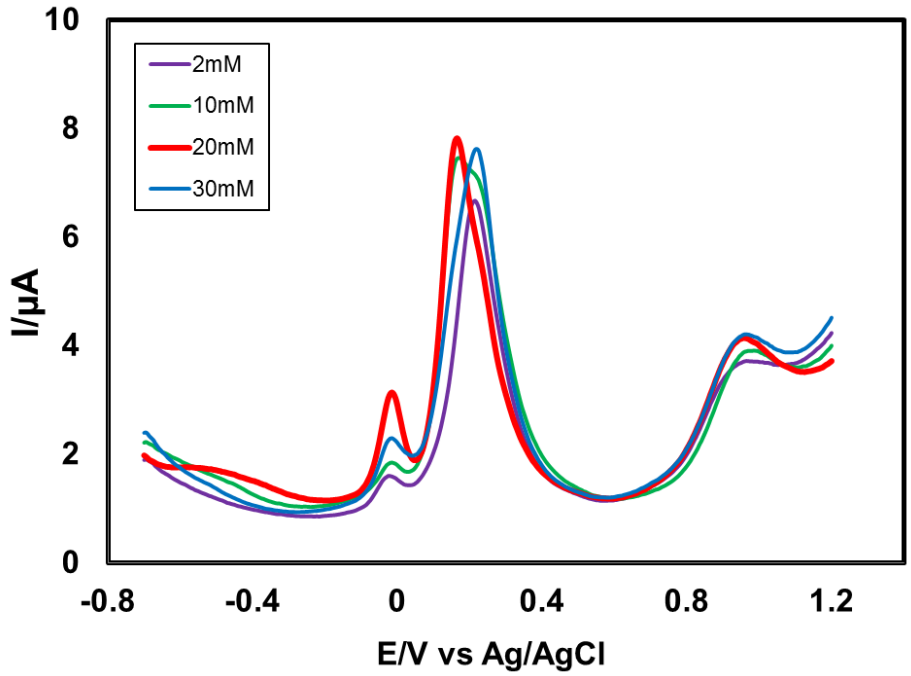

Fig. 4.38: Differential pulse voltammogram (DPV) of composition change of Imidazole (2, 10, 20 and 30mM) with the fixed composition of 2 mM Catechol in second scan of pH7 at *E*puls 0.02 V, tpuls 20ms of Au electrode and scan rate 0.1 Vs^{-1}.

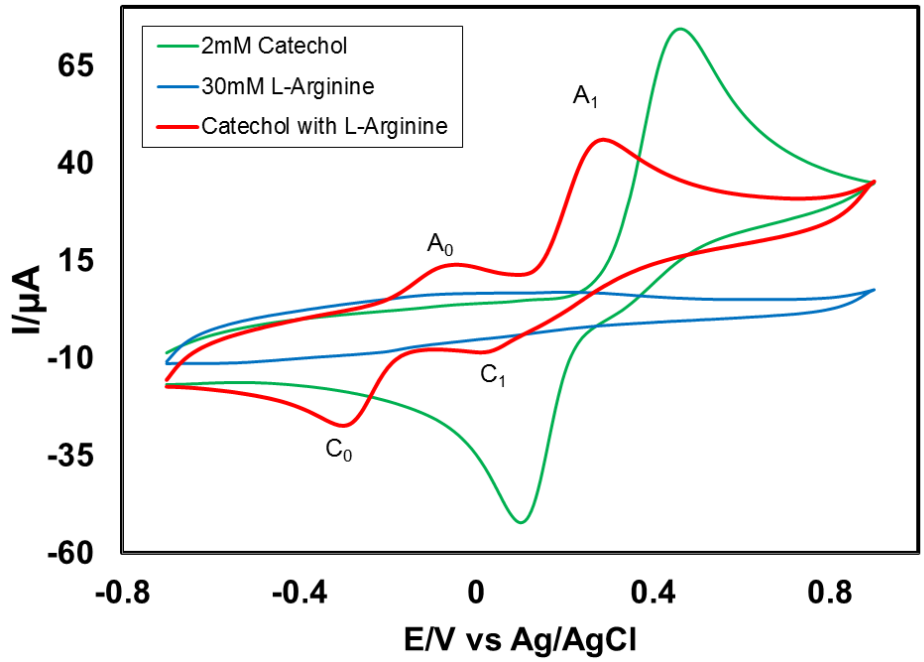

Fig. 4.39: Cyclic voltammogram of 2mM Catechol, 30mM L-Arginine and 2mM Catechol with 30mM L-Arginine of GC electrode in buffer solution (pH 7) at scan rate 0.1V/s (2nd cycle). A_0 and A_1 is appeared anodic peak and anodic peak, C_0 and C_1 is corresponding cathodic peak.

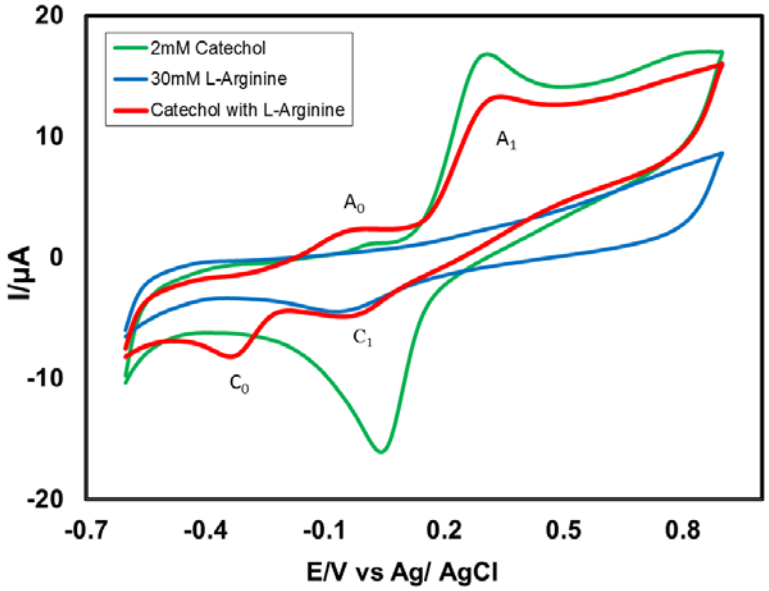

Fig. 4.40: Cyclic voltammogram of 2mM Catechol, 30mM L-Arginine and 2mM Catechol with 30mM L-Arginine of Pt electrode in buffer solution (pH 7) at scan rate 0.1V/s (2nd cycle). A_0 and A_1 is appeared anodic peak and anodic peak, C_0 and C_1 is corresponding cathodic peak.

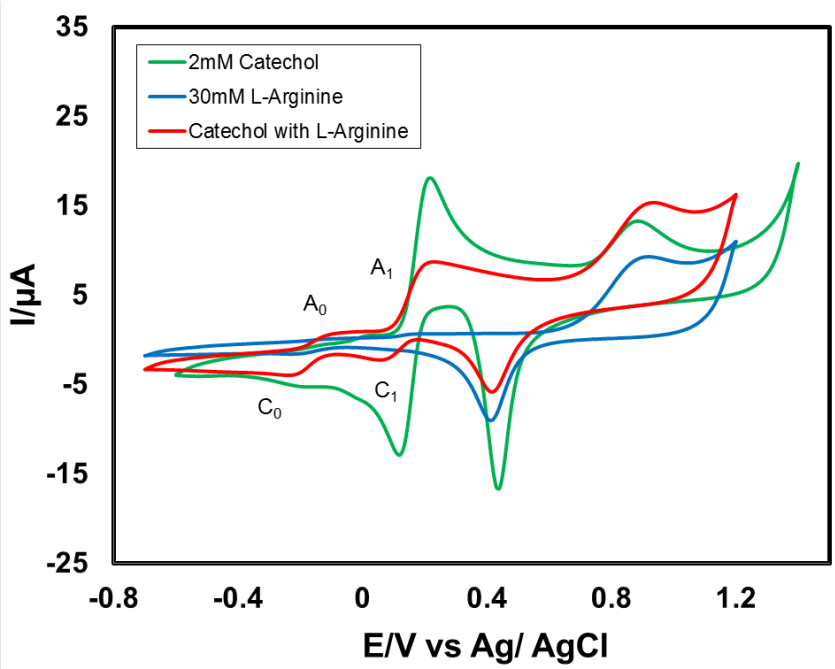

Fig. 4.41: Cyclic voltammogram of 2mM Catechol, 30mM L-Arginine and 2mM Catechol with 30mM L-Arginine of Au electrode in buffer solution (pH 7) at scan rate 0.1V/s (2nd cycle). A_0 and A_1 is appeared anodic peak and anodic peak, C_0 and C_1 is corresponding cathodic peak.

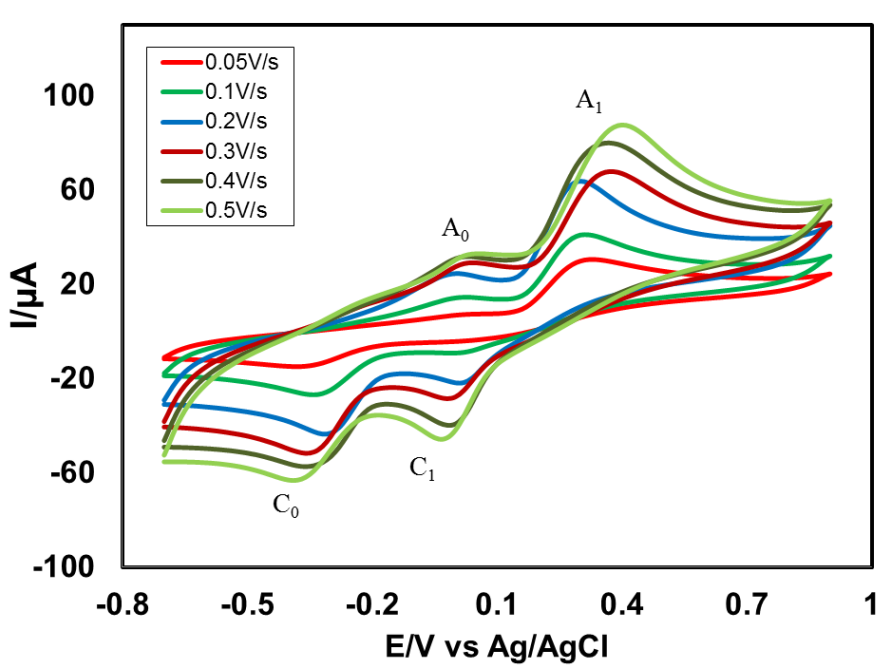

Fig. 4.42: Cyclic voltammogram of 2mM Catechol with 30mM L-Arginine in the second scan of potential at GC electrode in buffer solution (pH 7) at scan rate 0.05V/s to 0.5V/s.

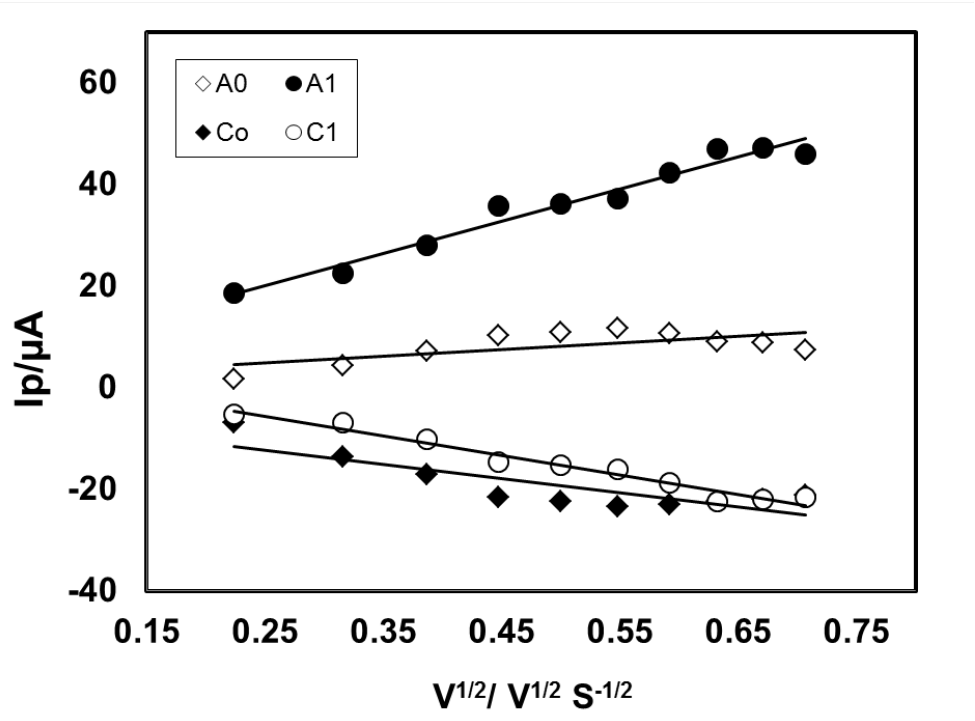

Fig. 4.43: Plots of peak current (I_p) versus square root of scan rate ($v^{1/2}$) of 2mM Catechol with 30mM L-Arginine of GC electrode in buffer solution (pH 7) (2^{nd} cycle).

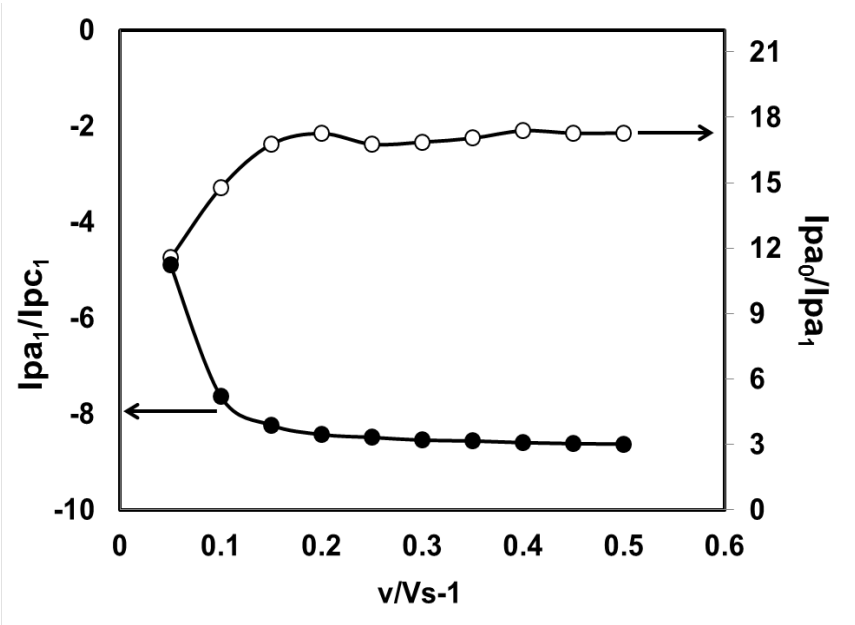

Fig. 4.44: Variation of peak current ratio of corresponding peak (I_{pa1}/I_{pc1}) and anodic peak (I_{pa0}/I_{pa1}) vs scan rate (v) of 2mM Catechol with 30mM L-Arginine of GC electrode in buffer solution (pH 7) at scan rate 0.1V/s in the second scan of potential.

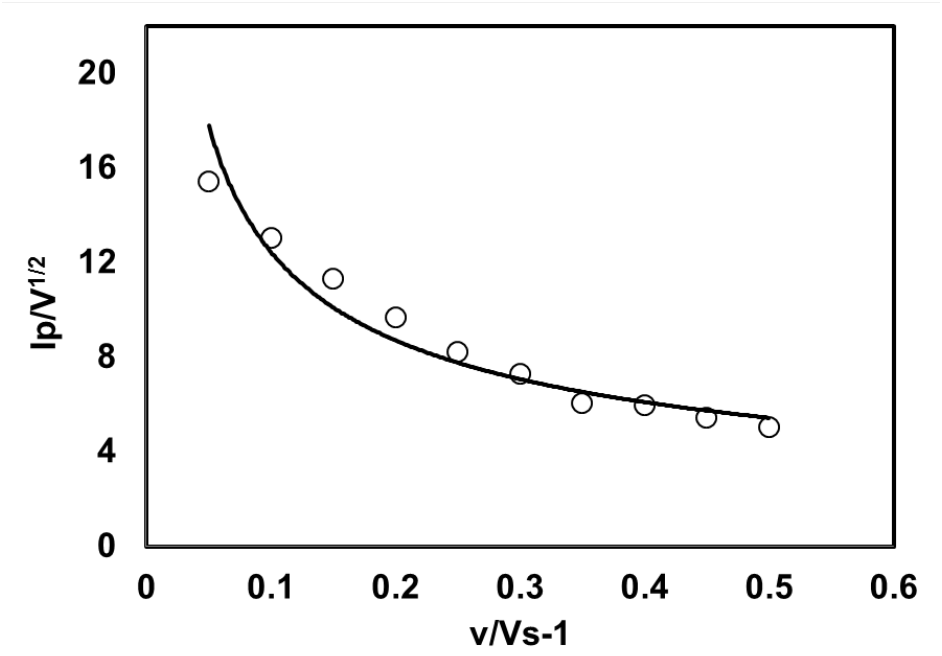

Fig.4.45: Plot of current function ($I_p/v^{1/2}$) versus scan rate (v) of 2mM Catechol with 30mM L-Arginine of GC electrode in buffer solution (pH 7) of the Appeared anodic peak(A_0).

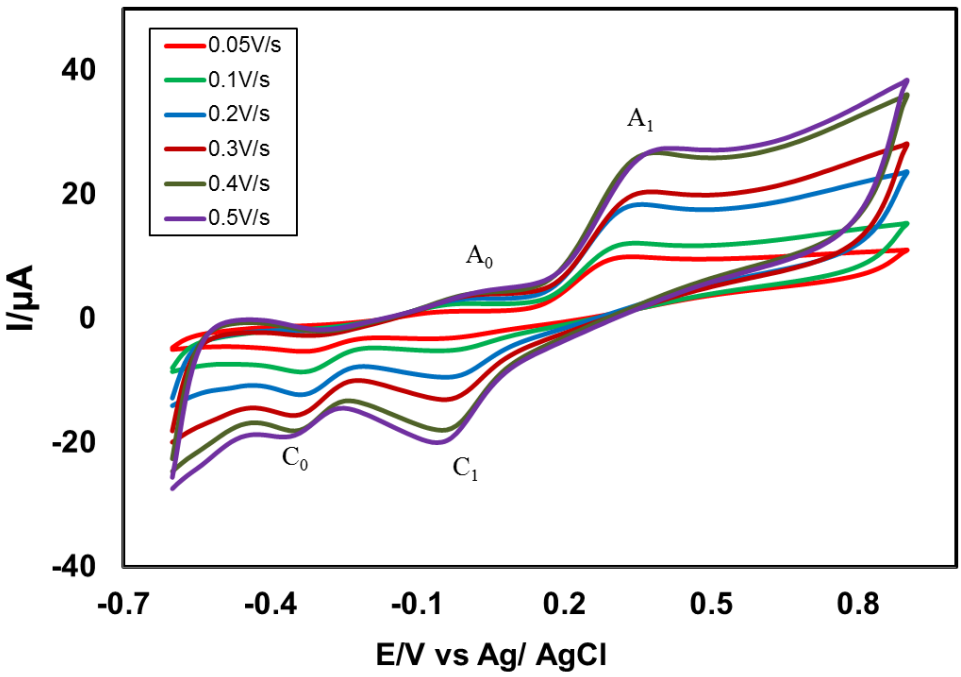

Fig. 4.46: Cyclic voltammogram of 2mM Catechol with 30mM L-Arginine in the second scan of potential at Pt electrode in buffer solution (pH 7) at scan rate 0.05V/s to 0.5V/s.

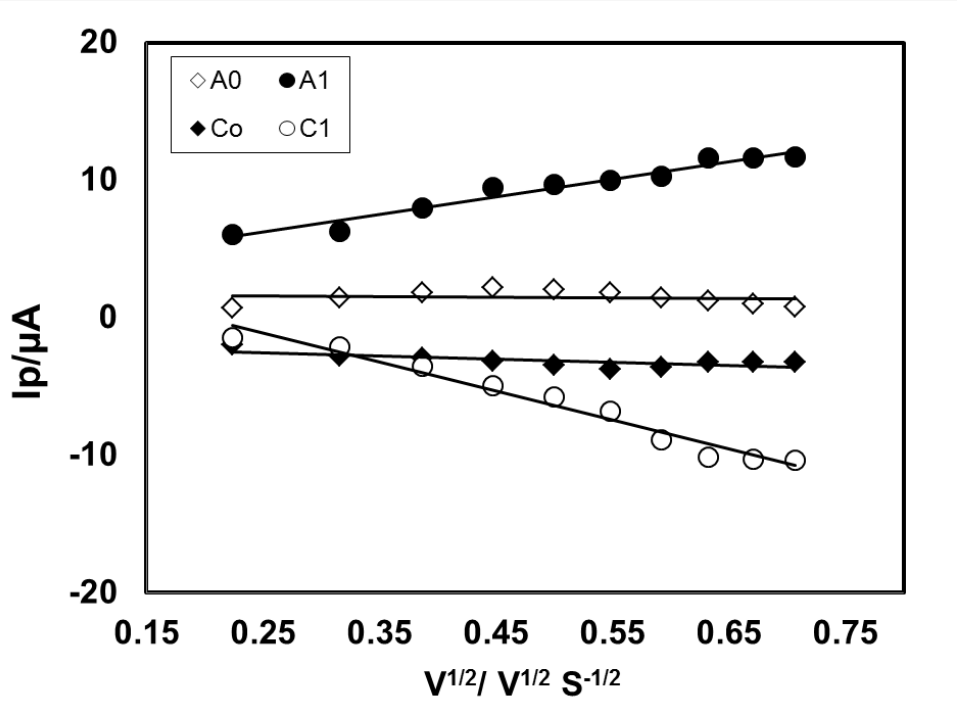

Fig. 4.47: Plots of peak current (I_p) versus square root of scan rate ($v^{1/2}$) of 2mM Catechol with 30mM L-Arginine of Pt electrode in buffer solution (pH 7) (2^{nd} cycle).

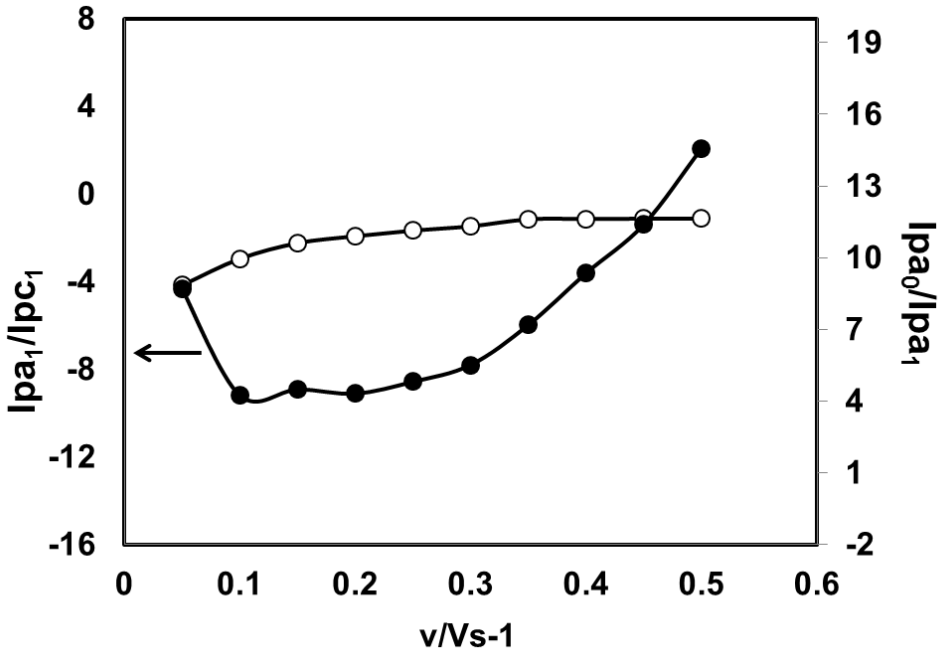

Fig. 4.48: Variation of peak current ratio of corresponding peak (I_{pa1}/I_{pc1}) and anodic peak (I_{pa0}/I_{pa1}) vs scan rate (v) of 2mM Catechol with 30mM L-Arginine of Pt electrode in buffer solution (pH 7) at scan rate 0.1V/s in the second scan of potential.

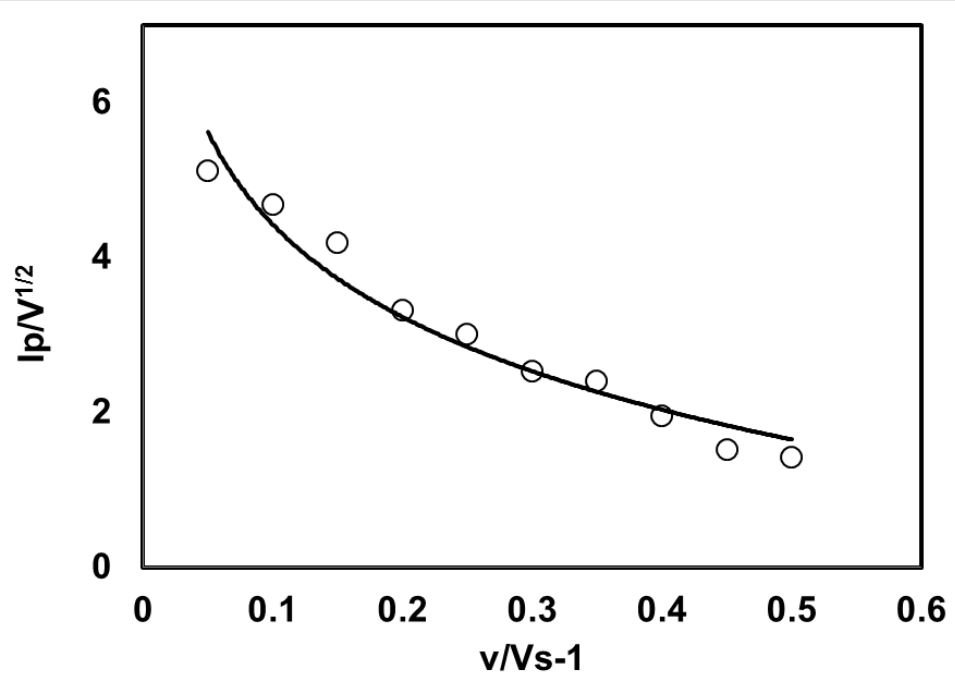

Fig. 4.49: Plots of current function ($I_p/v^{1/2}$) versus scan rate (v) of 2mM Catechol with 30mM L-Arginine of Pt electrode in buffer solution (pH 7) of the Appeared anodic peak (A_0).

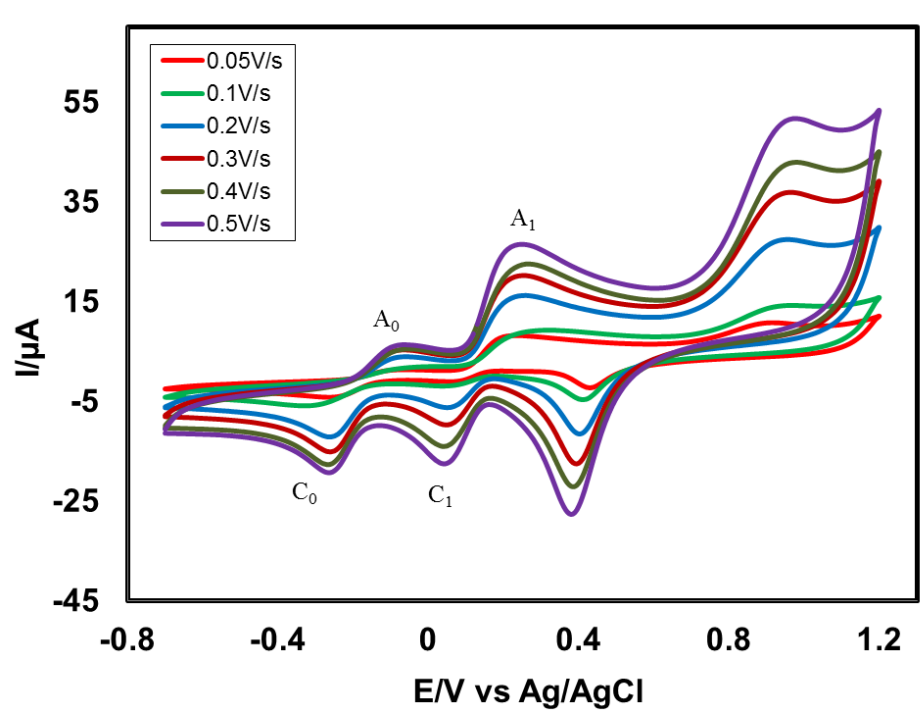

Fig. 4.50: Cyclic voltammogram of 2mM Catechol with 30mM L-Arginine in the second scan of potential at Au electrode in buffer solution (pH 7) at scan rate 0.05V/s to 0.5V/s.

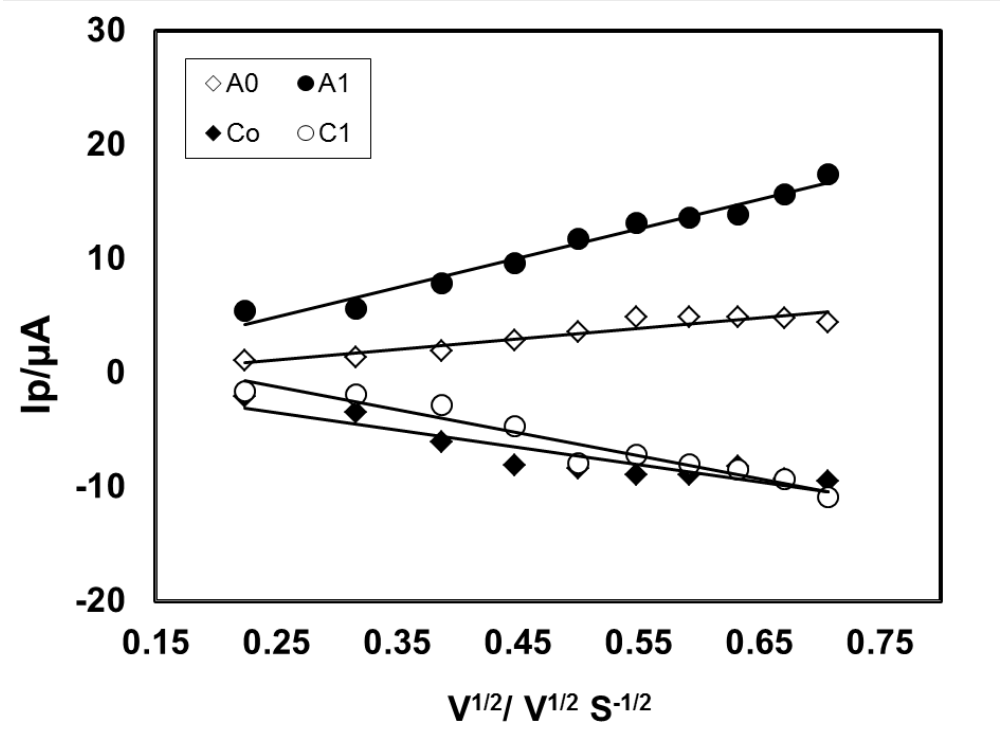

Fig. 4.51: Plots of peak current (I_p) versus square root of scan rate ($v^{1/2}$) of 2mM Catechol with 30mM L-Arginine of Au electrode in buffer solution (pH 7) (2^{nd} cycle).

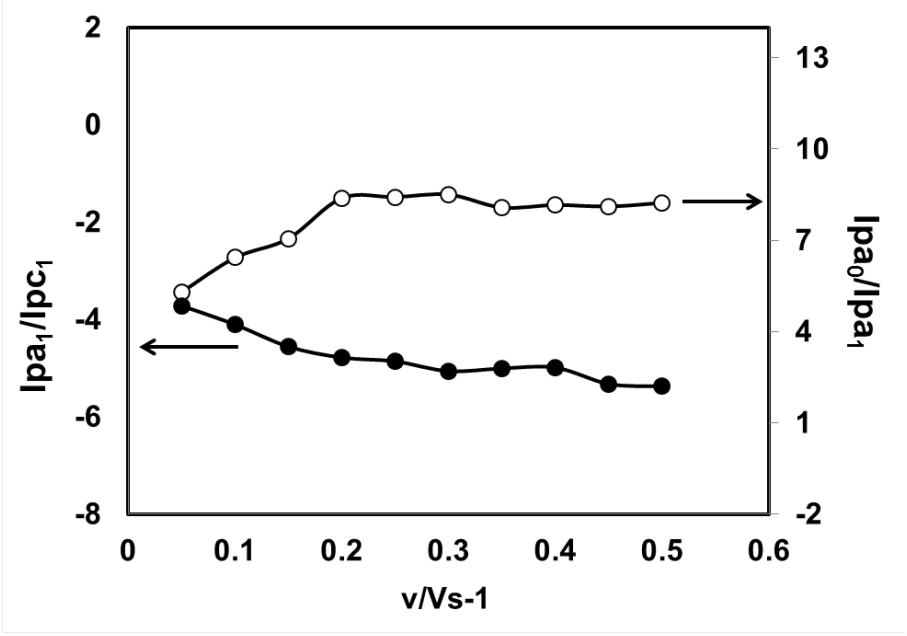

Fig. 4.52: Variation of peak current ratio of corresponding peak (I_{pa1}/I_{pc1}) and anodic peak (I_{pa0}/I_{pa1}) vs scan rate (v) of 2mM Catechol with 30mM L-Arginine of Au electrode in buffer solution (pH 7) at scan rate 0.1V/s in the second scan of potential.

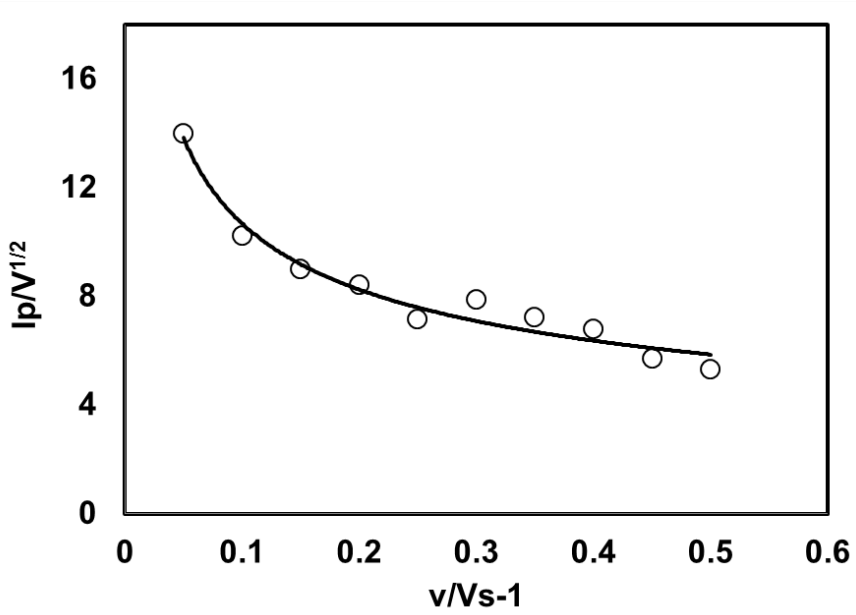

Fig. 4.53: Plots of current function ($I_p/v^{1/2}$) versus scan rate (v) of 2mM Catechol with 30mM L-Arginine of Au electrode in buffer solution (pH 7) of the Appeared anodic peak (A_0).

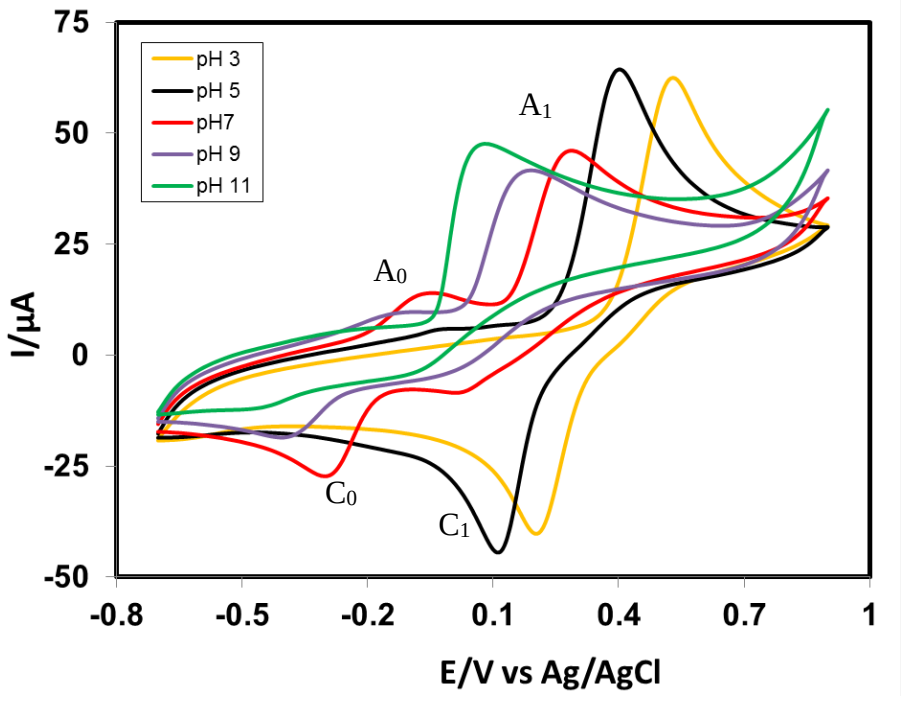

Fig. 4.54: Cyclic voltammogram of 2mM Catechol with 30mM L-Arginine of GC (3mm) electrode in different pH (3, 5, 7, 9 and 11) at scan rate 0.1V/s.

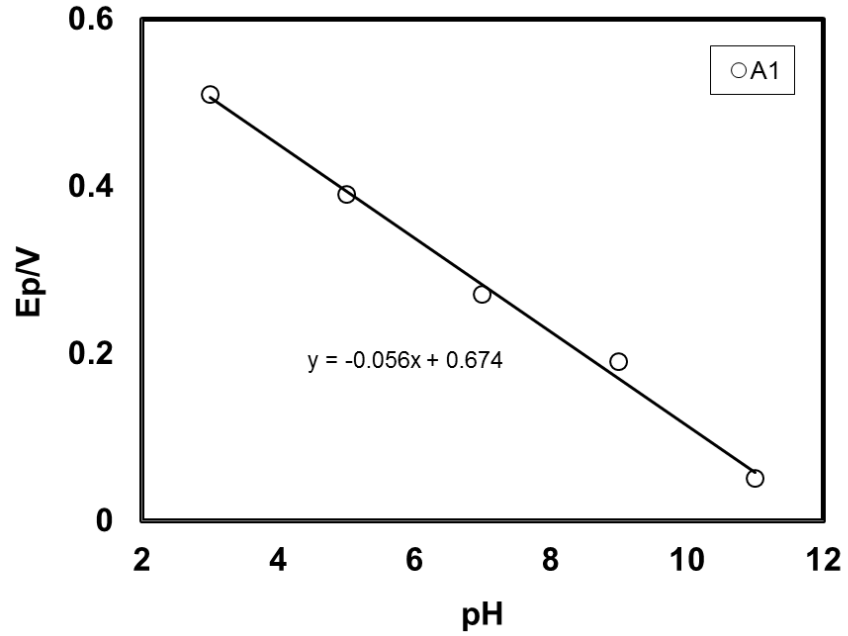

Fig. 4.55: Plots of peak potential (E_p) versus pH (3, 5, 7, 9 and 11) of 2mM Catechol with 30mM L-Arginine of GC electrode at scan rate 0.1V/s (2^{nd} cycle).

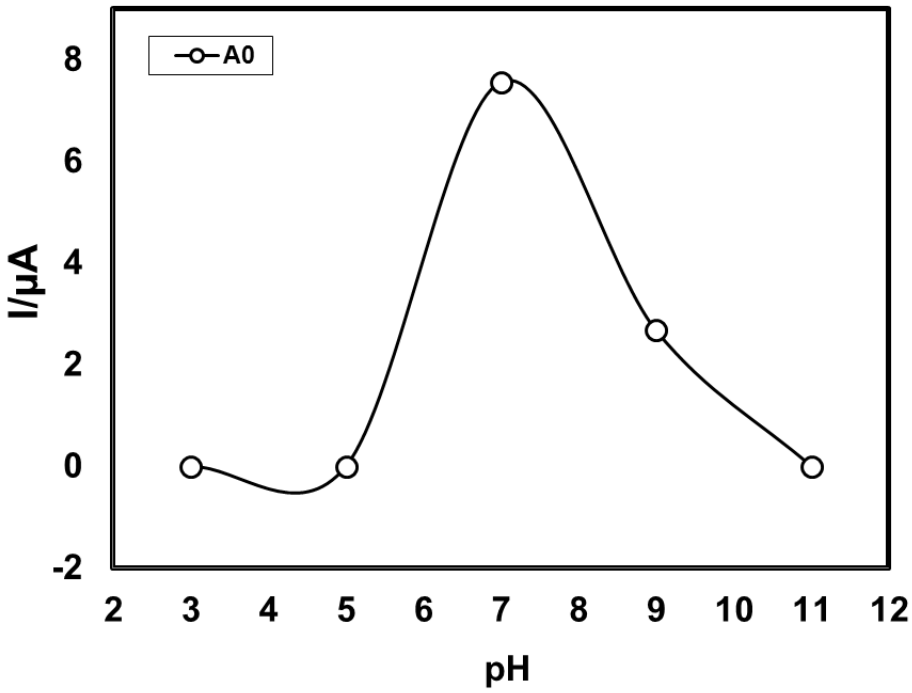

Fig. 4.56: Plot of peak current (I_p) versus pH (3, 5, 7, 9 and 11) of 2mM Catechol with 30mM L-Arginine of GC electrode at scan rate 0.1V/s (2^{nd} cycle).

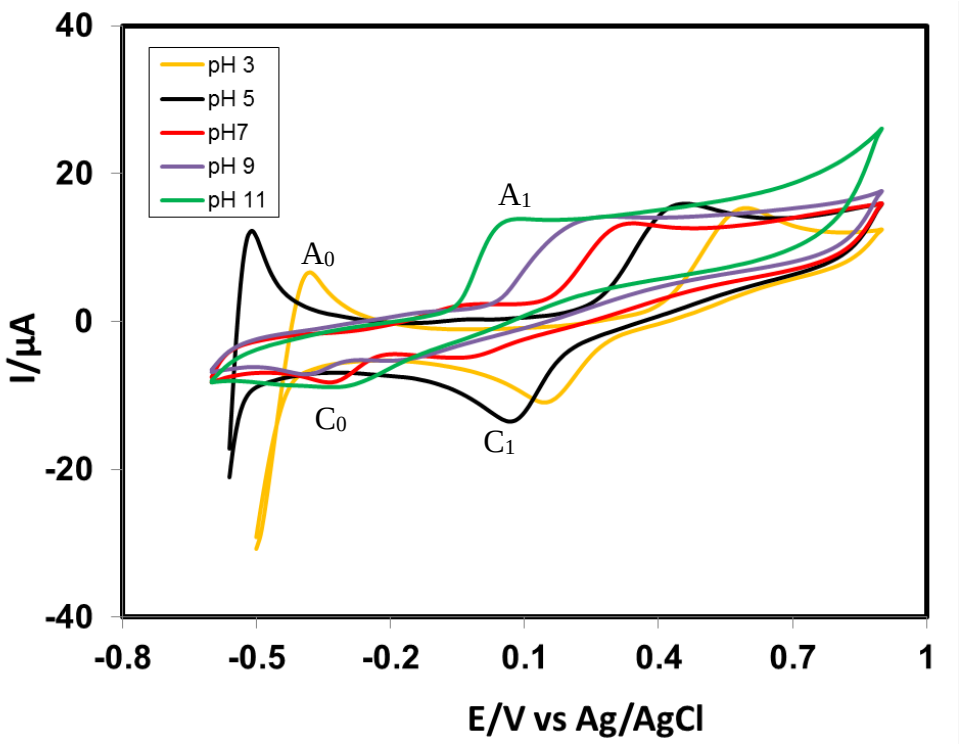

Fig. 4.57: Cyclic voltammogram of 2mM Catechol with 30mM L-Arginine of Pt electrode in different pH (3, 5, 7, 9 and 11) at scan rate 0.1V/s.

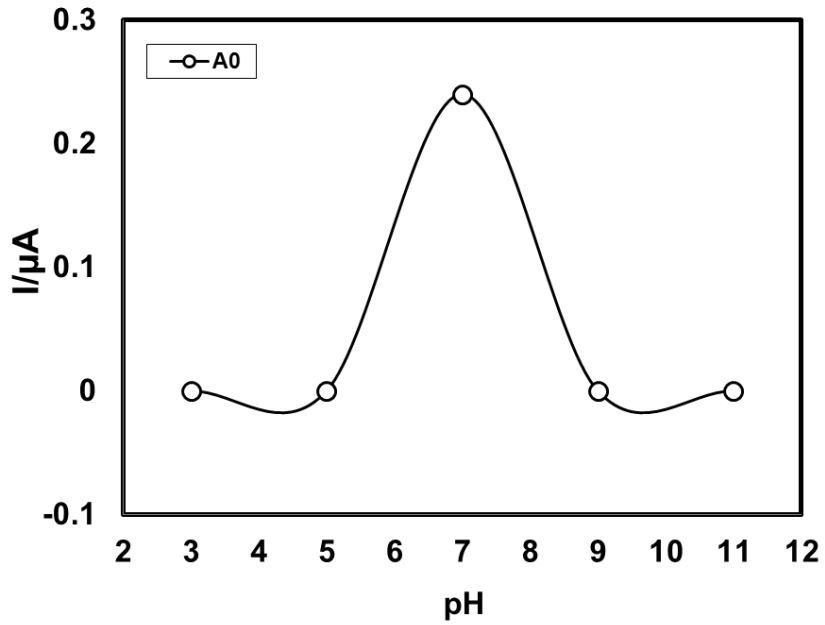

Fig. 4.58 Plots of peak current (I_p) versus pH (3, 5, 7, 9 and 11) of 2mM Catechol with 30mM L-Arginine of Pt electrode at scan rate 0.1V/s (2^{nd} cycle).

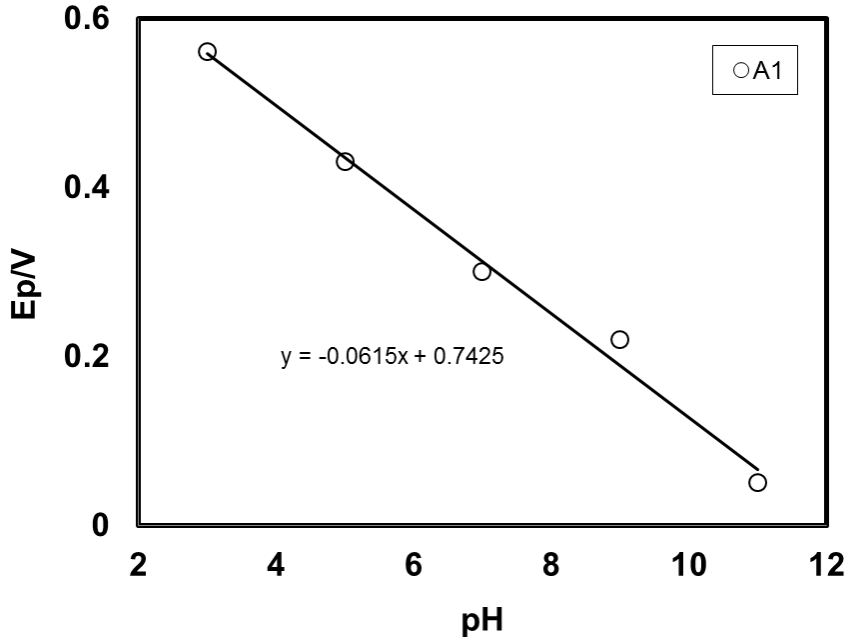

Fig. 4.59: Plot of peak potential (E_p) versus pH (3, 5, 7, 9 and 11) of 2mM Catechol with 30mM L-Arginine of Pt electrode at scan rate 0.1V/s (2nd cycle).

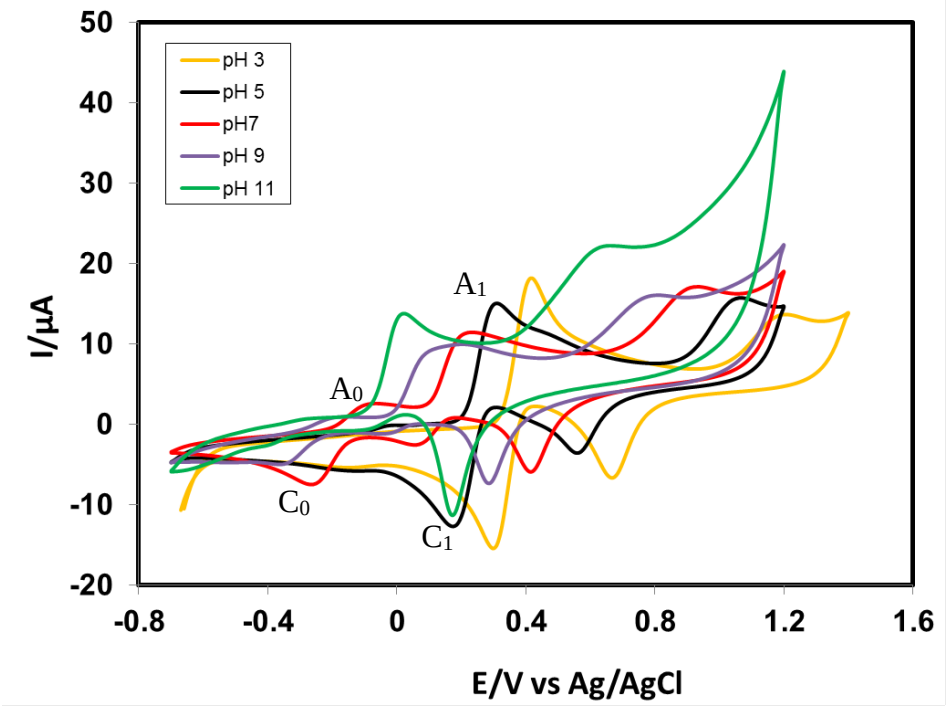

Fig. 4.60: Cyclic voltammogram of 2mM Catechol with 30mM L-Arginine of Au electrode in different pH (3, 5, 7, 9 and 11) at scan rate 0.1V/s.

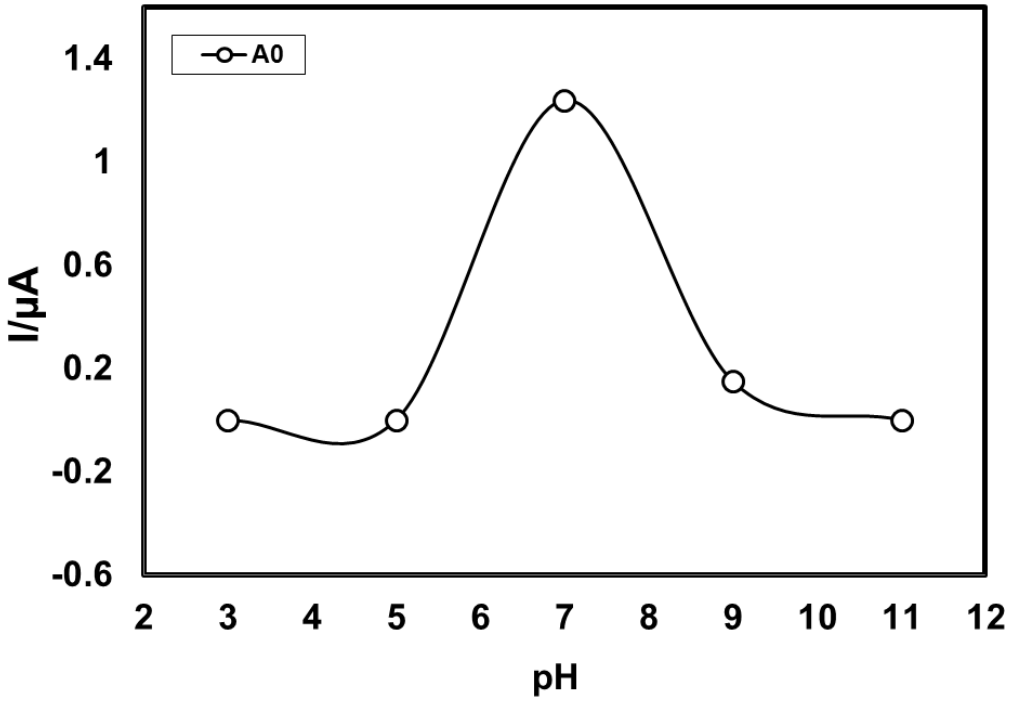

Fig. 4.61: Plots of peak current (I_p) versus pH (3, 5, 7, 9 and 11) of 2mM Catechol with 30mM L-Arginine of Au electrode at scan rate 0.1V/s (2^{nd} cycle).

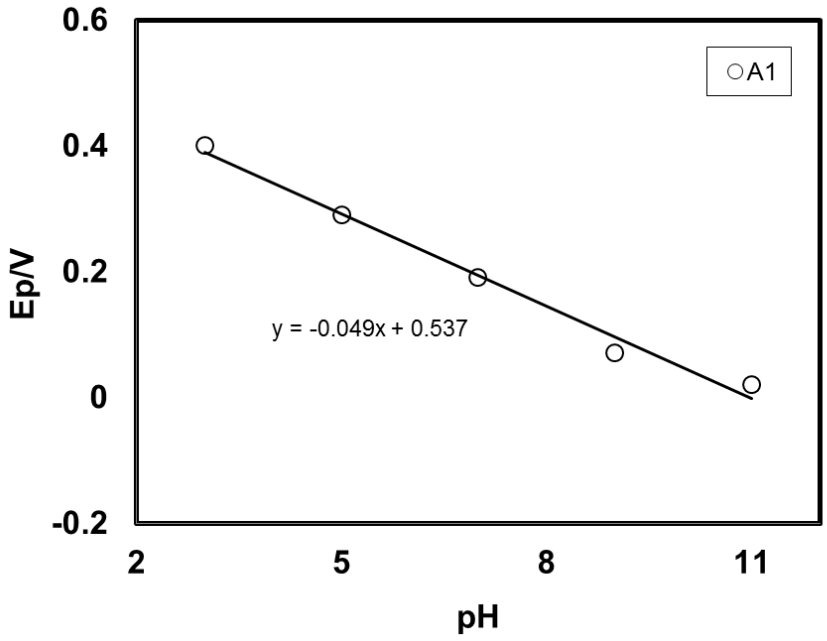

Fig. 4.62: Plot of peak potential (E_p) versus pH (3, 5, 7, 9 and 11) of 2mM Catechol with 30mM L-Arginine of Au electrode at scan rate 0.1V/s (2nd cycle).

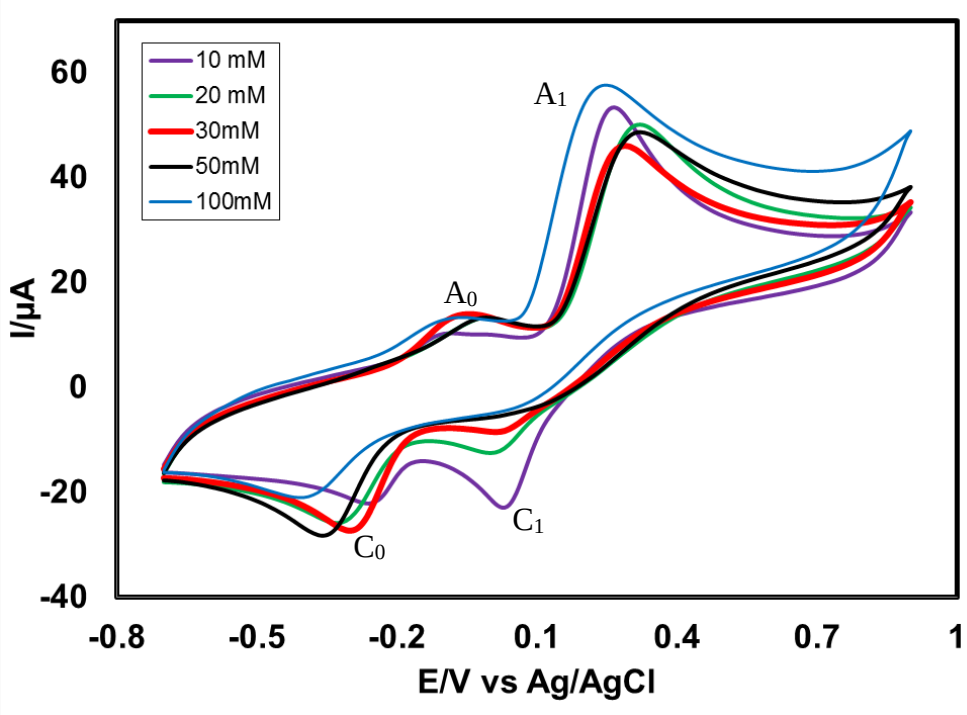

Fig. 4.63: CV of composition changes of L-Arginine (10, 20, 30, 50 and 100 mM) with fixed 2mM Catechol of GC electrode at pH 7 and scan rate 0.1V/s.

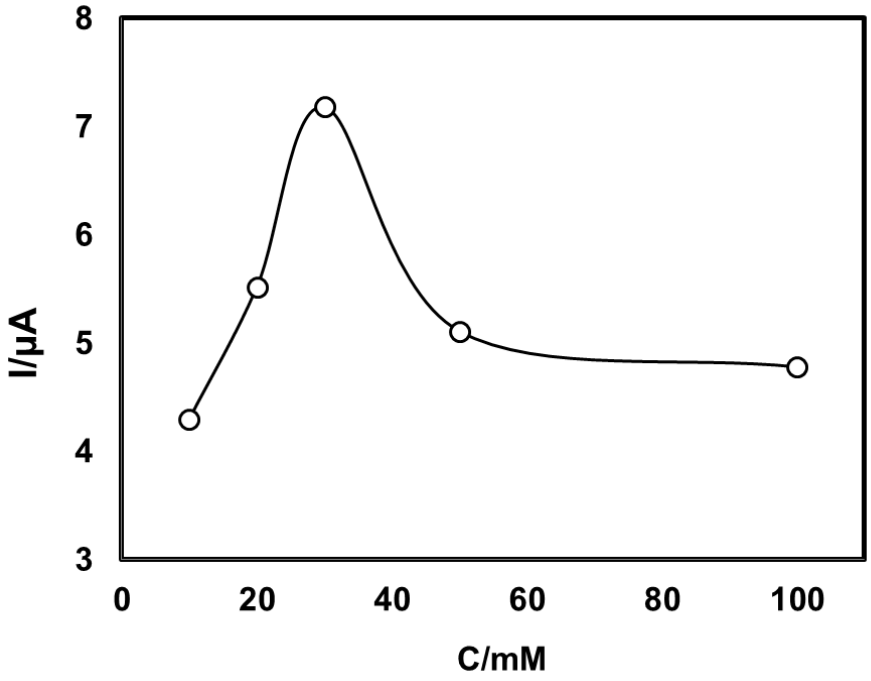

Fig. 4.64: Comparison of cyclic voltammogram of different concentration (10, 20, 30, 50 and 100 mM) of 2mM Catechol with 50mM L-Arginine of GC electrode in buffer solution (pH 7) at scan rate 0.1V/s (2nd cycle).

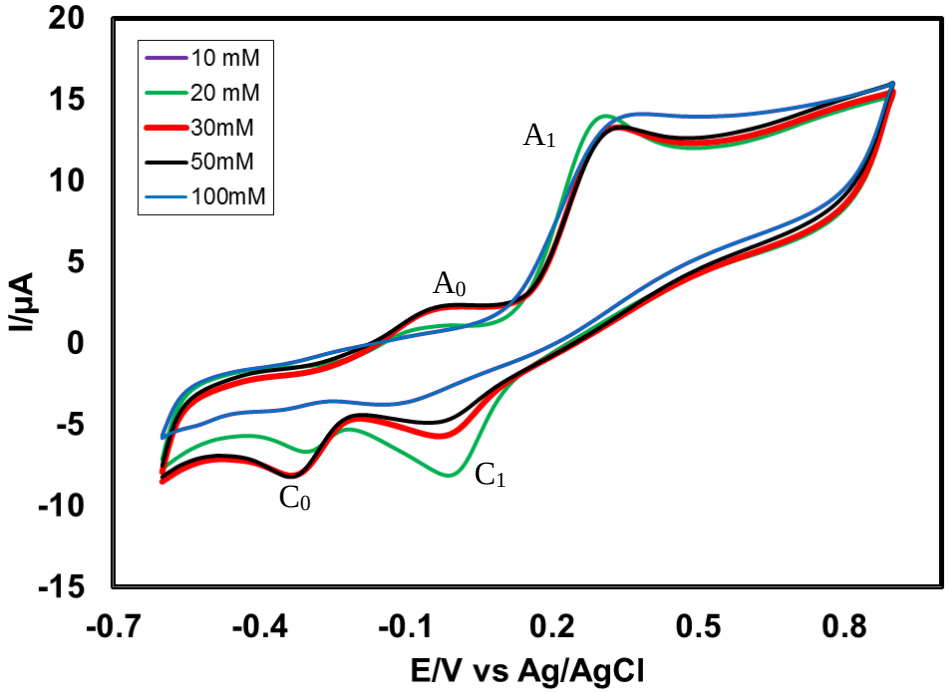

Fig. 4.65: CV of composition changes of L-Arginine (10, 20, 30, 50 and 100 mM) with fixed 2mM Catechol of Pt electrode at pH 7 and scan rate 0.1V/s.

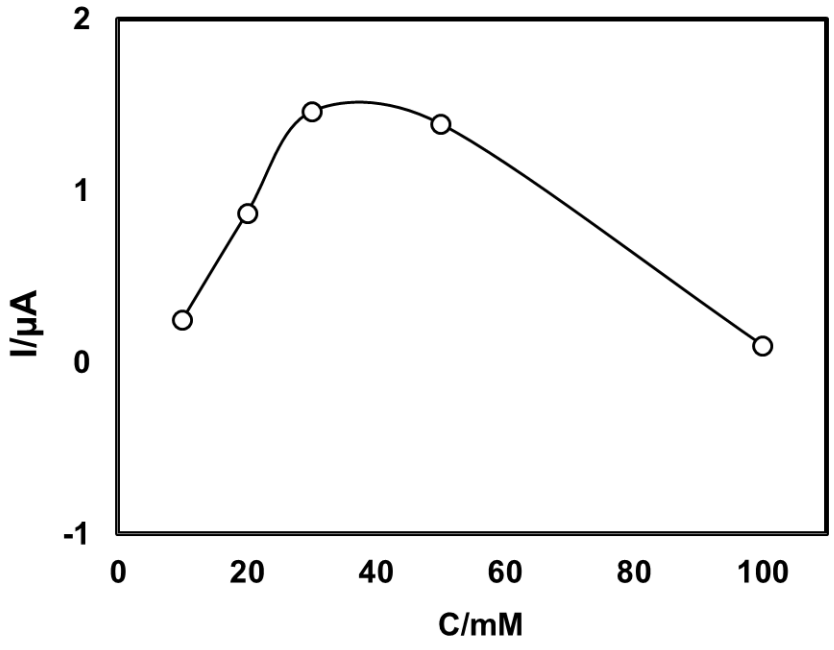

Fig. 4.66: Plots of peak current (I_p) versus concentration (C) of L-Arginine (10, 20, 30, 50 and 100 mM) with fixed 2mM Catechol of Pt electrode in buffer solution (pH) at 7 scan rate 0.1V/s (2^{nd} cycle).

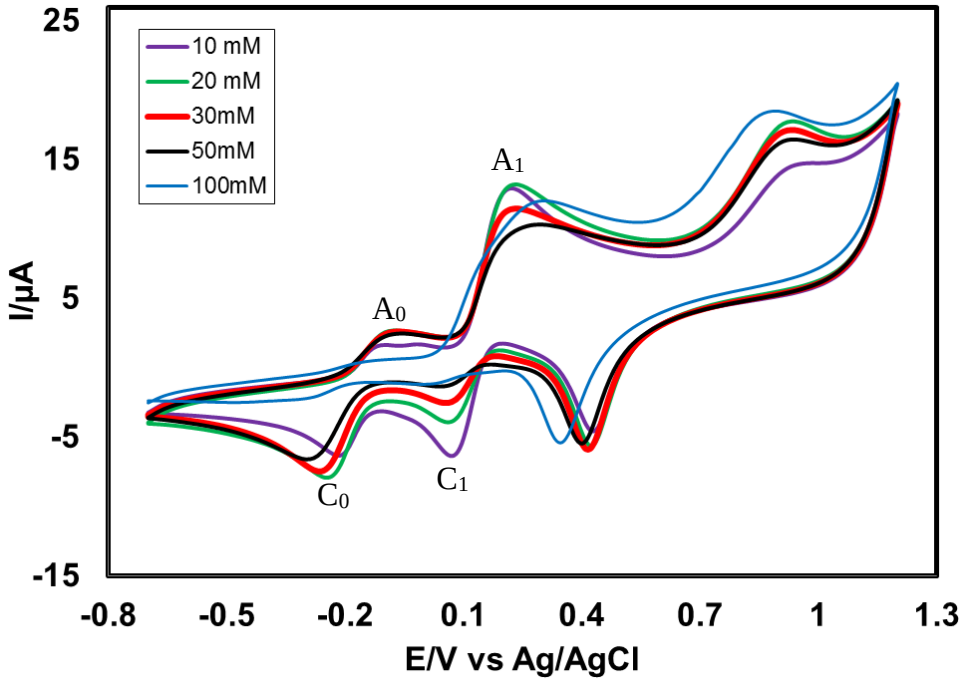

Fig. 4.67: CV of composition changes of L-Arginine (10, 20, 30, 50 and 100 mM) with fixed 2mM Catechol of Au electrode at pH 7 and scan rate 0.1V/s.

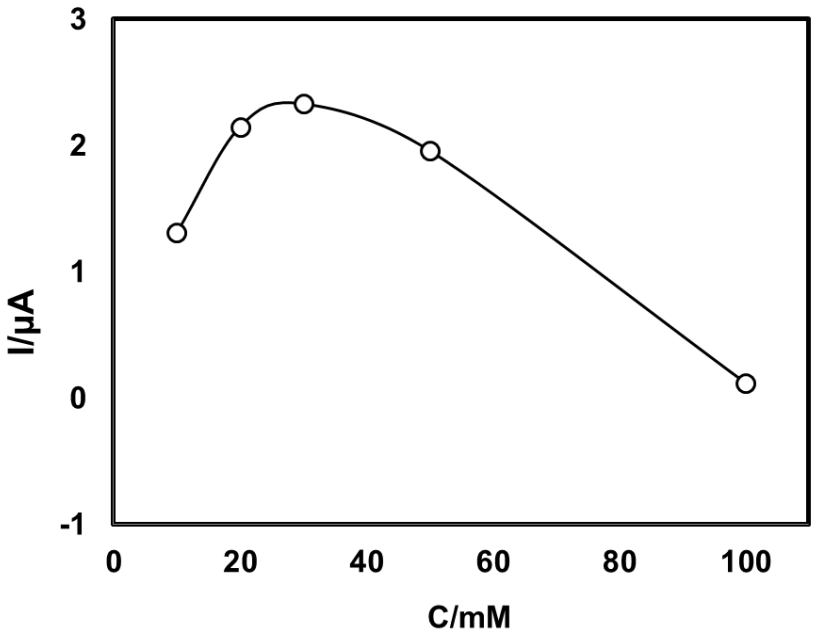

Fig. 4.68: Plots of peak current (I_p) versus concentration (C) of L-Arginine (10, 20, 30, 50 and 100 mM) with fixed 2mM Catechol of Au electrode in buffer solution (pH 3) at scan rate 0.1V/s (2^{nd} cycle).

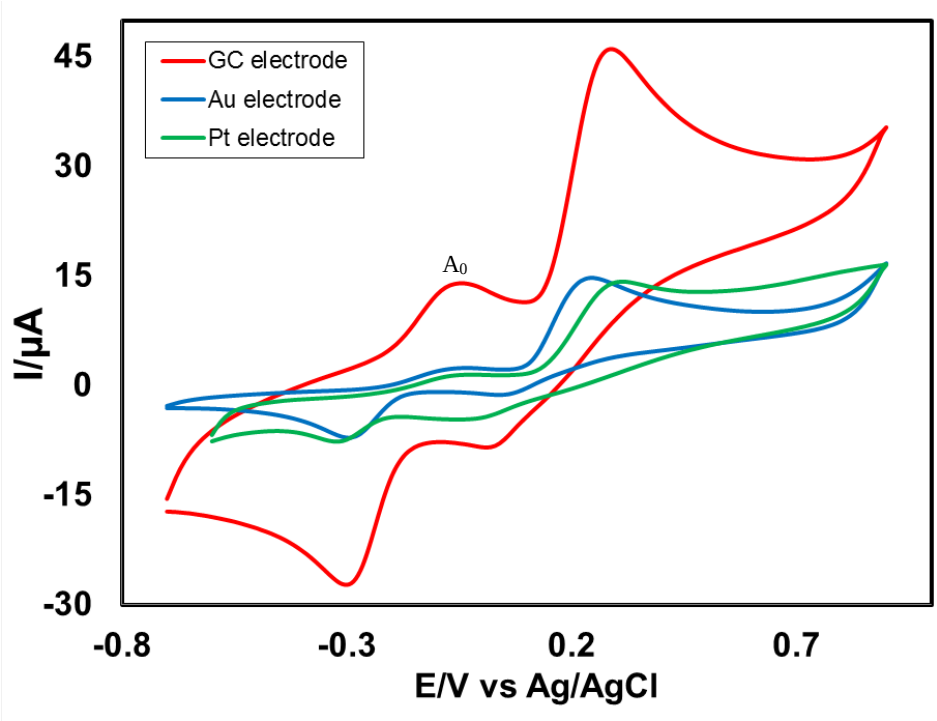

Fig. 4.69: Cyclic voltammogram (CV) of 2mM catechol with 30mM L-Arginine in GC electrode (3.0mm), Gold electrode (1.6mm) and Platinum electrode (1.6mm) at pH 7 and scan rate 0.1V/s.

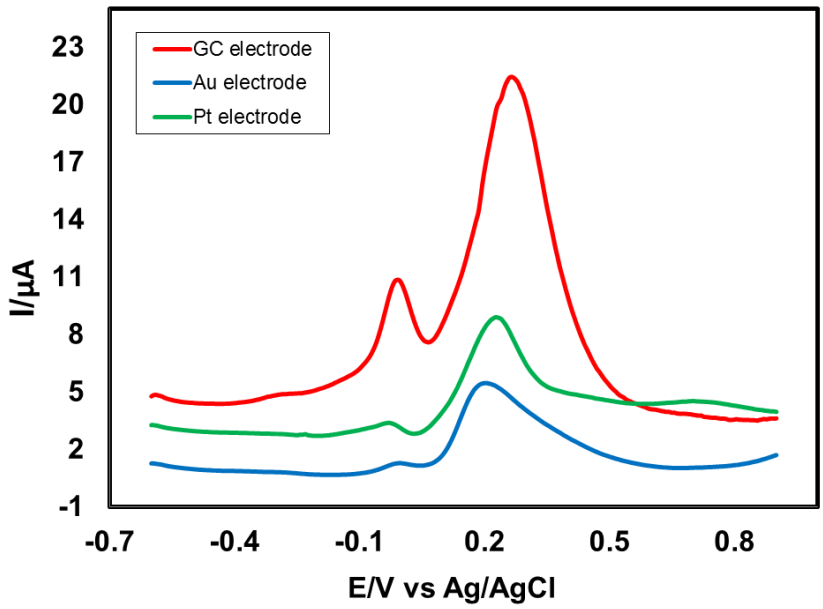

Fig. 4.70: Differential pulse voltammogram (DPV) of 2mM catechol with 30mM L-Arginine in GC electrode (3.0mm), Gold electrode (1.6mm) and Platinum electrode (1.6mm) at pH 7 and scan rate 0.1V/s.

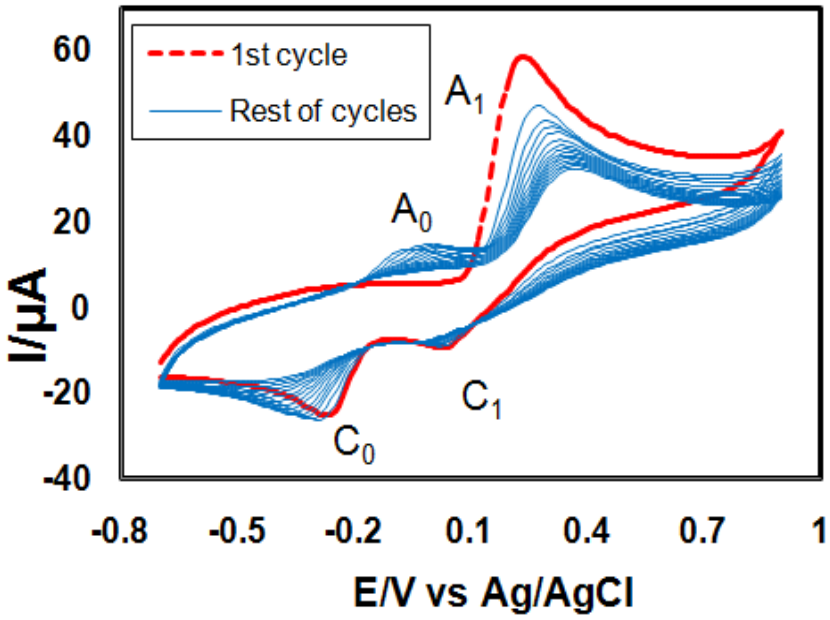

Fig. 4.71: Cyclic voltammogram of 2mM Catechol with 30mM L-Arginine of GC (3mm) electrode in the buffer solution of pH 7 at scan rate 0.1 V/s (15 cycles). The appeared anodic peak current (A_0) and cathodic peak current (C_0) increased with the iteration scan from the first cycle.

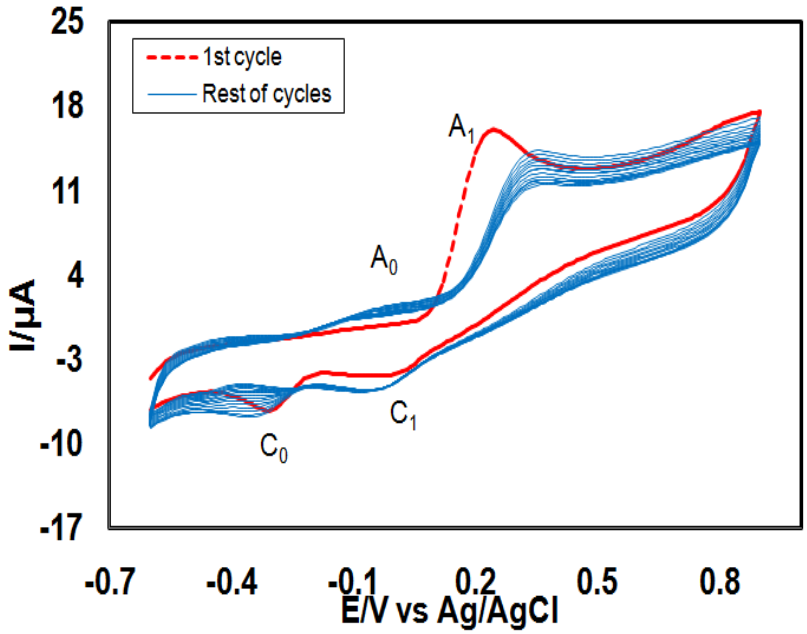

Fig. 4.72: Cyclic voltammogram of 2mM Catechol with 30mM L-Arginine of Pt electrode in the buffer solution of pH 7 at scan rate 0.1 V/s (5 cycles). The appeared anodic peak current (A_0) and cathodic peak current (C_0) increased with the iteration scan from the first cycle.

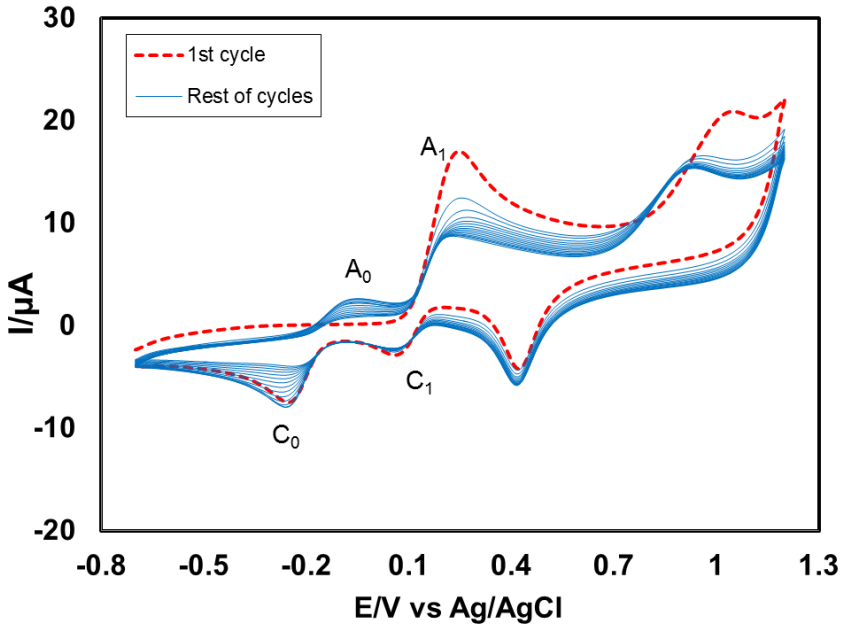

Fig. 4.73: Cyclic voltammogram of 2mM Catechol with 30mM L-Arginine of Au electrode in the buffer solution of pH 7 at scan rate 0.1 V/s (15 cycles). The appeared anodic peak current (A_0) and cathodic peak current (C_0) increased with the iteration scan from the first cycle.

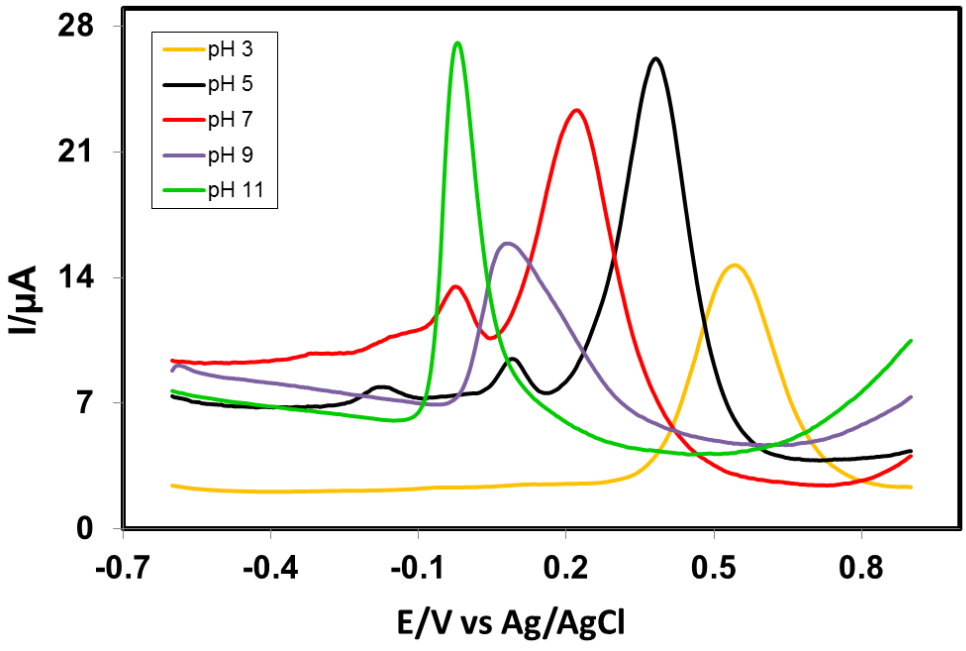

Fig. 4.74: Differential pulse voltammogram (DPV) of 2mM Catechol with 30mM L-Arginine of GC electrode in second scan of different pH (3, 5, 7, 9 and 11) and scan rate 0.1V/s.

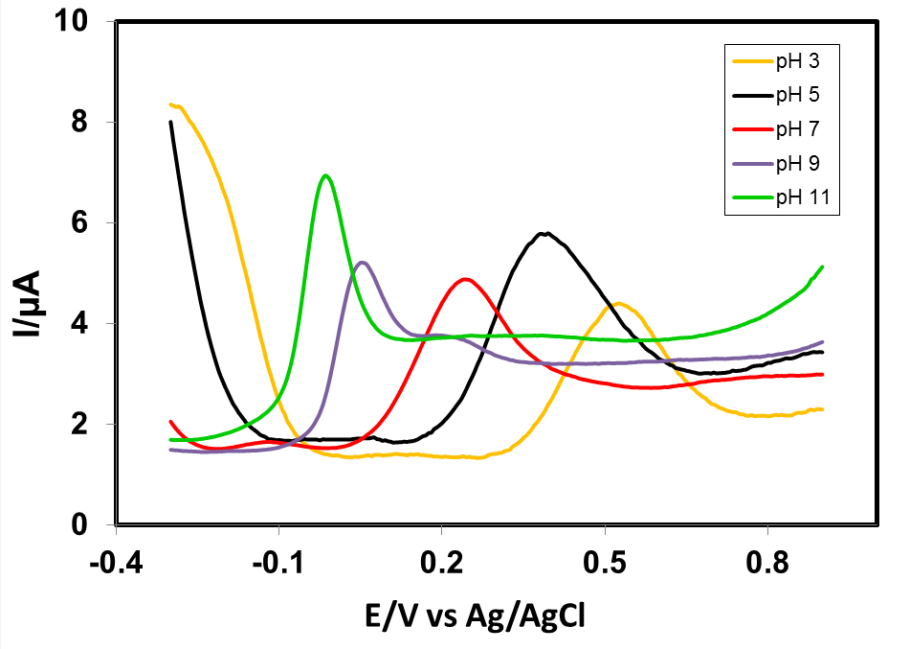

Fig. 4.75: Differential pulse voltammogram (DPV) of 2mM Catechol with 30mM L-Arginine of Pt electrode in second scans of different pH (3, 5, 7, 9 and 11) and scan rate 0.1V/s.

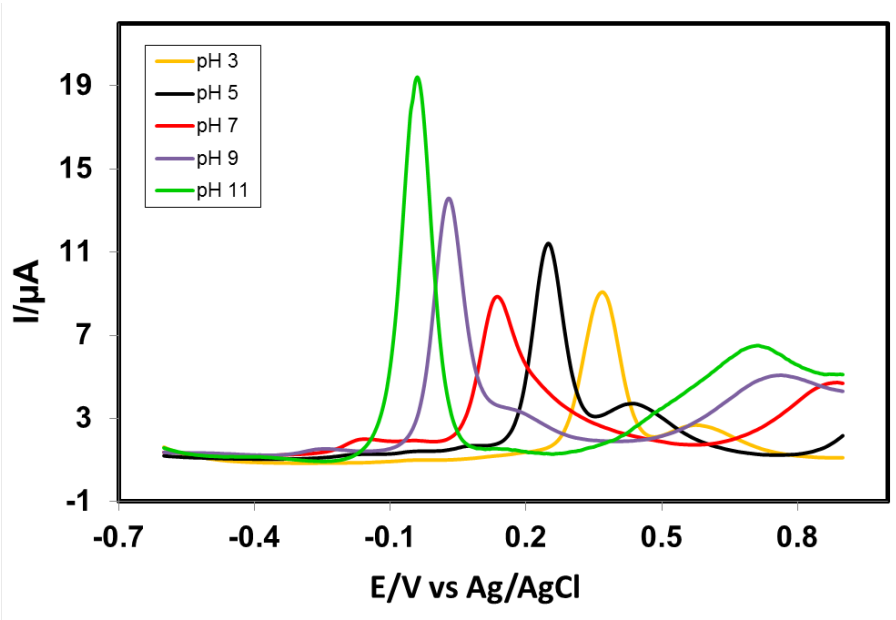

Fig. 4.76: Differential pulse voltammogram (DPV) of 2mM Catechol with 30mM L-Arginine of Au electrode in second scans of different pH (3, 5, 7, 9 and 11) and scan rate 0.1V/s.

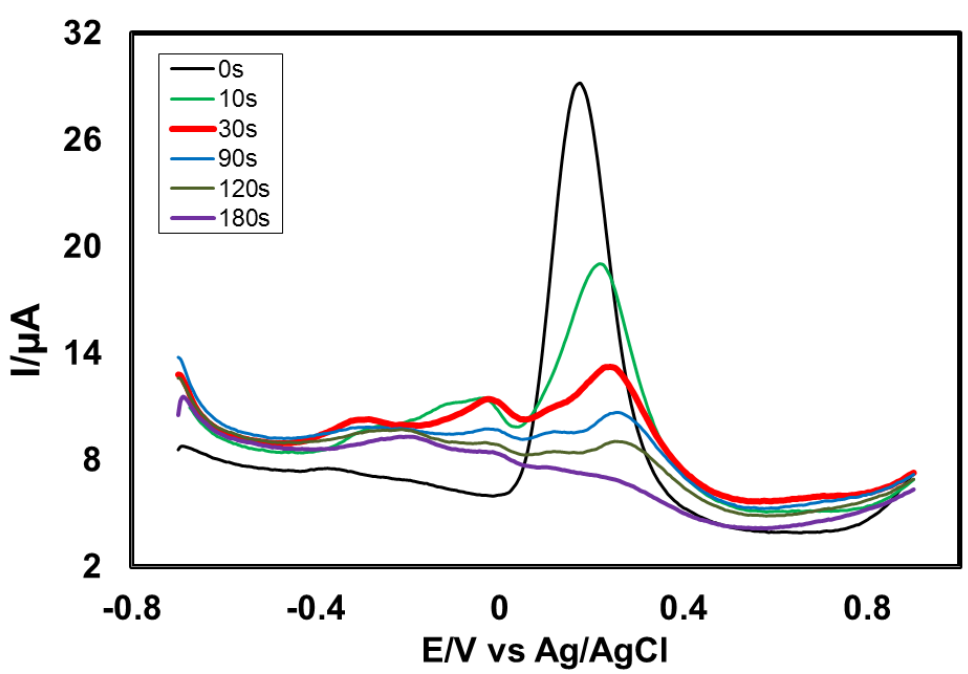

Fig. 4.77: Differential pulse voltammogram (DPV) of deposition time change (0, 10, 30, 60, 90,120 and 180s) of 2mM catechol with 30mM L-Arginine of pH 7 at *E*puls 0.02V, tpuls 20ms and scan rate 0.1Vs^{-1}.

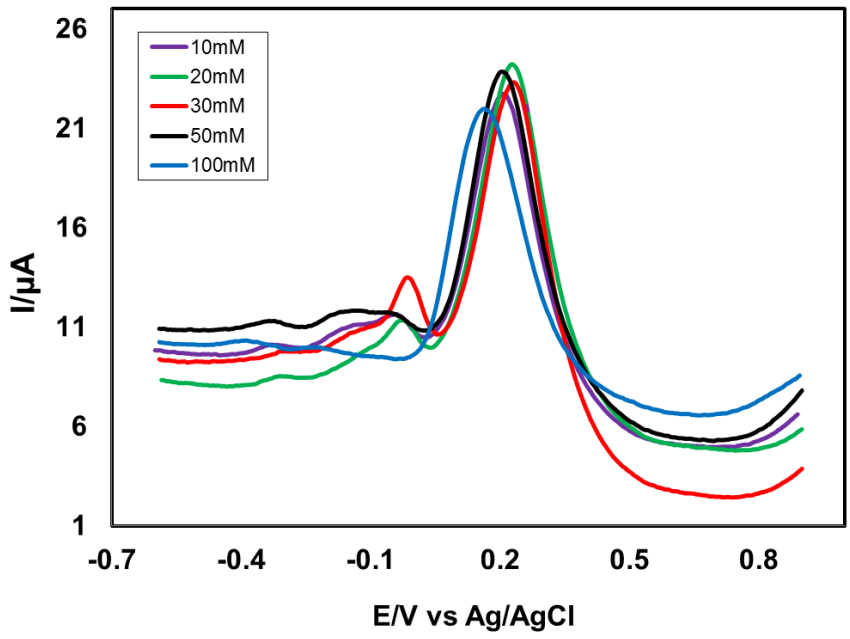

Fig. 4.78: Differential pulse voltammogram (DPV) of composition change of L-Arginine (10, 20, 30, 50 and 100 mM) with the fixed composition of 2 mM Catechol in second scan of pH7 at *E*puls 0.02V, tpuls 20ms of GC electrode and scan rate 0.1Vs^{-1}.

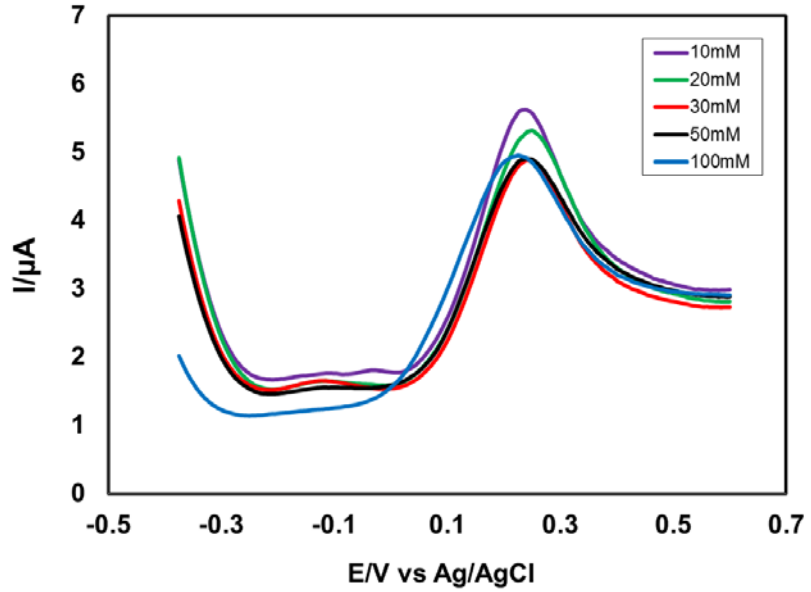

Fig. 4.79: Differential pulse voltammogram (DPV) of composition change of L-Arginine (10, 20, 30, 50 and 100 mM) with the fixed composition of 2 mM Catechol in second scan of pH 7 at *E*puls 0.02V, tpuls 20ms of Pt electrode and scan rate 0.1Vs^{-1}.

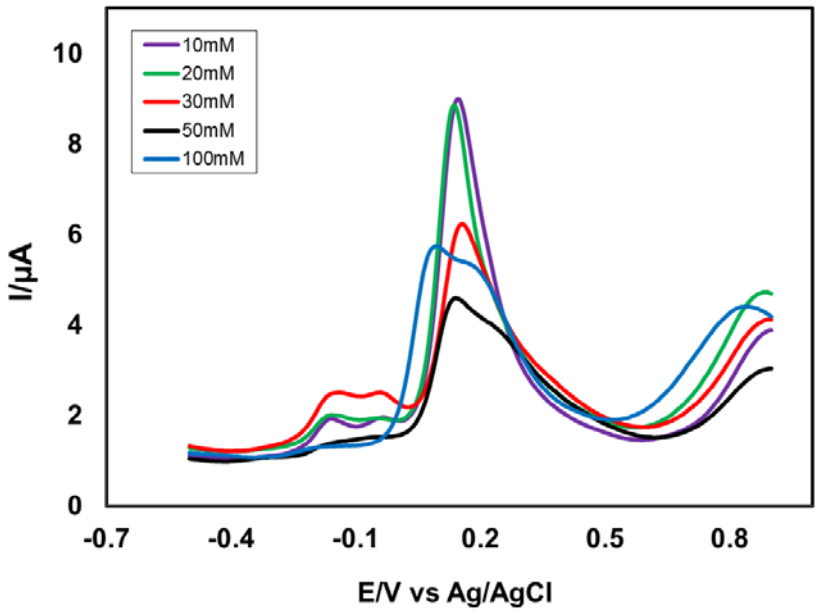

Fig. 4.80: Differential pulse voltammogram (DPV) of composition change of L-Arginine (10, 20, 30, 50 and 100 mM) with the fixed composition of 2 mM Catechol in second scan of pH7 at *E*puls 0.02V, tpuls 20ms of Au electrode and scan rate 0.1Vs^{-1}.

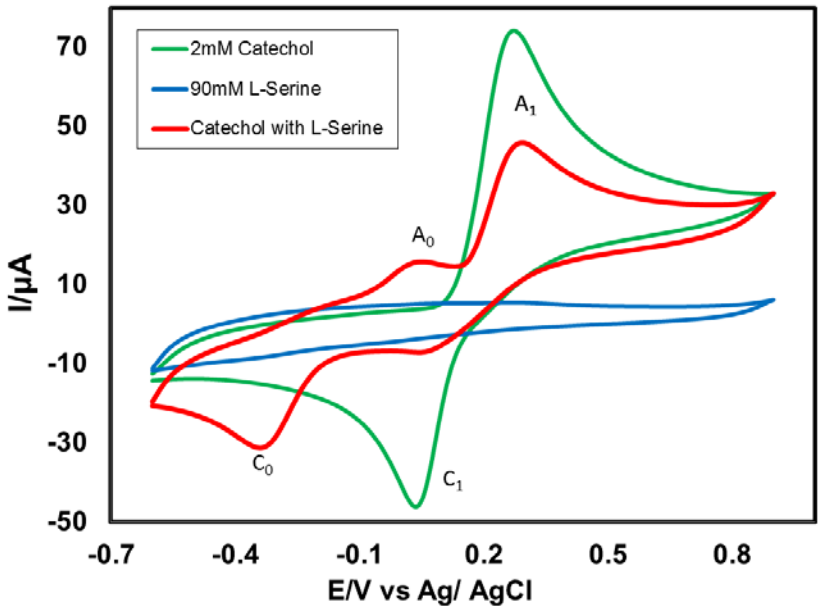

Fig. 4.81: Cyclic voltammogram of 2mM Catechol , 90mM L-Serine and 2mM Catechol with 90mM L-Serine of GC electrode in buffer solution (pH 7) at scan rate 0.1V/s (2nd cycle). A_0 and A_1 is appeared anodic peak and anodic peak, C_0 and C_1 is corresponding cathodic peak.

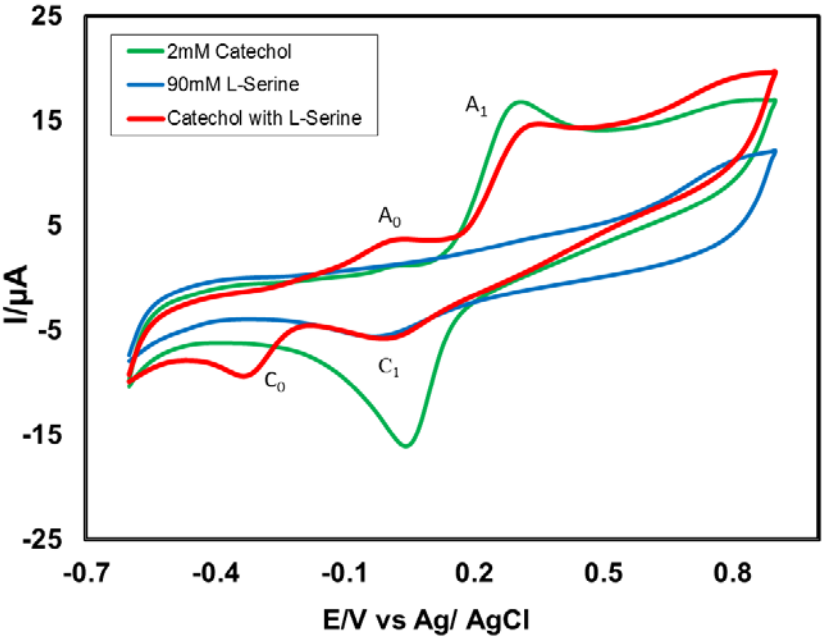

Fig. 4.82: Cyclic voltammogram of 2mM Catechol (dashed line), 90mM L-Serine (solid line) and 2mM Catechol with 90mM L-Serine (deep solid line) of Pt electrode in buffer solution (pH 7) at scan rate 0.1V/s (2nd cycle). A_0 and A_1 is appeared anodic peak and anodic peak, C_0 and C_1 is corresponding cathodic peak.

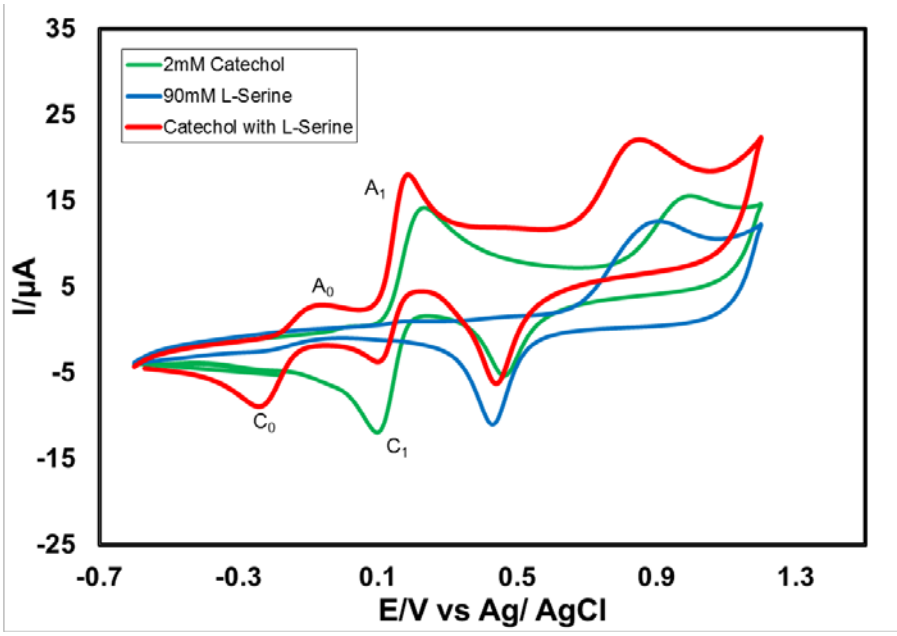

Fig. 4.83: Cyclic voltammogram of 2mM Catechol , 90mM L-Serine and 2mM Catechol with 90mM L-Serine of Au electrode in buffer solution (pH 7) at scan rate 0.1V/s (2nd cycle). A_0 and A_1 is appeared anodic peak and anodic peak, C_0 and C_1 is corresponding cathodic peak.

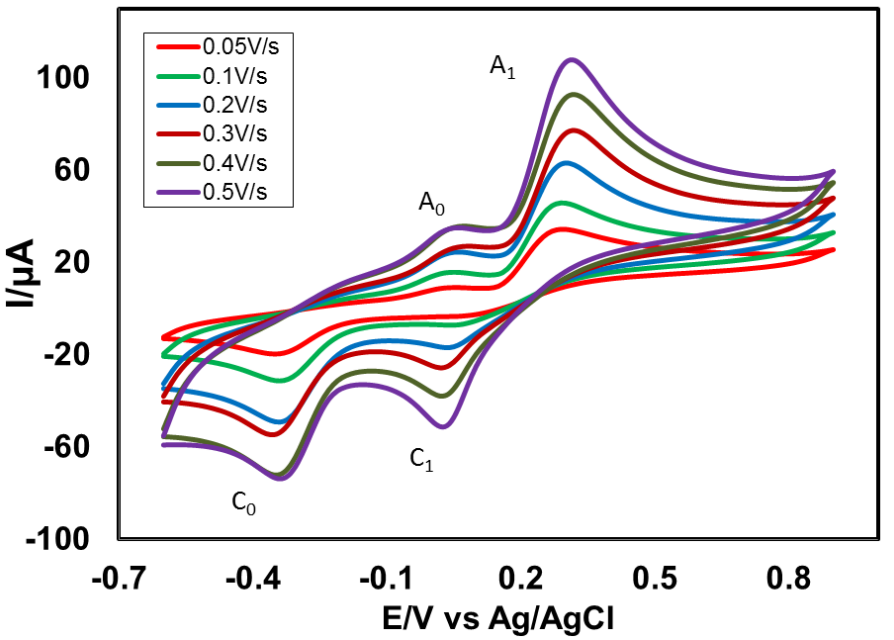

Fig. 4.84: Cyclic voltammogram of 2mM Catechol with 90mM L-Serine in the second scan of potential at GC electrode in buffer solution (pH 7) at scan rate 0.05V/s to 0.5V/s.

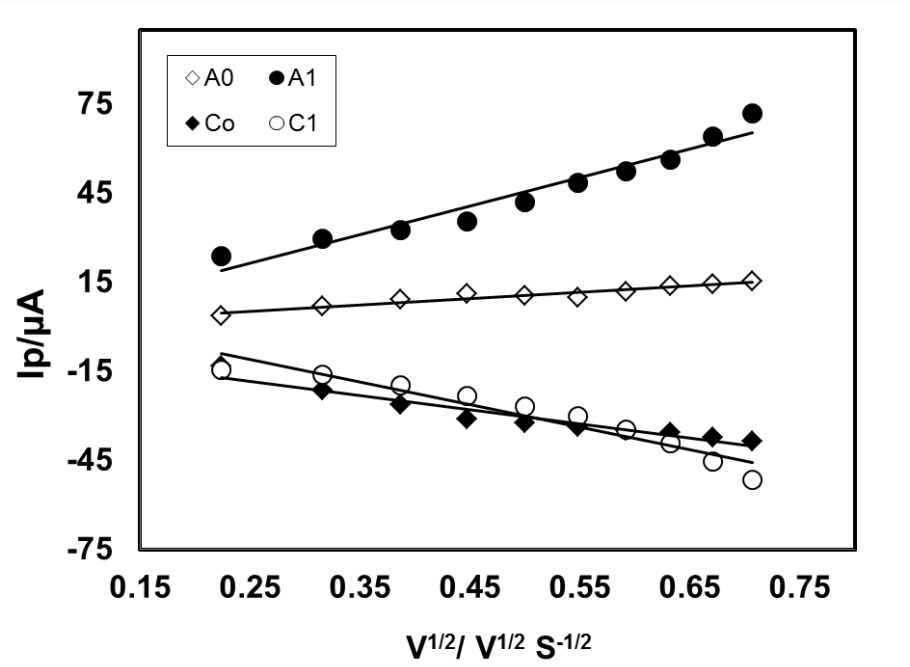

Fig. 4.85: Plots of peak current (I_p) versus square root of scan rate ($v^{1/2}$) of 2mM Catechol with 90mM L-Serine of GC electrode in buffer solution (pH 7) (2^{nd} cycle).

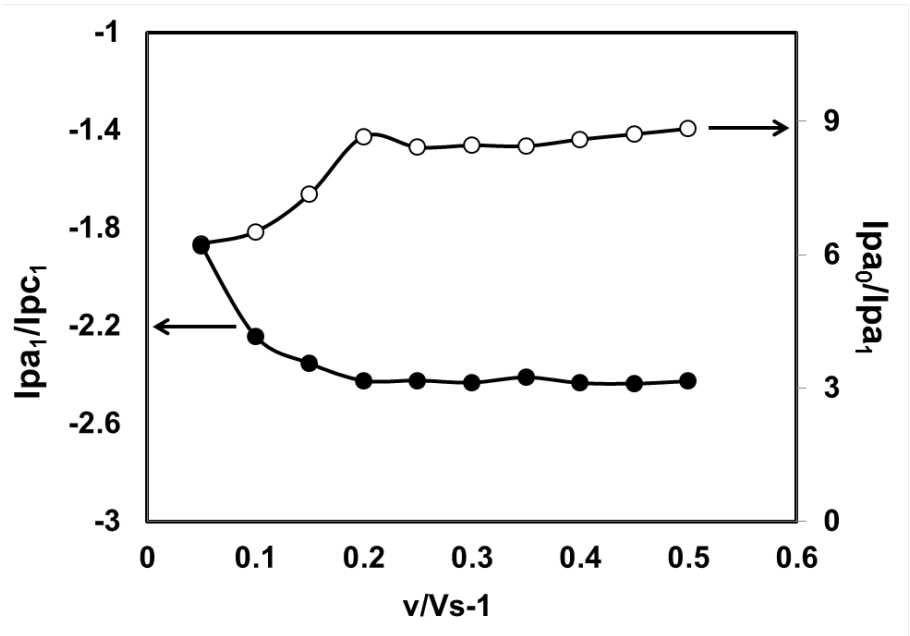

Fig. 4.86: Variation of peak current ratio of corresponding peak (I_{pa1}/I_{pc1}) and anodic peak (I_{pa0}/I_{pa1}) vs scan rate (v) of 2mM Catechol with 90mM L-Serine of GC electrode in buffer solution (pH 7) at scan rate 0.1V/s in the second scan of potential.

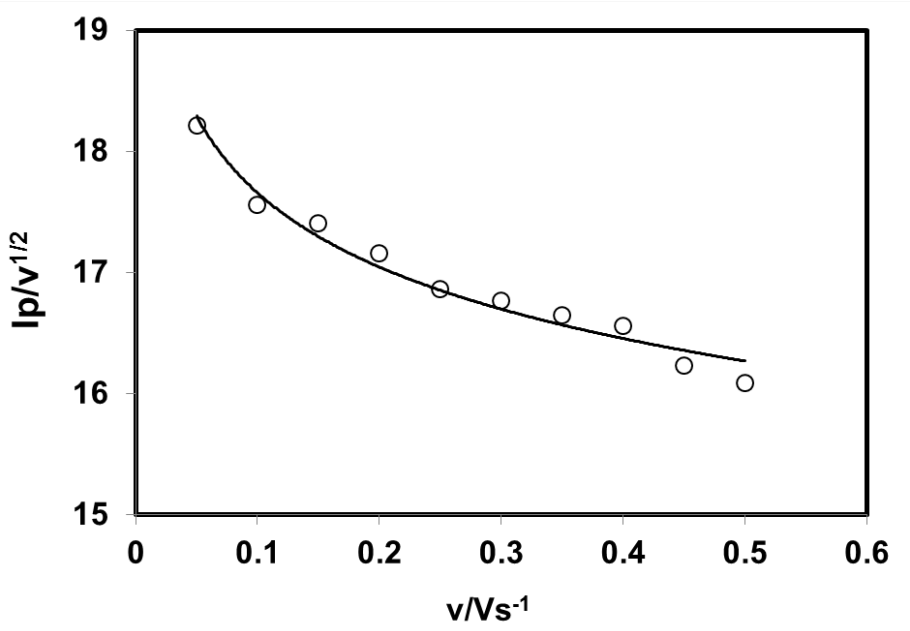

Fig. 4.87: Plot of current function ($I_p/v^{1/2}$) versus scan rate (v) of 2mM Catechol with 20mM L-Serine of GC electrode in buffer solution (pH 7) of the Appeared anodic peak (A_0).

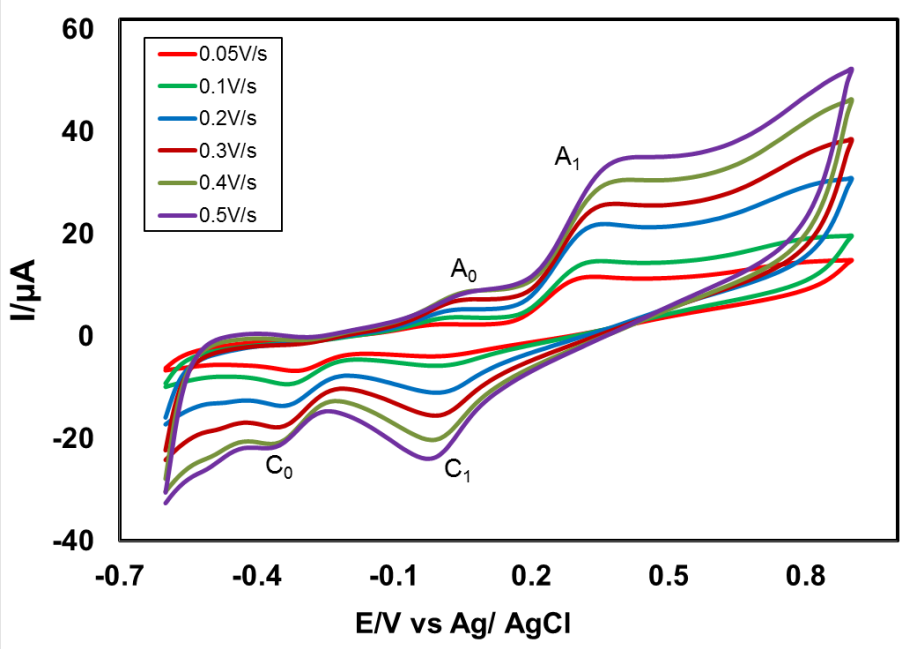

Fig. 4.88: Cyclic voltammogram of 2mM Catechol with 90mM L-Serine in the second scan of potential at Pt electrode in buffer solution (pH 7) at scan rate 0.05V/s to 0.5V/s.

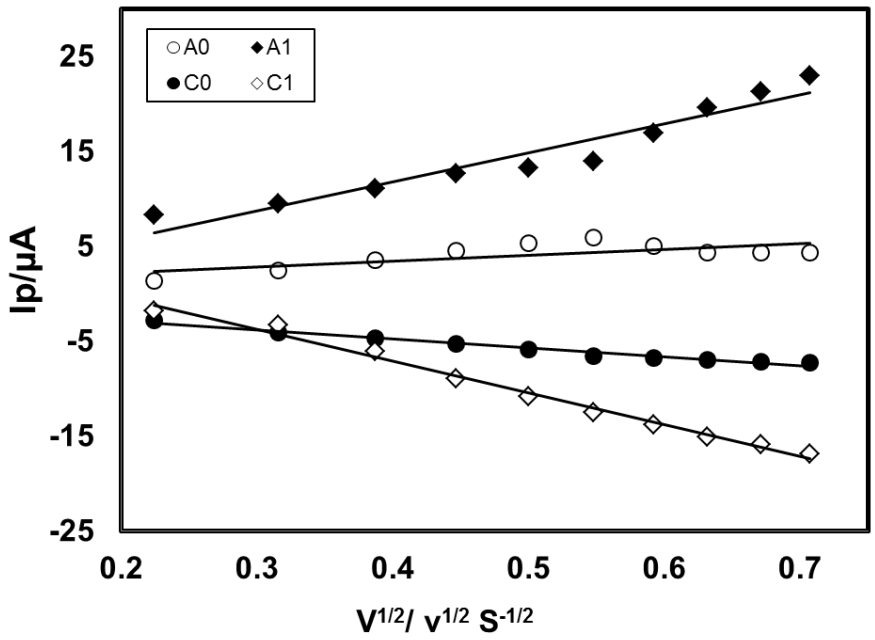

Fig. 4.89: Plots of peak current (I_p) versus square root of scan rate ($v^{1/2}$) of 2mM Catechol with 90mM L-Serine of Pt electrode in buffer solution (pH 7) (2^{nd} cycle).

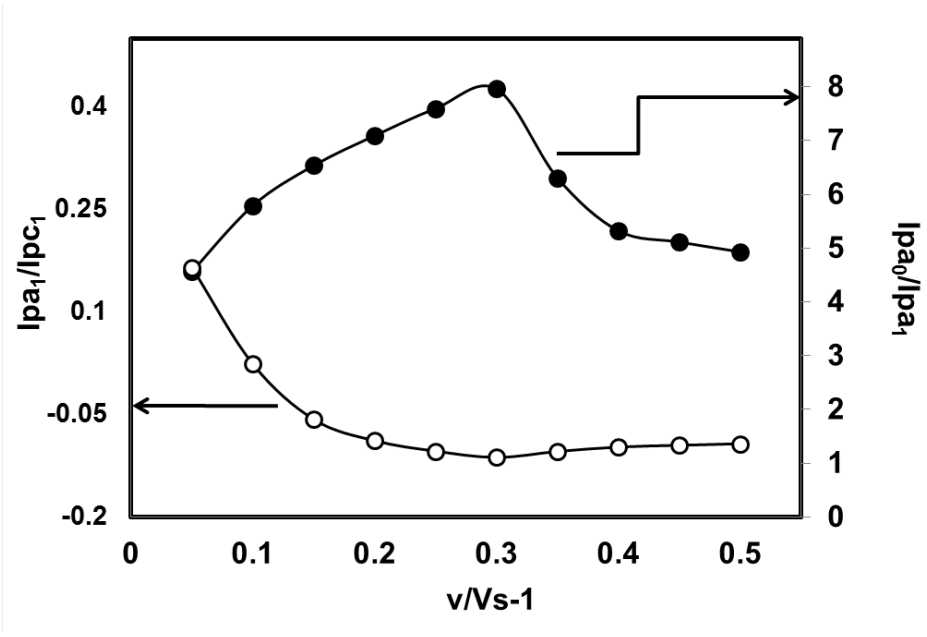

Fig. 4.90: Variation of peak current ratio of corresponding peak (I_{pa1}/I_{pc1}) and anodic peak (I_{pa0}/I_{pa1}) vs scan rate (v) of 2mM Catechol with 90mM L-Serine of Pt electrode in buffer solution (pH 7) at scan rate 0.1V/s in the second scan of potential.

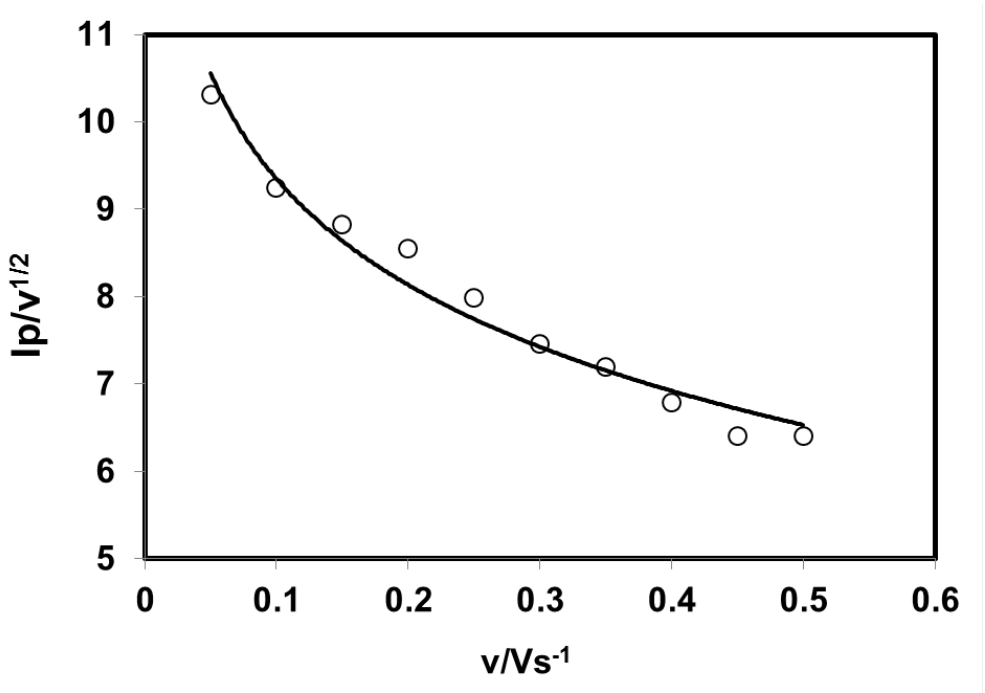

Fig. 4.91: Plots of current function ($I_p/v^{1/2}$) versus scan rate (v) of 2mM Catechol with 90mM L-Serine of Pt electrode in buffer solution (pH 7) of the Appeared anodic peak (A_0).

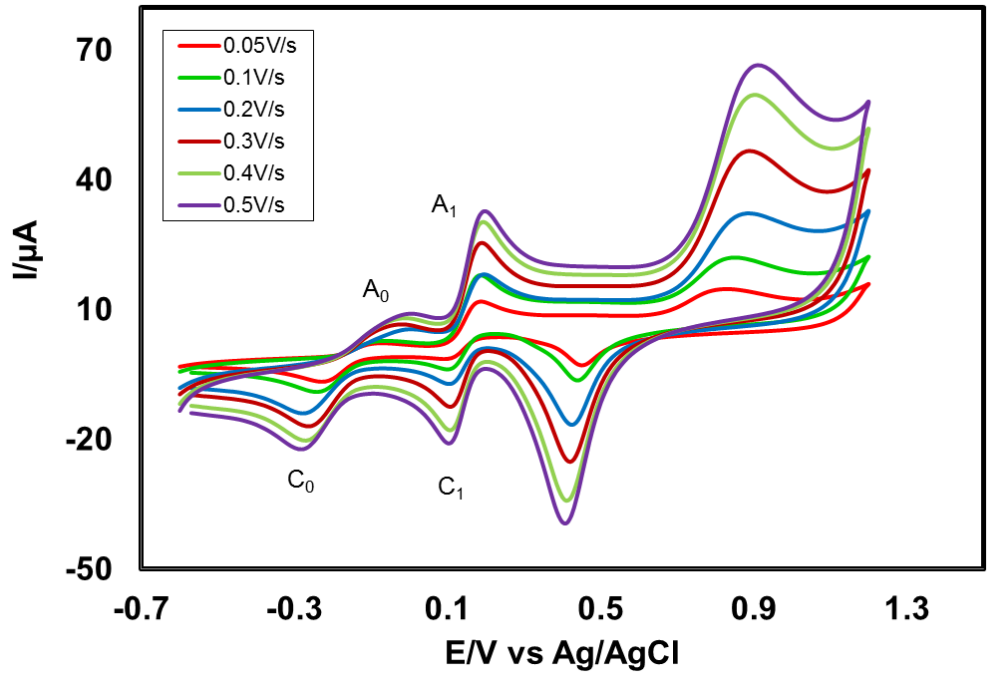

Fig. 4.92: Cyclic voltammogram of 2mM Catechol with 90mM L-Serine in the second scan of potential at Au electrode in buffer solution (pH 7) at scan rate 0.05V/s to 0.5V/s.

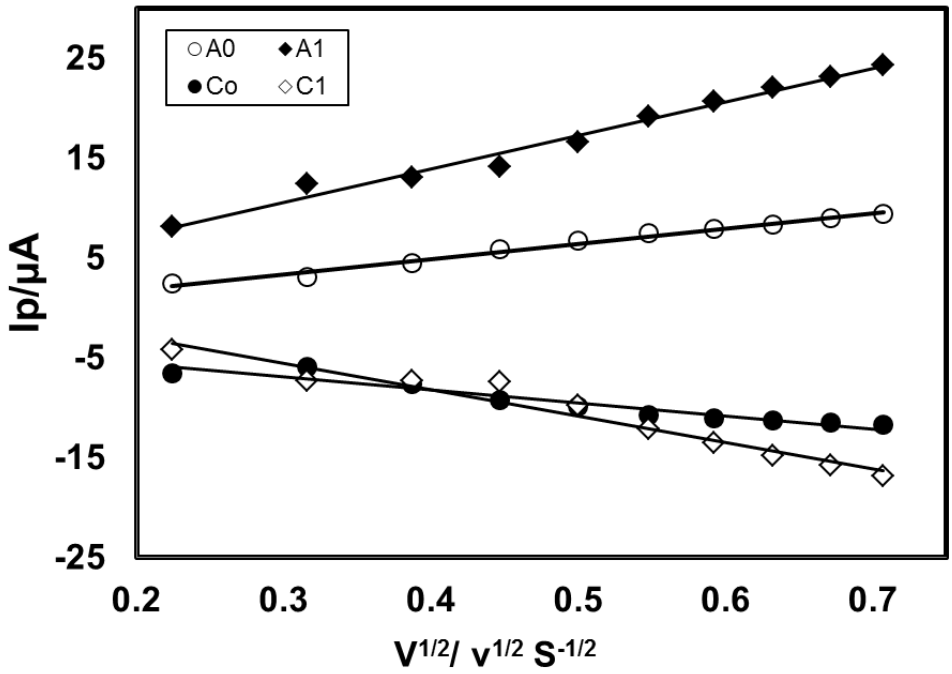

Fig. 4.93: Plots of peak current (I_p) versus square root of scan rate ($v^{1/2}$) of 2mM Catechol with 90mM L-Serine of Au electrode in buffer solution (pH 7) (2^{nd} cycle).

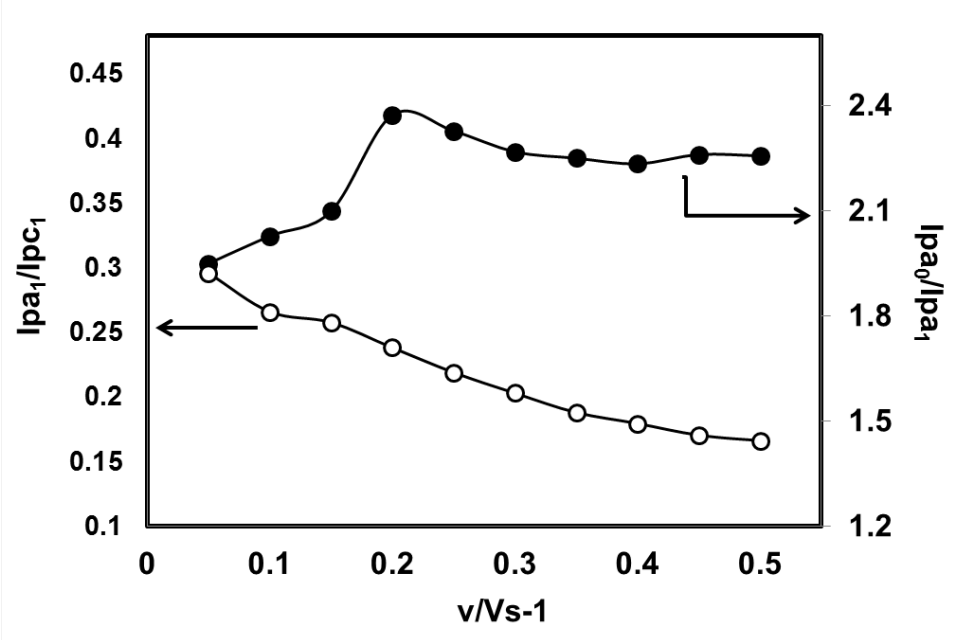

Fig. 4.94: Variation of peak current ratio of corresponding peak (I_{pa1}/I_{pc1}) and anodic peak (I_{pa0}/I_{pa1}) vs scan rate (v) of 2mM Catechol with 90mM L-Serine of Au electrode in buffer solution (pH 7) at scan rate 0.1V/s in the second scan of potential.

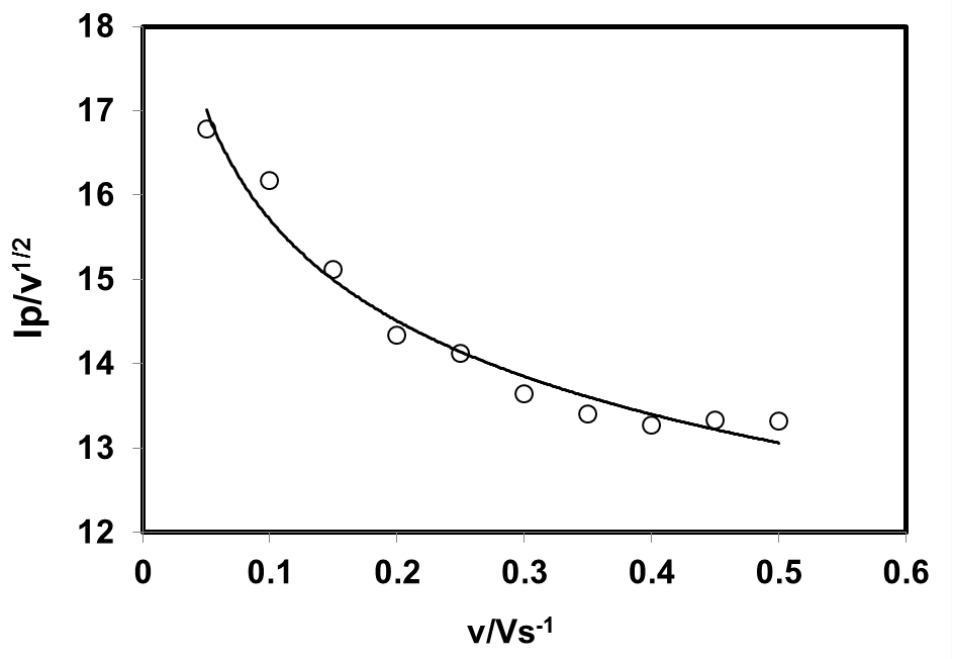

Fig. 4.95: Plots of current function ($I_p/v^{1/2}$) versus scan rate (v) of 2mM Catechol with 90mM L-Serine of Au electrode in buffer solution (pH 7) of the Appeared anodic peak(A_0).

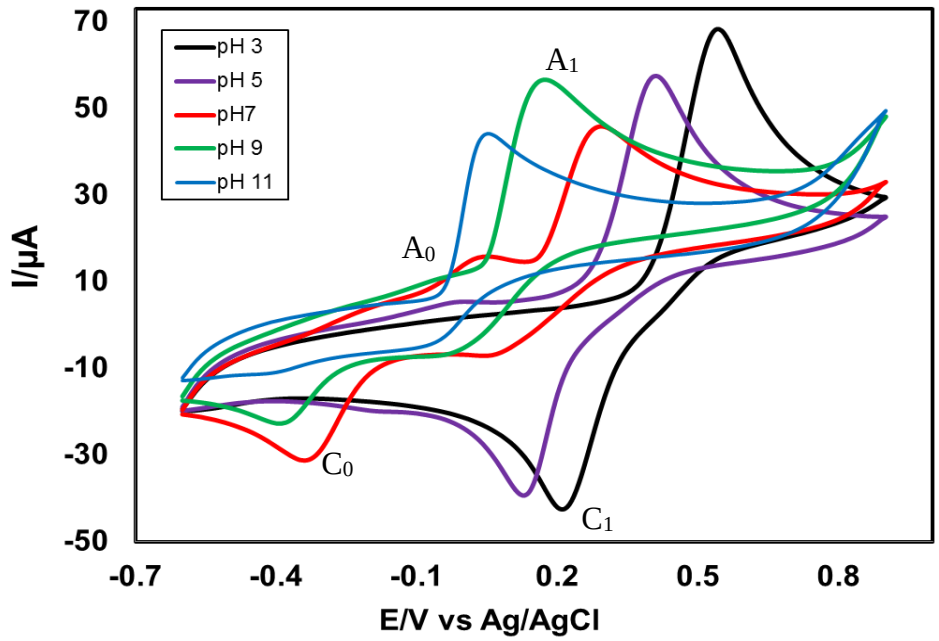

Fig. 4.96: Cyclic voltammogram of 2mM Catechol with 90mM L-Serine of GC (3mm) electrode in different pH (3, 5, 7, 9 and 11) at scan rate 0.1V/s.

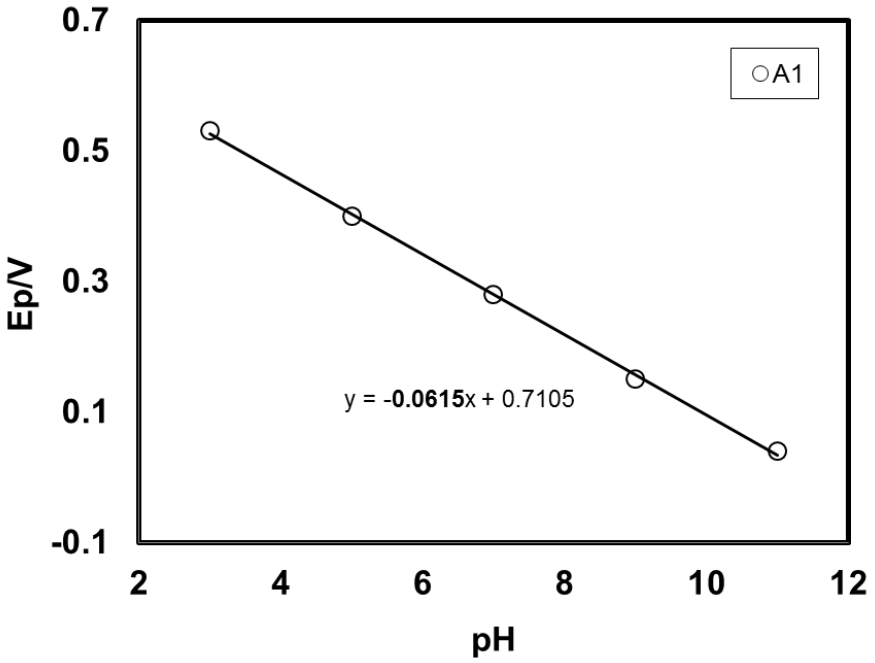

Fig. 4.97: Plots of peak potential (E_p) versus pH (3, 5, 7, 9 and 11) of 2mM Catechol with 90mM L-Serine of GC electrode at scan rate 0.1V/s (2^{nd} cycle).

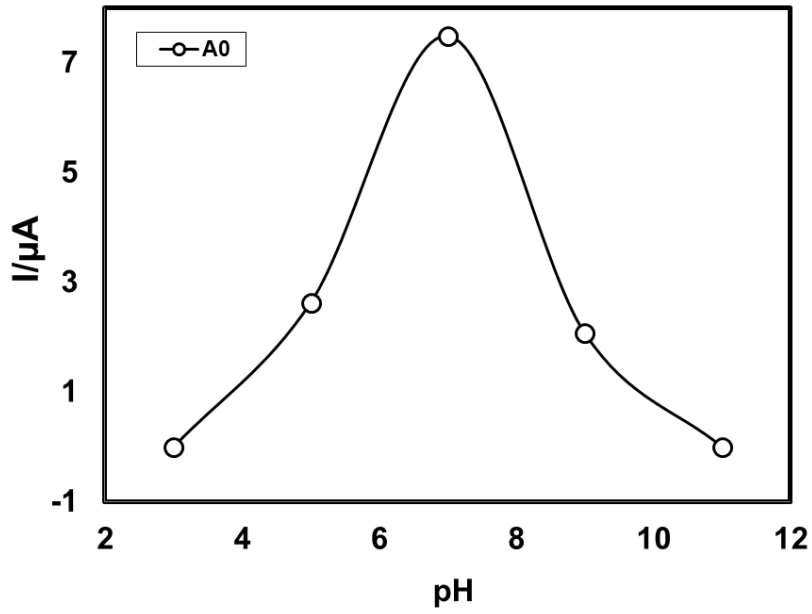

Fig. 4.98: Plot of peak current (I_p) versus pH (3, 5, 7, 9 and 11) of 2mM Catechol with 90mM L-Serine of GC electrode at scan rate 0.1V/s (2^{nd} cycle).

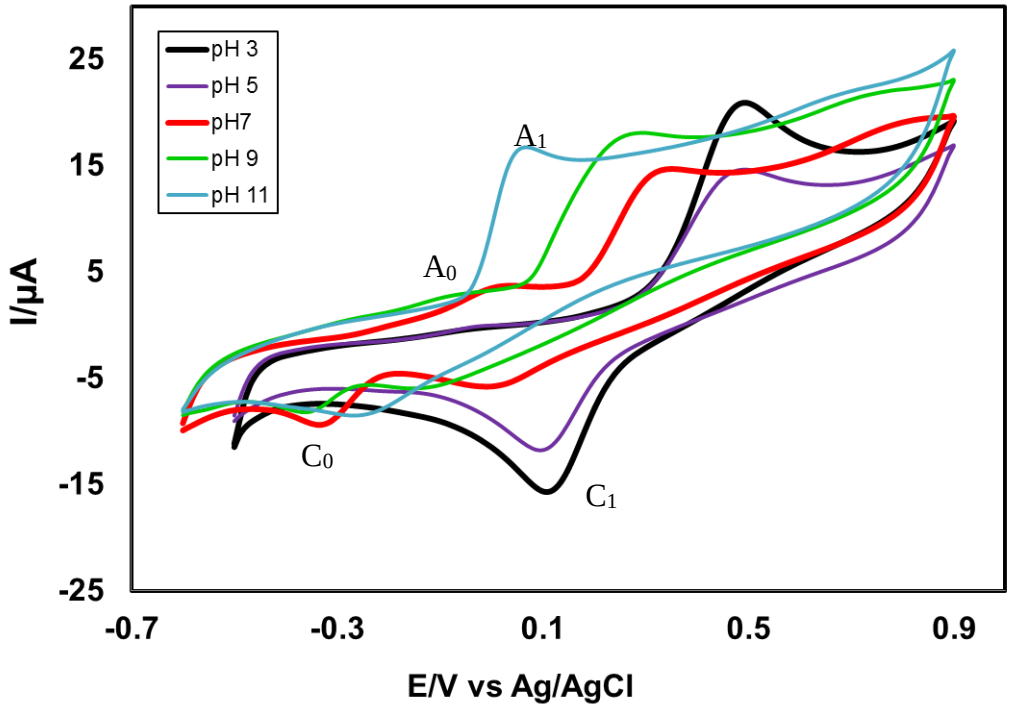

Fig. 4.99: Cyclic voltammogram of 2mM Catechol with 90mM L-Serine of Pt electrode in different pH (3, 5, 7, 9 and 11) at scan rate 0.1V/s.

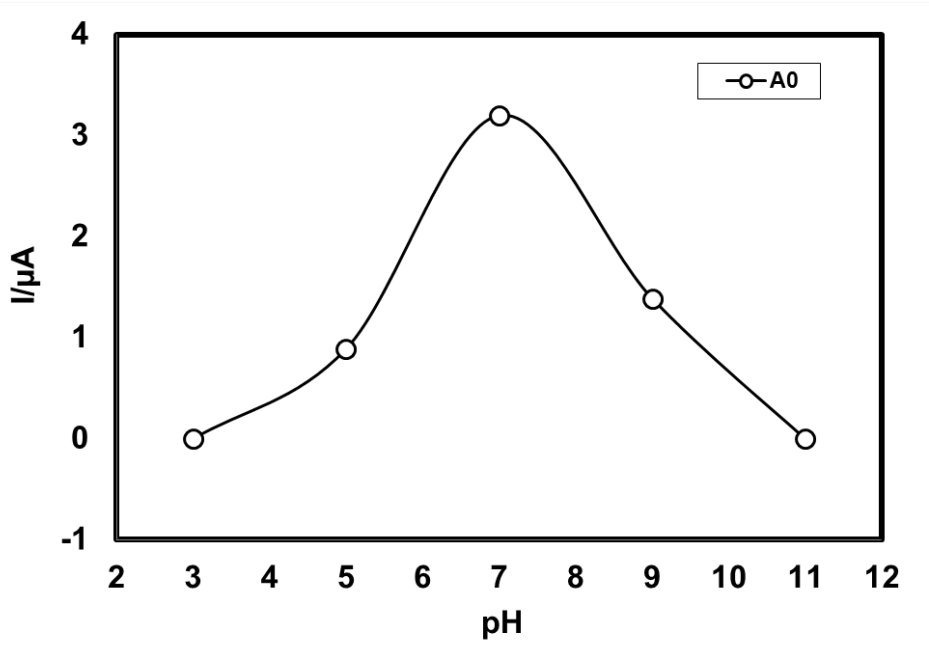

Fig. 4.100: Plots of peak current (I_p) versus pH (3, 5, 7, 9 and 11) of 2mM Catechol with 90mM L-Serine of Pt electrode at scan rate 0.1V/s (2^{nd} cycle).

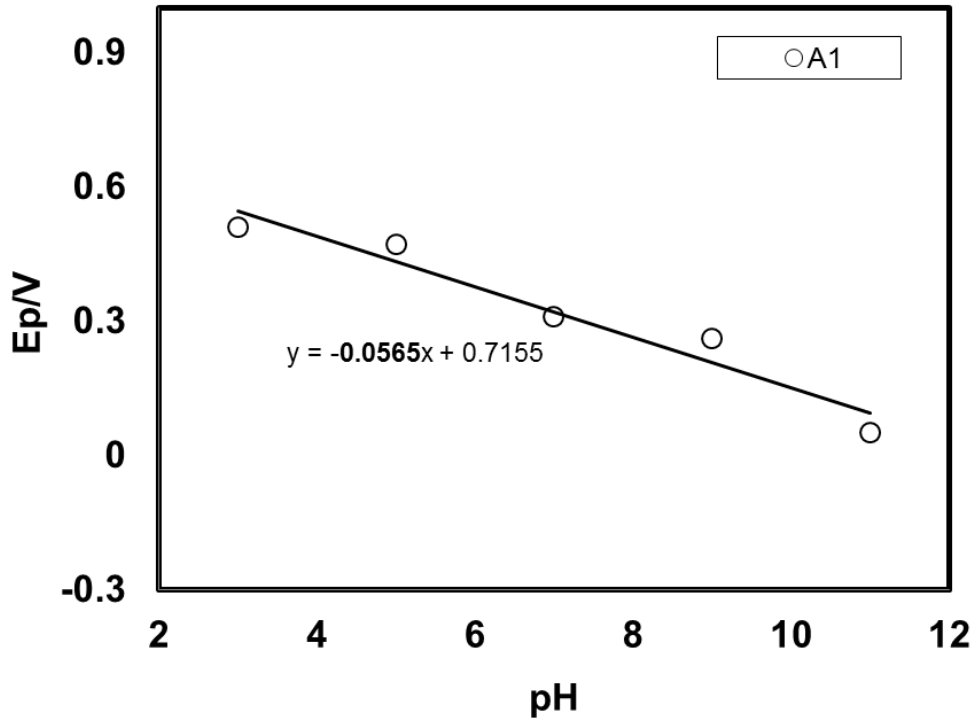

Fig. 4.101: Plot of peak potential (E_p) versus pH (3, 5, 7, 9 and 11) of 2mM Catechol with 90mM L-Serine of Pt electrode at scan rate 0.1V/s (2nd cycle).

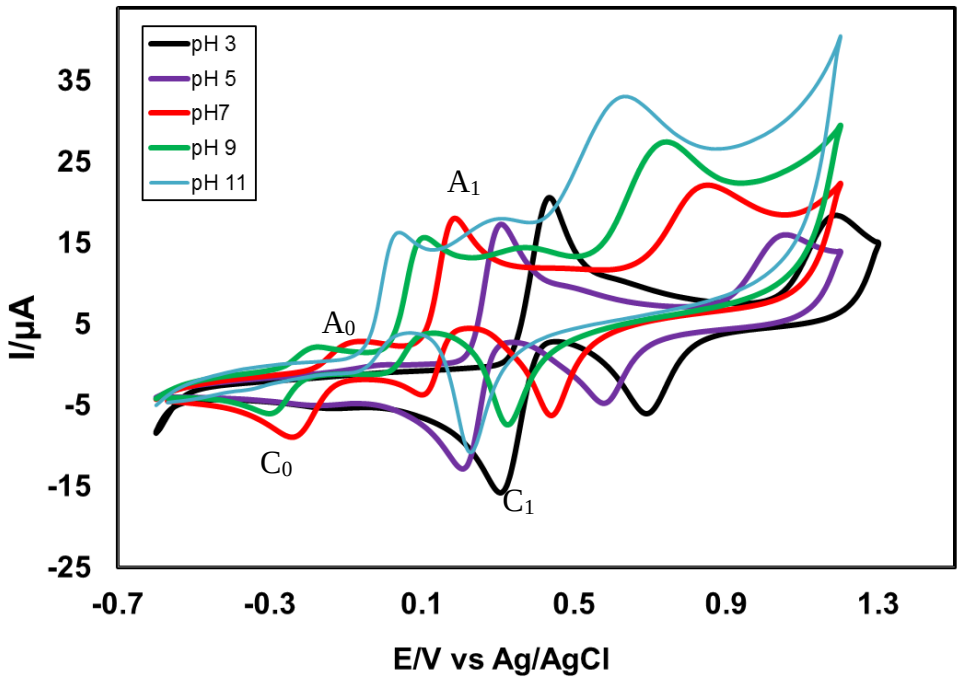

Fig. 4.102: Cyclic voltammogram of 2mM Catechol with 90mM L-Serine of Au electrode in different pH (3, 5, 7, 9 and 11) at scan rate 0.1V/s.

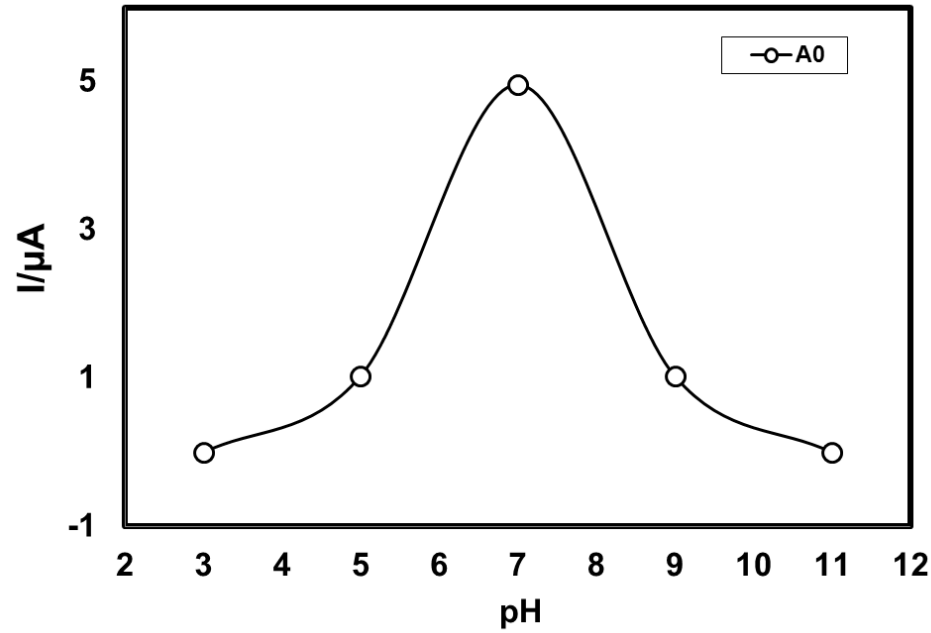

Fig. 4.103: Plots of peak current (I_p) versus pH (3, 5, 7, 9 and 11) of 2mM Catechol with 90mM L-Serine of Au electrode at scan rate 0.1V/s (2^{nd} cycle).

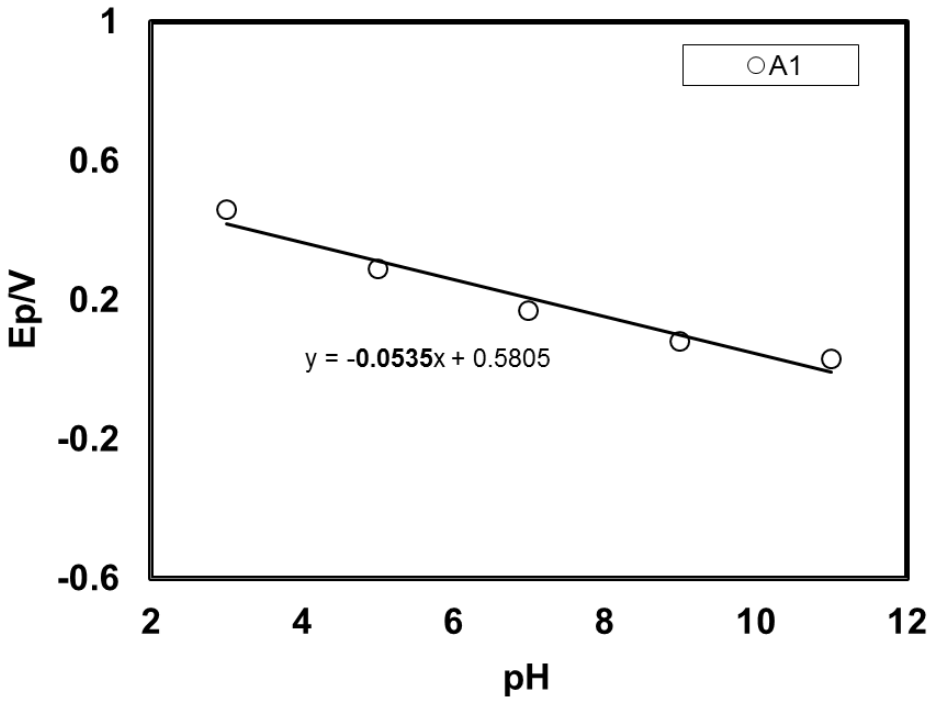

Fig. 4.104: Plot of peak potential (E_p) versus pH (3, 5, 7, 9 and 11) of 2mM Catechol with 90mM L-Serine of Au electrode at scan rate 0.1V/s (2nd cycle).

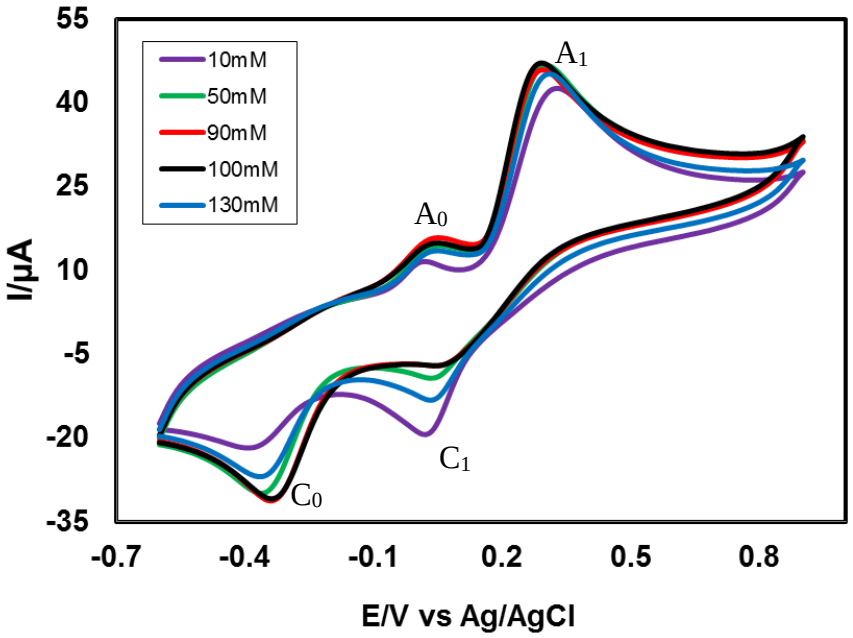

Fig. 4.105: CV of composition changes of L-Serine (10, 50, 90, 100 and 130mM) with fixed 2mM Catechol of GC electrode at pH 7 and scan rate 0.1V/s.

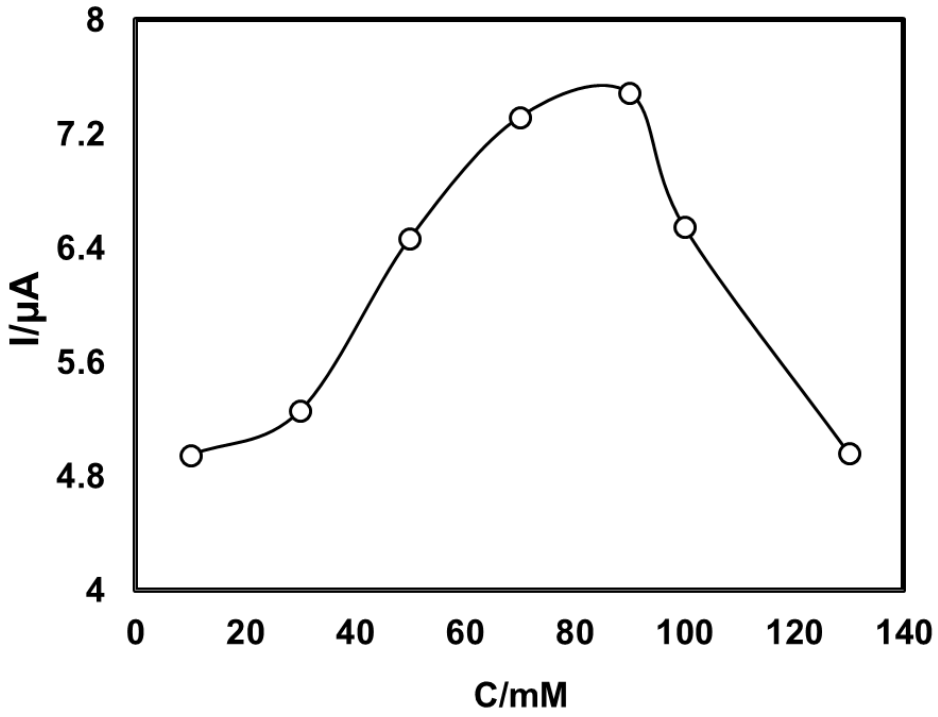

Fig. 4.106: Comparison of cyclic voltammogram of different concentration (10, 50, 90, 100 and 130mM) of L-Serine with 2mM Catechol in buffer solution (pH 7) at scan rate 0.1V/s (2nd cycle).

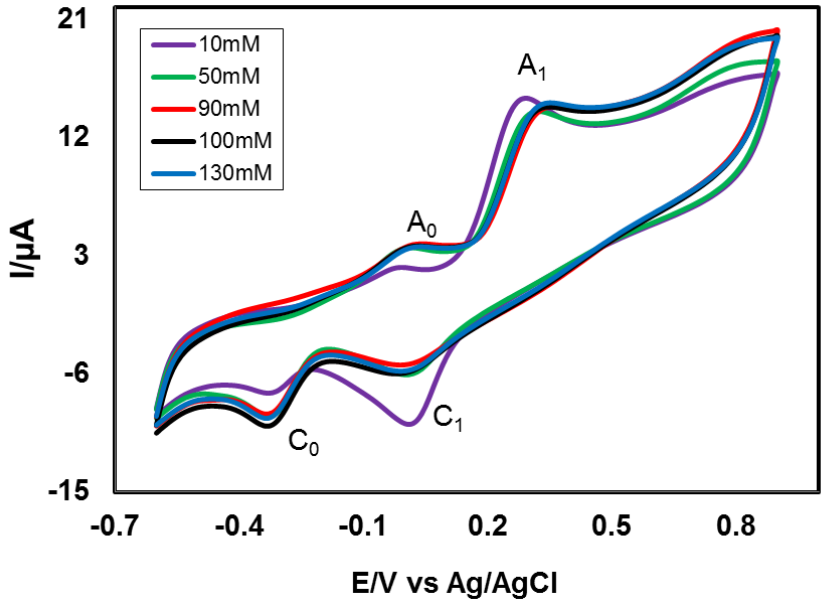

Fig. 4.107: CV of composition changes of L-Serine (10, 50, 90, 100 and 130mM) with fixed 2mM Catechol of Pt electrode at pH 7 and scan rate 0.1V/s.

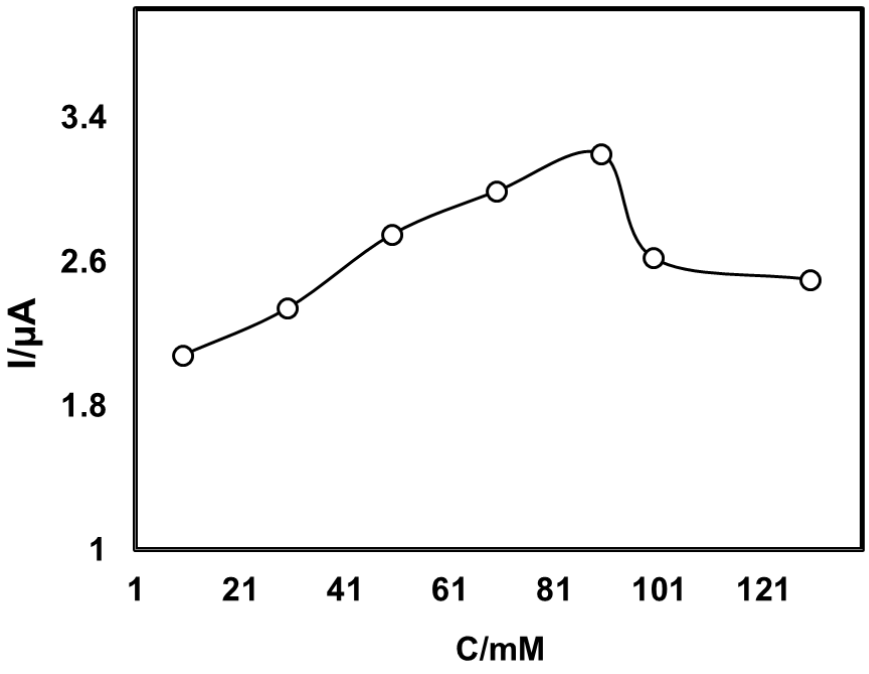

Fig. 4.108: Plots of peak current (I_p) versus concentration (C) of L-Serine (10, 50, 90, 100 and 130mM) with fixed 2mM Catechol of Pt electrode in buffer solution (pH) at 7 scan rate 0.1V/s (2^{nd} cycle).

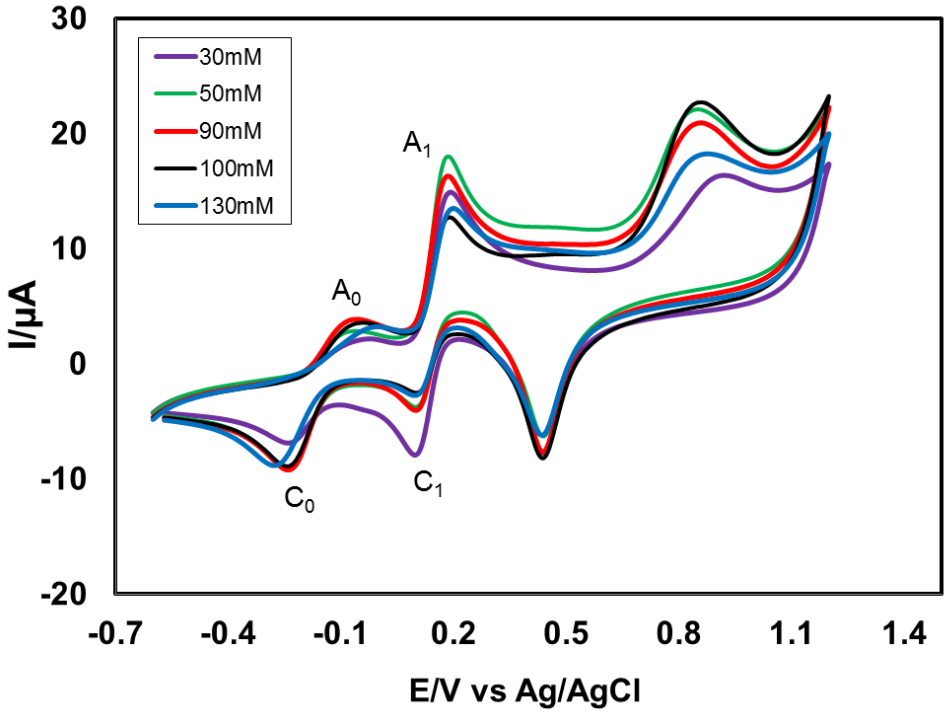

Fig. 4.109: CV of composition changes of L-Serine (30, 50, 90, 100 and 130mM) with fixed 2mM Catechol of Au electrode at pH 7 and scan rate 0.1V/s.

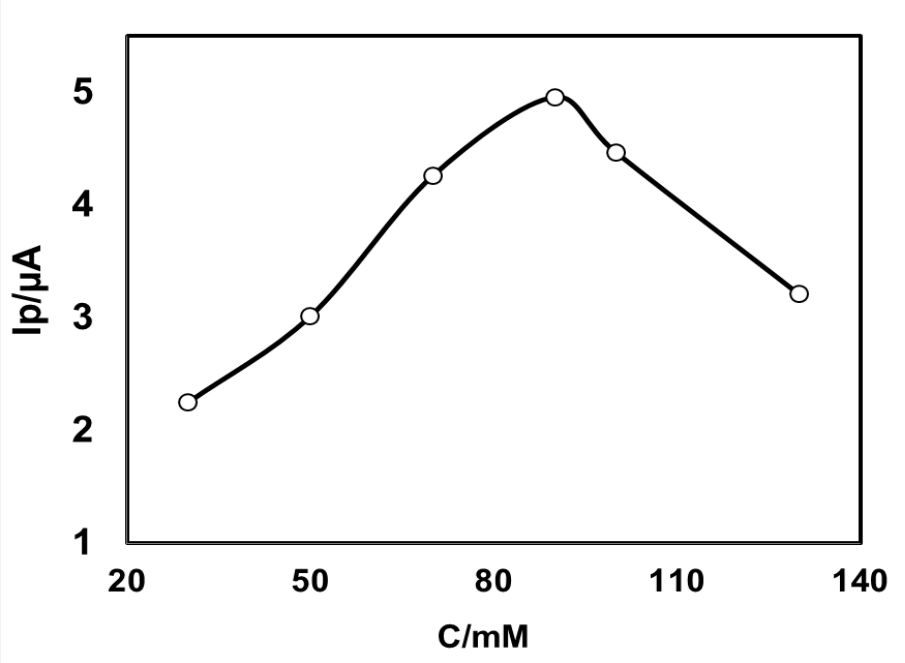

Fig. 4.110: Plots of peak current (I_p) versus concentration (C) of L-Serine (10, 50, 90, 100 and 130mM) with fixed 2mM Catechol of Au electrode in buffer solution (pH 7) at scan rate 0.1V/s (2^{nd} cycle).

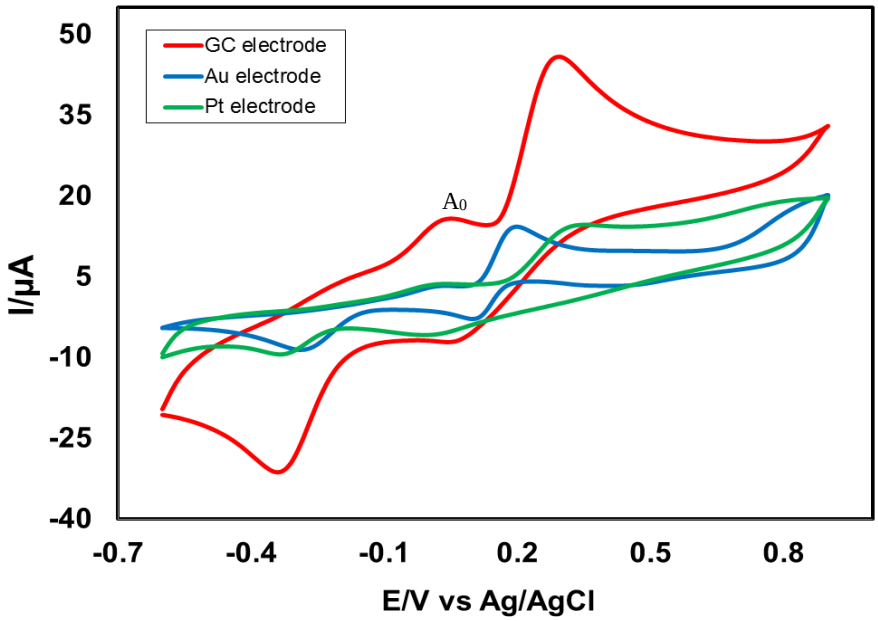

Fig. 4.111: Cyclic voltammogram (CV) of 2mM catechol with 90mM L-Serine in GC electrode (3.0mm), Gold electrode (1.6mm) and Platinum electrode (1.6mm) at pH 7 and scan rate 0.1V/s.

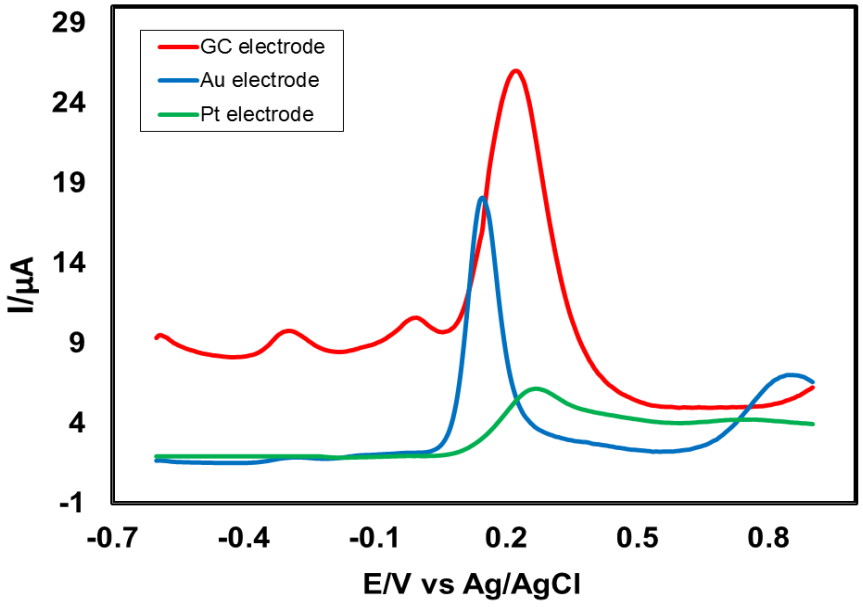

Fig. 4.112: Differential pulse voltammogram (DPV) of 2mM catechol with 90mM L-Serine in GC electrode (3.0mm), Gold electrode (1.6mm) and Platinum electrode (1.6mm) at pH 7 and scan rate 0.1V/s.

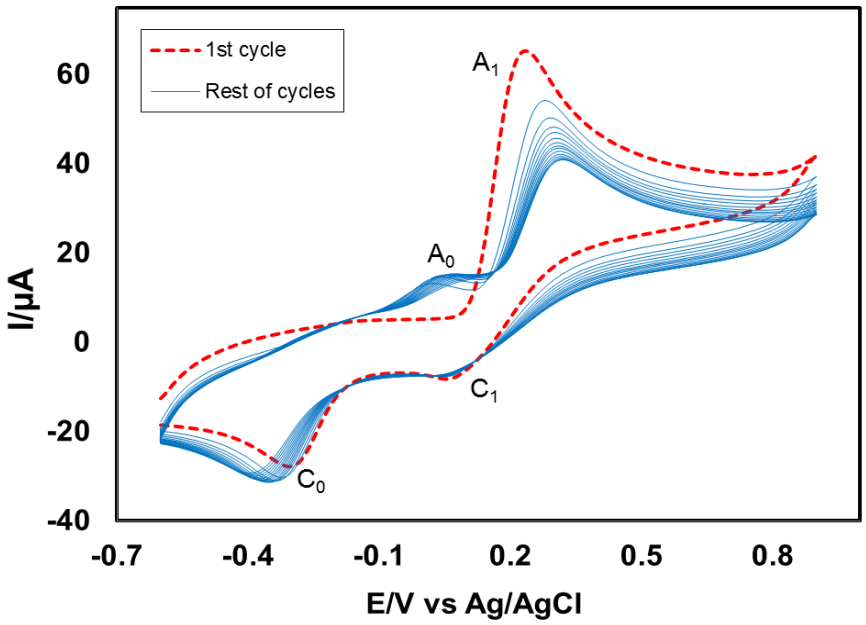

Fig. 4.113: Cyclic voltammogram of 2mM Catechol with 90mM L-Serine of GC (3mm) electrode in the buffer solution of pH 7 at scan rate 0.1 V/s (15 cycles). The appeared anodic peak current (A_0) and cathodic peak current (C_0) increased with the iteration scan from the first cycle.

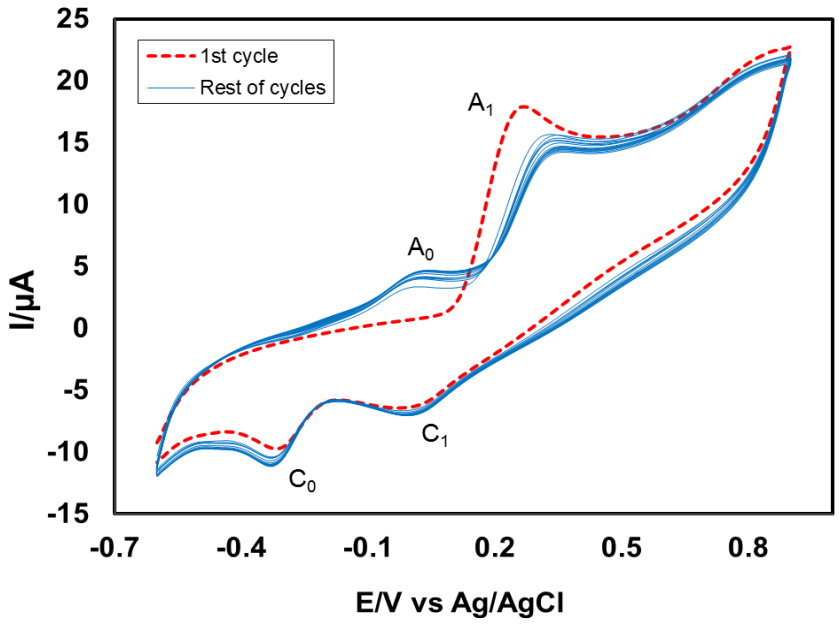

Fig. 4.114: Cyclic voltammogram of 2mM Catechol with 90mM L-Serine of Pt electrode in the buffer solution of pH 7 at scan rate 0.1 V/s (15 cycles). The appeared anodic peak current (A_0) and cathodic peak current (C_0) increased with the iteration scan from the first cycle.

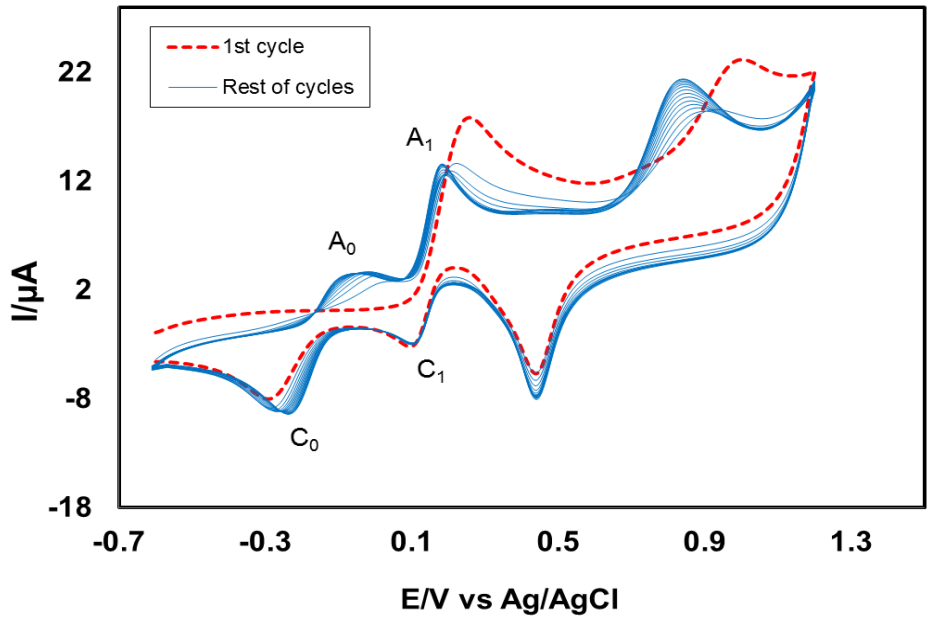

Fig. 4.115: Cyclic voltammogram of 2mM Catechol with 90mM L-Serine of Au electrode in the buffer solution of pH 7 at scan rate 0.1 V/s (15 cycles). The appeared anodic peak current (A_0) and cathodic peak current (C_0) increased with the iteration scan from the first cycle.

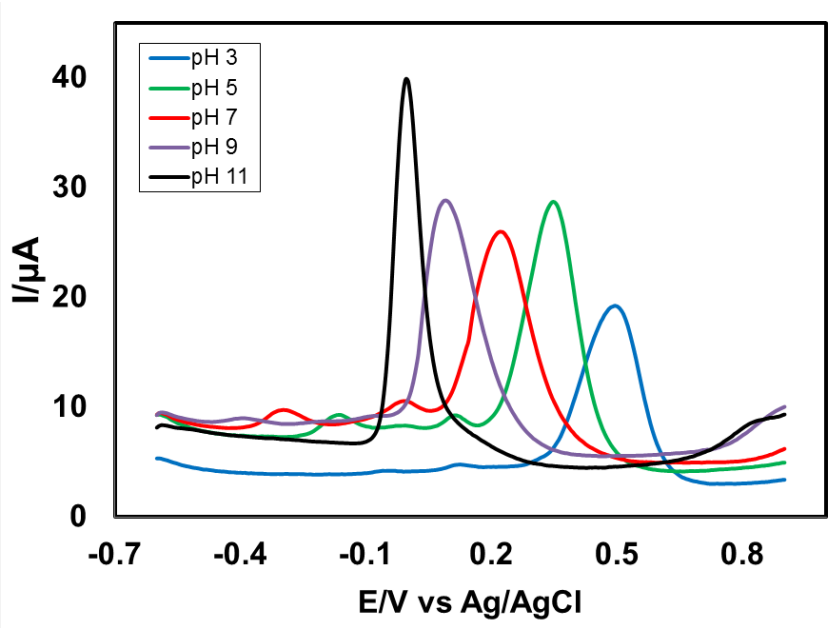

Fig. 4.116: Differential pulse voltammogram (DPV) of 2mM Catechol with 90mM L-Serine of GC electrode in second scan of different pH (3, 5, 7, 9 and 11) and scan rate 0.1V/s.

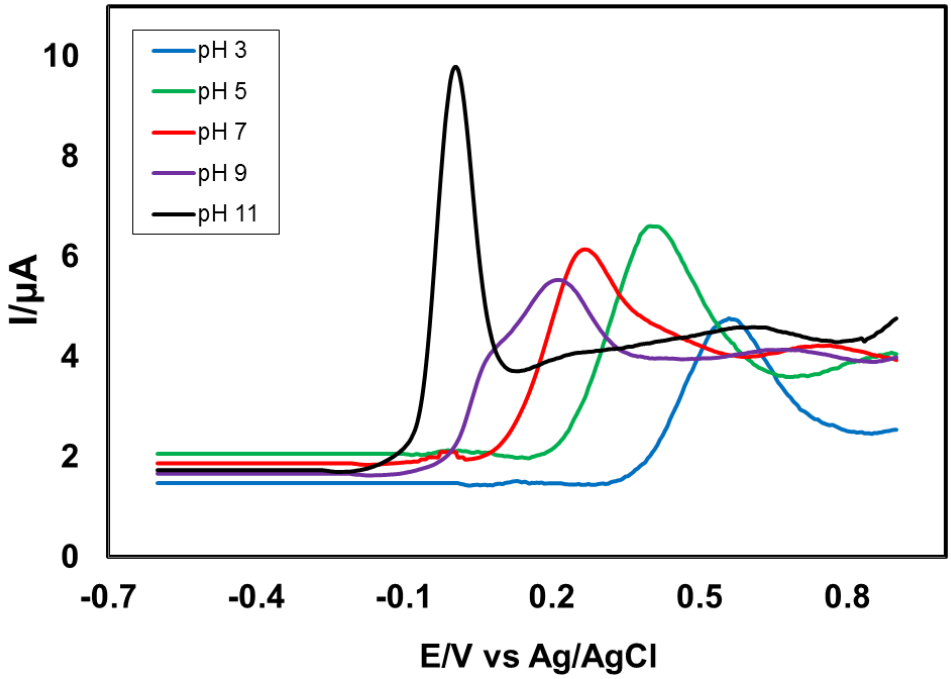

Fig. 4.117: Differential pulse voltammogram (DPV) of 2mM Catechol with 90mM L-Serine of Pt electrode in second scans of different pH (3, 5, 7, 9 and 11) and scan rate 0.1V/s.

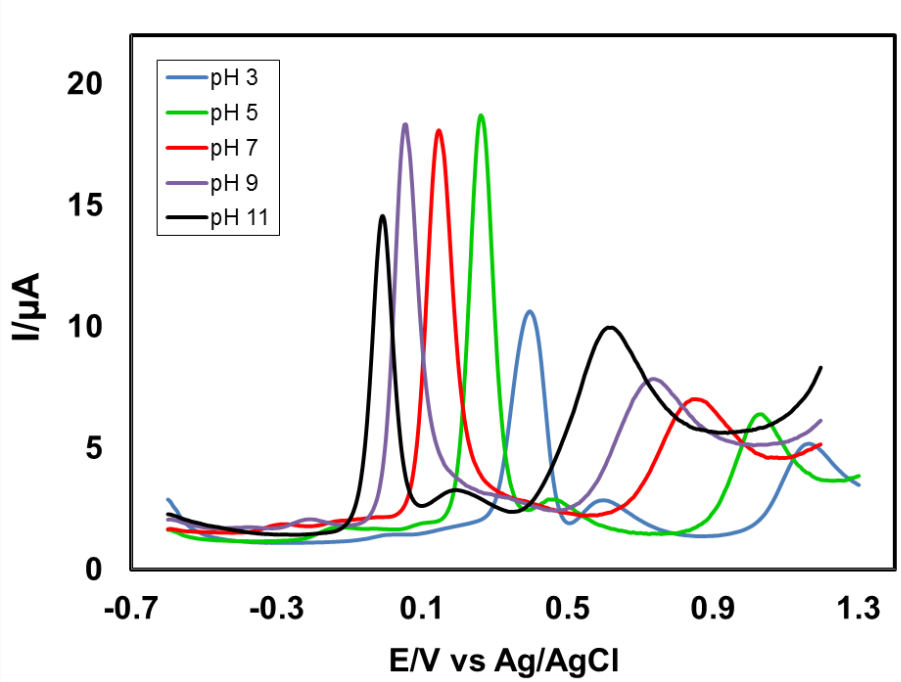

Fig. 4.118: Differential pulse voltammogram (DPV) of 2mM Catechol with 90mM L-Serine of Au electrode in second scans of different pH (3, 5, 7, 9 and 11) and scan rate 0.1V/s.

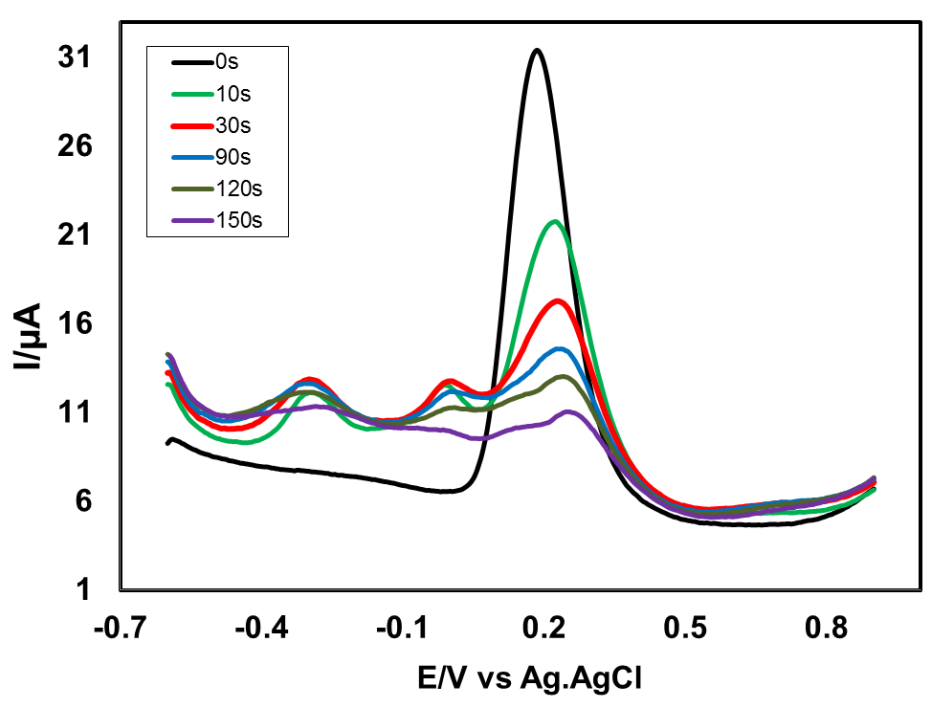

Fig. 4.119: Differential pulse voltammogram (DPV) of deposition time change (0, 10, 30, 90,120 and 150s) of 2mM catechol with 90mM L-Serine of pH 7 at *E*puls 0.02V, tpuls 20ms and scan rate 0.1Vs^{-1}.

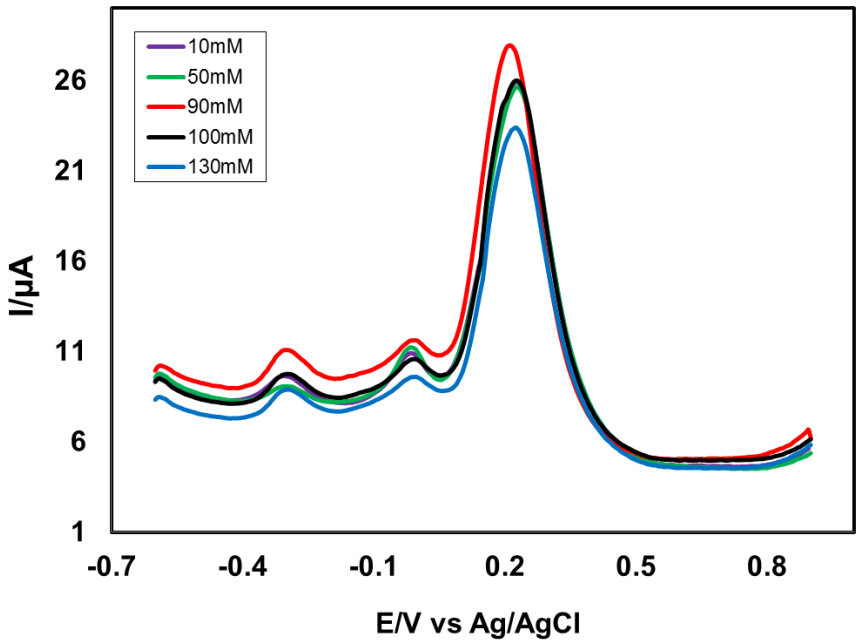

Fig. 4.120: Differential pulse voltammogram (DPV) of composition change of L-Serine (10, 50, 90, 100 and 130mM) with the fixed composition of 2 mM Catechol in second scan of pH7 at *E*puls 0.02V, tpuls 20ms of GC electrode and scan rate 0.1Vs^{-1}.

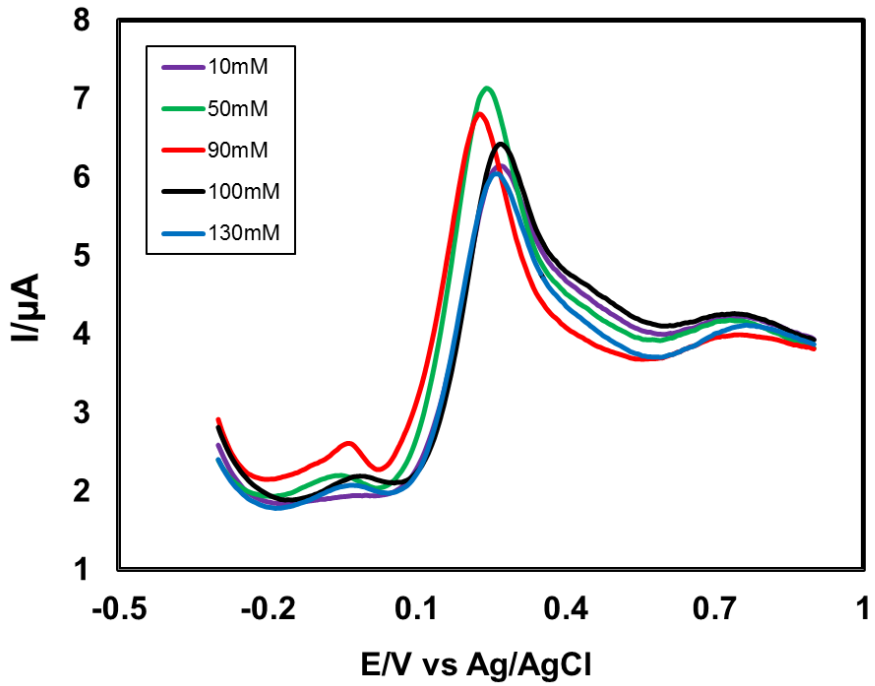

Fig. 4.121: Differential pulse voltammogram (DPV) of composition change of L-Serine (10, 50, 90, 100 and 130mM) with the fixed composition of 2 mM Catechol in second scan of pH 7 at *E*puls 0.02V, tpuls 20ms of Pt electrode and scan rate 0.1Vs^{-1}.

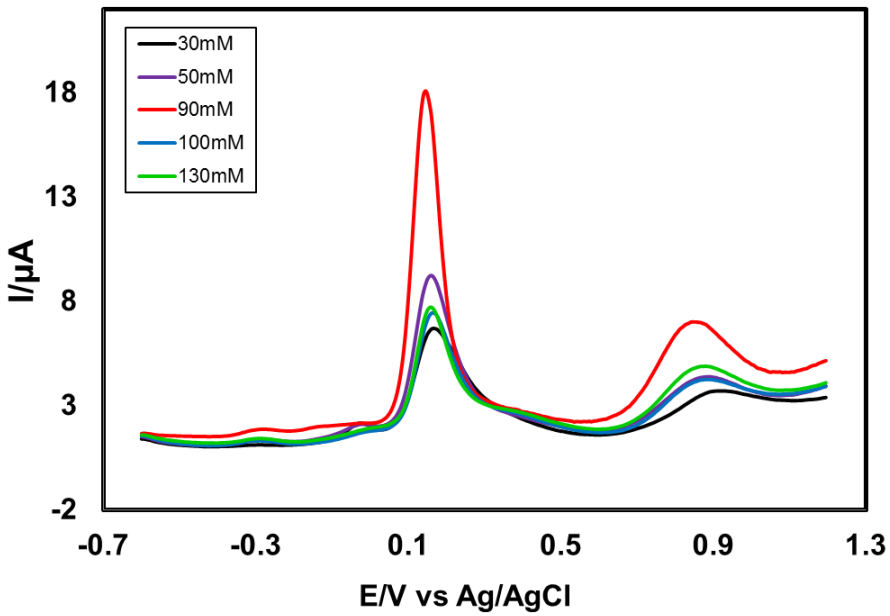

Fig. 4.122: Differential pulse voltammogram (DPV) of composition change of L-Serine (10, 50, 90, 100 and 130mM) with the fixed composition of 2 mM Catechol in second scan of pH7 at *E*puls 0.02V, tpuls 20ms of Au electrode and scan rate 0.1Vs^{-1}.

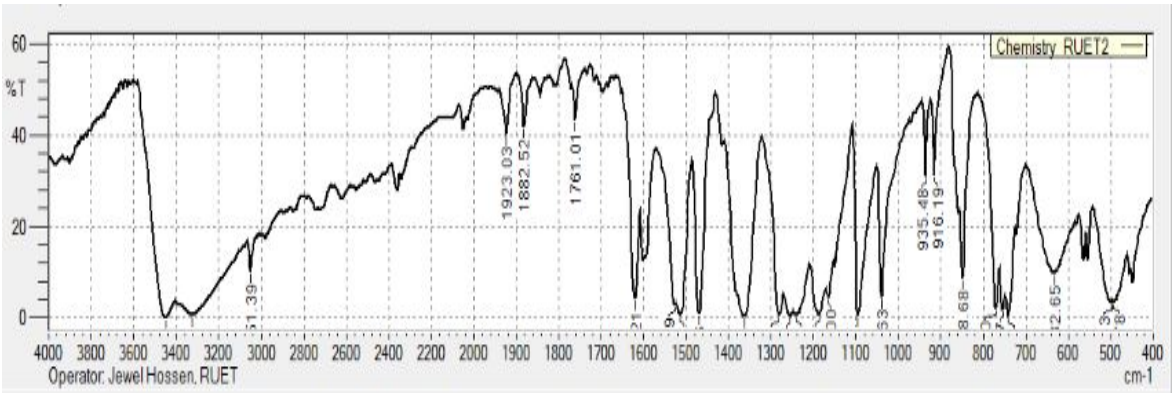

(a)

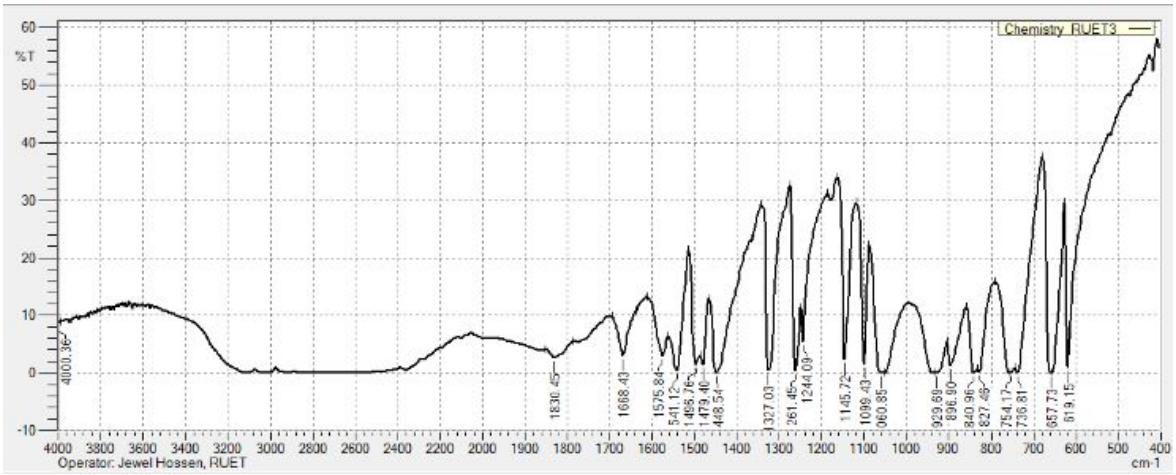

(b)

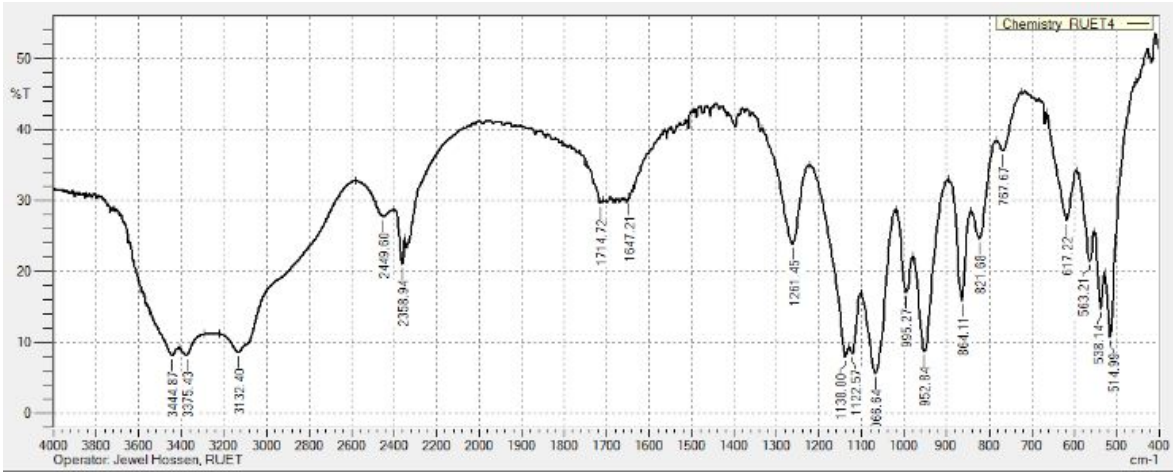

(c)

Fig. 4.123: Comparison of FTIR spectra of only (a) catechol, (b) only imidazole and catechol- imidazole adduct(c)

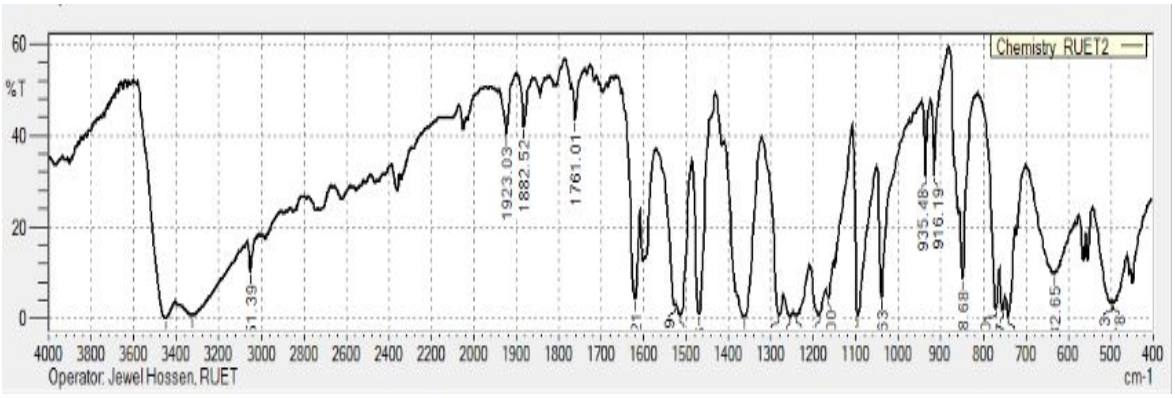

(a)

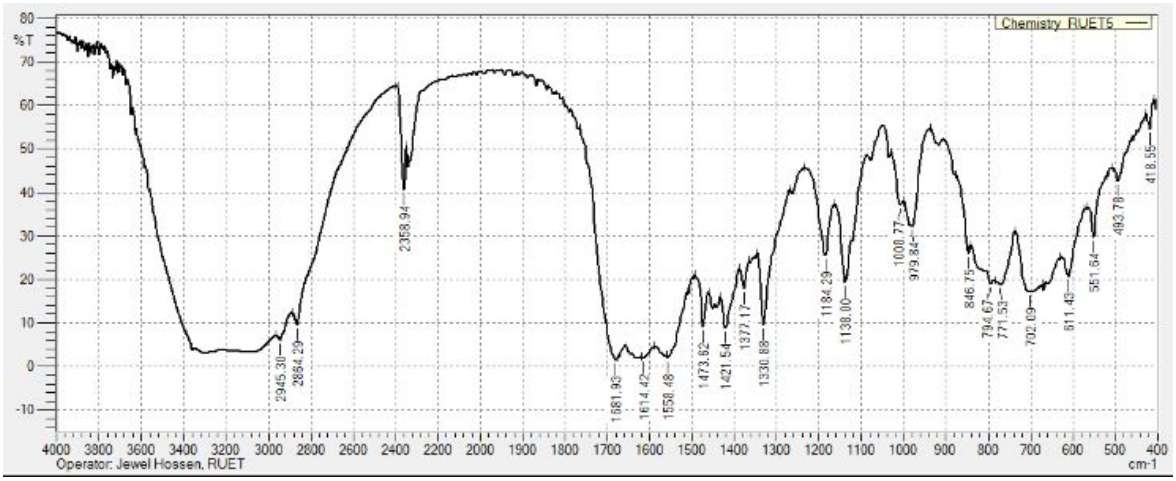

(b)

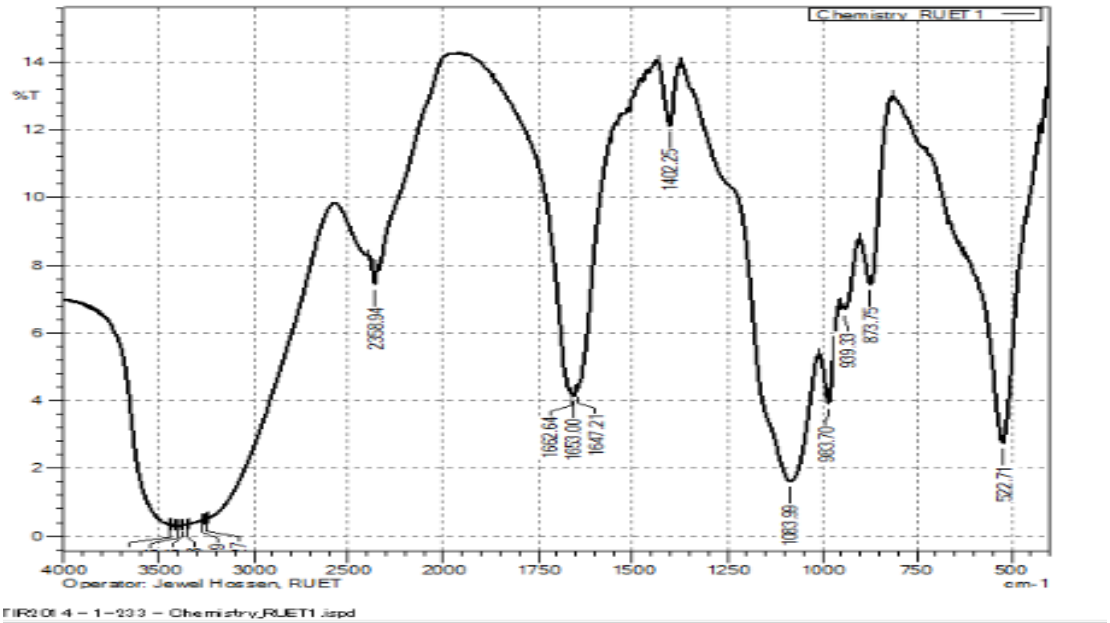

(c)

Fig. 4.124: Comparison of FTIR spectra of only catechol (a), only Arginine (b) and catechol-Arginine adduct (c)

Table 4.1: Peak potential (E_p), corresponding peak potential difference (ΔE), peak separation ($\Delta E_{1/2}$), peak current (I_p), corresponding peak current ratio (I_{pa}/I_{pc}) of 2mM catechol in aqueous buffer solution (pH 7) of GC electrode at different scan rate

v/Vs^{-1}	E_{pa1} /V	E_{pc1} /V	$\Delta E = E_{pc1} \sim E_{pa1}$	I_{pa1} /μA	I_{pc1} /μA	I_{pa1}/ I_{pc1}
0.05	0.37	0.04	0.33	5.23	-5.22	1.01
0.10	0.38	0.03	0.34	5.89	-5.75	1.03
0.15	0.38	0.04	0.34	3.78	-8.23	0.46
0.20	0.40	0.04	0.36	3.99	-7.46	0.53
0.25	0.42	0.03	0.39	5.27	-7.59	0.69
0.30	0.43	0.03	0.40	3.53	-7.64	0.46
0.35	0.50	0.01	0.49	3.64	-7.27	0.69
0.40	0.51	-0.03	0.54	3.52	-8.21	0.43
0.45	0.52	-0.04	0.56	4.61	-9.99	0.46

Table 4.2: Peak current (I_p), corresponding peak current ratio (I_{pa}/I_{pc}) of 2mM Catechol with 20mM Imidazole in buffer solution (pH 7) of GC electrode at different scan rate (2nd cycle)

v/Vs^{-1}	I_{pa0} /μA	I_{pa1} /μA	I_{pc1}/μA	I_{pa0}/I_{pa1}	I_{pa1}/I_{pc1}
0.05	1.5	26.92	-21.34	0.05	1.26
0.10	2.15	38.47	-35.49	0.05	1.08
0.15	2.75	47.89	-45.74	0.05	1.04
0.20	3.44	57.32	-56.4	0.06	1.01
0.25	4.26	61.19	-62.31	0.06	0.98
0.30	5.18	64.93	-68.43	0.07	0.94
0.35	5.79	71.71	-77.58	0.08	0.92
0.40	6.25	78.39	-86.93	0.07	0.90
0.45	6.49	85.67	-90.35	0.07	0.94
0.50	6.78	93.15	-94.02	0.07	0.99

Table 4.3: Peak Current I_p (μA), peak potential E_p (V) of 2mM Catechol with 20mM Imidazole of GC electrode at scan rate 0.1V/s in different pH media (2nd cycle)

pH	Peak Current I_p (μA)	Peak potential E_p (V)
	Oxidation, A_0	Oxidation, A_1
3	-0.9	0.65
5	-1.03	0.56
7	3.43	0.35
9	-1.09	0.32

Table 4.4: Peak Current I_p (µA), peak potential E_p (V) of 2mM Catechol with 20mM Imidazole of Au electrode at scan rate 0.1V/s in different pH media (2^{nd} cycle)

pH	Peak Current I_p (µA)	Peak potential E_p (V)
	Oxidation, A_0	Oxidation, A_0
3	0.00	0.58
5	0.00	0.43
7	1.05	0.28
9	0.00	0.09
11	0.00	0.00

Table 4.5. Peak Current I_p (µA), peak potential E_p (V) of 2mM Catechol with 20mM Imidazole of Pt electrode at scan rate 0.1V/s in different pH media (2^{nd} cycle)

pH	Peak Current I_p (µA)	Peak potential E_p (V)
	Oxidation, A_0	Oxidation, A_0
3	0.00	0.42
5	0.00	0.42
7	1.05	0.26
9	0.00	0.07
11	0.00	-0.01

Table 4.6: Peak Current I_p (µA) of 2mM Catechol with various concentration of Imidazole of GC electrode at scan rate 0.1V/s in pH 7 (2^{nd} cycle)

Concentration	Peak Current I_p (µA)
	Oxidation, A_0
2	1.57
10	1.97
20	2.37
30	1.99
50	1.49

Table 4.7: Peak Current I_p (μA) of 2mM Catechol with various concentration of Imidazole of Au electrode at scan rate 0.1V/s in pH 7 (2^{nd} cycle)

Concentration	Peak Current I_p (μA)
	Oxidation, A_0
2	0.57
10	0.88
20	1.05
30	0.89
50	0.55

Table 4.8: Peak Current I_p (μA) of 2mM Catechol with various concentration of Imidazole of Pt electrode at scan rate 0.1V/s in pH 7 (2^{nd} cycle)

Concentration	Peak Current I_p (μA)
	Oxidation, A_0
2	0.65
10	0.89
20	1.05
30	0.98
50	0.54

Table 4.9: Peak current (I_p), corresponding peak current ratio (I_{pa}/I_{pc}) of 2mM Catechol with 30mM Arginine in buffer solution (pH 7) of GC electrode at different scan rate (2^{nd} cycle)

v/Vs^{-1}	I_{pa0} /μA	I_{pa1} /μA	I_{pc0}/μA	I_{pc1}/μA	I_{pa0}/I_{pa1}	I_{pa1}/I_{pc1}
0.05	1.66	18.65	-6.88	-5.15	0.08	-3.62
0.10	4.36	22.64	-13.62	-6.89	0.19	-3.28
0.15	7.22	28.03	-16.98	-10.07	0.25	-2.78
0.20	10.38	35.82	-21.59	-14.58	0.28	-2.45
0.25	10.89	36.15	-22.35	-15.18	0.30	-2.38
0.30	11.68	37.28	-23.37	-15.96	0.31	-2.33
0.35	10.68	42.26	-23.02	-18.75	0.25	-2.25
0.40	9.06	47.09	-22.34	-22.44	0.19	-2.09
0.45	8.87	47.33	-21.97	-22.01	0.1	-2.15
0.50	7.44	46.05	-21.05	-21.46	0.16	-2.14

Table 4.10: Peak current (I_p), corresponding peak current ratio (I_{pa}/I_{pc}) of 2mM Catechol with 30mM Arginine in buffer solution (pH 7) of Au electrode at different scan rate (2nd cycle)

v/Vs^{-1}	I_{pa0} /μA	I_{pa1} /μA	I_{pc0}/μA	I_{pc1}/μA	I_{pa0}/I_{pa1}	I_{pa1}/I_{pc1}
0.05	1.12	5.43	-2.09	-1.58	4.84	-3.43
0.10	1.33	5.63	-3.42	-1.833	4.23	-2.73
0.15	1.89	7.89	-6.01	-2.78	3.50	-2.33
0.20	2.87	9.61	-8.07	-4.66	3.14	-1.50
0.25	3.58	11.79	-8.41	-7.94	3.02	-1.48
0.30	4.87	13.15	-8.91	-7.17	2.70	-1.43
0.35	4.89	13.65	-8.97	-8.03	2.79	-1.69
0.40	4.93	13.89	-8.18	-8.43	2.81	-1.64
0.45	4.78	15.68	-9.34	-9.34	2.28	-1.67
0.50	4.47	17.41	-9.45	-10.87	2.19	-1.60

Table 4.11: Peak current (I_p), corresponding peak current ratio (I_{pa}/I_{pc}) of 2mM Catechol with 30mM Arginine in buffer solution (pH 7) of Pt electrode at different scan rate (2nd cycle)

v/Vs^{-1}	I_{pa0} /μA	I_{pa1} /μA	I_{pc0}/μA	I_{pc1}/μA	I_{pa0}/I_{pa1}	I_{pa1}/I_{pc1}
0.05	0.70	6.08	-1.96	-1.46	-0.32	-4.18
0.10	1.48	6.27	-2.79	-2.12	-0.44	-2.95
0.15	1.78	7.99	-2.97	-3.56	-0.37	-2.24
0.20	2.2	9.49	-3.15	-4.92	-0.33	-1.92
0.25	2.01	9.67	-3.45	-5.79	-0.35	-1.67
0.30	1.81	9.98	-3.78	-6.76	-0.37	-1.47
0.35	1.43	10.28	-3.61	-8.88	-0.35	-1.15
0.40	1.24	11.6	-3.22	-10.17	-0.27	-1.14
0.45	1.02	11.62	-3.2	-10.29	-0.20	-1.12
0.50	0.80	11.66	-3.23	-10.35	-0.27	-1.12

Table 4.12: Peak Current I_p (μA), peak potential E_p (V) of 2mM Catechol with 30mM Arginine of GC electrode at scan rate 0.1V/s in different pH media (2nd cycle)

pH	Peak Current I_p (μA)	Peak potential E_p (V)
	Oxidation, A_0	Oxidation, A_1
3	0.00	0.51
5	0.00	0.39
7	7.56	0.27
9	2.67	0.19
11	0.00	0.05

Table 4.13: Peak Current I_p (µA), peak potential E_p (V) of 2mM Catechol with 30mM Arginine of Au electrode at scan rate 0.1V/s in different pH media (2^{nd} cycle)

pH	Peak Current I_p (µA)	Peak potential E_p (V)
	Oxidation, A_0	Oxidation, A_0
3	0.00	0.40
5	0.00	0.29
7	1.24	0.19
9	0.15	0.07
11	0.00	0.02

Table 4.14: Peak Current I_p (µA), peak potential E_p (V) of 2mM Catechol with 30mM Arginine of Pt electrode at scan rate 0.1V/s in different pH media (2^{nd} cycle)

pH	Peak Current I_p (µA)	Peak potential E_p (V)
	Oxidation, A_0	Oxidation, A_0
3	0.00	0.56
5	0.00	0.43
7	0.24	0.30
9	0.00	0.22
11	0.00	0.05

Table 4.15: Peak Current I_p (µA) of 2mM Catechol with various concentration of Arginine of GC electrode at scan rate 0.1V/s in pH 7 (2^{nd} cycle)

Concentration	Peak Current I_p (µA)
	Oxidation, A_0
10	4.30
20	5.52
30	7.18
50	5.11
100	4.78

Table 4.16: Peak Current I_p (µA) of 2mM Catechol with various concentration of Arginine of Au electrode at scan rate 0.1V/s in pH 7 (2nd cycle)

Concentration	Peak Current I_p (µA)
	Oxidation, A_0
10	1.31
20	2.15
30	2.33
50	1.96
100	0.12

Table 4.17: Peak Current I_p (µA) of 2mM Catechol with various concentration of Arginine of Pt electrode at scan rate 0.1V/s in pH 7 (2nd cycle)

Concentration	Peak Current I_p (µA)
	Oxidation, A_0
10	0.25
20	0.87
30	1.46
50	1.39
100	0.10

Table 4.18: Peak current (I_p), corresponding peak current ratio (I_{pa}/I_{pc}) of 2mM Catechol with 90mM Serine in buffer solution (pH 7) of GC electrode at different scan rate (2nd cycle)

v/Vs^{-1}	I_{pa0} /µA	I_{pa1} /µA	I_{pc0}/µA	I_{pc1}/µA	I_{pa0}/I_{pa1}	I_{pa1}/I_{pc1}
0.05	3.84	23.85	-13.3	-14.52	-0.33	-1.86
0.10	7.10	29.62	-21.4	-16.05	-0.31	-1.81
0.15	9.15	32.55	-26.22	-19.58	-0.28	-1.66
0.20	11.2	35.49	-31.04	-23.27	-0.26	-1.42
0.25	10.58	42.07	-32.28	-26.80	-0.23	-1.46
0.30	9.87	48.61	-33.69	-30.07	-0.20	-1.46
0.35	11.77	52.31	-34.86	-34.66	-0.19	-1.46
0.40	13.71	56.43	-35.7	-39.26	-0.18	-1.43
0.45	14.45	64.21	-37.05	-45.34	-0.15	-1.41
0.50	15.34	71.99	-38.41	-51.66	-0.13	-1.39

Table 4.19: Peak current (I_p), corresponding peak current ratio (I_{pa}/I_{pc}) of 2mM Catechol with 90mM Serine in buffer solution (pH 7) of Au electrode at different scan rate (2nd cycle)

v/Vs^{-1}	I_{pa0} /μA	I_{pa1} /μA	I_{pc0}/μA	I_{pc1}/μA	I_{pa0}/I_{pa1}	I_{pa1}/I_{pc1}
0.05	2.46	8.11	-6.54	-4.22	0.30	1.92
0.10	3.06	12.46	-5.89	-7.28	0.24	1.71
0.15	4.48	13.03	-7.58	-7.318	0.34	1.78
0.20	5.91	14.13	-9.27	-7.43	0.41	1.90
0.25	6.72	16.57	-9.91	-9.79	0.40	1.69
0.30	7.48	19.19	-10.75	-12.15	0.38	1.57
0.35	7.935	20.62	-11.04	-13.52	0.38	1.52
0.40	8.39	22.05	-11.22	-14.77	0.38	1.49
0.45	8.94	23.08	-11.53	-15.82	0.38	1.45
0.50	9.42	24.36	-11.74	-16.87	0.38	1.44

Table 4.20: Peak current (I_p), corresponding peak current ratio (I_{pa}/I_{pc}) of 2mM Catechol with 90mM Serine in buffer solution (pH 7) of Pt electrode at different scan rate (2nd cycle)

v/Vs^{-1}	I_{pa0} /μA	I_{pa1} /μA	I_{pc0}/μA	I_{pc1}/μA	I_{pa0}/I_{pa1}	I_{pa1}/I_{pc1}
0.05	1.31	8.26	-2.79	-1.78	0.15	4.64
0.10	2.42	9.47	-4.08	-3.33	0.25	2.84
0.15	3.48	11.08	-4.7	-6.10	0.31	1.81
0.20	4.54	12.69	-5.32	-8.94	0.35	1.41
0.25	5.26	13.23	-5.93	-10.79	0.39	1.22
0.30	5.93	13.92	-6.55	-12.55	0.42	1.10
0.35	4.98	16.85	-6.81	-13.81	0.29	1.22
0.40	4.29	19.63	-7.01	-15.07	0.21	1.30
0.45	4.3	21.27	-7.135	-15.93	0.20	1.33
0.50	4.31	22.96	-7.26	-16.84	0.18	1.36

Table 4.21: Peak Current I_p (µA), peak potential E_p (V) of 2mM Catechol with 90mM Serine of GC electrode at scan rate 0.1V/s in different pH media (2nd cycle)

pH	Peak Current I_p (µA)	Peak potential E_p (V)
	Oxidation, A_0	Oxidation, A_1
3	0.00	0.53
5	2.63	0.40
7	7.49	0.28
9	2.07	0.15
11	0.00	0.04

Table 4.22: Peak Current I_p (µA), peak potential E_p (V) of 2mM Catechol with 90mM Serine of Au electrode at scan rate 0.1V/s in different pH media (2nd cycle)

pH	Peak Current I_p (µA)	Peak potential E_p (V)
	Oxidation, A_0	Oxidation, A_0
3	0.00	0.46
5	1.03	0.29
7	4.96	0.17
9	1.03	0.08
11	0.00	0.03

Table 4.23: Peak Current I_p (µA), peak potential E_p (V) of 2mM Catechol with 90mM Serine of Pt electrode at scan rate 0.1V/s in different pH media (2nd cycle)

pH	Peak Current I_p (µA)	Peak potential E_p (V)
	Oxidation, A_0	Oxidation, A_0
3	0.00	0.51
5	0.89	0.47
7	3.2	0.31
9	1.39	0.26
11	0.00	0.05

Table 4.24: Peak Current I_p (µA) of 2mM Catechol with various concentration of Serine of GC electrode at scan rate 0.1V/s in pH 7 (2^{nd} cycle)

Concentration	Peak Current I_p (µA)
	Oxidation, A_0
10	4.95
30	5.26
50	6.47
70	7.32
90	7.49
100	6.55
130	4.96

Table 4.25: Peak Current I_p (µA) of 2mM Catechol with various concentration of Serine of Au electrode at scan rate 0.1V/s in pH 7 (2^{nd} cycle)

Concentration	Peak Current I_p (µA)
	Oxidation, A_0
30	2.25
50	3.015
70	4.26
90	4.96
100	4.47
130	3.21

Table 4.26: Peak Current I_p (µA) of 2mM Catechol with various concentration of Serine of Pt electrode at scan rate 0.1V/s in pH 7 (2^{nd} cycle)

Concentration	Peak Current I_p (µA)
	Oxidation, A_0
10	2.08
30	2.34
50	2.75
70	2.99
90	3.2

CHAPTER IV

Results and Discussion

The nucleophilic substitution reaction of Catechol in presence of Imidazole, L-Arginine and L-Serine has been carried out in buffer solution of different pH, at different scan rates by Cyclic voltammetry (CV), Controlled potential coulometry (CPC), Differential pulse voltammetry (DPV) and Chronoamperometry (CA) techniques using Glassy carbon (GC), Gold (Au) and Platinum (Pt) electrodes. By conducting these investigation we have extracted precious information regarding nucleophilic substitution reaction of Catechol with Imidazole, L-Arginine and L-Serine which have been discussed elaborately in the following section.

4.1.1 Electrochemical behavior of Catechol

Fig. 4.1 represents the cyclic voltammogram of the first 15 cycles of 2 mM catechol of GC (3 mm) electrode in buffer solution of pH 7. The voltammogram at the $0.1Vs^{-1}$ scan rate has one anodic peak at 0.38 V and corresponding cathodic peak at 0.03 V versus Ag/AgCl. In the subsequent potential cycles no new anodic peak appeared. This can be attributed that catechol showed one anodic peak related to its transformation to *o*-quinone and corresponding cathodic peak related to its transformation to catechol from *o*-quinone (Scheme 1) within a quasi-reversible two-electron transfer process. The anodic and corresponding cathodic peak current ratios at different scan rates are nearly unity at low scan rate which is tabulated in Table 4.1 it indicates that the redox reactions are quasi-reversible.

4.1.2 Electrochemical nature of Catechol in presence of Imidazole

Fig. 4.2 shows the cyclic voltammogram of only Catechol (Green line), only Imidazole (Blue line) and Catechol with Imidazole (Red line) at GC (3 mm) electrode in buffer solution of pH 7 and scan rate 0.1 V/s. The cyclic voltammogram of Catechol shows one anodic peak at A_1 (0.26 V) and corresponding cathodic peak at C_1 (0.05 V) related to its

transformation to *o*-quinone and vice versa. Pure Imidazole is electrochemically inactive amino acid hence no redox couple was observed in the potential range investigated (Fig. 4.2, blue line). Cyclic voltammogram of Catechol in the presence of Imidazole in buffer solution at pH 7 shows one anodic peak in the first cycle of potential and on the reverse scan the corresponding cathodic peak slowly decreases. In the second cycle of potential a new anodic peak A_0 is also observed at less positive potential at 0.02 V. Due to formation of new anodic peak the current intensity of Catechol reduces. This phenomenon can be explained by the fact of nucleophilic attack of Imidazole to o-benzoquinone. Due to the nucleophilic substitution reaction of Imidazole with Catechol, the o-benzoquinone concentration in reaction layer reduces; consequently the A_1 and C_1 peaks reduce. Whereas in the same time Catechol-Imidazole adducts produces and consequently the new peak A_0 appears. The peak current ratio for the peaks A_1 and C_1 (I_{Pa1}/I_{pc1}) decreased noticeably, which indicated the chemical reaction of Imidazole (2) with the o-quinone (1a) produced at the surface of electrode. These observations may ascribe the formation of 4-(1H-imidazole-1-yl)benzene-1,2-diol through nucleophilic substitution reaction (Scheme 1). If the constituent is such that the potential for the oxidation of product is lower, then further oxidation of the product is lower, the further oxidation and further addition may occur [83]. According to this concept it can be said that, the oxidation of Catechol-Imidazole is easier than the oxidation of parent Catechol in the presence of excess amount of nucleophile and this substituted product can be further attacked by Imidazole. However, it was not observed in cyclic voltammogram because of the low activity of o-quinone 4 toward 2. This behavior is in agreement with that reported by other research groups for similar electrochemically generated compounds such as Catechol and different nucleophiles [83-91]. In the absence of other nucleophiles, water or hydroxide ion often adds to the o-benzoquinone [92].

Fig. 4.3 shows the CV of second scan of potential of 2 mM Catechol with 20 mM Imidazole at Platinum (Pt) (1.6 mm) electrode in pH 7 and at scan rate 0.1 V/s. This cyclic voltammogram shows the comparison of only 2 mM Catechol (green line), pure Imidazole (blue line) and Catechol (2 mM) with Imidazole (20 mM) (Red line) in the second scan of potential at the same condition. A new reduction peak (C_0) appears at -0.47 V after the addition of 20 mM Imidazole to the solution at first scan of potential. The peak current decreases significantly with respect to the only Catechol. In the second scan of potential Catechol with Imidazole shows two anodic peaks at - 0.01 V and 0.25 V and the

corresponding two cathodic peaks at - 0.47 V and - 0.02 V, respectively. Upon addition of Imidazole to Catechol solution, the cathodic peak C_1 decreases and a new cathodic peak C_o appears. Also, in the second scan of potential a new anodic peak A_0 appears and anodic peak A_1 decreases similar to GC electrode. This observation can be stated by considering nucleophilic attack of Imidazole to o-benzoquinone. The nucleophilic attack of Imidazole to o-benzoquinone reduces the o-benzoquine concentration in reaction layer. Accordingly the A_1 and C_1 peaks reduce, whereas in the same time produces Catechol-Imidazole adduct and consequently the peak A_0 and C_0 appears (Scheme 1).

A similar behavior is observed when we used a Gold (Au) electrode for the investigation of same solution in the same condition. Fig. 4.4 shows the CV of Catechol (2 mM) in the presence of Imidazole (20 mM) at Au electrode in the second scan of potential. Upon addition of Imidazole to Catechol solution at the Gold (Au) electrode it shows three anodic and three cathodic peaks for the second scan of potential. The newly appearance of A_0 and C_0 peak, and decrease of A_1 and C_1 peak, and also shifting of the positions of peaks A_1 and C_1 also indicates that it is due to follow up reaction of Catechol with Imidazole (Scheme 1) at Au electrode. In case of GC and Pt electrodes, it shows two anodic and two cathodic peaks. The third peak of Au electrodes is due to the oxidation of Au in buffer solution. This unlike behavior has been discussed in the effect of electrode materials section.

4.1.3 Effect of scan rate of Catechol with Imidazole

Fig. 4.5 shows different scan rate comparison graph of 2 mM Catechol with 20 mM Imidazole at pH 7 and all required data has been tabulated in table 4.2. According to this voltammogram it can be seen that the peak current intensity of newly appeared peak gradually increases with the increase of scan rates. The cathodic peaks shift towards left whereas the anodic peaks move to the right direction with increase of scan rate. Fig. 4.6 shows plot of the anodic and cathodic net peak currents for second cycle against the square-root of the scan rates where the net current means the second peak subtracted from the first one by the scan-stopped method in the same condition [83]. The nearly proportional ratio in between redox couple indicates that the peak current of the reactant at each redox reaction is controlled by diffusion process. It can be seen in Fig. 4.7, the

cathodic peak for reduction of o-benzoquinone is almost disappeared in the scan rate of 0.05 V/s. By increasing the scan rate, the cathodic peak for reduction of o-benzoquinone starts to appear and increasing. The corresponding peak current ratio (I_{pa1}/I_{pc1}) vs scan rate for a mixture of Catechol and Imidazole decreases with increasing scan rate gradually (Fig. 4.7). The anodic peak current ratio (I_{pa0}/I_{pa1}) vs scan rate for a mixture of Catechol and Imidazole firstly increases and then after 0.4 V/s scan rate the peak current remains constant in (Fig. 4.7). On the other hand, the value of current function ($Ip/v^{1/2}$) is found to be decreased with increasing scan rate (Fig. 4.8). The exponential nature of the current function versus the scan rate plot indicates the ECE mechanism for electrode process [93]. This confirms the reactivity of o-benzoquinone (1a) towards Imidazole (2) firstly increases at slow scan rate and then at higher scan rate it decreases.According to the results, it was assumed that Imidazole (2) undergoes the 1,4-Michael addition reaction with o-benzoquinone (1a) leads to product 3. The oxidation of this compound (3) was observed easier than the oxidation of parent molecule (1) by virtue of the presence of electron donating amine group.

Step-1:

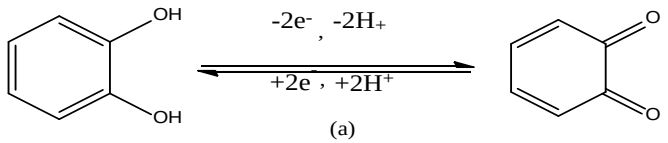

Catechol
1

o-benzoquinone
1a

Step-2:

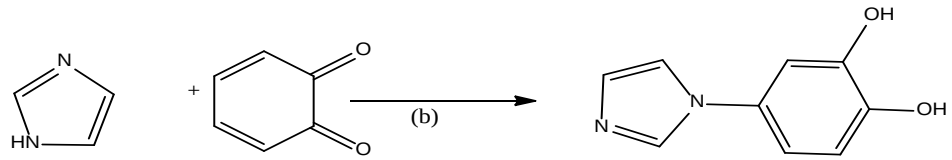

Imidazole
2

o-benzoquinone
1a

4-(1*H*-imidazol-1-yl)benzene-1,2-diol
3

Step-3:

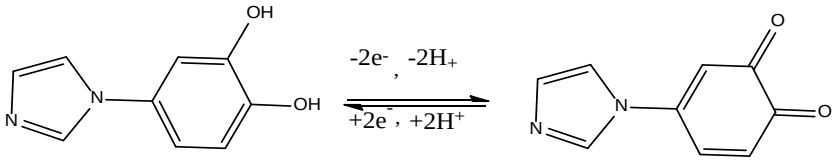

4-(1*H*-imidazol-1-yl)benzene-1,2-diol
3

4-(1*H*-imidazol-1-yl)cyclohexa-3,5-diene-1,2-dione
4

Scheme-1

Figures 4.9-4.10 show the CV of second scan of potential at Pt and Au electrode of 2 mM Catechol with 20 mM Imidazole at pH 7 and different scan rate. The peak current of both the anodic and cathodic peaks increases with the increase of scan rate. The anodic peaks are shifted towards right direction and the cathodic peaks are to the left with increase in the scan rate. But it was difficult to calculate the anodic peak current of newly appeared peak by base current consideration. According to this behavior it can be said that the nucleophilic substitution reaction of imidazole with catechol is suitable at GC electrode.

4.1.4 Influence of pH on Catechol with Imidazole

Cyclic voltammogram of Catechol in presence of 20 mM Imidazole of GC (3 mm) electrode was studied at pH from 3 to 9 (Fig. 4.11). The voltammetric behavior of Catechol at pH 3, 5, and 9 in the presence of 20 mM Imidazole show no new anodic peak appeared after repetitive cycling indicating that the reaction between o-benzoquinone and Imidazole has not occurred. This can be attributed to the fact that at pH 3-5, the nucleophilic property of amine groups is diminished through protonation (Fig. 4.11). This can be explained by the fact that at pH 5 or lowers, the amino group undergoes protonation by excess proton and forms zwitterion. Whereas, in the higher pH range (e.g., pH 9-11), the cyclic voltammograms of Catechol show irreversible behavior. It was thus suggested that the oxidation of Catechol followed by an irreversible chemical reaction with hydroxyl ion, especially in alkaline solutions [94]. However amines in this condition can also act as nucleophiles. The peak position of the redox couple is found to be dependent upon pH. The anodic peak potential of Catechol shifted towards left with the increase of pH. Fig. 4.12 shows the plot of the peak potential, E_p against pH at second cycle in the same condition. The slopes of the plot were determined (60 mV/pH for anodic peak A_1) which is close to theoretical value for two step one electron, one proton transfer process. Fig. 4.13 shows the plot of oxidation peak (A_0) current, I_p against pH of solution. From this figure it can be seen that the maximum peak current was obtained at pH 7 (Table 4.3). At this pH, the difference between the peak current ratio (I_{pC0}/I_{pA0}) in the presence of Imidazole is observed maximum. Consequently, pH 7 was selected as optimum condition for electrochemical study of Catechol, at which the electro oxidation was facilitated in neutral media and hence the rate of electron transfer was faster.

CV of Catechol in presence of 20 mM Imidazole at Platinum (Pt) (1.6 mm) electrode in the second scan of potential has been studied in pH 3 to 11(Fig. 4.14). The voltammetric behavior of 2 mM Catechol at pH 3-5 in the presence of 20 mM Imidazole shows one anodic peak and corresponding cathodic peak after repetitive cycling expressing that the reaction between o-quinone and Imidazole has not occurred. This can be assigned to the fact that in acidic media, the nucleophilic property of amine groups is diminished through protonation. In the pH 7, the o-quinone undergoes Imidazole attack by the amine through a Michael addition reaction suggests that voltammetric new anodic peak A_0 appeared after repetitive cycling. However amines in this condition can also act as nucleophiles. The peak position of the redox couple is found to be dependent upon pH. Fig. 4.15 shows the plot of oxidation peak current, I_p against pH solution. It is seen that the maximum peak current is obtained at pH 7 (Table 4.4). Fig. 4.16 shows the plot of peak potential, E_p vs pH. The slope value of the plot is obtained 75.0mV/pH which is nearer to the value of one electron, one proton transfer process.

The effect of pH on the cyclic voltammogram of 2 mM Catechol in presence of 20 mM Imidazole at Au (1.6 mm) electrode in the second scan of potential was studied at pH from 3 to 11 (Fig. 4.17). The influence of pH for Au electrode in the same systems, the voltammetric properties are slightly different from GC electrode. The voltammetric behavior of Catechol acidic media in the presence of Imidazole shows no new peak in the second scan of potential. This can be indicated to the fact that in lower pH, the nucleophilic property of amine groups is diminished through protonation. In the neutral media, the o-benzoquinone undergoes Imidazole attack by the amine through Michael addition reaction reflected that voltammetric new anodic peak A_0 appeared after repetitive cycling. In the higher pH (e.g., pH 9-11), no new anodic peak appeared in the second scan of potential. However, the peak position of the redox species is found to be dependent upon pH. Fig. 4.18 shows the plots of oxidation peak current, I_p against pH of solution. It is seen that the maximum peak current is obtained at pH 7 (Table 4.5) attributed that nucleophilic addition reaction is most favorable in neutral media. Fig. 4.19 shows the plot of the peak potential, E_p against pH at second cycle in the same condition. The slopes of the plot were (60.5 mV/pH for anodic peak A_1) which is close to theoretical value for two step one electron, one proton transfer process.

4.1.5 Concentration effect of Imidazole

The effect of composition change of Imidazole from 2 mM to 30 mM with fixed composition of Catechol was studied with the help of cyclic voltammetry of GC electrode at pH 7 and scan rate 0.1 V/s (fig. 4.20). Upon addition of Imidazole the anodic peaks shifts positively and a new peak appears at 0.01 V which suggests that the nucleophilic attack takes place and consequently Catechol-Imidazole adduct deposits on the electrode surface. The peak current intensity of the newly appeared anodic and cathodic peak increases with the increase of Imidazole concentration up to 20 mM and after that the redox peak current is started to be decreased (Fig. 4.21). The nucleophilic substitution reaction of Catechol in presence of Imidazole was maximum favorable up to 20 mM of Imidazole at pH 7. The corresponding peak current ratio (I_{pc1}/I_{pa1}) changes with the concentration of Imidazole. This was related to the increase of the homogenous reaction rate of following chemical reaction between o-benzoquinone 1a and Imidazole 2 with increasing concentration of Imidazole up to 20 mM (Table 4.6). At higher concentration of Imidazole (>20 mM), the excess electro-inactive Imidazole may be deposited on the electrode surface and consequently the peak current decreased.

In addition of different concentration of Imidazole (2, 10, 20 and 30 mM) into fixed concentration of Catechol (2 mM) at Gold (Au) and Platinum (Pt) electrodes has been also examined in the same conditions (Fig. 4.22 and fig. 4.24). In the first scan of potential a new cathodic peak (C_0) is appeared at -0.46 V and -0.1 V at Pt and Au electrodes respectively. Upon addition of Imidazole in the second scan of potential, the anodic peaks shifted and a new anodic peak appeared at - 0.02 V and - 0.01 V at Pt and Au electrodes respectively which suggests the formation of Catechol-Imidazole adduct. The net current intensity of the newly appeared anodic and cathodic peak increases with the increase of composition up to 20 mM of Imidazole. After further addition of Imidazole (>20 mM), the anodic and cathodic peak current gradually decreases (Table 4.7-4.8). At higher concentration of Imidazole (>20 mM), the excess electro inactive Imidazole may be accumulated on the electrode surface and the peak current decreased. Therefore, the concentration effects of Imidazole into the fixed concentration of Catechol (2 mM) for Au and Pt electrodes are few different from GC electrode.

4.1.6 Effect of electrode materials

In absence and presence of 20 mM Imidazole with the fixed composition of 2 mM Catechol the effect of electrode material on Electrochemical properties of Catechol was studied with the help of both cyclic voltammetry (CV) and differential pulse voltammetry (DPV) by using different electrodes like GC, Au and Pt at different pH at scan rate 0.1 V/s has shown in Fig. 4.26 and Fig. 4.27. The nature of voltammogram, the peak position and current intensity for the studied systems are different for different electrodes although the diameter of GC electrode (3 mm) was higher than Au and Pt (1.6 mm). The CV of GC electrode is significantly different from those of the Au and Pt electrodes based on peak current consideration. All electrodes show two anodic and corresponding cathodic peaks in the potential range of investigation. Among them the peak current intensity of GC electrode is much higher than Au and Pt electrodes in Figures 4.26-4.27. In the case of second cycle of potential a new oxidation and reduction peak appear at lower oxidation potential which can be attributed to the oxidation of adduct formed between the o-benzoquinone and Imidazole. Electrochemical properties of Catechol with Imidazole for example change of pH, concentration, scan rate etc. were studied in detail using Pt and Au electrodes. But among the electrodes, the voltammetric response of GC electrode was better than Pt and Au electrodes in the studied systems.

According to DPV electrode comparison graph (Fig. 4.27) it can be seen that GC electrode shows better voltammetric response having two anodic peak at -0.02 V and 0.23 V. We considered the Catechol-Imidazole adduct peak at -0.01 V and another peak at more lower potential. Among GC, Pt and Au electrode the peak current and voltammetric response of GC electrode was found much better than Pt electrode under this investigation. Therefore, GC electrode was chosen as electrode material for this investigation.

4.1.7 Subsequent cycles of CV of Catechol-Imidazole

Fig. 4.28 shows the cyclic voltammogram of the first 15 cycles of 2 mM Catechol with 20 mM Imidazole of GC (3 mm) electrode in buffer solution of pH 7 for the potential range between - 0.6 V to 0.9 V. The voltammogram at the scan rate 0.1 Vs^{-1} has one anodic peak at 0.25 V and corresponding cathodic peak at 0.05 V when considered the first scan of potential (red line). In the subsequent potential cycles a new anodic peak appeared at

0.04 V and intensity of the first anodic peak current increased progressively on cycling but the second anodic peak current decreases and shifted positively on cycling. This can be attributed to produce of the Catechol-Imidazole adduct through nucleophilic substitution reaction in the surface of electrode (Scheme 1). The successive decrease in the height of the Catechol oxidation and reduction peaks with cycling can be ascribed to the fact that the concentrations of Catechol-Imidazole adduct formation increased by cycling leading to the decrease of concentration of Catechol or quinone at the electrode surface. The positive shift of the second anodic peak in the presence of Imidazole is probably due to the formation of a thin film of product at the surface of the electrode, inhibiting to a certain extent the performance of electrode process. Along with the increase in the number of potential cycles the first anodic peak current increased up to 10 cycles and then the peak current almost unchanged with subsequent cycle (Fig. 4.28). This may be due to the block of electrode surface by the newly formed species after more cycling.

The effect of the cyclic voltammograms of the first 15 cycles of 2 mM Catechol with 20 mM Imidazole of Gold (Au) electrode and Platinum (Pt) electrode in buffer solution of pH 7 were also studied in the same condition (Fig. 4.29). In Fig. 4.30 at Au electrode there were two anodic peaks at 0.25 V and 1.06 V and three cathodic peaks at - 0.11 V, 0.03 V and 0.43 V respectively in the first scan of potential (red line). In the subsequent scan of potential Au electrode shows a new anodic peak at - 0.02 V with another three anodic peaks (blue line). But at Pt electrode there is one anodic peaks at 0.3 V and two cathodic peaks at - 0.47 V and - 0.01 V in the first scan of potential (red line) (Fig. 4.29). In the subsequent potential cycles a new anodic peak appeared at - 0.02 V and the first anodic peak current increased progressively on cycling but the second anodic peak current decreases and shifted positively on cycling. This can be suggested to produce the Catechol-Imidazole adduct through nucleophilic substitution reaction in the surface of electrode (Scheme 1).

4.1.8 Controlled-potential coulometry of Catechol with Imidazole

Controlled-potential coulommetry was performed to monitor the electrolysis progress with the help CV in aqueous solution containing 1 mM of Catechol and 10 mM of Imidazole at 0.45 V in pH 7 which has been showed in (Fig. 4.31). This voltammogram indicates that,

during the course of coulometry the peaks A_0 appears and the height of the A_0 peak increases to the advancement of coulometry, parallel to the decrease in height of anodic peak A_1. After some couples of hour both redox couple of appeared peak does not increase with the successive decrease of concentration of Catechol which has been showed by CV. This observation could lead us to draw a concept that the capacitive current was increased or side reactions were taken place. These observations allow us to propose the pathway in Scheme 1 for the electro-oxidation of Catechol (1) in the presence of Imidazole (2). According to our results, it seems that the 1,4 addition reaction of 2 to *o*-quinone (1a) reaction (2) was faster than other secondary reactions, leading to the intermediate 3. The oxidation of this compound (3) was easier than the oxidation of parent starting molecule (1) by virtue of the presence of electron-donating group. Like *o*-quinone**1a**, *o*-quinone **4** can also be attacked from the C-5 position by Imidazole (2). However, no over reaction was observed during the voltammetric experiments because of the low activity of the *o*-quinone **4** toward 1,4-Michael addition reaction with Imidazole (2).

4.1.9 pH effect of DPV of Catechol with Imidazole

Voltammogram obtained from 2 mM Catechol in the presence of 20 mM Imidazole in second scan in different pH (3-9) at GC electrode has shown in Fig. 4.32 to make clearer for the nucleophilic substitution reaction of Imidazole with Catechol. In the buffer solution of pH 7, Catechol shows two well-developed peaks at 0.02 V and 0.22 V respectively in the presence of Imidazole (Fig. 4.32). It also can be seen that at acidic and basic media there are no oxidation peak observed whereas completely separated anodic peaks with high current intensity were observed in pH 7, which can be attributed to the oxidations of o-benzoquinone-Imidazole new compound and Catechol, respectively.

Gold (Au) electrode is also used for the investigation of DPV of 2 mM Catechol with 20 mM Imidazole in different buffer solution at 0.1 Vs^{-1}. Fig. 4.34 shows the first and second scan of potential of Catechol + Imidazole solution at different pH, respectively. However, in pH 7 new peak A_0 appeared which may be attributed to the formation of Catechol-Imidazole adduct. But, in lower and higher pH media no new anodic peak appeared. In the buffer solution of pH 7, the voltammogram shows two well-developed peak ascribed the formation of adduct similar to GC electrode.

The effect of pH on the DPV technique was also employed to make clearer for Catechol-Imidazole addition reaction at Pt electrode in same condition. DPV of 2 mM Catechol in the presence of 20 mM Imidazole in first and second scan of potential at different pH (3-11) were shown in Fig. 4.33 (Epulse 0.02 V, tpulse 20 ms and scan rate 0.1 V/s). It is noticed that the peak positions of the DPV of Catechol with Imidazole shifts negatively this indicates that the nucleophilic reaction is easier at pH 7. But, in pH 3, pH 5, pH 9 and pH 11 no new peak appears in the second scan of potential. High current intensity is observed at pH 7, which can be attributed to the formation of Catechol-Imidazole adduct. The DPV of Au and Pt electrodes are consistent with the GC electrode in the studied systems at the same condition.

4.1.10 Effect of deposition time change of DPV of Catechol + Imidazole

Fig. 4.35, we considered the DPV of deposition time change (0, 10, 60, 120, 150 and 240 s) of 2 mM Catechol 20 mM Imidazole of pH 7. According to this figure, increasing of deposition time leads to develop a new peak at -0.01 V. At 10s a new peak is observed and when the deposition time increases 60s, more nucleophilic attack occurred and consequently more Catechol-Imidazole adduct was formed which leads to decreasing in the concentration of o-benzoquinone and increasing in the concentration of Catechol-Imidazole adduct at the surface of electrode. Maximum peak intensity was obtained up to 60s. For further increase of deposition time from 60s to 240s, both first and second anodic peak current decreases. This confirmed that with the increase of time decreases the concentration of o-benzoquinone due to follow up the reaction.

4.1.11 Effect of concentration of DPV of Catechol + Imidazole

The effect of different composition of Imidazole on Catechol was studied by using the differential pulse voltammetry. DPV of 2 mM Catechol with 2 to 30 mM Imidazole at pH 7 has been shown in fig. 4.36. There we observe again two separated anodic peaks appeared after addition of different concentration of Imidazole into Catechol similar to Fig. 4.20. In this case, the gradual increasing of the concentration of Imidazole up to 20 mM leads to increasing of first anodic peak current. For further increase of concentration, all anodic peak decreases gradually. In lower concentration of Imidazole (<20 mM), the

nucleophilic substitution reaction take place in comparable degree, whereas increasing the concentration of Imidazole (20 mM) make favorable nucleophilic attack of Imidazole toward o-benzoquinone generated at the surface of electrode. For further addition of Imidazole (>20 mM) into Catechol solution, the excess electro inactive Imidazole deposited on the electrode surface and hence the peak current decreases.

The effect of Imidazole concentration on the DPV of Catechol was also studied by using Pt (1.6 mm) electrode in the same condition. Fig. 4.38 shows DPV for 2 mM of Catechol solution containing buffer (pH 7) in the presence of various concentration of Imidazole from 2 mM to 30 mM at the surface of Pt electrode for the first and second scan of potential. As reported in Fig. 4.37, in the second scan there are two separated anodic peaks appeared after addition of Imidazole into Catechol. In lower concentration of Imidazole (<20 mM), the nucleophilic substitution reaction take place in comparable degree, whereas increasing the concentration of Imidazole (20 mM) make susceptible for nucleophilic attack of Imidazole towards o-benzoquinone generated at the surface of electrode. For more addition of Imidazole (> 20 mM) into Catechol solution, the excess electro inactive Imidazole accumulated on the electrode surface and hence the peak current decreases.

Gold (Au) electrode was also used for the investigation on the DPV of fixed 2 mM Catechol with different concentration (2-30 mM) of Imidazole in buffer solution pH 7 at 0.1 Vs^{-1}. Fig. 4.38 shows the second scan of potential of the studied systems at different concentration, respectively. In second scan of potential an appeared peak, A_0 was obtained which may be attributed the formation of Catechol-Imidazole adduct.

In this investigation different concentration 2-30 mM of Imidazole was used to determine the optimum condition for the nucleophilic substitution reaction on Catechol. As the reaction was occurred at moderately high concentration of nucleophiles, consequently the voltammetric peaks (CV and DPV) for adduct appeared noticeably. In contrast, comparatively low concentration of Imidazole was not favorable for the study of electrochemical oxidation of Catechol because the appearing peak was not so prominent.
From the experimental study it is noticeable that Imidazole acts properly as a nucleophile at pH 7. When the pH is below 7 that is acidic media, the nucleophilic activity of Imidazole reduces due to the protonation of amine. Whereas at basic condition, other

nucleophiles such as –OH produce in solution, therefore, the activity of amines decreases and the oxidation of Catechol followed by an irreversible chemical reaction with hydroxyl ion [66].

Therefore, from the above discussion it was clear that the nucleophilic substitution reaction of Catechol in presence of Imidazole is maximum favorable at 20 mM of Imidazole and at pH 7 which is consistent with both CV and DPV. All above observations could be attributed to the reaction between Imidazole and o-benzoquinone species produced at the surface of electrode, with the new anodic peak being attributed to the oxidation of newly formed o-benzoquinone- imidazole adduct.

4.2.1. Electrochemical nature of Catechol in presence of L-Arginine

Fig. 4.39 indicates the cyclic voltammogram of only catechol (Green line), only L-Arginine (Blue line) and catechol with L-Arginine (Red line) at GC (3mm) electrode in buffer solution of pH 7 and scan rate 0.1V/s. According to this cyclic voltammogram it can be seen that catechol shows one anodic peak at A_1 (0.44V) and corresponding cathodic peak at C_1 (0.12V) related to its transformation to *o*-benzoquinone and vice versa. As pure L-Arginine is an electrochemically inactive amino acid hence no sharp redox couple was observed in the potential range of investigation (Fig. 4.39, blue line). Cyclic voltammogram of catechol in the presence of L-Arginine in buffer solution of pH 7 shows one anodic peak in the first cycle of potential and on the reverse scan the corresponding cathodic peak slowly decreases and new peak C_0 is observed at less positive potential -0.28V. In the second cycle of potential a new anodic peak A_0 is also observed at less positive potential at -0.07V. Due to formation of new redox couple the current intensity of catechol reduces. This phenomenon can be explained by the fact of nucleophilic attack of Arginine to o-benzoquinone. Due to the conduction of nucleophilic substitution reaction of L-Arginine with catechol, the o-benzoquinone concentration in reaction layer reduces, consequently the A_1 and C_1 peaks reduce. Whereas in the same time catechol L-Arginine adduct produces and consequently the new peak A_0 appears. The peak current ratio for the peaks A_1 and C_1 (I_{Pa1}/I_{pc1}) decreased noticeably, which indicated the chemical reaction of Arginine (2) with the o-quinone (1a) produced at the surface of electrode. These observations may ascribe the formation of 2-amino-4-(1-(3,4-dioxocyclohexa-1,5-dien-1-

yl) guanidine)-4-oxobutanoic acid through nucleophilic substitution reaction (Scheme 2). If the constituent is such that the potential for the oxidation of product is lower, then further oxidation of the product is lower, the further oxidation and further addition may occur [83]. According to this concept it can be drawn that, the oxidation of catechol-Arginine is easier than the oxidation of parent catechol in the presence of excess amount of nucleophile and this substituted product can be further attacked by L-Arginine. However, it was not observed in cyclic voltammogram because of the low activity of o-quinone 4 toward 2. This behavior is in agreement with that reported by other research groups for similar electrochemically generated compounds such as catechol and different nucleophiles [83-91]. In the absence of other nucleophiles, water or hydroxide ion often adds to the o-benzoquinone [92].

Fig. 4.40 shows the CV of second scan of potential of 2 mM catechol with 30 mM L-Arginine at Platinum (Pt) (1.6mm) electrode in pH 7 and at scan rate 0.1V/s. This cyclic voltammogram shows the comparison of only 2mM catechol (green line), pure L-Arginine (blue line) and catechol (2 mM) with 30 mM L-Arginine (Red line) in the second scan of potential at the same condition. A new reduction peak (C_0) appears at -0.28 V after the addition of 30 mM L-Arginine to the solution at first scan of potential. The peak current decreases significantly with respect to the only catechol. In the second scan of potential catechol with L-Arginine shows two anodic peaks at - 0.04 V and 0.32 V and the corresponding two cathodic peaks at - 0.32 V and - 0.01 V, respectively. Upon addition of L-Arginine to catechol solution, the cathodic peak C_1 decreases and a new cathodic peak C_o appears. Also, in the second scan of potential a new anodic peak A_o appears and anodic peak A_1 decreases similar to GC electrode. This observation can be stated by considering nucleophilic attack of L-Arginine to o-benzoquinone. The nucleophilic attack of L-Arginine to o-benzoquinone reduces the o-benzoquine concentration in reaction layer. Accordingly the A_1 and C_1 peaks reduce, whereas in the same time produces catechol-Arginine adduct and consequently the peak A_0 and C_0 appears (Scheme 2).

A similar behavior is observed when we used a Gold (Au) electrode for the investigation of same solution in the same condition. Fig. 4.41 shows the CV of catechol (2 mM) in the presence of L-Arginine (30 mM) at Au electrode in the second scan of potential. Upon addition of L-Arginine to catechol solution at the Gold (Au) electrode it shows three

anodic and three cathodic peaks for the second scan of potential. The newly appearance of A_0 and C_0 peak, and decrease of A_1 and C_1 peak, and also shifting of the positions of peaks A_1 and C_1 also indicates that it is due to follow up reaction of catechol with L-Arginine (Scheme 2) at Au electrode. In case of GC and Pt electrodes, it shows two anodic and two cathodic peaks. The third peak of Au electrodes is due to the oxidation of Au in buffer solution. This unlike behavior has been discussed in the effect of electrode materials section.

4.2.2 Effect of scan rate of Catechol with L-Arginine

Fig. 4.42 show different scan rate comparison graph of 2mM catechol with 30mM L-Arginine at pH 7 and all required data has been tabulated in table 4.9. According to this voltammogram it can be seen that the peak current intensity of newly appeared peak gradually increases with the increase of scan rates. The cathodic peaks shift towards left whereas the anodic peaks move to the right direction with increase of scan rate. Fig. 4.43 shows plot of the anodic and cathodic net peak currents for second cycle against the square-root of the scan rates where the net current means the second peak subtracted from the first one by the scan-stopped method in the same condition [83]. The nearly proportional ratio in between redox couple indicates that the peak current of the reactant at each redox reaction is controlled by diffusion process. It can be seen in Fig. 4.42, the cathodic peak for reduction of o-benzoquinone is almost disappeared in the scan rate of 0.05 V/s. By increasing the scan rate, the cathodic peak for reduction of o-benzoquinone starts to appear and increasing. The corresponding peak current ratio (I_{pa1}/I_{pc1}) vs scan rate for a mixture of catechol and Arginine decreases with increasing scan rate firstly and then after 0.25 V/s, it remains almost unchanged (Fig 4.44). The anodic peak current ratio (I_{pa0}/I_{pa1}) vs scan rate for a mixture of catechol and Arginine firstly increases and then after 0.2 V/s scan rate the peak current remains constant in (Fig. 4.44). On the other hand, the value of current function ($Ip/v^{1/2}$) is found to be decreased with increasing scan rate (Fig. 4.45). The exponential nature of the current function versus the scan rate plot indicates the ECE mechanism for electrode process [93]. This also indicates the reactivity of o-benzoquinone (1a) towards Arginine (2) firstly increases at slow scan rate and then at higher scan rate it decreases.

The existence of a subsequent chemical reaction between o-benzoquinone **1a** and Arginine **2** is supported by the following evidence.

(i) In the presence of Arginine both I_{pc1} and I_{pa1} decreases during second cycle (fig. 4.44), this could be indicative of the fact that electrochemically generated *o*-benzoquinone **1a** is removed partially by chemical reaction with L-Arginine (**2**).

(ii) Corresponding peak current ratio (I_{pa1}/I_{pc1}) varies with potential sweep rate. In this case, a well-defined cathodic peak C_1 is observed at highest sweep rate. For lower sweep rates, the peak current ratio (I_{pa1}/I_{pc1}) is less than one and increases with increasing sweep rate. This is indicative of departure from intermediate and arrival to diffusion region with increasing sweep rate [83].

(iii) Increase in the scan rate causes a decrease in the progress of the chemical reaction of 1a with 2 during the period of recording the cyclic voltammogram and therefore, decease in peak current ratio (I_{pa0}/I_{pa1}) at higher scan rate.

(iv) The current function, $I_p/v^{1/2}$ for A_1 was found to be decreased exponentially with increasing scan rate. This indicates the reaction mechanism of the system was of ECE type (Scheme 2).

According to the results, it was assumed that Arginine (2) undergoes the 1,4-Michael addition reaction with o-benzoquinone (1a) leads to product 3. The oxidation of this compound (3) was observed easier than the oxidation of parent molecule (1) by virtue of the presence of electron donating amine group.

Step-1:

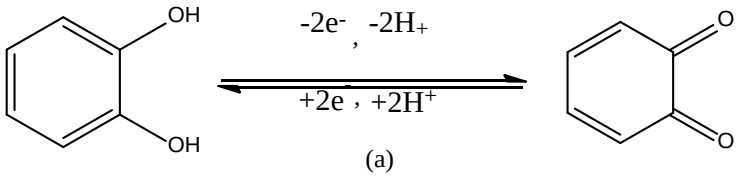

(a)

Catechol
1

o-benzoquinone
1a

Step-2:

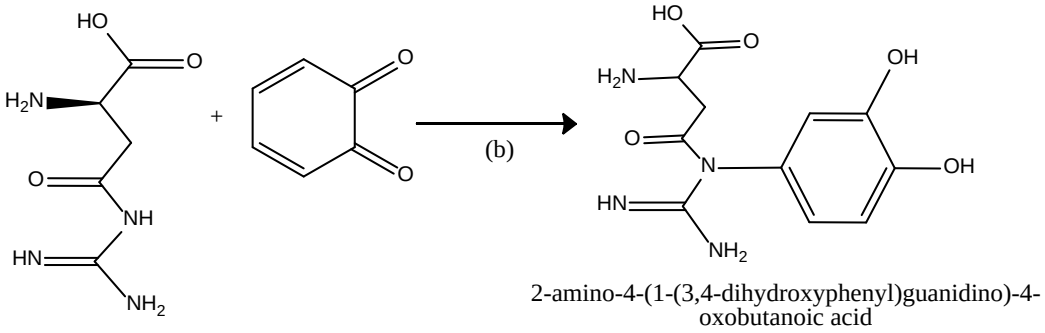

L-Arginine

2

1a

2-amino-4-(1-(3,4-dihydroxyphenyl)guanidino)-4-oxobutanoic acid

3

Step-3:

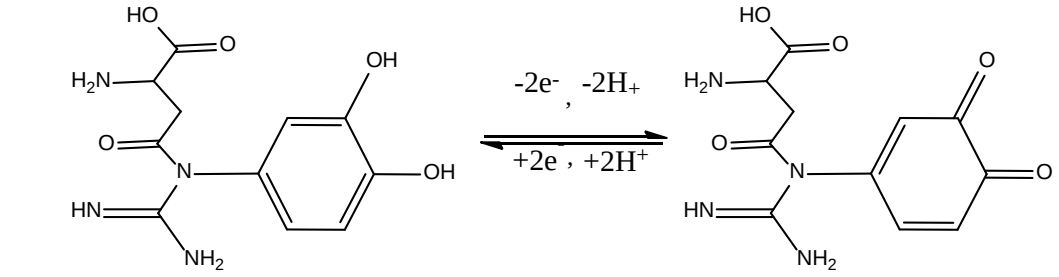

2-amino-4-(1-(3,4-dihydroxyphenyl)guanidino)-4-oxobutanoic acid

3

2-amino-4-(1-(3,4-dioxocyclohexa-1,5-dien-1-yl)guanidino)-4-oxobutanoic acid

4

Scheme-2:

Fig. 4.46 shows the CV of second scan of potential at Pt electrode of 2 mM catechol with 30 mM L-Arginine at pH 7 and different scan rate. The peak current of both the anodic and cathodic peaks increases with the increase of scan rate. The anodic peaks are shifted towards right direction and the cathodic peaks are to the left with increase in the scan rate. Fig. 4.47 shows plots of the anodic and cathodic peak currents for second scan of potential as a function of square-root of the scan rates. The proportionality of the anodic and the cathodic peaks ascribed that the peak current of the reactant at each redox reaction is controlled by diffusion process. The anodic and cathodic peak currents, peak potentials, corresponding peak potential differences and peak current ratio are tabulated in Table 4.11.

Fig. 4.48 shows variation of peak current ratio of corresponding peak (I_{pa1}/I_{pc1}) and anodic peak (I_{pa0}/I_{pa1}) vs scan rate (v) of 2mM Catechol with 30mM L-Arginine in the same

condition. The corresponding peak current ratio (I_{pa1}/I_{pc1}) vs scan rate for a mixture of catechol and L-Arginine decreases with increasing scan rate firstly and then after 0.2V/s, the peak current started to be increased (Fig. 4.48). The anodic peak current ratio (I_{pa0}/I_{pa1}) vs scan rate for a mixture of catechol and L-Arginine firstly increases and then after 0.1V/s scan rate the peak current remain unchanged (Fig. 4.48). Beside this, the value of current function ($Ip/v^{1/2}$) is found to be decreased with increasing scan rate (Fig. 4.49). The exponential nature of the current function versus the scan rate plot indicates the ECE mechanism for electrode process.

Similarly the voltammetric behavior of the above systems has been investigated at Au electrode. Fig. 4.50 shows the CV of catechol with 30 mM L-Arginine for second cycle of potential at different scan rate in pH 7. This voltammogram is consistent with fig. 4.42 and fig. 4.46. According to Fig. 4.51 and table 4.10 it can be seen that the anodic and cathodic net peak currents against the square-root of the scan rates is nearly proportional which suggests that the peak current of the reactant at each redox reaction is controlled by diffusion process. Fig. 4.52 shows variation of peak current ratio of corresponding peak (I_{pa1}/I_{pc1}) and anodic peak (I_{pa0}/I_{pa1}) vs scan rate (v) in the same condition. The (I_{pa1}/I_{pc1}) peak current ratio gradually decreasing with increasing scan rates whereas the anodic peak current ratio observed maximum at 0.2V/s and after that it remains almost unchanged with increasing scan rates(Table 4.10-4.11). The exponentially decreasing nature with increasing scan rates in fig. 4.53 indicates that the reaction is taken place by ECE mechanism. According to all system it can be said that, the nucleophilic substitution reaction of catechol in presence of L-Arginine is maximum favorable at slow scan rate by diffusion process.

4.2.3 Influence of pH on catechol with L-Arginine

Cyclic voltammogram of catechol in presence of 30 mM L-Arginine of GC (3mm) electrode has been studied at pH from 3 to 11 (Fig. 4.54). The voltammetric behavior of catechol at pH 3, 5, 9 and 11 in the presence of 30mM L-Arginine show no new appeared anodic peak after repetitive cycling indicating that the reaction between o-benzoquinone and L-Arginine has not occurred. This can be attributed to the fact that at pH 3-5, the nucleophilic property of amine groups is diminished through protonation (Fig. 4.54). This

can be explained by the fact that at pH 5 or lowers, the amino group undergoes protonation by excess proton and form zwitterion. Whereas, in the higher pH range (e.g., pH 9- 11), the cyclic voltammogram of catechol show irreversible behavior. It was thus suggested that the oxidation of catechol followed by an irreversible chemical reaction with hydroxyl ion, especially in alkaline solutions [94]. However amines in this condition can also act as nucleophiles. The peak position of the redox couple is found to be dependent upon pH (Fig. 4.55). The anodic peak potential of catechol shifted towards left with the increase of pH.

Fig. 4.56 shows the plot of oxidation peak (A_0) current, I_p against pH of solution. From this figure it was seen that the maximum peak current was obtained at pH 7 (table 4.12). At this pH, the difference between the peak current ratio (I_{pC0}/I_{pA0}) in the presence of Arginine is observed maximum. Consequently, pH 7 was selected as optimum condition for electrochemical study of catechol, at which the electro oxidation was facilitated in neutral media and hence the rate of electron transfer was faster.

CV of catechol in presence of 30 mM L-Arginine at Platinum (Pt) (1.6 mm) electrode in the second scan of potential has been studied in pH 3 to 11 (Fig. 4.57). The voltammetric behavior of 2 mM catechol at acidic and basic media in the presence of 30 mM L-Arginine shows one anodic peak and corresponding cathodic peak after repetitive cycling expressing that the reaction between o-quinone and L-Arginine has not occurred. This can be assigned to the fact that at acidic media, the nucleophilic property of amine groups is diminished through protonation. In the pH 7 the o-quinone undergoes L-Arginine attack by the amine through a Michael addition reaction suggests that voltammetric new anodic peak A_0 appeared after repetitive cycling. However amines in this condition can also act as nucleophiles. The peak position of the redox couple is found to be depended upon pH. Fig. 4.58 shows the plot of oxidation peak current, I_p against pH solution. It is seen that the maximum peak current is obtained at pH 7 (table 4.14). Fig. 4.59 shows the plot of peak potential, E_p vs pH. The slope value of the plot is obtained 61.5mV/pH which is nearer to the value of one electron, one proton transfer process.

The effect of pH on the cyclic voltammogram of 2 mM catechol in presence of 30 mM L-Arginine at Au (1.6 mm) electrode in the second scan of potential was studied at pH from 3 to 11 (Fig. 4.60). The influence of pH for Au electrode in the same systems, the

voltammetric properties are slightly different from GC electrode. The voltammetric behavior of catechol at pH 3, pH 5, pH 9 and pH 11 in the presence of L-Arginine shows no new peak in the second scan of potential. This can be indicated to the fact that in lower pH, the nucleophilic property of amine groups is diminished through protonation. In the pH 7, the o-benzoquinone undergoes L-Arginine attack by the amine through Michael addition reaction reflected that voltammetric new anodic peak A_0 appeared after repetitive cycling. In the higher pH (e.g., pH 11), no new anodic peak appeared in the second scan of potential. However, the peak position of the redox species is found to be dependent upon pH. Fig. 4.61 shows the plots of oxidation peak current, I_p against pH of solution. It is seen that the maximum peak current is obtained at pH 7 (table 4.13) attributed that nucleophilic addition reaction is most favorable in neutral media. Fig. 4.62 shows the plot of the peak potential, E_p against pH at second cycle in the same condition. The slope of the plot was calculated (49 mV/pH for anodic peak A_1) which is close to theoretical value for two step one electron, one proton transfer process.

4.2.4 Concentration effect of L-Arginine

The influence of composition change of L-Arginine from 10 mM to 100 mM with fixed composition of catechol has been studied with the help of cyclic voltammetry of GC electrode at pH 7 and scan rate 0.1V/s (fig. 4.63). Upon addition of L-Arginine the anodic peaks shifts negatively and a new peak appears at - 0.07V which suggests that the nucleophilic attack takes place and consequently catechol-Arginine adduct deposits on the electrode surface. The peak current intensity of the newly appeared anodic and cathodic peak increases with the increase of L-Arginine concentration up to 30 mM and after that the redox peak current is started to be decreased (Fig. 4.64). The nucleophilic substitution reaction of catechol in presence of Arginine was maximum favorable up to 30 mM of Arginine at pH 7 (table 4.15). The corresponding peak current ratio (I_{pc1}/I_{pa1}) changes with the concentration of Arginine. This was related to the increase of the homogenous reaction rate of following chemical reaction between o-benzoquinone 1a and Arginine 2 with increasing concentration of Arginine up to 30 mM. At higher concentration of Arginine (>30mM), the excess electro-inactive Arginine may be deposited on the electrode surface and consequently the peak current decreased.

In addition of different concentration of L-Arginine (10, 20, 30, 50 and 100 mM) into fixed concentration of catechol (2 mM) at Gold (Au) and Platinum (Pt) electrodes has been also examined in the same conditions (Fig. 4.65 - 4.68). In the first scan of potential a new cathodic peak (C_0) appears at -0.32 V and -0.24 V at Pt and Au electrodes respectively. Upon addition of L-Arginine in the second scan of potential, the anodic peaks shifted and a new anodic peak appeared at - 0.05 V and - 0.1 V at Pt and Au electrodes respectively which suggests the formation of catechol-Arginine adduct. The net current intensity of the newly appeared anodic and cathodic peak increases with the increase of composition up to 10 to 30 mM of L-Arginine (Table 4.16-4.17). After further addition of L-Arginine (>30 mM), the anodic and cathodic peak current gradually decreases. At higher concentration of L-Arginine (>30mM), the excess electroinactive L-Arginine may be accumulated on the electrode surface and the peak current decreased. Therefore, the concentration effects of L-Arginine into the fixed concentration of catechol (2 mM) for Au and Pt electrodes are few different from GC electrode.

4.2.5 Effect of electrode materials

In absence and presence of 30mM Arginine with the fixed composition of 2mM catechol the effect of electrode material on Electrochemical properties of catechol has been studied with the help of both cyclic voltammetry (CV) and Differential pulse voltammetry (DPV) by using different electrodes like GC, Au and Pt at different pH at scan rate 0.1V/s has shown in Fig. 4.69 and fig. 4.70. The nature of voltammogram, the peak position and current intensity for the studied systems are different for different electrodes although the diameter of GC electrode (3mm) was higher than Au and Pt (1.6mm). The CV of GC electrode is significantly different from those of the Au and Pt electrodes based on peak current consideration. All electrodes show two anodic and corresponding cathodic peaks in the potential range of investigation. Among them the peak current intensity of GC electrode is much higher than Au and Pt electrodes in Figures 4.69-4.70. Voltammetric measurements performed at an Au electrode in only buffer solution of without catechol and L-Arginine at pH 7, showed a peak at 1.1 V to the formation of Au(III) hydroxide. Consequently, the third peak (1.08 V) of Au electrode in presence of catechol and L-Arginine at pH 7 is due to the oxidation of Au in buffer solution. Similar behavior of oxidation of Au electrode in different pH has been reported [89]. In the case of GC and Pt

electrodes for the second cycle of potential a new oxidation and reduction peak appear at lower oxidation potential which can be attributed to the oxidation of adduct formed between the o-benzoquinone and L-Arginine. Electrochemical properties of catechol with L-Arginine for example change of pH, concentration, scan rate etc. were studied in detail using Pt and Au electrodes. But among the electrodes, the voltammetric response of GC electrode was better than Pt and Au electrodes in the studied systems.

According to DPV electrode comparison graph (Fig. 4.70) it can be seen that GC electrode showed better voltammetric response and two anodic peak at -0.32V and -0.02V. We considered the catechol-adduct peak at -0.02V and another very small peak at more lower potential -0.32 could be due to side reaction like polymerization, further oxidation of catechol-adduct or nucleophilic attract of hydroxyl ion. Among GC, Pt and Au electrode the peak current and voltammetric response of GC electrode was more suitable than Pt electrode under this investigation. Therefore, GC electrode was chosen as electrode material for this investigation.

4.2.6 Subsequent cycles of CV of Catechol+L-Arginine

Fig. 4.71 shows the cyclic voltammograms of the first 15 cycles of 2 mM catechol with 30 mM L-Arginine of GC (3 mm) electrode in buffer solution of pH 7 for the potential range between - 0.7 V to 0.9 V. The voltammogram at the scan rate 0.1 Vs^{-1} has one anodic peak at 0.22 V and two cathodic peaks at -0.26 V and 0.02 V when considered the first scan of potential (red line). In the subsequent potential cycles a new anodic peak appeared at -0.04V and intensity of the first anodic peak current increased progressively on cycling but the second anodic peak current decreases and shifted positively on cycling. This can be attributed to produce of the catechol-Arginine adduct through nucleophilic substitution reaction in the surface of electrode (Scheme 2). The successive decrease in the height of the catechol oxidation and reduction peaks with cycling can be ascribed to the fact that the concentrations of catechol-Arginine adduct formation increased by cycling leading to the decrease of concentration of catechol or quinone at the electrode surface. The positive shift of the second anodic peak in the presence of L-Arginine is probably due to the formation of a thin film of product at the surface of the electrode, inhibiting to a certain extent the performance of electrode process. Along with the increase in the number of

potential cycles the first anodic peak current increased up to 10 cycles and then the peak current almost unchanged with subsequent cycle (Fig. 4.71). This may be due to the block of electrode surface by the newly formed species after more cycling.

The effect of the cyclic voltammograms of the first 15 cycles of 2 mM Catechol with 30 mM L-Arginine of Gold (Au) electrode and Platinum (Pt) electrode in buffer solution of pH 7 were also studied in the same condition. In Fig. 4.73 at Au electrode there were two anodic peaks at 0.22V and 1.02 V and three cathodic peaks at - 0.24 V, 0.09 V and 0.44 V respectively in the first scan of potential (red line). In the subsequent scan of potential Au electrode shows a new anodic peak at - 0.08 V with another three anodic peaks (blue line). But at Pt electrode there is one anodic peaks at 0.22 V and two cathodic peaks at - 0.29 V and 0.01 V in the first scan of potential (red line) (Fig. 4.72). In the subsequent potential cycles a new anodic peak appeared at - 0.06 V and the first anodic peak current increased progressively on cycling but the second anodic peak current decreases and shifted positively on cycling. This can be suggested to produce the catechol-Arginine adduct through nucleophilic substitution reaction in the surface of electrode (Scheme 2).

4.2.7 pH effect of DPV of Catechol with L-Arginine

Voltammogram obtained from 2mM catechol in the presence of 30 mM L-Arginine in second scan in different pH (3-11) at GC electrode has shown in Fig. 4.74 to make clearer for the nucleophilic substitution reaction of Arginine on catechol. In the buffer solution of pH 7, catechol shows two well-developed wave at -0.035V and 0.21V respectively in the presence of L-Arginine. As can be seen two completely separated anodic peaks with high current intensity were observed in pH 7, which can be attributed to the oxidations of o-benzoquinone-Arginine new compound and catechol, respectively.

The effect of pH on the DPV technique was also employed to make clearer for catechol-Arginine addition reaction at Pt electrode in same condition. DPV of 2mM catechol in the presence of 30 mM L-Arginine in first and second scan of potential at different pH (3-11) has been shown in Fig. 4.75 (Epulse 0.02 V, tpulse 20 ms and scan rate 0.1 V/s). It is noticed that the peak positions of the DPV of catechol with L-Arginine shifts negatively this indicates that the nucleophilic reaction is easier at pH 7. But, in pH 3-5 no new peak

appears in the second scan of potential and in pH 9-11, the species are totally electroinactive. A new anodic peak is observed at pH 7, which can be attributed to the formation of catechol-Arginine adduct.Gold (Au) electrode is also used for the investigation of DPV of 2mM catechol with 30 mM L-Arginine in different buffer solution at 0.1 Vs^{-1}. Fig. 40769 shows the first and second scan of potential of catechol + L-Arginine solution at different pH, respectively. However, in pH 7 new peak A_0 appeared which may be attributed to the formation of catechol-Arginine adduct. But, in lower and higher pH media no new anodic peak appeared. In the buffer solution of pH 7, the voltammogram shows two well-developed peak ascribed the formation of adduct similar to GC electrode. The DPV of Au and Pt electrodes are consistent with the GC electrode in the studied systems at the same condition.

4.2.8 Effect of deposition time change of DPV of Catechol + L-Arginine

Fig. 4.77 we considered the DPV of deposition time change (0, 10, 30, 90, 120 and 180s) of 2 mM catechol 30 mM L-Arginine of pH 7. According to this Fig., increasing of deposition time leads to develop two new peaks at - 0.32V and - 0.04 V. When the deposition time increases 30s, more nucleophilic attack occurred and consequently more catechol-Arginine adduct was formed which leads to decreasing in the concentration of o-benzoquinone and increasing in the concentration of Catechol-Arginine adduct at the surface of electrode. Maximum peak intensity was obtained up to 30s. For further increase of deposition time from 60s to 180s, both first and second anodic peak current decreases. This confirmed that with the increase of time decreases the concentration of o-benzoquinone due to follow up the reaction.

4.2.9 Effect of concentration of DPV of Catechol + L-Arginine

The effect of different composition of L-Arginine on catechol was studied by using the differential pulse voltammetry. DPV of 2mM catechol with 10 to 100mM L-Arginine at pH 7 has been shown in fig. 4.78. We can see that there are again two separated anodic peaks appeared after addition of different concentration of L-Arginine into catechol similar to Fig. 4.63. In this case, the gradual increasing of the concentration of L-Arginine up to 30 mM leads to increasing of first anodic peak current. For further increase of

concentration from 40 to 100 mM, all anodic peak decreases gradually. In lower concentration of L-Arginine (<30 mM), the nucleophilic substitution reaction take place in comparable degree, whereas increasing the concentration of L-Arginine (30mM) make favorable nucleophilic attack of Arginine toward o-benzoquinone generated at the surface of electrode. For further addition of Arginine (>30mM) into catechol solution, the excess electroinactive L-Arginine deposited on the electrode surface and hence the peak current decreases.

The effect of L-Arginine concentration on the DPV of catechol was also studied by using Platinum (Pt) (1.6 mm) electrode in the same condition. Fig. 4.79 shows DPV for 2 mM of catechol solution containing buffer (pH 7) in the presence of various concentration of L-Arginine from 10 mM to 100 mM at the surface of Pt electrode for the first and second scan of potential. As reported in Fig. 4.78, in the second scan there are two separated anodic peaks appeared after addition of L-Arginine into catechol. In lower concentration of L-Arginine (< 30 mM), the nucleophilic substitution reaction take place in comparable degree, whereas increasing the concentration of L-Arginine (30 mM) make susceptible for nucleophilic attack of L-Arginine towards o-benzoquinone generated at the surface of electrode. For more addition of L-Arginine (> 30 mM) into catechol solution, the excess electroinactive L-Arginine accumulated on the electrode surface and hence the peak current decreases.

Gold (Au) electrode was also used for the investigation on the DPV of fixed 2 mM catechol with different concentration (10-100 mM) of L-Arginine in buffer solution pH 7 at 0.1 Vs^{-1}. Fig. 4.80 shows the second scan of potential of the studied systems at different concentration, respectively. In second scan of potential an appeared peak, A_0 was obtained which may be attributed the formation of catechol-Arginine adduct.

In this investigation different concentration 10-100mM of L-Arginine was used to determine the optimum condition for the nucleophilic substitution reaction on catechol. As the reaction was occurred at moderately high concentration of nucleophiles, consequently the voltammetric peaks (CV and DPV) for adduct appeared noticeably. In contrast, comparatively low concentration of L-Arginine was not favorable for the study of electrochemical oxidation of catechol because the appearing peak was not so prominent.

From the experimental study it is noticeable that Arginine acts properly as a nucleophile at pH 7. When the pH is below 7 that are at acidic media, the nucleophilic activity of L-Arginine reduces due to the protonation of amine. Whereas at basic condition, other nucleophiles such as –OH produce in solution, therefore, the activity of amines decreases and the oxidation of catechol followed by an irreversible chemical reaction with hydroxylion [66].

Therefore, from the above discussion it was clear that the nucleophilic substitution reaction of catechol in presence of Arginine is maximum favorable at 30mM of L-Arginine and at pH 7 which is consistent with both CV and DPV. All above observations could be attributed to the reaction between L-Arginine and o-benzoquinone species produced at the surface of electrode, with the new anodic peak being attributed to the oxidation of newly formed o-benzoquinone- Arginine adduct.

4.3.1. Electrochemical nature of Catechol in presence of L-Serine

Fig. 4.81 shows the cyclic voltammogram of only catechol (Green line), only L-Serine (Blue line) and catechol with L-Serine (Red line) at GC (3mm) electrode in buffer solution of pH 7 and scan rate 0.1V/s. The cyclic voltammogram of catechol shows one anodic peak at A_1 (0.26V) and corresponding cathodic peak at C_1 (0.05V) related to its transformation to *o*-quinone and vice versa. Pure L-Serine is electrochemically inactive amino acid hence no sharp redox couple was observed in the potential range investigated (Fig. 4.81, blue line). Cyclic voltammogram of catechol in the presence of L-Serine in buffer solution of pH 7 shows one anodic peak in the first cycle of potential and on the reverse scan the corresponding cathodic peak slowly decreases and new peak C_0 is observed at less positive potential -0.32V. In the second cycle of potential a new anodic peak A_0 is also observed at less positive potential at 0.02V. Due to formation of new redox couple the current intensity of catechol reduces. This phenomenon can be explained by the fact of nucleophilic attack of Serine to o-benzoquinone. Due to the conduction of nucleophilic substitution reaction of L-Serine with catechol, the o-benzoquinone concentration in reaction layer reduces, consequently the A_1 and C_1 peaks reduce. Whereas in the same time catechol-Serine adduct produces and consequently the new peak A_0 appears. The peak current ratio for the peaks A_1 and C_1 (I_{Pa1}/I_{pc1}) decreased

noticeably, which indicated the chemical reaction of Serine (2) with the o-quinone (1a) produced at the surface of electrode. These observations may ascribe the formation of 3-hydroxy-2-((3-hydroxy-4-oxocyclohexa-2,5-diene-1-ylidene)amino]propanoic acid through nucleophilic substitution reaction (Scheme 1). If the constituent is such that the potential for the oxidation of product is lower, then further oxidation of the product is lower, the further oxidation and further addition may occur [83]. According to this concept it can be drawn that, the oxidation of catechol-Serine is easier than the oxidation of parent catechol in the presence of excess amount of nucleophile and this substituted product can be further attacked by L-Serine. However, it was not observed in cyclic voltammogram because of the low activity of o-quinone 4 toward 2. This behavior is in agreement with that reported by other research groups for similar electrochemically generated compounds such as catechol and different nucleophiles [83-91]. In the absence of other nucleophiles, water or hydroxide ion often adds to the o-benzoquinone [92].

Fig. 4.82 shows the CV of second scan of potential of 2 mM catechol with 90 mM L-Serine at Platinum (Pt) (1.6mm) electrode in pH 7 and at scan rate 0.1V/s. This cyclic voltammogram shows the comparison of only 2mM catechol (green line), pure L-Serine (blue line) and catechol (2 mM) with L-Serine (90 mM) (Red line) in the second scan of potential at the same condition. A new reduction peak (C_0) appears at -0.27 V after the addition of 90 mM L-Serine to the solution at first scan of potential. The peak current decreases significantly with respect to the only catechol. In the second scan of potential catechol with L-Serine shows two anodic peaks at 0.0 V and 0.32 V and the corresponding two cathodic peaks at - 0.31 V and 0.03 V, respectively. Upon addition of L-Serine to catechol solution, the cathodic peak C_1 decreases and a new cathodic peak C_o appears. Also, in the second scan of potential a new anodic peak A_o appears and anodic peak A_1 decreases similar to GC electrode. This observation can be stated by considering nucleophilic attack of L-Serine to o-benzoquinone. The nucleophilic attack of L-Serine to o-benzoquinone reduces the o-benzoquine concentration in reaction layer. Accordingly the A_1 and C_1 peaks reduce, whereas in the same time produces catechol-Serine adduct and consequently the peak A_0 and C_0 appears (Scheme 3).

A similar behavior was observed when we used a Gold (Au) electrode for the investigation of same solution in the same condition. Fig. 4.83 shows the CV of catechol (2 mM) in the

presence of L-Serine (90 mM) at Au electrode in the second scan of potential. Upon addition of L-Serine to catechol solution at the Gold (Au) electrode it shows three anodic and three cathodic peaks for the second scan of potential. The newly appearance of A_0 and C_0 peak, and decrease of A_1 and C_1 peak, and also shifting of the positions of peaks A_1 and C_1 also indicates that it is due to follow up reaction of catechol with L-Serine (Scheme 3) at Au electrode. In case of GC and Pt electrodes, it shows two anodic and two cathodic peaks. The third peak of Au electrodes is due to the oxidation of Au in buffer solution. This unlike behavior has been discussed in the effect of electrode materials section.

4.3.2 Effect of scan rate of Catechol with L-Serine

Fig. 4.84 shows different scan rate comparison graph of 2mm catechol with 90mM Serine at pH 7. According to this voltammogram it can be seen that the peak current intensity of newly appeared peak gradually increases with the increase of scan rates. The cathodic peaks shift towards left whereas the anodic peaks move to the right direction with increase of scan rate. Fig. 4.85 shows plot of the anodic and cathodic net peak currents for second cycle against the square-root of the scan rates where the net current means the second peak subtracted from the first one by the scan-stopped method in the same condition [83]. The nearly proportional ratio in between redox couple indicates that the peak current of the reactant at each redox reaction is controlled by diffusion process. It can be seen in Fig. 4.84, the cathodic peak for reduction of o-benzoquinone is almost disappeared in the scan rate of 0.05 V/s. By increasing the scan rate, the cathodic peak for reduction of o-benzoquinone starts to appear and increasing (Table 4.18). The corresponding peak current ratio (I_{pa1}/I_{pc1}) vs scan rate for a mixture of catechol and Serine decreases with increasing scan rate firstly and then after 0.2V/s, it remains almost unchanged (Fig. 4.86). The anodic peak current ratio (I_{pa0}/I_{pa1}) vs scan rate for a mixture of catechol and Serine firstly increases and then after 0.2V/s scan rate the peak current remain unchanged (Fig. 4.86). On the other hand, the value of current function ($Ip/v^{1/2}$) is found to be decreased with increasing scan rate (Fig. 4.87). The exponential nature of the current function versus the scan rate plot indicates the ECE mechanism for electrode process [93]. This confirms the reactivity of o-benzoquinone (1a) towards Serine (2) firstly increases at slow scan rate and then at higher scan rate it decreases.

According to the results, it was assumed that Serine (2) undergoes the 1,4-Michael addition reaction with o-benzoquinone (1a) leads to product 3. The oxidation of this compound (3) was observed easier than the oxidation of parent molecule (1) by virtue of the presence of electron donating amine group.

Step-1:

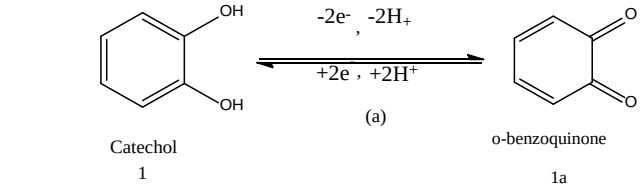

Catechol
1

o-benzoquinone
1a

Step-2:

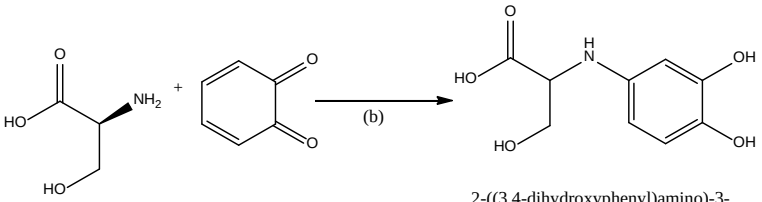

L-Serine
2

o-benzoquinone
1a

2-((3,4-dihydroxyphenyl)amino)-3-hydroxypropanoic acid
3

Step-3:

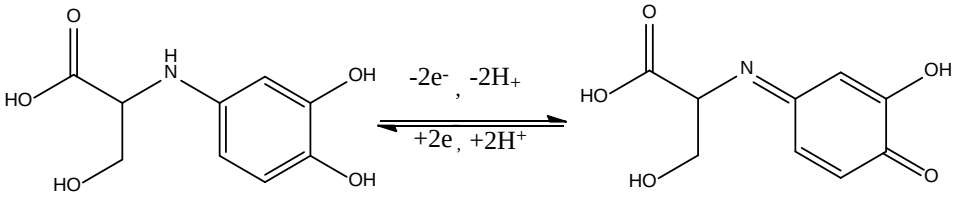

2-((3,4-dihydroxyphenyl)amino)-3-hydroxypropanoic acid
3

(*E*)-3-hydroxy-2-((3-hydroxy-4-oxocyclohexa-2,5-dien-1-ylidene)amino)propanoic acid
4

Scheme 3:

Fig. 4.88 shows the CV of second scan of potential at Pt electrode of 2 mM catechol with 90 mM L-Serine at pH 7 and different scan rate. The peak current of both the anodic and cathodic peaks increases with the increase of scan rate. The anodic peaks are shifted towards right direction and the cathodic peaks are to the left with increase in the scan rate. Fig. 4.89 shows plots of the anodic and cathodic peak currents for second scan of potential as a function of square-root of the scan rates. The proportionality of the anodic and the cathodic peaks ascribed that the peak current of the reactant at each redox reaction is controlled by diffusion process. The anodic and cathodic peak currents, peak potentials,

corresponding peak potential differences and peak current ratio are tabulated in Tables 4.19-4.20.

Fig. 4.90 shows variation of peak current ratio of corresponding peak (I_{pa1}/I_{pc1}) and anodic peak (I_{pa0}/I_{pa1}) vs scan rate (v) of 2mM Catechol with 90mM L-Serine in the same condition. The corresponding peak current ratio (I_{pa1}/I_{pc1}) vs scan rate for a mixture of catechol and L-Serine decreases with increasing scan rate firstly and then after 0.2V/s, it remains almost constant (Fig. 4.90). The anodic peak current ratio (I_{pa0}/I_{pa1}) vs scan rate for a mixture of catechol and Serine firstly increases and then after 0.3V/s scan rate the peak current suddenly starts to be decreased (Fig. 4.90). Beside this, the value of current function ($Ip/v^{1/2}$) is found to be decreased with increasing scan rate (Fig. 4.91). The exponential nature of the current function versus the scan rate plot indicates the ECE mechanism for electrode process.

Similarly the voltammetric behavior of the above systems has been investigated at Au electrode. Fig. 4.92 shows the CV of catechol with 90 mM L-Serine for second cycle of potential at different scan rate in pH 7. This voltammogram is consistent with Fig. 4.84 and Fig. 4.88. According to Fig. 4.93 it can be seen that the anodic and cathodic net peak currents against the square-root of the scan rates is nearly proportional which suggests that the peak current of the reactant at each redox reaction is controlled by diffusion process. Fig. 4.94 shows variation of peak current ratio of corresponding peak (I_{pa1}/I_{pc1}) and anodic peak (I_{pa0}/I_{pa1}) vs scan rate (v) in the same condition. The (I_{pa1}/I_{pc1}) peak current ratio decreases gradually whereas the anodic peak current ratio observed maximum at 0.2 V/s and after that it degreases with increasing scan rates(Table 4.19). The exponentially decreasing nature with increasing scan rates in Fig. 4.95 indicates that the reaction is taken place by ECE mechanism. According to all system it can be said that, the nucleophilic substitution reaction of catechol in presence of L-Serine is maximum favorable at slow scan rate by diffusion process.

4.3.3 Influence of pH on catechol with L-Serine

Cyclic voltammogram of catechol in presence of 90 mM L-Serine of GC (3mm) electrode was studied at pH from 3 to 11 (Fig. 4.96). The voltammetric behavior of catechol at pH 3,

5, 9 and 11 in the presence of 90mM L-Serine show no new anodic peak appeared after repetitive cycling indicating that the reaction between o-benzoquinone and L-Serine has not occurred. This can be attributed to the fact that at pH 5, the nucleophilic property of amine groups is diminished through protonation (Fig. 4.96). This can be explained by the fact that at pH 3-5 or lowers, the amino group undergoes protonation by excess proton and form zwitterion. But, in the higher pH 9-11 the cyclic voltammogram of catechol show irreversible behavior. It was thus suggested that the oxidation of catechol followed by an irreversible chemical reaction with hydroxyl ion, especially in alkaline solutions [20]. However amines in this condition can also act as nucleophiles. The peak position of the redox couple is found to be dependent upon pH. The anodic peak potential of catechol shifted towards left with the increase of pH.

Fig. 4.98 shows the plot of oxidation peak (A_0) current, I_p against pH of solution. From this Fig. it was seen that the maximum peak current was obtained at pH 7(Table 4.21). At this pH, the difference between the peak current ratio (I_{pC0}/I_{pA0}) in the presence of Serine is observed maximum. Consequently, pH 7 was selected as optimum condition for electrochemical study of catechol, at which the electro oxidation was facilitated in neutral media and hence the rate of electron transfer was faster.

CV of catechol in presence of 90 mM L-Serine at Platinum (Pt) (1.6 mm) electrode in the second scan of potential has been studied in pH 3 to 11(Fig. 4.99). The voltammetric behavior of 2 mM catechol at pH 7 in the presence of 90 mM L-Serine shows one anodic peak and corresponding cathodic peak after repetitive cycling expressing that the reaction between o-quinone and L-Serine has not occurred. This can be assigned to the fact that at acidic media, the nucleophilic property of amine groups is diminished through protonation. In the pH 7 the o-quinone undergoes L-Serine attack by the amine through a Michael addition reaction suggests that voltammetric new anodic peak A_0 appeared after repetitive cycling. However amines in this condition can also act as nucleophiles. The peak position of the redox couple is found to be depended upon pH. Fig. 4.100 shows the plot of oxidation peak current, I_p against pH solution. It is seen that the maximum peak current is obtained at pH 7 (Table 4.23). Fig. 4.101 shows the plot of peak potential, E_p vs pH. The slope value of the plot is obtained 56.5mV/pH which is nearer to the value of one electron, one proton transfer process.

The effect of pH on the cyclic voltammogram of 2 mM catechol in presence of 90 mM L-Serine at Au (1.6 mm) electrode in the second scan of potential was studied at pH from 3 to 11 (Fig. 4.102). The influence of pH for Au electrode in the same systems, the voltammetric properties are slightly different from GC electrode. The voltammetric behavior of catechol at acidic media in the presence of L-Serine shows no new peak in the second scan of potential. This can be indicated to the fact that in lower pH, the nucleophilic property of amine groups is diminished through protonation. In the pH 7 the o-benzoquinone undergoes L-Serine attack by the amine through Michael addition reaction reflected that voltammetric new anodic peak A_0 appeared after repetitive cycling. In the higher pH (e.g., pH 11), no new anodic peak appeared in the second scan of potential. However, the peak position of the redox species is found to be dependent upon pH. Fig. 4.103 shows the plots of oxidation peak current, I_p against pH of solution. It is seen that the maximum peak current is obtained at pH 7 (Table 4.22) attributed that nucleophilic addition reaction is most favorable in neutral media. Fig. 4.104 shows the plot of the peak potential, E_p against pH at second cycle in the same condition. The slopes of the plot were (53.5 mV/pH for anodic peak A_1) which is close to theoretical value for two step one electron, one proton transfer process.

4.3.4 Concentration effect of L-Serine

The effect of composition change of L-Serine from 10 mM to 130 mM with fixed composition of catechol was studied with the help of cyclic voltammetry of GC electrode at pH 7 and scan rate 0.1V/s (Fig. 4.105). Upon addition of L-Serine the anodic peaks shifts positively and a new peak appears at ~ 0.03V which suggests that the nucleophilic attack takes place and consequently catechol-Serine adduct deposits on the electrode surface. The peak current intensity of the newly appeared anodic and cathodic peak increases with the increase of L-Serine concentration up to 90 mM and after that the redox peak current is started to be decreased (Fig. 4.106). The nucleophilic substitution reaction of catechol in presence of Serine was maximum favorable up to 90 mM of Serine at pH 7 (Table 4.24). The corresponding peak current ratio (I_{pc1}/I_{pa1}) changes with the concentration of Serine. This was related to the increase of the homogenous reaction rate of following chemical reaction between o-benzoquinone 1a and L-Serine 2 with increasing concentration of Serine up to 90 mM. At higher concentration of Serine (>90mM), the

excess electro-inactive Serine may be deposited on the electrode surface and consequently the peak current decreased.

In addition of different concentration of L-Serine (10, 50, 90, 100 and 130mM) into fixed concentration of catechol (2 mM) at Gold (Au) and Platinum (Pt) electrodes has been also examined in the same conditions (Fig. 4.107 and Fig. 4.109). In the first scan of potential a new cathodic peak (C_0) is appeared at -0.32 V and -0.21 V at Pt and Au electrodes respectively. Upon addition of L-Serine in the second scan of potential, the anodic peaks shifted and a new anodic peak appeared at 0.01 V and - 0.07 V at Pt and Au electrodes respectively which suggests the formation of catechol-Serine adduct. The net current intensity of the newly appeared anodic and cathodic peak increases with the increase of composition up to 10 to 90 mM of L-Serine(Table 4.25-4.26). After further addition of L-Serine (>90 mM), the anodic and cathodic peak current gradually decreases. At higher concentration of L-Serine (>90mM), the excess electroinactive L-Serine may be accumulated on the electrode surface and the peak current decreased. Therefore, the concentration effects of L-Serine into the fixed concentration of catechol (2 mM) for Au and Pt electrodes are few different from GC electrode.

4.3.5 Effect of electrode materials

In absence and presence of 90mM Serine with the fixed composition of 2mM catechol the effect of electrode material on Electrochemical properties of catechol was studied with the help of both cyclic voltammetry (CV) and Differential pulse voltammetry (DPV) by using different electrodes like GC, Au and Pt at different pH at scan rate 0.1V/s has shown in Fig. 4.111 and Fig. 4.112. The nature of voltammogram, the peak position and current intensity for the studied systems are different for different electrodes although the diameter of GC electrode (3mm) was higher than Au and Pt (1.6mm). The CV of GC electrode is significantly different from those of the Au and Pt electrodes based on peak current consideration. All electrodes show two anodic and corresponding cathodic peaks in the potential range of investigation. Among them the peak current intensity of GC electrode is much higher than Au and Pt electrodes in Fig. 4.111. In the case of GC and Pt electrodes for the second cycle of potential a new oxidation and reduction peak appear at lower oxidation potential which can be attributed to the oxidation of adduct formed between the o-benzoquinone and L-Serine. Electrochemical properties of catechol with L-

Serine for example change of pH, concentration, scan rate etc. were studied in detail using Pt and Au electrodes. But among the electrodes, the voltammetric response of GC electrode was better than Pt and Au electrodes in the studied systems.

According to DPV electrode comparison graph (Fig. 4.112) it can be seen that GC electrode showed better voltammetric response and three anodic peak at -0.315V, -0.03V and 0.21V. We considered the catechol-adduct peak at -0.03V and another very small peak at more lower potential -0.315 V can be raised due to side reaction like polymerization, further oxidation of catechol-adduct or nucleophilic attract of hydroxyl ion. Among GC, Pt and Au electrode the peak current and voltammetric response of GC electrode was found much better than Pt electrode under this investigation. Therefore, GC electrode was chosen as electrode material for this investigation.

4.3.6 Subsequent cycles of CV of Catechol+L-Serine

Fig. 4.113 shows the cyclic voltammograms of the first 15 cycles of 2 mM catechol with 90 mM L-Serine of GC (3 mm) electrode in buffer solution of pH 7 for the potential range between - 0.6 V to 0.9 V. The voltammogram at the scan rate 0.1 Vs^{-1} has one anodic peak at 0.22 V and two cathodic peaks at -0.32 V and 0.08 V when considered the first scan of potential (red line). In the subsequent potential cycles a new anodic peak appeared at ~ 0.04V and intensity of the first anodic peak current increased progressively on cycling but the second anodic peak current decreases and shifted positively on cycling. This can be attributed to produce of the catechol-Serine adduct through nucleophilic substitution reaction in the surface of electrode (Scheme 3). The successive decrease in the height of the catechol oxidation and reduction peaks with cycling can be ascribed to the fact that the concentrations of catechol-Serine adduct formation increased by cycling leading to the decrease of concentration of catechol or quinone at the electrode surface. The positive shift of the second anodic peak in the presence of L-Serine is probably due to the formation of a thin film of product at the surface of the electrode, inhibiting to a certain extent the performance of electrode process. Along with the increase in the number of potential cycles the first anodic peak current increased up to 10 cycles and then the peak current almost unchanged with subsequent cycle (Fig. 4.113). This may be due to the block of electrode surface by the newly formed species after more cycling.

The effect of the cyclic voltammograms of the first 15 cycles of 2 mM Catechol with 90 mM L-Serine of Gold (Au) electrode and Platinum (Pt) electrode in buffer solution of pH 7 were also studied in the same condition. In Fig. 4.115 at Au electrode there were two anodic peaks at 0.25V and 0.97 V and three cathodic peaks at - 0.28 V, 0.11 V and 0.41 V respectively in the first scan of potential (red line). In the subsequent scan of potential Au electrode shows a new anodic peak at - 0.07 V with another three anodic peaks (blue line). But at Pt electrode there is one anodic peaks at 0.25 V and two cathodic peaks at - 0.3 V and 0.02 V in the first scan of potential (red line) (Fig. 4.114). In the subsequent potential cycles a new anodic peak appeared at - 0.01 V and the first anodic peak current increased progressively on cycling but the second anodic peak current decreases and shifted positively on cycling. This can be suggested to produce the catechol-Serine adduct through nucleophilic substitution reaction in the surface of electrode (Scheme 3).

4.3.7 pH effect of DPV of Catechol with L-Serine

Differential pulse Voltammogram obtained from the 1,4-Michaael addition reaction of 2mM catechol in the presence of 90 mM Serine in second scan in different pH (3-11) at GC electrode has shown in Fig. 4.116 to make clearer for the nucleophilic substitution reaction of Serine on catechol. In the buffer solution of pH 5-7, catechol gave two new well-developed waves at -0.19V, 0.09V (for pH 5) and -0.32V, 0.01V (for pH 7) respectively in the presence of L-Serine. As can be seen two completely separated anodic peaks with high current intensity were measured in pH 7, which can be attributed to the oxidations of o-benzoquinone-Serine new compound and catechol, respectively.

Gold (Au) electrode is also used for the investigation of DPV of 2mM catechol with 90 mM L-Serine in different buffer solution at 0.1 Vs^{-1}. Fig. 4.118 shows the first and second scan of potential of catechol + L-Serine solution at different pH, respectively. However, in pH 7 new peak A_0 appeared which may be attributed to the formation of Catechol-Serine adduct. But, in lower and higher pH media no new anodic peak appeared. In the buffer solution of pH 7, the voltammogram shows two well-developed peak ascribed the formation of adduct similar to GC electrode.

To investigate the effect of pH on the electro-oxidation of catechol, the DPV technique was also employed to make clearer for catechol-Serine addition reaction at Pt electrode in

the same condition. DPV of 2mM catechol in the presence of 90 mM L-Serine in first and second scan of potential at different pH (3-11) have been shown in Fig. 4.117 (E_{pulse} 0.02 V, t_{pulse} 20 ms and scan rate 0.1 V/s). It can be seen that the peak positions of the DPV of catechol with L-Serine shifts negatively this indicates that the nucleophilic reaction is easier at pH 7. But, in acidic media no new peak appears in the second scan of potential and in pH 9-11, the species are totally electroinactive. A new peak is observed at pH 7, which can be attributed to the formation of catechol-Serine adduct. The DPV of Au and Pt electrodes are consistent with the GC electrode in the studied systems at the same condition.

4.3.8 Effect of deposition time change of DPV of Catechol + L-Serine

In the Fig. 4.119, we have shown the DPV of deposition time change (0, 10, 30, 90, 120 and 150s) of 2 mM catechol 90 mM Serine of pH 7. According to this Figure it can be seen that, increasing of deposition time leads to develop two new peaks at – 0.32V and -0.01 V. When the deposition time increases 30s, more nucleophilic attack occurred and consequently more catechol-Serine adduct was formed which leads to decreasing in the concentration of o-benzoquinone and increasing in the concentration of catechol-Serine adduct at the surface of electrode. Maximum peak intensity was obtained up to 30s. For further increase of deposition time from 40s to 150s, both first and second anodic peak current decreases. This confirmed that with the increase of time decreases the concentration of o-benzoquinone due to follow up the reaction.

4.3.9 Effect of concentration of DPV of Catechol + L-Serine

The effect of different composition of Serine on catechol has been studied by using the differential pulse voltammetry. DPV of 2mM catechol with 10 to 130mM Serine at pH 7 has been mentioned in Fig. 4.120. There we can see three separated anodic peaks appeared after addition of different concentration of L-Serine into catechol similar to Fig. 11. In this case, the gradual increasing of the concentration of Serine up to 90 mM leads to increasing of first anodic peak current. For further increase of concentration from 100 to 130 mM, all anodic peak decreases gradually. In lower concentration of L-Serine (<90 mM), the nucleophilic substitution reaction take place in comparable degree, whereas increasing the

concentration of L-Serine (90mM) make favorable nucleophilic attack of Serine toward o-benzoquinone generated at the surface of electrode. For further addition of Serine (>90mM) into catechol solution, the excess electroinactive L-Serine deposited on the electrode surface and hence the peak current decreases.

The effect of L-Serine concentration on the DPV of catechol was also studied by using Platinum (Pt) (1.6 mm) electrode in the same condition. Fig. 4.121 shows DPV for 2 mM of catechol solution containing buffer (pH 7) in the presence of various concentration of L-Serine from 10 mM to 130 mM at the surface of Pt electrode for the first and second scan of potential. After the second scan there are two separated anodic peaks appeared after addition of L-Serine into catechol. In lower concentration of L-Serine (< 90 mM), the nucleophilic substitution reaction take place in comparable degree, whereas increasing the concentration of L-Serine (90 mM) make susceptible for nucleophilic attack of L-Serine towards o-benzoquinone generated at the surface of electrode. For more addition of L-Serine (> 90 mM) into catechol solution, the excess electroinactive L-Serine accumulated on the electrode surface and hence the peak current decreases.

Gold (Au) electrode was also used for the investigation on the DPV of fixed 2 mM catechol with different concentration (10-130 mM) of L-Serine in buffer solution pH 7 at 0.1 Vs^{-1}. Fig. 4.122 shows the second scan of potential of the studied systems at different concentration, respectively. In second scan of potential an appeared peak, A_0 was obtained which may be attributed the formation of catechol-Serine adduct.

Different concentration 10-130mM of L-Serine was used to determine the optimum condition for the nucleophilic substitution reaction on catechol. As the reaction was occurred at moderately high concentration of nucleophiles, consequently the voltammetric peaks (CV and DPV) for adduct appeared noticeably. In contrast, comparatively low concentration of L-Serine was not favorable for the study of electrochemical oxidation of catechol because the appearing peak was not so prominent. From the experimental study it is noticeable that Serine acts properly as a nucleophile at pH 7. When the pH is below 7 that are at acidic media, the nucleophilic activity of L-Serine reduces due to the protonation of amine. Whereas at basic condition, other nucleophiles such as –OH produce

in solution, therefore, the activity of amines decreases and the oxidation of catechol followed by an irreversible chemical reaction with hydroxyl ion [66].

Therefore, from the above discussion it was clear that the nucleophilic substitution reaction of catechol in presence of Serine is maximum favorable at 90mM of L-Serine and at pH 7 which is consistent with both CV and DPV. All above observations could be attributed to the reaction between L-Serine and o-benzoquinone species produced at the surface of electrode, with the new anodic peak being attributed to the oxidation of newly formed o-benzoquinone- Serine adduct.

4.4.1 Spectral analysis of Catechol + Imidazole

The FTIR spectral assignments of the vibrational modes of the Catechol-Imidazole adduct, Imidazole and Catechol were studied. The Imidazole showed N-H stretching sharp band at 2910 cm^{-1} and O-H stretching band at 3120 cm^{-1}. Catechol showed O-H stretching at 3467 cm^{-1}. The absorption peaks due to the O-H broad stretching vibration was appeared at 3444 cm^{-1} and C=O stretching at 1647 cm^{-1} for the Catechol-Imidazole adduct (Figure 4.123). The absorption peaks due to the N-H stretching vibration was disappeared at the wave number for the Catechol-Imidazole adduct.

4.4.2 Spectral analysis of Catechol + L-Arginine

The FTIR spectral assignments of the vibrational modes of the Catechol-Arginine adduct, Arginine and Catechol were studied (Figure 4.124). The Arginine showed the N-H stretching sharp band at 2864 $cm^{-1}$and O-H stretching band at 3320 cm^{-1}. Catechol showed O-H stretching at 3467 cm^{-1}. The absorption peaks due to the O-H broad stretching vibration was appeared at 3404 cm^{-1} and C=O stretching at 1653 $cm^{-1}$for the Catechol-Arginine adduct (Figure 4.124). The absorption peaks due to the N-H stretching vibration was disappeared at the wave number for the Catechol-Arginine adduct.

CHAPTER V

Conclusions

The reaction of electrochemically generated *o*-benzoquinone from oxidation of Catechol as Michael acceptors with Imidazole, L-Arginine and L-Serine has been studied in aqueous solution with various pH, different electrodes and different concentration of nucleophiles using Cyclic voltammetry (CV), Controlled potential coulometry (CPC), Differential pulse voltammetry (DPV) and Chronoamperometry (CA) techniques. The participation of reaction of *o*-benzoquinone with Imidazole, L-Arginine and L-Serine in the second scan of potential was observed.

Pure Imidazole, L-Arginine and L-Serine are electro-inactive whereas pure Catechol is electro-active. The redox reactions of Catechol are quasi-reversible. The products generated from the reaction that undergo electron transfer at more negative potentials than the Catechol. Electrode effects on CV and DPV of Catechol in presence of Imidazole, L-Arginine and L-Serine have been investigated. The voltammetric response of GC electrode is better than Au and Pt electrodes.

The nucleophilic substitution reaction of Imidazole, L-Arginine and L-Serine with Catechol is highly pH dependent and the maximum peak current is obtained at pH 7. The electro-oxidation of Catechol-amino acid and Catechol-imidazole adducts are facilitated in neutral media. The electro-oxidation of Catechol adducts take place via the $1e^{-}/1H^{+}$ process. This also suggests that during the reaction not only electron but also proton is released from the Catechol-amine adducts. The reactions are also concentration dependent. The reaction is mostly favorable in 30 mM of L-arginine, 90 mM of L-Serine and 20 mM of Imidazole with fixed 2 mM of Catechol.

All the studied system shows that peak current of both the anodic and the corresponding cathodic peaks increases with the increasing of scan rate. The peak current of the species at each redox reaction is controlled by diffusion process. The current function decreased

with the increasing of scan rate is ascribed that the nucleophilic addition of Catechol with mentioned nucleophiles occur through an ECE mechanism. The formation of Catechol-nucleophile adducts are also confirmed by coulometric measurement and FTIR spectra.

REFERENCES

1. Zayas Blanco, F. De , García Falcón, M.S. and SimalGándara J., 2004, J. Food. Contr., Vol. 15, p. 375.

2. Bult, A. Metal Ions in Biological Systems, Sigel, H., Ed., New York: Marcel Dekker, 1983, vol. 16, p. 261.

3. Golabi, S. M. and Nematollahi. D. P., 1992, J. Biomed. Anal., Vol. 10, p. 1035.

4. Petrova, S. A, Kolodyazhny, M. V and Ksenzhek, O. S., 1990, J. Electroanal. Chem., Vol. 227, p. 189.

5. Yu Katz, E, Borovkov, V. V and Evstigneeva, R. P., 1992, J. Electroanal. Chem., Vol. 320, p. 197.

6. Slavcheva, E, Sokolova, E. and Raicheva, S., 1993, J. Electroanal. Chem., Vol. 360, p. 271.

7. Kano, K. and Uno, B., 1993, Anal. Chem., Vol. 65, p. 1088.

8. Testa, A. C and Reinmuth, W. H., 1961, Anal. Chem., Vol. 33, p. 1320.

9. https://en.wikipedia.org/wiki/Diethylamine.

10. https://en.wikipedia.org/wiki/Sulfanilic_acid.

11. Kiani, A, Raoof, J. B, Nematollahi, D. and Ojani, R., 2005, J. Electroanal. Chem, Vol. 17, No. 19, pp. 1755 – 1760.

12. Khalafi, L, and Rafiee, M., 2010, J. Hazardous Materials, Vol. 174, p. 801.

13. Debus, H., 1858, "Ueber die Einwirkung des Ammoniaks auf Glyoxal". Annalen der Chemie und Pharmacie, Vol. 107, pp. 199–208.

14. Alan R. Katritzky, 1984, Comprehensive Heterocyclic Chemistry. Vol. 5, p.469-498,

15. Grimmett, M. Ross., 1997, Imidazole and Benzimidazole Synthesis. Academic Press.

16. Brown, E.G., 1998, Ring Nitrogen and Key Biomolecules. Kluwer Academic Press.

17. Pozharskii, A.F, et al., 1997, Heterocycles in Life and Society. John Wiley & Sons.

18. Heterocyclic Chemistry TL Gilchrist, The Bath press 1985 ISBN 0-582-01421-2

19. Hochachka, P.W. & G.N. Somero, 2002. Biochemical adaptation: mechanisms and process in physiological evolution. New York: Oxford University Press. 466 p.

20. Castaño T, Encinas A, Pérez C, Castro A, Campillo NE, Gil C., 2008, "Design, synthesis, and evaluation of potential inhibitors of nitric oxide synthase."Bioorg Med Chem., Vol, 16, pp. 6193-206.

21. Bogle RG, Whitley GS, Soo SC, Johnstone AP, Vallance P., 1994, "Effect of anti-fungal imidazoles on mRNA levels and enzyme activity of inducible nitric oxide synthase". Br J Pharmacol.. Vol. 111, pp. 1257-61.

22. http://aminoacidinformation.com/l-serine-benefits/

23. IUPAC-IUBMB Joint Commission on Biochemical Nomenclature. "Nomenclature and Symbolism for Amino Acids and Peptides". Recommendations on Organic & Biochemical Nomenclature, Symbols & Terminology etc.

24. Tapiero H, Mathé G, Couvreur P, Tew KD, 2002, "L-Arginine". (review). Biomedicine & Pharmacotherapy, Vol. 56, pp. 439–445.

25. Saini, Rashmi; Badole, Sachin L.; Zanwar, Anand A., 2013, "Arginine Derived Nitric Oxide: Key to Healthy Skin". In Watson, Ronald Ross; Zibadi, Sherma. Bioactive Dietary Factors and Plant Extracts in Dermatology. Nutrition and Health. pp. 73–82.

26. Morris SM, 2004, "Enzymes of arginine metabolism". (review). The Journal of Nutrition 134 (10 Suppl): 2743S–2747S; discussion 2765S–2767S.

27. Stechmiller JK, Childress B, Cowan L, 2005, "Arginine supplementation and wound healing". (review). Nutrition in Clinical Practice, Vol. 20, pp. 52–61.

28. Witte MB, Barbul A, 2003, "Arginine physiology and its implication for wound healing". (review). Wound Repair and Regeneration, Vol. 11, pp. 419–23.

29. Gokce N, 2004, "L-arginine and hypertension". The Journal of Nutrition 134 (10 Suppl): 2807S–2811S; discussion 2818S–2819S.

30. http://www.webmd.com/vitamins-supplements/ingredientmono-875-l-arginine.aspx?activeingredientid=875&

31. Nomenclature and symbolism for amino acids and peptides (IUPAC-IUB Recommendations 1983)", 1984, Pure Appl. Chem. Vol.56, pp. 595–624.

32. The Columbia Encyclopedia 6th ed. encyclopedia.com. *Retrieved 22 October 2012*.

33. https://en.wikipedia.org/wiki/Serine

34. http://www.foodchemadditives.com/applications-uses/1489#sthash.np8aLWWT.dpuf

35. Nematollahi, D. and Golabi, S. M., 2000, J. Electroanal. Chem., Vol. 481, p. 208.

36. Nematollahi, D. and Golabi, S. M., 1996, J. Electroanal. Chem., Vol. 405, p. 133.

37. Nematollahi, D. and Golabi, S. M., 2001, J. Electroanal. Chem., Vol. 13, p. 1008.

38. Nematollahi, D. and Golabi, S. M., 1997, J. Electroanal. Chem., Vol. 420, p. 127.

39. Nematollahi, D. and Golabi, S. M., 1997, J. Electroanal. Chem., Vol. 430, p. 141.

40. Nematollahi, D. and Golabi, S. M., 1998, Bull. Electrochem., Vol. 14, p. 97.

41. Nematollahi, D. and Golabi, S. M., 1997, Bull. Electrochem., Vol. 13, p. 156.

42. Nematollahi, D. and Goodarzi, H., 2001, Iran J. Electroanal. Chem., Vol. 510, p. 108.

43. Nematollahi, D. and Goodarzi, H., 1997, Iran J. Sci. Technol., Vol. 21, p. 121.

44. Nematollahi, D. and Forooghi, Z., 2002, Tetrahedron, Vol. 58, p. 4949.

45. Shahrokhian, S. and Hamzehloei, A., 2003, Electrochem. Commun., Vol. 5, p. 706.

46. Grujic, Z, Tabakovic, I. and Trkovnic, M., 1976, Tetrahedron Lett., Vol. 52, p. 4823.

47. Tabakovic, I, Grujic, Z. and Bejtovic, Z., 1983, J. Heterocyclic Chem., Vol. 20, p. 635.

48. Golabi, S. M, Nourmohammadi, F. and Saadnia, A., 2002, J. Electroanal. Chem., Vol. 529, p. 12.

49. Fotouhi, L, Kiani, S. T, Nematollahi, D. and Heravi, M. M., 2007, J. Electroanal. Chem., Vol. 10, p. 1002.

50. C.M.A. Brett and A.M.O. Brett, 1993, “Electrochemistry Principles, Methods and Applications”, Oxford University Press.

51. M. E. Hossain, 2014, “Electrochemical sensor simultaneous detection and estimation of environmental toxic pollutants”, M.Phil Thesis, KUET.

52. D.A. Skoog, F.J. Holler and T.A. Nieman, 2007, “Principles of Instrumental Analysis”, Thomson Brooks/ Cole, 6th Ed., pp. 349-351.

53. P.T. Kissinger and W.R. Heineman, 1996, “Laboratory Techniques in Electroanalytical Chemistry”, Marcel Dekker, Inc.

54. C.M.A. Brett and A.M.O. Brett, 1998, “Electroanalysis”, Oxford University Press.

55. Chaires, J.B., Dattagupta, N. and Crothers, D.M., 1982, Biochemistry, Vol. 21, p. 3933.

56. Randles, J.E.B., 1948, Transactions of the Faraday Society, Vol. 44, p. 327.

57. Sevcik, A., 1948, Collection of Czechoslovak Chemical Communications, Vol. 13, p. 349.

58. Bott, A.W., 1994, Curr. Seps., Vol. 13, p. 49.

59. Klinger, R.J. and Kochi, J.K., 1981, Journal of Physical Chemistry, Vol. 85, p. 12.

60. Afzal Shah, 2010, "Redox Behavior and DNA Binding Studies of Some Electroactive Compounds", Ph.D Thesis, Department of Chemistry, Quaid-i-Azam University, Islamabad.

61. Nicholson, R.S., 1965, "Analytical Chemistry", Vol. 37, p. 135.

62. Matsuda, H. and Ayabe, Y.Z., 1955, Electrochimica Acta, Vol. 59, p. 494.

63. Andrews, L.J., 1954, Chem. Revs., Vol. 54, p. 713.

64. A.J. Bard and L.R. Faulkner, 1980, "Electrochemical Methods, Fundamentals and Applications", John Wiley, New York.

65. Eyring, H., Glasstone, S. and Laidler, K.J., 1939, The Journal of Chemical Physics, Vol. 7, p. 1053.

66. Reinmuth, W.H., 1962, "Analytical Chemistry", Vol. 34, p. 144.

67. Laviron, E., 1983, J. Electrochim. Interfac. Electrochim., Vol. 1, p. 148.

68. Polcyn, D.S. and Shain, I., 1966, Analytical Chemistry, Vol. 38, p. 370.

69. Aoki, K. and Osteryoung, J., 1981, Journal of Electroanalytical Chemistry, Vol. 122, p. 19.

70. Aoki, K. and Osteryoung, J., 1984, Journal of Electroanalytical Chemistry, Vol. 160, p. 335.

71. Flanagan, J.B. and Marcoux, L., 1973, Journal of Physical Chemistry, Vol. 77, p. 1051.

72. Heinze, J., 1981, Journal of Electroanalytical Chemistry, Vol. 124, p. 73.

73. Shoup, D. and Szabo, A., 1982, Journal of Electroanalytical Chemistry, Vol. 140, p. 237.

74. Gavaghan, D.J. and Rollett, J.S., 1990, Journal of Electroanalytical Chemistry, Vol. 295, p. 1.

75. Qian, W., Jin, B., Diao, G., Zhang, Z. and Shi, H., 1996, Journal of Electroanalytical Chemistry, Vol. 414, p. 1.

76. Ikeuchi, H. and Kanakubo, M., 2000, Journal of Electroanalytical Chemistry, Vol. 493, p. 93.

77. Jr. D.K. Gosser, , 1993, "Cyclic Voltammetry (Simulation and analysis of reaction mechanisms)", Wiley-VCH, Inc.

78 F.M. Hawkridgein, P.T. Kissinger and W.R.(Eds.) Heieman, 1996, "Laboratory Techniques in Electroanalytical chemistry", Marcel Dekker Inc., New York. 2nd Ed.

79. J. Wang, 1994, "Analytical Electrochemistry", VCH Publishers Inc., New York.

80. E.R. Brown, R.F. Larg, A. Weissberger and B.(Eds.) Rossiter, 1971, Physical Methods of chemistry, Vol.1-Part IIA, Wiley-Interscience, New York.

81. Armada, P.G, Losada, J. and Perez, S.V., 1996, "Cation analysis scheme by differential pulse polarography", Vol. 73, pp. 544-546.

82. Zhang, J., 1972, Journal of Electroanalytical Chemistry, Vol. 331, p. 945.

83. Brun, A. and Rosset, R., 1974, Journal of Electroanalytical Chemistry, Vol. 49, p. 287.

84. Stum, D.I. and Suslov, S.N., 1979, Bio. Zika, Vol. 21, p. 40.

85. Rayn, M.D., Yueh, A. and Yu, C.W., 1980, Journal of Electrochemical Society, Vol. 127, p. 1489.

86. Md. Matiar Rahman, 2014, "Electrochemical characterization of biologically important electroactive metal ligand complexes with multi-electron transfer reaction", M.Phil Thesis, KUET.

87. Thibodeau, P.A. and Paquette, B., 1999, Free Radical Biology & Medicine, Vol. 27, p. 1367.

88. Mazzini, S, Monderelli, R, Ragg, E. and Scaglioni, L., 1995, Journal of the Chemical Society, Perkin Transactions, Vol. 2, p. 285.

89. Pasta, M., Mantia, F.L. and Cui, Y., 2010, Electrochimica Acta, Vol. 55, p. 5561.

90. Papouchado, L., Sandford, R.W., Petrie, G. and Adams, R.N., 1975, Journal of Electroanalytical Chemistry, Vol. 65, p. 275.

91. Khalafi, L., Rafiee, M., Shahbak, M., et al., 2013, Journal of Chemistry, Vol. 1, pp. 1-5.

92. Grujic, Z., Tabakovic, I. and Trkovnic, M., 1976, Tetrahedron Letters, Vol. 52, p. 4823.

93. Golabi, S.M., Nourmohammadi, F. and Saadnia, A., 2002, Journal of Electroanalytical Chemistry, Vol. 529, p. 12.

94. Belenky, P., Bogan, K.L. and Brenner, C., 2007, Trends in Biochemical Sciences, Vol. 32, p. 9.